Dissertation

submitted to the

Combined Faculty of Natural Sciences and Mathematics

of Heidelberg University, Germany

for the degree of

Doctor of Natural Sciences

Put forward by

Eileen Sophie Giesel

born in: Gunzenhausen

Oral examination: 11.01.2023

On astrophysical solutions in the constructive gravity program and cosmological tests for weakly birefringent spacetime

Referees:

Prof. Dr. Björn Malte Schäfer

Prof. Dr. Jan M. Pawlowski

Supervisors:

Prof. Dr. Björn Malte Schäfer

Prof. Dr. Frederic P. Schuller

Zusammenfassung

Mithilfe von gravitativem Abschluss konnten [Dü+18]; [Wol22]; [Due20]; [Wie18] zeigen, wie sich Gravitationstheorien systematisch basierend auf dem Materie-Inhalt der Raumzeit konstruieren lassen. Während diese Vorgehensweise erfolgreich die allgemeine Relativitätstheorie für eine metrische Raumzeit reproduziert, ist es bis jetzt noch nicht möglich gewesen, eine Lösung für die einfachste Verallgemeinerung der Maxwell-Elektrodynamik basierend auf einer Vakuumdoppelbrechung erlaubenden, flächen-metrischen Struktur zu finden. Für hoch-symmetrische FLRW-Raumzeiten konnte eine metrische, sowie eine flächen-metrische Lösung hergeleitet werden [Due20]; [Fis17]. Von diesem Ergebnis ausgehend soll das Programm der konstruktiven Gravitation auf sphärisch symmetrische, stationäre, metrische Raumzeiten angewendet werden. Desweiteren soll ein entsprechender Ansatz für flächenmetrische Geometrien ausgearbeitet werden, und die Schwierigkeiten, welche im Lösungsverfahren auftreten, diskutiert werden. Zudem wird im Fall schwacher flächen-metrischer Gravitation die Etherington-Dualität verletzt [Sch+17]; [Ale20b]; [SW17] und diese Verletzung soll durch schwache Gravitationslinsenexperimente untersucht werden. Die Observable ist die Flächenhelligkeit, die allerdings durch astrophysikalische Prozesse wie der physischen Wechselwirkung von Galaxien mit Gezeitenfeldern stark beeinflusst wird. Darüber hinaus wird untersucht, wie sich - ebenfalls durch Gezeitenwechselwirkung hervorgerufen - Galaxien verbiegen und wie stark diese Auswirkung verglichen zu ihrem analogen Gravitationslinseneffekt ist.

Abstract

Via gravitational closure [Dü+18]; [Wol22]; [Due20]; [Wie18] could show, how gravitational theories based on the matter content of spacetime can be systematically constructed. While this successfully reproduces general relativity for metric spacetimes, finding a solution for the simplest generalization of Maxwell electrodynamics with a vacuum birefringence allowing, area-metric structure has in general not been possible so far. For highly symmetric FLRW spacetimes a metric, as well as an area-metric solution could be derived [Due20]; [Fis17]. Based on this result, the constructive gravity program will be applied for spherically symmetric, stationary metric spacetimes. Furthermore, an according ansatz is worked out for area-metric geometries, and it is discussed which difficulties arise in finding a corresponding solution. Furthermore, the Etherington-duality is violated in the case of weakly area-metric gravitation [Sch+17]; [Ale20b]; [SW17], and this violation will be investigated with weak gravitational lensing experiments. The observable is the surface brightness, which is, however, heavily influenced by astrophysical processes like physical interaction of galaxies with tidal fields. Beyond that, it is studied how galaxies also get bent due to tidal interactions and how strong this effect is compared to its analog in gravitational lensing.

I am still confused – but on a higher level.
Enrico Fermi

Contents

0 Introduction

In 1933, Fritz Zwicky discovered a discrepancy between the observed luminous matter contained in a galaxy and the virial velocities of the same galaxy [Zwi33]. His findings hinted at the concept of dark matter to explain for these discrepancies. This was further underpinned and clarified by Vera Rubin and Kent Ford, as well as Kenneth Freeman in the 1970s, who studied the rotational velocities of spiral galaxies: These were significantly larger than expected at higher radii, and could not be explained by classical models with luminous matter alone [SBD17].
With the observations by [Rie+98], it became also evident that a concept of dark energy has to make up a significant amount of the energy-momentum content of the Universe as source of repulsive gravity. It drives apart everything on cosmological scales in an accelerated fashion. The studies of [Rie+98] confirm this for distant supernovae as a prominent example.
A lot of scientific effort was put into understanding the nature of dark matter and dark energy. Especially for dark matter, physicists discussed various different particle models that shall account for the discrepancies in the observations. Unfortunately, as of now, none of these particles were detected in experiments. This lead to the idea that the gravitational interaction requires modification and needs to be refined.
However, since Einstein's theory of general relativity, it is known how deeply matter and gravity are related and that the two can hardly be discussed independent of each other. In fact, Einstein had the fundamental insight that classical electrodynamics can be understood in a geometric way, while the equivalence principle guided him from special relativity (1905) to general relativity (1915) as theory of gravity. It turns out to be a purely geometric effect rather than an actual force (see [Bla20] and references therein).
Spinors on a curved metric spacetime are another example for a matter theory providing crucial additional input to the gravity action, since this spacetime might still possess torsion as additional geometric structure. The starting point is the Dirac equation, that contains a connection form that also includes a torsion degree of freedom. Following the arguments of [Cli+12]; [DL03]; [Tra06], the gravity action consists of the Einstein-Hilbert action and an additional part containing a contorsion tensor that is a function of the torsion. This is called Einstein-Cartan-Sciama-Kibble theory (ECSK). Variation of the gravity action with respect to metric and contorsion yields the corresponding gravitational field equations. From the matter part two sources of gravity are thus found: The energy-momentum stress tensor by variation

of the matter action with respect to the metric, as well as the spin angular momentum tensor by variation with respect to the contorsion. Outside of matter with spin and for low spin-densities general relativity is then recovered.
Both examples, general relativity connected to Maxwell theory, as well as ECSK which is assumed to be connected to matter with intrinsic spin, illustrate, that there is a deep connection between gravity and the underlying matter theory. Or as John Archibald Wheeler famously put it with the following sentence [MSW73]: *"Spacetime tells matter how to move; matter tells spacetime how to curve."*
Thus, it is not surprising that for a consistent description of physical problems, where the interplay between matter and gravity plays an important role, one must always keep in mind, what a modification of one of these might imply for the other. This interplay needs to be put into a precise mathematical language though, and the spacetime dynamics must be rigorously derived thereafter.
Initially, [HKT76] showed how to construct the ADM-representation [ADW08] of the Einstein-Hilbert action, i.e. general relativity in a canonical formalism. They carried out this construction starting from a Lorentzian metric as according geometry of the spacetime manifold. The constructive gravity program in its most recent version worked out by [Dü+18]; [Due20]; [Wol22]; [Sch20] builds up on the conceptual ideas by [HKT76]. The program further generalizes the idea of systematically constructing a gravity theory from some specific input geometry of spacetime, which is always implicitly part of the matter equations of motion. Hence, a way is established to formulate the interplay between matter and gravity in terms of countably many partial differential equation. The kinematics of matter hereby serves as an input, to deliver the corresponding gravitational dynamics as an output. The construction of general relativity from Maxwell electrodynamics can then be performed successfully as a case study in this framework.
This serves as a strong motivation to study different matter models as input for a gravitational theory, systematically following the constructive gravity program. Another interesting matter theory candidate is the Dirac equation with a spinor coupling to the torsion. This has not been studied in the constructive gravity program, but it would be interesting to see whether this leads to a gravitational theory similar to ECSK.
One can also take one step further back, and consider the simplest generalization of Maxwell electrodynamics, namely general linear electrodynamics (see for instance [Rub02] for a review). While in the action of Maxwell electrodynamics the two field strength tensors F_{ab} couple via two inverse Lorentzian metrics g^{ab}, the theory of general linear electrodynamics features a 4-rank tensor object G^{abcd} as linear constitutional relation, to which the field strength tensors couple instead. The object G^{abcd} to which these matter fields couple, and

which hence determines the structure of the matter equations of motion, is also called area-metric. As implied by its name, it defines a genuine measure of area instead of length, unlike a metric. Interestingly, with the area-metric as the according geometric field of the spacetime manifold, this electrodynamic theory generally allows for vacuum birefringence. This might sound unusual, since birefringence is something one rather expects due to light traversing some kind of anisotropic material instead of a gravitational field. But then, one could also ask why the spacetime as a medium should be isotropic everywhere in the first place. Therefore, the question arises whether vacuum birefringence would be possible or not, and if it is possible, what the corresponding implications would be.

Now in this context, it must be stressed, that if one was ever to observe vacuum birefringence, Maxwell theory would not hold anymore. But since general relativity is - in its entire construction - deeply connected to Maxwell electrodynamics, it becomes evident that the gravity theory would need to be adjusted accordingly.

The most noticeable difference compared to general relativity is, that concepts from Riemannian geometry which rely on a metric cannot be used any longer to postulate a gravitational action. It is for instance not clear how to build a Riemann tensor or Ricci tensor from an area-metric [Scha]. Hence, a systematic way to construct gravity theories for different matter theories is needed, such that postulating curvature invariants from the geometric spacetime structure is not required.

Now, that is what constructive gravity aims to achieve. Starting from area-metric geometry to find the corresponding gravity action is an important case study in this context, which is for instance discussed in more detail by [Dü+18]; [Due20]; [Wol22]; [Sch+17]; [Fis17]; [Ale20b] and references therein.

Interestingly, recent work has shown cosmic birefringence by analyzing polarization data from Planck 2018 [MK20]. With these results, the authors of [Fuj+21] studied the according implications for properties of hypothetical axion-like particles as possible causes for this effect. Alternatively, one can also ask whether the findings by [MK20] could set experimental bounds for birefringence due to an area-metric background. However, it is also important to stress that in this context classical effects like Faraday rotation will arise as well. The question is of course how these limit the precision and resolvability of exotic physics effects. But still, exploring the implications of general linear electrodynamics in this case would be very interesting.

While it has, as of now, not been possible to construct a general gravity action for general linear electrodynamics [Dü+18]; [Due20]; [Wol22]; [Sch+17], a solution for highly symmetric FLRW spacetimes [Due20]; [Fis17] could be derived successfully via symmetry-reduced gravitational closure. Of course, it would also be desirable to find an appropriate solution

for less symmetric cases like for a Schwarzschild spacetime in area-metric geometry for two reasons:

First of all, it is important to understand how solutions of area-metric gravity would look like in the strong gravity regime. Since the Schwarzschild solution, and its physical implications within this spacetime structure, are the first step in understanding the physics for compact astrophysical black holes, it is natural to ask how to construct those for modified gravity theories. And indeed, with modern gravitational wave experiments like LIGO, data from strong gravity events like black hole mergers can be studied, and signatures which hint at deviations from general relativity can be searched. Similarly, this is the case for the event horizon telescope (EHT), where models for the black hole shadow can be investigated. It is expected, that, if there are any deviations from general relativity, corresponding signatures may be found in the shape of the black hole shadow, as for instance addressed by [Daa+22].

Secondly, it is an interesting case study from a conceptual point of view, since working out the ansatz to perform the construction may also point at current difficulties in the constructive gravity program itself. Thus, it will turn out that finding an area-metric Schwarzschild solution is highly non-trivial. How one can still try to approach this problem, was the central motivation of this thesis.

A further example, where the construction of non-metric solutions via gravitational closure proved to be successful, was for the weak field limit [Sch+17]; [Wol22]; [Wie18]. The corresponding solutions for weakly birefringent spacetime are in detail discussed by [Sch+17]; [Wol22]; [Ale20b].

Now, an important aspect for probing the large-scale distribution of dark matter, or even further whether and where modifications of general relativity might play a role is through observations, for instance via weak gravitational lensing: Due to light deflection in gravitational fields one can directly probe gravity itself. Especially the solutions for weakly birefringent spacetime are a perfect basis to study possible signatures of an area-metric spacetime geometry using weak lensing. As an example, [SW17] predict a violation of the Etherington distance duality relation.

However, when using weak lensing to search for new physics one also has to ensure, that sources for systematic errors from classical astrophysics are well understood and under control: An important source for systematic errors in weak lensing is intrinsic alignment, meaning intrinsic shape and size distortions, as well as orientations within local tidal fields of the large-scale structure. Interestingly, these intrinsic alignment effects will lead, as shown in this work, to a similar phenomenology as expected from a violation of the Etherington distance duality relation because of a weakly birefringent spacetime.

Outline of this thesis

In Chapter 1, basic ideas on constructive gravity, as established by [Dü+18]; [Due20]; [Wol22]; [Wie18] will be summarized.
It will also be studied, guided by preceding works by [Due20]; [Fis17]; [Dü+20], how the metric Schwarzschild solution and related solution types can be systematically constructed in Chapter 2. This will especially serve as a consistency check for the theory, inspiring however how this problem might be solved for spacetimes with a different geometric structure.
Next, in Chapter 3, it will be discussed how one can derive a symmetry reduced ansatz for the constructive gravity program for an area-metric spacetime with Schwarzschild symmetries, being guided by previous works by [PWS09]. It is furthermore summarized briefly, what open question in this program is in general most obstructive to find an according area-metric Schwarzschild solution in the future.
In Chapter 4, a linear alignment model based as further development of [GDS21] will be discussed in order to derive intrinsic gravitational flexions in a Newtonian intrinsic alignment model. Its observability is to be compared with the one of the weak lensing flexion as analog effect. Many methods discussed in Chapter 4 which concern the calculation of spectra and cumulated signal-to-noise ratio plots will then be needed in the subsequent part of this thesis. There, in Chapter 5, it will be discussed how the Etherington distance duality violation in weakly birefringent spacetimes as derived by [SW17], will lead to a violation of the surface brightness conservation law from general relativity. The corresponding surface brightness variations are estimated, and their magnitude is compared to a similar effect caused by classical intrinsic alignment in the Newtonian limit. Furthermore, the impact of the Etherington distance duality modification on the quasar magnification bias is investigated.
Finally, in Chapter 6, the main topics addressed in this thesis will be summarized briefly, and an outlook will be given for each of them.

Notational remarks

Throughout this thesis, and if not stated otherwise the Latin letters $a, b, \cdots$ will denote spacetime indices, while Greek letters $\alpha, \beta \cdots$ denote spatial indices. Furthermore, only equations which are referred to explicitly in the text are numbered.

1 Constructive Gravity

In this chapter the basic principles of the constructive gravity program will be reviewed briefly. First it is discussed, which matter theories would be physically viable to consider, what kinematic structure they posses and how this leads to the gravitational dynamics in the end. Therefore, the physical idea behind this whole program is that the matter dynamics already contain all the relevant information for the spacetime geometry dynamics, such that gravity becomes a mere consistency condition (see [Due20]; [Wol22]; [Dü+18]; [Sch20]). The constructive gravity program can be considered as a conceptual generalization of geometrodynamics [Kuc74]; [HKT76].

1.1 Gravitational closure in the context of modified gravity

Basically, constructive gravity or also called gravitational closure (see for instance [Dü+18]; [Due20]; [Wol22]) aims at systematically finding the according gravitational dynamics implied by the kinematic structure imprinted on spacetime by an underlying matter theory, which is defined through the action S_{matter}. As discussed in [Dü+18] the matter dynamics must thus be closed under variation of the associated gravity action S_{geo}, where the total action is given by

$$S\left[\boldsymbol{\Phi}(\boldsymbol{x}); G(x)\right] = S_{\text{geo}}\left[G(x)\right] + S_{\text{matter}}\left[\boldsymbol{\Phi}(\boldsymbol{x}); G(x)\right).$$

The bracket notation is adapted from [Dü+18] and means the following: While the []-backet denotes a dependency on the field and higher order derivatives, the ()-backet denotes an explicit dependence on the field only. This kind of notation will be used on different occasions throughout this chapter.

Since the gravitational closure procedure makes it possible to derive the gravitational dynamics, one natural setup to consider is given by Maxwell electrodynamics. From this general relativity can be derived [Dü+18]; [Due20]; [Wol22], what confirms the result by [Kuc74]; [HKT76] in a more general setting.

This result not surprising: Lovelock's theorem states, that if one considers four dimensions, a metric as underlying geometry, and at most second derivatives thereof, as well as symmetric, locally divergence-free field equations, the gravity action should be given by the Einstein-Hilbert action (see [Cli+12] for reference). Thus, as stated in [Cli+12], at least one of these

requirements should be violated for a modification of gravity to become sensible. For example different fields (for instance scalars in case of Horndeski gravity [Hor74]) may be introduced, or higher-order derivatives, and non-local field equations (see for instance [Boo21] and references therein).
However, gravitational closure follows a different approach: The philosophy of the program implies that one cannot modify the gravitational dynamics without considering its effect on matter theories and vice versa. This is an important insight, especially concerning the quest of searching for dark matter and energy, respectively modified gravity theories, or both.
The following chapter is a summary of the basic ideas of the constructive gravity program in its latest form[1] worked out by [Dü+18]; [Wie18]; [Due20]; [Sch20]; [Wol22].

1.2 Spacetime kinematics from matter fields

At first it will be summarized, based upon [RRS11]; [Due20]; [Wol22]; [Wie18], what requirements need to be imposed upon matter fields such that they can be considered as canonically quantizable. The canonical quantization will hereby not play a role for the constructive gravity program per se, since here only classical fields are considered. However, in a bigger picture, which also includes other fundamental branches of physics like Quantum field theory, one would also need to be able to describe these matter fields accordingly. Therefore, any proposed classical matter theory which cannot be quantized is outruled.
The canonical quantizability will also define the kinematics and the causual structure of the dispersion relations of these matter theories within a specfic spacetime geometry. From this structure the gravitational dynamics will be derived later.
Take a matter theory, similar to [Wol22],

$$S_{\text{matter}}\left[\boldsymbol{\Phi}(\boldsymbol{x}); G(x)\right) = \int_M \mathrm{d}^4x\, \mathcal{L}_{\text{matter}}\left(\boldsymbol{\Phi}(\boldsymbol{x}), \partial\boldsymbol{\Phi}(x), \cdots, \partial^n\boldsymbol{\Phi}(x); G(x)\right),$$

where M is the 4-dimensional spacetime manifold with $x \in M$, with $G(x)$ as some spacetime geometry to which a set of matter fields $\boldsymbol{\Phi}(x) \coloneqq (\Phi_1(x), \cdots, \Phi_N(x))$ couple. By virtue of Hamilton's principle variation of this matter action with respect to the matter fields will lead to the equations of motion with

$$\frac{\delta S_{\text{matter}}}{\delta \Phi_i(x)} = 0.$$

[1] An earlier ansatz for the constructive gravtiy program was worked out by [Gie+12]; [Wit14]; [SW14] for instance.

For a quasi-linear matter theory the according equation of motion will generally form a system of partial differential equations given by [Wol22]

$$Q^{i_1,\cdots,i_n}_{\mathcal{AB}}\left(\mathbf{\Phi}(\boldsymbol{x}),\partial\mathbf{\Phi}(x),\cdots,\partial^{n-1}\mathbf{\Phi}(x);G(x)\right)\left(\partial_{i_1}\cdots\partial_{i_n}\mathbf{\Phi}^{\mathcal{B}}\right)(x)+\mathcal{O}\left(\partial^{n-1}\mathbf{\Phi}\right)=0. \tag{1.1}$$

Here $Q^{i_1,\cdots,i_n}_{\mathcal{AB}}$ denotes the coefficient in front of all the terms containing the highest derivative order of the matter fields, and which appears linearly in the equations of motion. Even though only partial derivatives of $\mathbf{\Phi}(x)$ appear in (1.1), the whole expressions still transforms covariantly, since all lower order derivative terms cancel any excess partial derivatives of jacobians due to coordinate transformations of the term $\partial_{i_1}\cdots\partial_{i_n}\mathbf{\Phi}^{\mathcal{B}}$, which is clearly not a tensor. Contrary, the highest order derivative coefficient $Q^{i_1,\cdots,i_n}_{\mathcal{AB}}$ is a tensor density of weight one - which can be de-densitized to become a tensor - and encodes the kinematic information that is relevant in the following. As discussed in [RRS11]; [Due20]; [Wol22]; [Wie18] $\mathcal{A}$ and $\mathcal{B}$ are multiindices, containing all matter fields of the theory, as well as their respective components. Further restricting to linear matter models, the matter fields do not even appear in the highest order coefficient $Q^{i_1,\cdots,i_n}_{\mathcal{AB}}(G(x))$, but only the geometry. This implies that the amplitude of the matter field can be scaled down to arbitrarily small values. It can hence be considered as test matter, to avoid any back-reaction of the fields to the spacetime geometry (see discussion by [Due20]; [Wol22] for instance).

Generally, one cannot read off the highest derivative order coefficient directly from the equations of motion derived from variation, but also needs to ensure, that the system of partial differential equations is in involutive form. Involutivity is an involved concept that needs to be elaborated in more detail, what is beyond the scope of this work. Essentially, if a system of partial differential equations is in involutive form, this means that all hidden integrability conditions are made explicit. Consequently, seemingly irrelevant lower order terms may possibly contribute to the coefficient $Q^{i_1,\cdots,i_n}_{\mathcal{AB}}$. An according review on involutivity of a system of partial differenential equations with some applicative examples can be found in [Sei10]; [Wie18]; [Wol22].

Now, a WKB (Wentzel-Kramers-Brillouin) ansatz [Wie18]; [Wol22]

$$\Phi^{\mathcal{A}}(x)=\mathrm{Re}\left(\exp\left[\mathrm{i}S(x)/\lambda\right]\left(\phi^{\mathcal{A}}+\mathcal{O}(\lambda)\right)\right)$$

for the amplitudes of the matter fields is inserted. It is evaluated in the geometric optical limit $\lambda\to\infty$, where the matter fields are indistinguishable from massless particle modes, with $k_a=-\partial_a S(x)$ as wave co-vector. Then, the so-called principal symbol [Wol22] is given by

$$T(x,k)_{\mathcal{AB}}=Q^{i_1,\cdots,i_n}_{\mathcal{AB}}(x)k_{i_1}\cdots k_{i_n}.$$

The corresponding equations of motion read

$$T(x,k)_{\mathcal{AB}}\phi^{\mathcal{A}} = 0,$$

for all non-vanishing solutions of $\phi^{\mathcal{A}}$. This means, that $T(x,k)_{\mathcal{AB}}$ must not be invertible, and thus have vanishing determinant. If the matter theory is however a gauge theory, one has to be careful, since seemingly non-zero solutions of $\phi^{\mathcal{A}}$ can actually just be gauge artifacts, and therefore physically equivalent to $\phi^{\mathcal{A}} = 0$. Thus, the gauge freedom needs to be reduced from the prinicpal symbol according to the techniques laid out in detail in [Dü+18]; [Wol22]; [Wie18] for instance, and summarized here:
Take $\phi^{\mathcal{A}}$ to be a gauge field with gauge transformation

$$\phi^{\mathcal{A}} \to \phi^{\mathcal{A}} + \partial_a \chi^{a\mathcal{A}}_{(\sigma)},$$

where $\sigma = 1, \cdots, s$ denotes s linearly independent coefficients $\chi^{a\mathcal{A}}_{(\sigma)}$. This implies that the solution space of $T(x,k)_{\mathcal{AB}}\phi^{\mathcal{A}} = 0$ is at least s-dimensional, however with solutions that are purely gauge, and at least one physical solution is required. As discussed by [Iti09]; [Dü+18]; [Wie18]; [Wol22] this means that the rank of $T(x,k)_{\mathcal{AB}}$ must thus be $R-s$ dimensional, where R is the number of mulitindices $\mathcal{A}$, and thus for the adjunct matrix it needs to hold that

$$T^{[\mathcal{A}_1\cdots\mathcal{A}_s][\mathcal{B}_1\cdots\mathcal{B}_s]}(x,k) = \frac{\partial^s \left(\det_{\mathcal{A},\mathcal{B}} T(x,k)\right)}{\partial T_{\mathcal{A}_1\mathcal{B}_1}\cdots\partial T_{\mathcal{A}_s\mathcal{B}_s}} = 0.$$

Then, as argued by [Dü+18]; [Wol22]; [Wie18] and references therein, the principal polynomial density $\tilde{P}(x,k)$ can be read off from

$$T^{[\mathcal{A}_1\cdots\mathcal{A}_s][\mathcal{B}_1\cdots\mathcal{B}_s]}(x,k) = \epsilon^{\sigma_1\cdots\sigma_s}\epsilon^{\tau_1\cdots\tau_s}\chi^{a_1\mathcal{A}_1}_{(\sigma_1)}\cdots\chi^{a_s\mathcal{A}_s}_{(\sigma_s)}\chi^{b_1\mathcal{B}_1}_{(\tau_1)}\cdots\chi^{b_s\mathcal{B}_s}_{(\tau_s)}k_{a_1}\cdots k_{a_s}k_{b_1}\cdots k_{b_s}\tilde{P}(x,k).$$

Thus, the principal polynmial density $\tilde{P}(x,k)$, or after de-densitization the principal polynomial

$$P(x,k) = P^{a_1\cdots a_n}k_{a_1}\cdots k_{a_n} = 0$$

needs to vanish. Here $P^{a_1\cdots a_n}$ is the principal tensor field, while n is the degree of the principal polynomial. This polynomial hence defines the massless dispersion relation in spacetime, since it was derived from the geometrical optical limit.

1.2.1 Matter conditions

As worked out in detail by [RRS11] and discussed further for instance in [Dü+18]; [Wol22]; [Due20]; [Wie18] not *all* principal polynomials are suitable for physical theories. Only if three conditions are fulfilled by the matter theory and its underlying background geometry, they are viable to extract physical relevant statements from the theories. These conditions can be shown to be necessary requirements once for canonical quantization of the matter theory (see [RRS11] and [RS11] for explicit applications).

First of all, the matter dynamics must be **predictive**, meaning that there is a well-defined initial value formulation: Initial data on a Cauchy hypersurface has to develop in an unambiguous way to hypersurfaces at later instances. For this to be possible the equations of motion of the matter theory shall be hyperbolic, what implies the **hyperbolicity of the principal polynomial** $P(x,k)$ itself.
This means that [Dü+18]; [RRS11]

$$\begin{aligned}&\exists h \in T^*_x M \text{ such that } P(x,h) \neq 0,\\ &\text{For } P(x, q+\lambda h) = 0 \text{ and } \forall q \in T^*_x M, \text{ solved by only real roots} \lambda(x) \in \mathbb{R}.\end{aligned}$$

Here, $T^*_x M$ denotes the co-tangent space, with h and q as according co-vectors. The co-vector h is then called hyperbolic, and lies within an open set $h \in C_x(P,h) \subset T^*_x M$ of hyperbolic co-vectors, which form a convex cone, called the hyperbolicity cone.
If the principal polynomial can be reduced to a product of n lower order polynomials according to [RRS11]

$$P(x,k) = P_1(x,k) \cdots P_n(x,k),$$

each of these lower order polynomials $P_i(x,k)$ must be hyperbolic to ensure the hyperbolicity of $P(x,k)$. Repeated factors of lower order polynomials should be removed, such that the principal polynomial can be written as a product of irreducible lower order polynomials. As elaborated in more detail in [RRS11] and briefly mentioned in the discussion of the next matter condition, this is an important technical requirement. Additionally, removing repeated factors from the principal polynomial also does not pose a problem, for they contain no further information on the roots [RRS11].
The hyperbolicity cone belonging to $P(x,k)$ is then given by the intersection of the single hyperbolicity cones belonding to the lower order polynomials as [Dü+18]; [RRS11]

$$C(P,k) = C_1(P_1,h) \cap \cdots \cap C_n(P_n,h).$$

Momenta for massless particles can thus be interpreted as those co-vectors lying on the boundary of the hyperbolicity cones. As an example, in metric theory it is the momenta of photons which form the boundary of the Minkowskian light cones, and $P(x,k) = g^{ab}k_a k_b = 0$ is the massless dispersion relation.

Next, it is important to establish a **duality between momenta and velocities of massless particles**. This means that it has to be possible to describe the trajectories $x(\eta)$, with η as affine parameter, of massless particles both as stationary curves of a Hamiltonian action and Lagrangian action. To enable this switching between the Hamiltonian and Lagrangian description in a well-defined way, one needs to transform between the massless momenta $k \in C_x(P,k)$ forming the boundary of the convex hyperbolicity cone, and the tangent vectors $v = \mathrm{d}x/\mathrm{d}\eta \equiv \dot{x}$. This is done via a so-called Gauss map (see [RRS11]), which is defined through a dual principal polynomial

$$P^{\#}(x,v) \coloneqq P_1^{\#}(x,v)\cdots P_n^{\#}(x,v).$$

This polynomial can also be written in terms of irreducible factors, and maps from the tangent space to the real numbers.
Now, $P^{\#}(x,v)$ exists if $P(x,k)$ is hyperbolic [RRS11] and relates to the principal polynomial $P(x,k)$ via (see also [Dü+18]; [Wol22]; [Due20])

$$P_i^{\#}\left(x, \frac{\partial P_i}{\partial k}(x,k)\right) = 0,\ \forall k \in N_i \text{ with } \frac{\partial P_i}{\partial k} \in T_xM,$$
$$\text{where } N_i \coloneqq \left\{k \in T_x^*M | P_i(x,k) = 0 \text{ and} \frac{\partial P_i}{\partial k}(x,k) \neq 0\right\}.$$

So the gradients of the principal polynomial with respect to the momenta are the roots of the dual principal polynomial. As stated previously, the repeated factors for $P(x,k)$ need to be removed to derive this dual polynomial by means of projective algebraic geometry (see [RRS11] for a detailed discussion).
If one furthermore requires for the massless case, that the dual prinicpal polynomial is hyperbolic as well, in a similar sense as already discussed for $P(x,k)$, the velocities v form the boundary of the convex dual hyperbolicity cone $v \in C_x(P^{\#},v) \subset T_xM$. Requiring that both $P(x,k)$ and the dual $P^{\#}(x,v)$ are hyperbolic is called **bi-hyperbolicity**. It implies that the prinicpal polynomial can be retrieved by the double dual $P(x) \sim P(x)^{\#\#}$. This means, as shown by [RRS11], that it becomes possible to switch back and forth between the Hamiltonian

description of the massless matter action

$$S[k, x; \rho) = \int \mathrm{d}\eta \left[k_a(\eta)\dot{x}^a(\eta) - \rho(\eta)P(x(\eta), k(\eta))\right],$$

and the according Lagrangian description

$$S[x; \mu) = \int \mathrm{d}\eta \rho(\eta) P^{\#}(x(\eta), \dot{x}(\eta)), \tag{1.2}$$

with Lagrange multiplier $\rho(\eta)$.

To summarize the previous paragraph, the bi-hyperbolicity ensures the definition of convex open hyperbolicity cones in tangent and co-tangent space, as well as a duality between them for massless modes. Now, as discussed by [RRS11]; [Dü+18]; [Wol22]; [Due20]; [Wie18] these cones are also required to define local observers in $O_x \subset T_xM$, with according worldline tangents $U \in T_xM$, who need to agree on whether a massless momentum they measure is of positive or negative energy. This is the **energy distinction** condition: There must always be a clear distinction if a massless momentum $k \in T_x^*M$ lies in the cone of positive energies $k \in O_x^+$, or in the cone of negative energies $k \in O_x^-$. The cone O_x^+ of positive massless momenta is defined as [RRS11]; [Dü+18]; [Wol22]; [Due20]; [Wie18]

$$O_x^+ := \{k \in T_x^*M | k(U) > 0 \ \forall U \in O_x\}.$$

Thus, the set of massless momenta N will disjointly decompose into a positive and negative energy part via

$$N - \{0\} = N^+ \dot{\cup} N^-, \quad \text{with } N^\pm := (\pm O_x^+).$$

If this condition is fulfilled any hyperbolicity cone $C_x(P^{\#}, U) \subset T_xM$ contains an according observer cone O_x [RRS11]; [Dü+18]; [Wol22]; [Due20]. Thus, as discussed in [RRS11]; [Dü+18]; [Wol22]; [Due20]; [Wie18], a time-orientation for this observer cone O_x can be chosen freely via a smooth vector field T hyperbolic to $P^{\#}$ with $O_x = C_x\left(P^{\#}, T\right)$.
Additionally, as mentioned by [Gie+12] this observer independent energy split of the massless modes is necessary for the according split into positive and negative energy modes during canonical quantization of matter fields, and hence for quantizability in general.

1.2.2 Observer definitions

To further define the observer frame, there are now two different approaches, involving two alternative ways to define a dual correspondence between the tangent and co-tangent space for

massive observers and particles. Their worldlines, with tangents $\dot{x} \in O_x$, and corresponding momenta $q \in C_x \subset O_x^+$ do not lie on the boundaries, but within the convex hyperbolicity cones O_x, as well as the positive energy cones $C_x \subset O_x^+$ in co-tangent space.

At first, the **observer definition** based on [RRS11] and described in detail for instance in [Dü+18]; [Wol22]; [Due20] will be summarized briefly. This observer definition is based on the postualte of a massive dispersion relation (1.3). Choosing a positive sign for the principal polynomial within the interior of the cone C_x, i.e. [Due20]

$$P(x, C_x) > 0,$$

the massive dispersion relation

$$P(x, q) = m^{\deg P} \tag{1.3}$$

is postulated with $\deg P$ as the degree of the principal polynomial. In the metric case, where $\deg P = 2$, this results in the well-known 4-momentum normalization. According to [RRS11] the dispersion relation (1.3) can be enforced via the following free-particle action

$$S_{\text{massive}}[x, q; \mu) = \int \mathrm{d}\lambda \left[q_a(\lambda)\dot{x}^a(\lambda) - \mu(\lambda) m \ln P\left(x(\lambda), m^{-1} q(\lambda)\right)\right],$$

by variation with respect to the Lagrange multiplier $\mu(\lambda)$.
Since C_x is an open convex cone, one can now perform Legendre transformations to switch from the free-particle action in x and q to a free particle action in x only. This is ensured by the Legendre map given as [RRS11]; [Dü+18]; [Due20]; [Wol22]

$$L_x : C_x \to T_x M, \quad L_x(q) = \frac{1}{\deg P} \frac{\partial \ln P}{\partial q}(x, q),$$

in components:

$$(L_x(q))_a = \frac{P^{a b_1 \cdots b_{d-1}} q_{b_1} \cdots q_{d-1}}{P(x, q)} \text{ with } d = \deg P,$$

for which an inverse exists given that the three matter conditions are implemented [RRS11]. It maps from the tangent space $L_x(C_x) \subset T_x M$ back to the co-tangent cone C_x for massive positive energy particles via

$$L_x^{-1} : L_x(C_x) \to C_x.$$

It is in general not possible to express the inverse Legendre map analytically, but in particular it can be shown to be non-polynomial in general [Wit14]. As becomes apparent from the component definition of the Legendre map L_x, one receives a vector by insertion of a co-vector,

such that the Legendre map effectively raises the indices, similarly to the inverse metric in the special case of general relativity.
With the generally non-polynomial function $P^*(x,v) \coloneqq P\left(x, L_x^{-1}(\dot{x})\right)^{-1}$ which maps the subspace $L_x(C_x) \subset T_xM$ of the tangent space to the real numbers, the Legendre transformed massive particle action is then given by [RRS11]

$$S_{\text{massive}}[x] = \int \mathrm{d}\lambda m \left(P^*\left(x(\lambda), \dot{x}(\lambda)\right)\right)^{1/\deg P}.$$

According to [RRS11], a proper time parameterization can now be chosen for a local observer with $P^*(x,\dot{x}) = 1$ along the worldline. Consequently, one can show, that the duality $\dot{x} = L_x(q/m)$ between velocity and momenta for massive particle holds. The tangent vectors of the local observer lie, as discussed in the context of the energy distinction property, within the observer cone $\dot{x} \in O_x = C_x(P^\#, T) \subset L_x\left(C_x(P,k)\right)$, where $C_x(P,k)$ is the hyperbolcity cone of positive energy momenta. Thus, it follows that the co-tangent vectors dual to the observer tangents are within the set $L_x^{-1}(O_x) \subset C_x(P,k)$. Hence, the local observer have - except for metric theory - only access to a subset of all hyperbolic co-normals to initial data hypersurfaces in general [Scha]; [Wie18]; [Wol22].

This issue can be fixed with an **alternative observer definition** according to [Sch20]; [Wie18]; [Wol22], which is summarized in the following: Instead of defining the Legendre map as the map from the co-tangent space to the tangent space via L_x one can alternatively define it vice versa from the tangent space to the co-tangent space.
Then this new Legendre map ℓ_x in the alternative observer definition is, according to [Sch20]; [Wol22]; [Wie18], given by:

$$\begin{aligned} &\ell_x : C_x(P^\#, v) \to T_x^*M, \quad \ell_x(v) = \frac{1}{\deg P^\#} \frac{\partial \ln P^\#}{\partial v}(x,v), \\ &\text{in components:} \\ &(\ell_x(v))_a = \frac{P^\#_{ab_1\cdots b_{d-1}} v^{b_1} \cdots v^{d-1}}{P^\#(x,v)} \text{ with } d = \deg P^\#. \end{aligned} \tag{1.4}$$

Here, the Legendre map ℓ_x now takes a vector and returns a co-vector, and thus effectively lowers the index, similarly to the metric in general relativity. Crucially however, ℓ_x is not the inverse of the Legendre map L_x in the observer definition by [RRS11], but an entirely different Legendre map. It is again invertible with

$$\ell_x^{-1} : \ell_x\left(C_x^\#\right) \to C_x^\#,$$

mapping from the co-tangent space back to the hyperbolicity cone $C_x^{\#} \equiv C_x\left(P^{\#}, T\right)$ in tangent space, where T denotes again the time-orientation. There is now, according to [Sch20]; [Scha]; [Wol22]; [Wie18], a conceptual advantage compared to the former observer definition: An observer cone $O_x \subset C_x^{\#}$ can be chosen, such that the set of co-tangents $q \in C_x \subset \ell_x\left(C_x^{\#}\right)$, which are dual to the tangents along the worldlines of the local observers, contains all admissible co-normals within C_x of the Cauchy hypersurfaces via

$$\ell_x\left(O_x\right) = C_x. \tag{1.5}$$

A time-like vector $U \in O_x$ can now be defined such, that its image under the Legendre map ℓ_x must lie within the hyperbolicity cone in co-tangent space. The sign of the principal polynomial in the interior of C_x is again chosen to be positive:

$$\ell_x\left(U\right) \in C_x \quad \text{with } P\left(x, C_x\right) > 0.$$

Although the choice of a suitable hyperbolicity cone for the observer becomes clearer in this alternative, new observer definition, introduced by [Sch20]; [Wie18]; [Wol22], it still lacks a massive dispersion relation, as well as a massive particle action, unlike the observer definition by [RRS11]. Even if the dispersion relation (1.3) needed to be postulated, it is still useful to have one for defining a massive particle action. This will be discussed in the following paragraph.

The construction of an according action for the alternative observer definition, as introduced by [Sch20]; [Wie18]; [Wol22], will closely follow the arguments laid out in detail in [RRS11] for the previous observer definition. A massive dispersion relation can now be imposed in a similar way via the following set-up: One may postulate, that for momenta $q \in C_x$

$$P^{*\#}\left(x, q\right) = m^{\deg P^{\#}},$$

holds for the massive dispersion relation[2], where $P^{*\#}\left(x, q\right)$ is given by

$$P^{*\#}\left(x, q\right) = P^{\#}\left(x, \ell_x^{-1}(q)\right)^{-1},$$

by inversion of (1.5). It can be confirmed, that this ansatz reproduces the massive dispersion relation in the metric case, where the dual principal polynomial has degree $\deg P^{\#} = 2$ and given by the metric.

[2]This idea was also discussed together and in accordance with [Wie].

In this case, the inverse Legendre map is just given by

$$\left(\ell_x^{-1}(q)\right)^a = \frac{g^{ab}q_b}{g^{cd}q_c q_d},$$

similarly to [Wit14] for instance. Insertion into the postulated dispersion relation yields

$$P^{*\#}(x,q) = \left(g_{ab}\left(\ell_x^{-1}(q)\right)^a\left(\ell_x^{-1}(q)\right)^b\right)^{-1} = g^{cd}q_c q_d = m^2,$$

as expected. As discussed in [RRS11] the inverse Legendre map can be defined via a fibre derivative[3] D with respect to q

$$\ell_x^{-1}(q) = -Df(q) = \frac{1}{\mathrm{deg}P^{\#}}\frac{\partial \ln P^{*\#}(x,q)}{\partial q} = \frac{1}{\mathrm{deg}P^{\#}}\frac{DP^{*\#}(x,q)}{P^{*\#}(x,q)}.$$

Here, $f(q)$ with $f_x : C_x \to \mathbb{R}$ is supposed to be - by analogy to the construction in [RRS11] - a convex function with

$$f(q) = -\frac{1}{\mathrm{deg}P^{\#}}\ln P^{*\#}(x,q),$$

such that it can mapped to a Legendre dual f_x^L. Now, using that the dual principal polynomial is homogeneous of degree $\mathrm{deg}P^{\#}$, while the inverse Legendre map is homogeneous of degree -1 [RRS11], the massive dispersion relation can be rewritten as

$$P^{*\#}\left(x, \frac{q}{m}\right) = 1.$$

An ansatz for the free massive particle action can then by given - similarly to [RRS11] - by

$$S_{\,\mathrm{massive}}\left[x,q;\lambda\right) = \int \mathrm{d}\tau q_a \dot{x}^a - \lambda(\tau)m\ln P^{*\#}\left(x, q/m\right),$$

with Lagrange multiplier λ to enforce the massive dispersion relation, and $\dot{x} \in C_x^{\#}$ is the associated velocity. In a subsequent step, this action is varied with respect to the momentum q to yield

$$\dot{x}^a(\tau) = -\lambda\frac{\partial \ln\left(P^{\#}(x,v)\right)}{\partial v^b}\frac{\partial\left(\ell_x^{-1}(q/m)\right)^b}{\partial(q/m)_a} = \lambda\,\mathrm{deg}P^{\#}\left(\ell_x^{-1}(q/m)\right)^a,$$

after some steps of calculation, where

$$v^a := \left(\ell_x^{-1}(q/m)\right)^a \in C_x^{\#}.$$

[3] For more information on this kind of construction see [RRS11] for reference.

Thus, the momenta are given by

$$q = \ell_x\left(\frac{\dot{x}}{\lambda \mathrm{deg} P^{\#}}\right),$$

what can be inserted into the massive free particle action to rewrite it as a function of x. Hence, one needs to insert the Legendre dual function $f_x^L: \ \ell_x^{-1}(C_x) = C_x^{\#} \to \mathbb{R}$ with

$$f_x^L(v) = -\ell_x(v) \cdot v - f_x\left(\ell_x(v)\right),$$

similarly to [RRS11], into the massive particle action. After a few steps omitted here this results in

$$S_{\text{massive}}[x;\lambda) = -m\mathrm{deg} P^{\#} \int \mathrm{d}\tau \left(\lambda f_x^L(\dot{x}) + \lambda \ln\left(\lambda \mathrm{deg} P^{\#}\right)\right),$$

for the action, where $f^L(\alpha v) = f^L(v) - \ln\alpha$ was used, similar to [RRS11]. Then variation with respect to λ results in

$$\lambda = -\lambda f_x^L(\dot{x}) - \lambda \ln\left(\lambda \mathrm{deg} P^{\#}\right),$$

what leads to

$$\lambda = \frac{\exp\left(-f_x^L(\dot{x}) - 1\right)}{\mathrm{deg} P^{\#}} = \frac{\exp\left(f_x\left(\ell_x(\dot{x})\right)\right)}{\mathrm{deg} P^{\#}},$$

due to the normalization $\ell_x(\dot{x})(\dot{x}) = 1$, similarly to [RRS11].
Consequently, the following free massive particle action is found:

$$\begin{aligned} S_{\text{massive}}[x] =& m \int \mathrm{d}\tau \exp\left(f_x\left(\ell_x(\dot{x})\right)\right) = m \int \mathrm{d}\tau \exp\left(-\frac{1}{\mathrm{deg} P^{\#}} \ln P^{*\#}\left(x, \ell_x(\dot{x})\right)\right) \\ =& m \int \mathrm{d}\tau \exp\left(\frac{1}{\mathrm{deg} P^{\#}} \ln P^{\#}\left(x, \ell_x^{-1}\left(\ell_x(\dot{x})\right)\right)\right) = m \int \mathrm{d}\tau \left(P^{\#}(x,\dot{x})\right)^{1/\mathrm{deg} P^{\#}}. \end{aligned} \quad (1.6)$$

The proper time parameterization is then achieved via

$$\left(P^{\#}(x,\dot{x})\right)^{1/\mathrm{deg} P^{\#}} = 1,$$

which specializes to the well-known 4-velocity normalization

$$\sqrt{g_{ab}\dot{x}^a\dot{x}^b} = 1$$

in the metric case. Thus, as expected for the metric case, the massive particle action is just given via the square root of the line-element. Since

$$P^{*\#}\left(x, \ell_x(\dot{x})\right) = P^{\#}(x,\dot{x})^{-1},$$

it becomes apparent, that

$$P^{*\#}\left(x, \ell_x\left(\dot{x}\right)\right) = P^{*\#}\left(x, q/m\right) = 1,$$

such that velocities of massive particles can be associated to their momenta via

$$\ell_x\left(\dot{x}\right) = \frac{q}{m}.$$

Similar to [RRS11] variation of $S_{\text{massive}}\left[x\right]$ with respect to x generally yields a geodesic equation, but now with Finsler function $F\left(x, \dot{x}\right) = P^{\#}\left(x, \dot{x}\right)^{1/\deg P^{\#}}$ (see [She01] for more details on Finsler geometries). The according Finsler metric is then given, similarly to [RRS11]; [Wol22], by

$$g_{m,n}\left(x, v\right) u^m w^n \coloneqq \frac{1}{2}\frac{\partial^2}{\partial s \partial t}\left(P^{\#}\left(x, v + s \cdot u + t \cdot w\right)^{2/\deg P^{\#}}\right)\Big|_{s=0, t=0},$$

with the corresponding massive point particle action

$$S_{\text{massive}}\left[x\right] = \int \mathrm{d}\tau m \sqrt{g_{mn}\left(x(\tau), \dot{x}(\tau)\right) \dot{x}^m(\tau) \dot{x}^n(\tau)}.$$

To summarize, following the steps laid out in [RRS11] it is also possible to construct a massive point particle action in the alternative observer defnition, similar to the construction for the previous observer definition. However, the caveat is that the massive dispersion relation has to be postulated again in an even less straightforward way as before.

1.3 Spacetime dynamics and gravitational closure

After having discussed in what way the spacetime kinematics is defined by the underlying matter theory under consideration, this section should summarize, particularly based on [Dü+18]; [Wol22]; [Due20]; [Wie18], how gravitational dynamics can be constructed from that. Following ideas similar to classical geometrodynamics [Kuc74]; [HKT76] the aim is to express the spacetime geometry and its dynamics in a canoncial formulation. The first step for this is to perform a 3 + 1-split of spacetime [ADW08] to describe the initial data on Cauchy hypersurfaces, and then to canoncially evolve it. The dynamics will specifically be defined by a set of algebra relations called Dirac brackets, which will also contain information about the Legendre map and thus the kinematic structure set up by the matter model. These bracket relations will form the basis of the gravitational closure equations, from which the gravity theory can then - in principle - be constructed.

1.3.1 3 + 1-split of spacetime

The first step of the program is to split spacetime into a foliation of hyperbolic spatial hypersurfaces carrying the initial data, which undergo a time-evolution from one slice to the next[4]. This is done via the following embedding of a 3-dimensonal spatial screen manifold Σ into the four dimensional spacetime manifold M via

$$X_t : \Sigma \hookrightarrow M,$$

where X_t are a one-parameter family of embedding maps. Thus, $X_t(\Sigma)$ is a hyperbolic hypersurface at some instant in time t with hyperbolic co-normal $\epsilon_0(t,\sigma)$ at each point with $\sigma \in \Sigma$ and $t \in \mathbb{R}$. An according orthonormal spacetime vector frame can then be constructed from the Legendre map ℓ_x in the alternative[5] observer definition and the pushforward of the embedding map via [Sch20]; [Wie18]; [Wol22]

$$e_0(t,\sigma) \coloneqq \ell^{-1}_{X_t(\sigma)}\left(\epsilon^0(t,\sigma)\right), \quad e_\alpha(t,\sigma) \coloneqq X_{t*}\left(\left(\frac{\partial}{\partial y^\alpha}\right)_\sigma\right),$$

$$\text{in components:} \quad e^a_0 = \left(\ell^{-1}_{X_t(\sigma)}\left(\epsilon^0(t,\sigma)\right)\right)^a, \quad e^a_\alpha = \frac{\partial X^a}{\partial y^\alpha}.$$

Here y^α denote the coordinates in a chart of the screen manifold Σ. To clarify notation one more, Latin indices will from now on, and if not stated otherwise, denote the spacetime indices, while Greek indices correspond to the spatial indices only.
Now, the basis vector e_0 corresponds to a hypersurface orthogonal vector, while e_α summarize the hypersurface tangential basis vectors. An according dual basis dual basis $\left(\epsilon^0, \epsilon^\beta\right)$ to this foliation frame $(e_0, e_\alpha) \equiv (\partial_0, \partial_\alpha)$ is defined via the relations [Dü+18]

$$\begin{aligned}
&\epsilon^\beta_a\left(e^a_\alpha\right) = \delta^\alpha_\beta, \\
&\epsilon^0_a\left(e^a_\alpha\right) = 0, \quad \text{annihilation condition,} \\
&\epsilon^0_a\left(e^a_0\right) = 1, \quad \text{normalisation condition,} \\
&\delta^a_b = \epsilon^0_b\left(e^a_0\right) + \epsilon^\alpha_b\left(e^a_\alpha\right), \quad \text{completeness relation.}
\end{aligned}$$

Using the orthonormal frame, the tangent vector $\dot{X}_t \equiv \partial_t$ of integral curves connecting $X_{t_0}(\sigma)$ with any later instance in time $X_{t_0+t'}(\sigma)$ is given by

$$\partial_t = Ne_0 + N^\alpha e_\alpha,$$

[4] This 3 + 1-split is a standard technique in general relativity as discussed for instance in [ADW08]; [Str13].
[5] The whole construction described here was initially performed using the observer definition with Legendre map L_x instead [Dü+18]; [Due20]; [Wol22]. Both constructions yield in principle the same results.

with lapse $N \coloneqq \epsilon^0(\partial_t)$ and shift $N^\alpha \coloneqq \epsilon^\alpha(\partial_t)$ (confirm [Dü+18];[Str13]). The according co-vector basis can then be shown to be given by

$$\mathrm{d}t = \frac{\epsilon^0}{N}, \ \mathrm{d}x^\alpha = -\frac{N^\alpha \epsilon^0}{N} + \epsilon^\alpha, \tag{1.7}$$

as discussed for instance in [Wol22]. Equipped with these orthonormal frames and co-frames, any tensorial quantity can now be projected onto the hypersurface by contraction with the orthonormal frame (e_0, e_α) for lower indices, or co-frame $\left(\epsilon^0, \epsilon^\alpha\right)$ for upper indices.
The projection of the dual principal polynomial onto the hypersurface is for example given by [Wol22]; [Wie18] as

$$\begin{aligned} & P^\#_{\alpha_1 \cdots \alpha_i}(t,\sigma) \coloneqq P^\#_{X_t(\sigma)}\left(e_{\alpha_1}(t,\sigma), \cdots e_{\alpha_i}(t,\sigma), e_0(t,\sigma), \cdots e_0(t,\sigma)\right), \\ \text{in components:} \quad & P^\#_{\alpha_1 \cdots \alpha_i 0 \cdots 0} = P^\#_{a_1 \cdots a_d} e^{a_1}_{\alpha_1} \cdots e^{a_i}_{\alpha_i} e^{a_{i+1}}_0 \cdots e^{a_d}_0, \end{aligned}$$

and similarly by [Due20]; [Dü+18] for the principal polynomial. Here i ranges from 0 to $d = \deg P^\#$. Using the orthonormality of the frame vectors e_α and e_0 together with the explicit expression of the Legendre map (1.4) one finds that

$$P^\#_\alpha = P^\#_{\alpha 000} = 0, \quad \text{annihilation condition,} \tag{1.8}$$

$$P^\# = P^\#_{0000} = 1, \quad \text{normalization condition,} \tag{1.9}$$

as discussed for instance in [Wie18]; [Wol22]. More examples on how the hypersurface projection works are discussed in sections 1.4 and 1.5.
The geometry induced on the hypersurface is similarly given as the according projection of the tensor field $\boldsymbol{g}^{\mathcal{A}}$ with valence set by the according spacetime geometry $G(x)$ to which the matter fields couple. Here $\mathcal{A}$ denotes an arbitrary multiindex of the induced tensor field.

1.3.2 Hypersurface dynamics

After having performed a foliation of spacetime the next step is to describe the dynamical evolution of an arbitary projected field $\boldsymbol{g}^{\mathcal{A}}$ with

$$\boldsymbol{g}\left(X_t(z), e_0\left[X_t(z)\right], e_\alpha\left[X_t(z)\right], \epsilon^0\left[X_t(z)\right], \epsilon^\alpha\left[X_t(z)\right]\right),$$

as discussed in detail in [Wol22] and summarized here. How these fields change with time, is - at least to linear order (see also [Wie18]) - encoded in the total time derivative via [Wol22]

$$\begin{aligned}\frac{\mathrm{d}}{\mathrm{d}t}\boldsymbol{g}^{\mathcal{A}}\left[X_t\right] &= \int_\Sigma \mathrm{d}^3 z \dot{X}_t(z)\frac{\delta \boldsymbol{g}^{\mathcal{A}}}{\delta X_t^a(z)} = \int_\Sigma \mathrm{d}^3 z \left(N e_0^a + N^\alpha e_\alpha^a\right)(z)\frac{\delta \boldsymbol{g}^{\mathcal{A}}}{\delta X_t^a(z)} \\ &=: \mathcal{H}\left(N\left(X_t\right)\right)\boldsymbol{g}^{\mathcal{A}}\left[X_t\right] + \mathcal{D}\left(\vec{N}\left(X_t\right)\right)\boldsymbol{g}^{\mathcal{A}}\left[X_t\right].\end{aligned}$$

Here, the functional differential operator

$$\mathcal{H}\left(N\right) \coloneqq \int_\Sigma \mathrm{d}^3 z N(z) e_0^a(t,z)\frac{\delta}{\delta X_t^a(z)}$$

encodes deformations of the field normal to the hypersurface, while

$$\mathcal{D}\left(\vec{N}\right) \coloneqq \int_\Sigma \mathrm{d}^3 z N^\alpha(z) e_\alpha^a(t,z)\frac{\delta}{\delta X_t^a(z)}$$

describes deformations tangential to the hypersurface. Additionally, as has already been shown by [HKT76] and is more generally reviewed by [Wol22] these operators can be interpreted in the following way: On the one hand, the tangential deformation corresponds to a Lie derivative of the field $\boldsymbol{g}^{\mathcal{A}}$ along the shift vector $\vec{N}$ via [Wol22]

$$\mathcal{D}\left(\vec{N}\right)\boldsymbol{g}^{\mathcal{A}}\left[X_t\right](y) = N^\mu(y)\partial_\mu \boldsymbol{g}^{\mathcal{A}}(y) - \left(\partial_\gamma N^\mu(y)\right)\boldsymbol{F}^{\mathcal{A}}{}_\mu{}^\gamma(y) = \mathcal{L}_{\vec{N}}\boldsymbol{g}^{\mathcal{A}}(y). \tag{1.10}$$

Here the so-called tangential deformation coefficient, which appears in the definition of the Lie-derivative is given by [Wol22]

$$\boldsymbol{F}^{\mathcal{A}}{}_\mu{}^\gamma(y) = e_\mu^a(y)\frac{\partial \boldsymbol{g}^{\mathcal{A}}}{\partial \partial_\gamma X^a}(y).$$

On the other hand, the normal deformation yields the abstract relation [Wol22]

$$\mathcal{H}\left(N\right)\boldsymbol{g}^{\mathcal{A}}\left[X_t\right](y) = N(y)k(y) + \left(\partial_\gamma N\right)(y)\boldsymbol{M}^{\mathcal{A}\gamma}(y). \tag{1.11}$$

Here the first term is local in the lapse $N(y)$, and the according pre-factor $k(y)$ is defined as the velocity of $\boldsymbol{g}^{\mathcal{A}}$. The second term on the right-hand side of equation (1.11) collects all contributions, which are derivatives of $N(y)$ and thus non-local in the lapse. The prefactor $\boldsymbol{M}^{\mathcal{A}\gamma}(y)$ is defined as non-local deformation coefficient with [Dü+18]

$$\boldsymbol{M}^{\mathcal{A}\gamma}(y) = e_0^a(y) \frac{\partial \boldsymbol{g}^{\mathcal{A}}}{\partial \partial_\gamma X^a}(y).$$

The normal and tangential deformation coefficient of an arbitrary projection are explicitly calculated by variation of the frame vectors, and dual frame vectors with respect to the embedding map. These variations can be derived similarly to [Wit14]; [Wol22] via the definition of the frame vector e_α in terms of the embedding map, the Legendre map (1.4), as well as the annihilation (1.8) and normalization conditions (1.9), and the completeness relation to yield

$$\begin{aligned}
\frac{\delta e_\alpha^a(y)}{\delta X^b(z)} =& -\delta_b^a \partial_\alpha \delta_y(z), \\
\frac{\delta e_0^a(y)}{\delta X^b(z)} =& -e_0^a \left(\mathrm{deg} P^\#\right)^{-1} \partial_b P^\#_{c\, j_2 \cdots j_d} e_0^c e_0^{j_2} \cdots e_0^{j_d} \delta_y(z) \\
&+ e_\alpha^a \epsilon_b^0 \left(\mathrm{deg} P^\# - 1\right)^{-1} \left(P^{\#-1}\right)^{\alpha\beta} \partial_\beta \delta_y(z), \\
\frac{\delta \epsilon_a^0(y)}{\delta X^b(z)} =& \partial_b P^\#_{a j_2 \cdots j_d} e_0^{j_2} \cdots e_0^{j_d} \delta_y(z) \\
&- \frac{\mathrm{deg} P^\# - 1}{\mathrm{deg} P^\#} \epsilon_a^0 \partial_b P^\#_{c j_2 \cdots j_d} e_0^c e_0^{j_2} \cdots e_0^{j_d} \delta_y(z) \\
&+ \epsilon_a^\alpha \epsilon_b^0 \partial_\alpha \delta_y(z), \\
\frac{\delta \epsilon_a^\alpha(y)}{\delta X^b(z)} =& \epsilon_b^\alpha \epsilon_a^\beta \partial_\beta \delta_y(z) - \epsilon_a^0 \epsilon_b^0 \left(\mathrm{deg} P^\#\right)^{-1} \left(P^{\#-1}\right)^{\alpha\beta} \partial_\beta \delta_y(z),
\end{aligned}$$

in the alternative observer definition, with delta distribution $\delta_y(z)$ and $d = \mathrm{deg} P^\#$. From these relations it can be read off, that the derivatives of the vectors and co-vectors with respect to $\partial_\gamma X^a$ are similar to the previous observer definition (see for instance [Dü+18]; [Due20]; [Wol22]). They are given by [Wie18]; [Wol22]

$$\begin{aligned}
\frac{\partial e_0^m}{\partial\left(\partial_\gamma X^a\right)} &= -\left(\mathrm{deg} P^\# - 1\right)^{-1} e_\sigma^m \epsilon_a^0 \left(P^{\#-1}\right)^{\sigma\gamma}, & \frac{\partial e_\mu^m}{\partial\left(\partial_\gamma X^a\right)} &= \delta_a^m \delta_\mu^\gamma, \\
\frac{\partial \epsilon_m^\mu}{\partial\left(\partial_\gamma X^a\right)} &= -\epsilon_a^\mu \epsilon_m^\gamma + \left(\mathrm{deg} P^\# - 1\right)^{-1} \epsilon_m^0 \epsilon_a^0 \left(P^{\#-1}\right)^{\mu\gamma}, & \frac{\partial \epsilon_m^0}{\partial\left(\partial_\gamma X^a\right)} &= -\epsilon_a^0 \epsilon_m^\gamma.
\end{aligned} \tag{1.12}$$

A very important observation is now, that the tangential and normal deformation operators $\mathcal{D}\left(\vec{N}\right)$ and $\mathcal{H}(N)$ are vector fields over the manifold of embeddings (see [HKT76] what is

further reviewed in [Dü+18]; [Due20]; [Wol22]), and thus form a commutator algebra. It can be explicitly evaluated by successive application of the operators to an arbitrary functional, where the variations of the frame fields with respect to the embedding is important in the calculation. The commutator algebra is then given by

$$[\mathcal{H}(N),\mathcal{H}(M)] = -\mathcal{D}\Big(\big(\mathrm{deg}P^{\#}-1\big)^{-1}\left(P^{\#-1}\right)^{\alpha\beta}\big(M\partial_\beta N - N\partial_\beta M\big)\,\partial_\alpha\Big), \tag{1.13}$$

$$\Big[\mathcal{D}\big(\vec{N}\big),\mathcal{H}\,(M)\Big] = -\mathcal{H}\left(\mathcal{L}_{\vec{N}}M\right), \tag{1.14}$$

$$\Big[\mathcal{D}\big(\vec{N}\big),\mathcal{D}\big(\vec{M}\big)\Big] = -\mathcal{D}\big(\mathcal{L}_{\vec{N}}\vec{M}\big), \tag{1.15}$$

as discussed in more detail in [Dü+18]; [Due20]; [Wie18] and especially [Wol22]. The commutator relations (1.13)-(1.15) are also called hypersurface deformation algebra and encode the time evolution of hypersurface functionals and fields, and thus the gravitational dynamics in the spacetime picture. Emphasis is placed on the first algebra relation (1.13), which contains the component $\left(P^{\#-1}\right)^{\alpha\beta}$ of the inverse dual polynomial on the right-hand side of the equation.

Now, as was discussed before, the kinematic information on the matter theory under consideration is encoded within the observer frames, and thus the observer definition given in terms of the Legendre map. This map in turn is given via the (dual) principal polynomial, which is defined on the spacetime geometry, whose dynamics one aims to determine in the course of this program. The kinematic information is then indirectly injected into the gravity theory via (1.13), what, however, also implies as a downside that the commutator relations form no Lie algebra [Dü+18]; [Due20]; [Wol22]. But this actually turns out to be beneficial and a technical necessity as will be addressed in the next section.

Eventually, the first two algebra relations (1.13)-(1.14) will lead to the system of gravitational closure equations from which the gravity theory can be constructed.

1.3.3 Canonical dynamics

The next step in the constructive gravity program consists of translating the evolution in spacetime to a canonical evolution on the hypersurface with initial data in phase space, as worked out by [Dü+18]; [Due20]; [Wol22] for instance. In other words, while in the spacetime picture the full geometry $G(x)$ is known at any point and any instant and the hypersurface geometry $\boldsymbol{g}^{\mathcal{A}}$ is induced from that, the canonical picture aims to construct the (generally) unknown spacetime geometry from known initial data in phase space, as also remarked in [Due20]. In this context, [Wit14]; [Dü+18]; [Wol22] introduced the following metaphor: While a physical observer would only able to determine canonical phase space data within their spatial hyper-

surface at a specific instant in time and find rules to evolve it (*human view*), they cannot simply read off all relevant information at any spacetime point and derive the according hypersurface projection from that, unlike some omniscient being (*divine view*).
Thus, as discussed in [Dü+18]; [Due20]; [Wol22] in detail, the canonical geometry $g^{\mathcal{A}}$ is now directly imposed, and has the same valence as the induced geometry $\boldsymbol{g}^{\mathcal{A}}$ in the spacetime picture. Also lapse N and shift N^{α} are introduced as independent fields on the hypersurface Σ in the canonical description. One also imposes the fields $p^{\#}_{\alpha_1\cdots\alpha_i}$ with $i = 1, \cdots \deg P^{\#}$ as canonical quantities on the hypersurface. These depend on $g^{\mathcal{A}}$ in the same way as the projected components of the principal polynomial $P^{\#}_{\alpha_1\cdots\alpha_i}$ depended on the induced geometry $\boldsymbol{g}^{\mathcal{A}}$ in the *divine view*. Symmetry conditions for $g^{\mathcal{A}}$ are then enforeced to mimic the symmetries of the induced hypersurface geometry via the linear projection [Due20]

$$g^{\mathcal{A}} = \Pi^{\mathcal{A}}_{\mathcal{B}} g^{\mathcal{B}},$$

as well as the non-linear annihilation and normalization conditions on the frame.
Due to these symmetries and the non-linear frame conditions it proves (see for instance [Dü+18]; [Due20]; [Wol22] useful and also necessary to parameterize the F geometric degrees of freedom of $g^{\mathcal{A}}$ via generalized coordinates - also called configuration fields - $\varphi^A(t, \sigma) \in \Phi$ with $A = 1, \cdots, F$ and Φ being an F-dimensional manifold[6] via the following map:

$$\hat{g}^{\mathcal{A}} : \Phi \to \mathbb{R}, \quad \text{with } g^{\mathcal{A}} \text{ invoked by } \hat{g}^{\mathcal{A}}\left(\varphi^1, \cdots, \varphi^F\right).$$

The annihilation and normalization condition can thus be enforced by [Due20]

$$p^{\#}_{\alpha}(\hat{g}(\varphi)) = 0, \quad \text{and } p(\hat{g}(\varphi)) = 1.$$

Thus, the configuration fields are constructed such, that these conditions are always fulfilled, especially under time evolution [Dü+18]; [Due20]; [Wol22].
Analogously, if the canonical geometry is built from the configuration fields, these fields can be directly re-extracted from the geometry according to the inverse map [Dü+18]; [Due20]; [Wol22]

$$\hat{\varphi}^A(\hat{g}(\varphi)) = \varphi^A.$$

[6] Strictly speaking, as discussed in [Dü+18] in more detail, the configuration fields are sections of the Φ-fibre bundle over the hypersurface Σ.

Consequently, one can define the non-constant intertwiners

$$\frac{\partial\hat{\varphi}^A}{\partial g^{\mathcal{A}}}\left(\hat{g}(\varphi)\right), \quad \text{and} \quad \frac{\partial\hat{g}^{\mathcal{A}}}{\partial\varphi^A}\left(\varphi\right),$$

between $g^{\mathcal{A}}$ and the fields φ^A. From these the relations

$$\frac{\partial\hat{\varphi}^A}{\partial g^{\mathcal{A}}}\left(\hat{g}(\varphi)\right)\frac{\partial\hat{g}^{\mathcal{A}}}{\partial\varphi^B}\left(\varphi\right) = \delta^A_B, \quad \text{and} \quad \frac{\partial\hat{g}^{\mathcal{A}}}{\partial\varphi^A}\left(\varphi\right)\frac{\partial\hat{\varphi}^A}{\partial g^{\mathcal{B}}}\left(\hat{g}(\varphi)\right) = \mathcal{T}^{\mathcal{A}}_{\mathcal{B}},$$

with projector $\mathcal{T}^{\mathcal{A}}_{\mathcal{B}}$ can be derived [Dü+18]; [Due20]; [Wol22]. The role of the intertwiner $\partial\hat{g}^{\mathcal{A}}/\partial\varphi^A$ is to map from the representation of the geometric degrees of freedom as configuration fields φ^A to the according representation as hypersurface geometry fields $\hat{g}^{\mathcal{A}}$, while $\partial\hat{\varphi}^A/\partial g^{\mathcal{A}}$ maps accordingly from the representation in terms of the hypersurface geometry $\hat{g}^{\mathcal{A}}$ to the configuration fields φ^A.

Besides the generalized coordinates φ^A one also introduces the canonically conjugate momentum densities π_A to complete the phase space, as well as the Poisson bracket given by [Due20]

$$\{F, G\} \coloneqq \int_\Sigma \mathrm{d}^3x \left(\frac{\delta F}{\delta\varphi^A(x)}\frac{\delta G}{\delta\pi_A(x)} - \frac{\delta G}{\delta\varphi^A(x)}\frac{\delta F}{\delta\pi_A(x)}\right),$$

with functionals $F\left[\varphi,\pi\right]$, $G\left[\varphi,\pi\right]$.

As mentioned by [Dü+18]; [Due20]; [Wol22] this leads to the definition of the phase space functionals

$$\hat{\mathcal{H}}\left(N\right) \coloneqq \int_\Sigma \mathrm{d}^3x\, N(x)\hat{\mathcal{H}}\left[\varphi(x),\pi(x)\right], \quad \text{and} \quad \hat{\mathcal{D}}\left(\vec{N}\right) \coloneqq \int_\Sigma \mathrm{d}^3x\, N^\alpha(x)\hat{\mathcal{D}}_\alpha\left[\varphi(x),\pi(x)\right].$$

They are constructed such, that they mimic the hypersurface deformation operators in the canonical description. It is hence required that these space functionals fulfill the following consistency relations

$$\mathcal{H}\left(N\right)\boldsymbol{g}^{\mathcal{A}} \simeq -\left\{\hat{\mathcal{H}}(N), g^{\mathcal{A}}\right\}, \tag{1.16}$$

$$\mathcal{D}\left(\vec{N}\right)\boldsymbol{g}^{\mathcal{A}} \simeq -\left\{\hat{\mathcal{D}}\left(\vec{N}\right), g^{\mathcal{A}}\right\}, \tag{1.17}$$

in a symbolic sense (see [Dü+18]; [Due20]; [Wol22] for more details), since $\boldsymbol{g}^{\mathcal{A}}$ on the left-hand sides and $g^{\mathcal{A}}$ on the right-hand sides of these equations are strictly speaking two different mathematical objects [Wol22]. However, the functional dependency of the left-hand sides of these relations on $\boldsymbol{g}^{\mathcal{A}}$ is carried over to the canonical description, and is translated into a function of the canonical fields $g^{\mathcal{A}}$ instead. Only then, it becomes possible to actually

equate the according expressions to the right-hand sides of the consistency relations [Dü+18]; [Due20]; [Wol22]. Then, the Poisson algebra

$$\left\{\hat{\mathcal{H}}(N), \hat{\mathcal{H}}(M)\right\} = \hat{\mathcal{D}}\left(\left(\deg P^{\#} - 1\right)^{-1} \left(p^{\#-1}\right)^{\alpha\beta} \left(M\partial_\beta N - N\partial_\beta M\right)\partial_\alpha\right), \tag{1.18}$$

$$\left\{\hat{\mathcal{D}}\left(\vec{N}\right), \hat{\mathcal{H}}(M)\right\} = \hat{\mathcal{H}}\left(\mathcal{L}_{\vec{N}} M\right), \tag{1.19}$$

$$\left\{\hat{\mathcal{D}}\left(\vec{N}\right), \hat{\mathcal{D}}\left(\vec{M}\right)\right\} = \hat{\mathcal{D}}\left(\mathcal{L}_{\vec{N}} \vec{M}\right), \tag{1.20}$$

needs to hold, too, to ensure consistency with the hypersurface deformation algebra relations (1.13) to (1.15). Consequently, the kinematic information encoded in the component $\left(p^{\#-1}\right)^{\alpha\beta} =: p^{\#\,\alpha\beta}$ of the input coeffcient, which mimics the inverse component $\left(P^{\#-1}\right)^{\alpha\beta}$ of the dual principal polynomial, is inserted into the gravity theory via the first Poisson algebra relation.

In the previous section it was mentioned that the hypersurface deformation algebra is not a Lie algebra because of the structure function $\left(P^{\#-1}\right)^{\alpha\beta}$ appearing in (1.13). Now, in order to represent the hypersurface deformation commutators in the *divine view* as Poisson algebra in the canonical *human view*, specific constraints on $\hat{\mathcal{H}}$ and $\hat{\mathcal{D}}$ need to be imposed, as discussed in detail in [Dü+18]; [Due20]; [Wol22]. These constraints actually provide an abstract notion of spacetime diffeomorphism invariance in the canonical picture. This - as for instance discussed in [IK85a]; [IK85b] - can be obtained by demanding path independence [Dü+18]; [Due20]; [Wol22]; [HKT76]: If an arbitrary functional F on a hypersurface $X_{t_0}(\Sigma)$ at initial time t_0 is evolved to a final hypersurface $X_{t_1}(\Sigma)$ at t_1, the according change δF must be independent of the single foliations between the initial and the final hypersurface. As discussed for instance in [HKT76]; [Dü+18]; [Wol22] this path independence also implies the following constraints for the local functionals

$$\hat{\mathcal{H}}\left[\varphi(x), \pi(x)\right] = 0, \quad \text{and } \hat{\mathcal{D}}_\alpha\left[\varphi(x), \pi(x)\right] = 0,$$

such that the total Hamiltonian density in the gravitational action

$$\begin{aligned} S_{\text{geo}} &= \int \mathrm{d}t \int_\Sigma \mathrm{d}^3x \dot{\varphi}^A(x)\pi_A(x) - \int \mathrm{d}t H\left[\varphi, \pi, N, N^\alpha\right] \\ &= \int \mathrm{d}t \int_\Sigma \mathrm{d}^3x \dot{\varphi}^A(x)\pi_A(x) - \int \mathrm{d}t \int_\Sigma \mathrm{d}^3x \left(N(x)\hat{\mathcal{H}}\left[\varphi(x), \pi(x)\right] + N^\alpha(x)\hat{\mathcal{D}}_\alpha\left[\varphi(x), \pi(x)\right]\right), \end{aligned} \tag{1.21}$$

splits up into the so-called superhamiltonian $\hat{\mathcal{H}}(x)$ and the supermomentum $\hat{\mathcal{D}}(x)$ with

$$H\left[\varphi, \pi; N, N^{\alpha}\right) = \hat{\mathcal{H}}(N) + \hat{\mathcal{D}}(\vec{N}),$$

(see for instance [Dü+18]; [Due20]; [Wol22]). The supermomentum can be determined from the consistency relation (1.17), as well as the algebra bracket (1.20). One finds from (1.17) that [Dü+18]; [Due20]; [Wol22]

$$\left(\mathcal{L}_{\vec{N}} g\right)^{\mathcal{A}}(x) = N^{\mu}\partial_{\mu} g^{\mathcal{A}} - \left(\partial_{\gamma} N^{\mu}\right) F^{\mathcal{A}}{}_{\mu}{}^{\gamma} = \frac{\partial \hat{g}^{\mathcal{A}}}{\partial \varphi^{A}} \frac{\delta \hat{\mathcal{D}}\left(\vec{N}\right)}{\delta \pi_{A}(x)}, \tag{1.22}$$

where (1.10) was inserted, however as functions of $g^{\mathcal{A}}$ instead of $\boldsymbol{g}^{\mathcal{A}}$. Thus, in the canonical description the kinematical input $F^{A}{}_{\mu}{}^{\gamma}$ representing the coeficient arising in tangential deformations is given via the Lie derivative of the configuration field along the shift as

$$\frac{\partial \hat{\varphi}^{A}}{\partial g^{\mathcal{A}}}\left(\hat{g}(\varphi)\right)\left(\mathcal{L}_{\vec{N}} \hat{g}(\varphi)\right)^{\mathcal{A}} =: N^{\mu}\partial_{\mu}\varphi^{A} - \left(\partial_{\gamma} N^{\mu}\right) F^{A}{}_{\mu}{}^{\gamma}, \tag{1.23}$$

with

$$F^{A}{}_{\mu}{}^{\gamma} := \frac{\partial \hat{\varphi}^{A}}{\partial g^{\mathcal{A}}}\left(\hat{g}(\varphi)\right) F^{\mathcal{A}}{}_{\mu}{}^{\gamma},$$

(see [Due20]; [Wol22]; [Dü+18] for a detailed discussion). Now, as stated by [Dü+18]; [Due20]; [Wol22], integration of equation (1.22) and insertion into the algebra relation (1.20) leads to the final result for supermomentum

$$\hat{\mathcal{D}}\left(\vec{N}\right) = \int_{\Sigma} \mathrm{d}^{3}x \pi_{A}(x) \frac{\partial \hat{\varphi}^{A}}{\partial g^{\mathcal{A}}}\left(\hat{g}(\varphi)\right)\left(\mathcal{L}_{\vec{N}} \hat{g}(\varphi)\right)^{\mathcal{A}}(x). \tag{1.24}$$

Next, the consistency relation (1.16) for the superhamiltonian yields, as discussed by [Dü+18]; [Due20]; [Wol22], that

$$\frac{\delta \hat{\mathcal{H}}}{\delta \pi_{A}(x)} = N(x) k^{A}(x) + \left(\partial_{\gamma} N\right)(x) \boldsymbol{M}^{A\gamma}(x), \tag{1.25}$$

via the relation (1.11) acting on $\boldsymbol{g}^{\mathcal{A}}$ with

$$k^{A}(x) = \frac{\partial \hat{\varphi}^{A}}{\partial g^{\mathcal{A}}}\left(\hat{g}(\varphi)\right) k^{\mathcal{A}}$$

as generalized velocities, collecting terms with prefactor $N(x)$ of the local part of the Hamiltonian. The according non-local deformation coefficient due to deformations normal to the

hypersurfaces is then given by [Due20]; [Wol22]; [Dü+18]

$$M^{A\gamma} \coloneqq \frac{\partial \hat{\varphi}^A}{\partial g^{\mathcal{A}}} \left(\hat{g}(\varphi)\right) e_0^a \frac{\partial \boldsymbol{g}^{\mathcal{A}}}{\partial \left(\partial_\gamma X^a\right)} = \frac{\partial \hat{\varphi}^A}{\partial g^{\mathcal{A}}} \left(\hat{g}(\varphi)\right) \boldsymbol{M}^{\mathcal{A}\gamma}. \tag{1.26}$$

Its explicit expression is derived from the definition of $\boldsymbol{g}^{\mathcal{A}}$ in terms of the frame vectors and their corresponding variations with respect to the derivatives of the hypersurface embedding map. After evaluation of all the variations, the hypersurface fields are then replaced by the canonical equivalents, which are as functions of the configuration fields φ.
As furthermore shown by [Wol22] an important observation is that the non-local normal deformation coefficient $M^{A\gamma}$ depends on higher order components of the dual prinicpal polynomial via

$$M^{A\gamma} \frac{\partial p^{\#}_{\alpha_1 \cdots \alpha_I}}{\partial \varphi^A} p^{\#}_{\epsilon\gamma} \left(\mathrm{deg} P^{\#} - 1\right) = I \left(\mathrm{deg} P^{\#} - 1\right) p^{\#}_{(\alpha_2 \cdots \alpha_I} p^{\#}_{\alpha_1)\epsilon} - \left(\mathrm{deg} P^{\#} - I\right) p^{\#}_{\alpha_1 \cdots \alpha_I \epsilon}.$$

This relation can be derived by the non-local normal deformation coefficient for arbitrary projection of the dual principal polynomial

$$\boldsymbol{M}^{\gamma}_{\alpha_1 \cdots \alpha_I} = e_0^a(x) \frac{\partial P^{\#}_{\alpha_1 \cdots \alpha_I}}{\partial \left(\partial_\gamma X^a_I\right)},$$

and then successive application of the chain rule to relate it to the coefficient $M^{A\gamma}$ [Wol22]. To conclude, since the coefficient $M^{A\gamma}$ depends on higher order projections of the principal polynomial, these will also be indirectly injected into the gravity theory.
Now, from the relation (1.25) one finds the superhamiltonian to be given by [Due20]; [Wol22]; [Dü+18]

$$\hat{\mathcal{H}}(N) = \int_\Sigma \mathrm{d}^3 x \left(\hat{\mathcal{H}}_{\mathrm{local}} \left[\varphi; \pi\right) - \partial_\gamma \left(M^{A\gamma} \pi_A\right)\right)(x), \tag{1.27}$$

with non-local part $-\partial_\gamma \left(M^{A\gamma} \pi_A\right)$ and a local part, which is related to a still to be determined Lagrangian density $\mathcal{L}$ via Legendre tranform as

$$\hat{\mathcal{H}}_{\mathrm{local}} \left[\varphi; \pi\right) = \pi_A k^A \left[\varphi; \pi\right) - \mathcal{L} \left[\varphi; k \left[\varphi; \pi\right)\right).$$

The generalized velocities k^A are given by

$$k^A \left[\varphi, \pi\right) \coloneqq \frac{\partial \hat{\mathcal{H}}_{\mathrm{local}}}{\partial \pi_A} \left[\varphi, \pi\right),$$

and the associated momenta π_A by

$$\pi_A\left[\varphi, k\right) = \frac{\partial \mathcal{L}}{\partial k^A}\left[\varphi, k\right).$$

As initially realized by [Kuc74]; [HKT76] and also applied in the constructive gravity program by [Due20]; [Wol22]; [Dü+18] this Legendre transform of the local Hamiltonian to the Lagrangian picture will simplify the evaluation of the Poisson algebra relation (1.18) a lot, since it will become linear in $\mathcal{L}$. An ansatz, originally introduced by [Kuc74] and generalized by [Due20]; [Wol22]; [Dü+18] for this Lagrange density is then given as the following expansion

$$\mathcal{L} = \sum_{N=0}^{\infty} C_{A_1 \cdots A_N}(x) k^{A_1}(x) \cdots k^{A_N}(x). \tag{1.28}$$

Here the coefficient functionals $C_{A_1 \cdots A_N}[\varphi(x)]$ will play an important role in the construction of the gravity theory and are called the output coefficients, whose solution one aims to find. Now, as discussed by [Wol22]; [Due20]; [Dü+18] evaluation of the Hamiltonian equation of motion

$$\begin{aligned}\dot{\varphi}^A(t,x) &= \left\{\varphi^A(t,x), H\left[\varphi, \pi; N, N^\alpha\right)\right\} = \\ &= \int_\Sigma \mathrm{d}^3 x \left(\left\{\varphi^A(t,x), \hat{H}\left[\varphi(t,x), \pi(t,x)\right]\right\} N(t,x) + \left\{\varphi^A(t,x), \hat{D}_\alpha\left[\varphi(t,x), \pi(t,x)\right]\right\} N^\alpha(t,x)\right),\end{aligned}$$

and insertion of the consistency relations (1.16) and (1.17) as funtions of the canonical variables will lead to an explicit expression for the generalized velocities

$$k^A = \frac{1}{N}\left(\dot{\varphi}^A - \left(\partial_\gamma N\right) M^{A\gamma} - N^\alpha \partial_\alpha \varphi^A + \left(\partial_\gamma N^\mu\right) F^A{}_\mu{}^\gamma\right). \tag{1.29}$$

As shown by [Wol22]; [Due20]; [Dü+18] insertion of the solution for the supermomentum (1.24) as well as the superhamiltonian (1.27), expressed in terms of the local and non-local contribution, and elimination of $\dot{\varphi}^A(t,x)$ by insertion of (1.29) into the gravity action (1.21) leads to the following action

$$S_{\text{geo}}\left[\varphi, \pi, N, \vec{N}\right] = \int \mathrm{d}t \int_\Sigma \mathrm{d}^3 x N(t,x)\left(\pi_A(t,x) k^A(t,x) - \hat{H}_{\text{local}}\left[\varphi(t,x); k(t,x)\right)\right).$$

Interestingly, this action only contains local terms, and the integrand is just the Legendre transformation back to the local Lagrange density (1.28). So finally the gravitational action

for a specific matter theory as input is given by [Wol22]; [Due20]; [Dü+18]

$$S_{\text{geo}}\left[\varphi, N, \vec{N}\right] = \int \mathrm{d}t \int_{\Sigma} \mathrm{d}^3x\, N(t,x)\mathcal{L}\Big[\varphi^A(t,x); \frac{1}{N(t,x)}\left(\dot{\varphi}^A - \left(\partial_\gamma N\right)(t,x) M^{A\gamma}\left(\varphi(t,x)\right)\right.$$
$$\left. -N^\alpha \partial_\alpha \varphi^A + \left(\partial_\gamma N^\mu\right) F^A{}_\mu{}^\gamma\right)\Big].$$

For the gravitational Lagrange density is only determined by the local part described by the ansatz (1.28) in terms of the output coefficients $C_{A_1\cdots A_N}$, it suffices to solve them to set up the gravity theory.

Now, the question is of course how to construct the solutions for the output coefficients in the first place. This is achieved by careful evaluation of the two Poisson algebra relations (1.18) and (1.19), which is derived in detail in [Wol22]; [Due20] for reference.

For the first algebra relation (1.19) the solutions of the supermomentum and superhamiltonian are inserted. Here, the local part is accordingly replaced by the ansatz (1.28) for the Lagrange density and the associated momenta are replaced by $\pi_A = \partial\mathcal{L}/\partial k^A$. Then, evaluation of all functional derivatives allows to rewrite the algebra relation as a functional differential equation for $\mathcal{L}$. These can then be recast into a countable set of partial differential equations for the output coefficients $C_{A_1\cdots A_N}$, where the kinematic input comes from the coefficients $p^{\#\alpha\beta}$, $M^{A\gamma}$, $F^A{}_\mu{}^\gamma$ and higher order spatial derivatives of the configuration fields $\partial^n\varphi^A$. These coefficients are thus called kinematic input coefficients. As discussed by [Wol22]; [Due20]; [Dü+18] the gravitational closure equations derived from this algebra relation lead to equations which connect output coefficients from different orders. During the evaluation of the equation [Dü+18]; [Due20]; [Wol22] receive that the output coefficients $C_{A_1\cdots A_N}$ with $N \geq 3$ depend at most on second spatial derivatives of the configuration fields, i.e. $C_{A_1\cdots A_N}\left(\varphi, \partial\varphi, \partial^2\varphi\right)$. Unfortunately, $C\left(\varphi, \partial\varphi, \cdots \partial^n\varphi\right)$, $C_A\left(\varphi, \partial\varphi, \cdots \partial^n\varphi\right)$ and $C_{AB}\left(\varphi, \partial\varphi, \cdots \partial^n\varphi\right)$ can gnerally depend on arbitrary order of spatial derivatives of the configuration field, what is sometimes referred to as the collapse problem [Dü+18]; [Due20]; [Wol22].

Similarly, the second algebra relation (1.19) is evaluated and recasted into a functional differential equation first. This equation is then rewritten into countably many partial differential equations for the output coefficients, which mainly ensure that the final gravitational Lagrange density transforms as a scalar density [Wit14]; [Wol22]. Thus, they are also called the covariance part of the closure equations.

All gravitational closure equations as derived by [Dü+18]; [Due20]; [Wol22] are summarized in an overview in the Appendix A for reference. Their solution would allow to construct the gravity action. However, for the full field the total action $S = S_{\text{geo}} + S_{\text{matter}}$ needs to be varied. How the matter action S_{matter}, with according gravitational source tensor, looks like in detail depends on the type of matter under consideration, but also on the geometry that serves as

gravitational field. One finds a generalized notion of gravitational sources for arbitrary geometries based on [GM01] for instance, which will also be summarized briefly in chapter 5. Further details and applications in cosmology can be found in preliminary works by [Due20]; [Fis17] for instance.

1.4 Example: Maxwell electrodynamics

This section summarizes how one can describe the input kinematics of the gravitational theory based on Maxwell electrodynamics as underlying matter theory, mainly following [Dü+18]; [Wie18]; [Due20]; [Wol22].
From the matter action of Maxwell electrodynamics

$$S_{\text{matter}}[A; g) = -\frac{1}{4}\int d^4x\,\sqrt{-\det g(x)}\,g^{ac}(x)g^{bd}(x)F_{ab}(x)F_{cd}(x),$$

with field strength tensor $F_{ab} = \partial_a A_b - \partial_b A_a$ the massless dispersion relation is derived from the according equations of motion by variation with respect to the matter field A_b, and subsequent reduction of gauge ambiguities, as discussed for instance in detail in [SW14]; [Due20]; [Wol22]; [Wie18]; [Dü+18]. From the equation of motion the highest order derivative term in the fields is collected (see [Due20])

$$0 = \sqrt{-\det g}\,g^{ab}g^{cd}\partial_a\partial_b A_c + O(\partial A)\,.$$

Then, a WKB-ansatz is inserted for the field amplitudes and evaluated in the limit of infinite frequencies. This leads to the well-known result, that the inverse Lorentzian metric defines the massless dispersion relation

$$0 = g^{ab}k_a k_b = P(k),$$

with wave co-vector k_a and principal polynomial $P(k)$. Accordingly, the dual prinicpal polynomial is just given in terms of the metric

$$P^{\#}(v) = g_{ab}v^a v^b,$$

with vector v^a. At the same time the metric g_{ab} is also the fundamental geometric field of the theory, determining the gravitational dynamics.
Next, a 3+1-split is performed and it is studied how the evolution of hypersurface data is driven by the canonical geometry. The induced hypersurface geometry, as well as the normalization and annihilation conditions of the principal polynomial, can be directly derived from

the metric g_{ab} as

$$\boldsymbol{g}_{\alpha\beta} = \boldsymbol{g}\left(e_\alpha, e_\beta\right), \ \boldsymbol{g}_{00} = \boldsymbol{g}_{e_0,e_0} = 1,$$
$$\boldsymbol{g}_{\alpha 0} = \boldsymbol{g}_{0\alpha} = \boldsymbol{g}\left(e_\alpha, e_0\right) = P^{\#}_{\alpha} = 0.$$

In the previous observer definition by [RRS11]; [Dü+18] the inverse metric g^{ab} is used as according hypersurface geometry. The canonical geometry $g_{\alpha\beta}(t, \sigma)$ on the hypersurface Σ_t with $\sigma \in \Sigma_t$, as well as its parameterization in terms of the configuration fields φ^A, with A running from 1 to 6 to account for the 6 degrees of freedom of the symmetric hypersurface metric $\boldsymbol{g}_{\alpha\beta}$, can be expressed as

$$\hat{g}_{\alpha\beta}(\varphi) = I_{\alpha\beta A}\varphi^A, \tag{1.30}$$

with the according constant intertwiner

$$I_{\alpha\beta A} = 1/\sqrt{2}\begin{pmatrix} \sqrt{2} & 0 & 0 & 0 & 0 & 0 \\ 0 & 1 & 0 & 0 & 0 & 0 \\ 0 & 0 & 1 & 0 & 0 & 0 \\ 0 & 1 & 0 & 0 & 0 & 0 \\ 0 & 0 & 0 & \sqrt{2} & 0 & 0 \\ 0 & 0 & 0 & 0 & 1 & 0 \\ 0 & 0 & 1 & 0 & 0 & 0 \\ 0 & 0 & 0 & 0 & 1 & 0 \\ 0 & 0 & 0 & 0 & 0 & \sqrt{2} \end{pmatrix}_{\alpha\beta A}. \tag{1.31}$$

Then, the configuration fields can be derived from the canonical geometry via the inverse map

$$\hat{\varphi}(g) = I^{A\alpha\beta} g_{\alpha\beta},$$

with constant intertwiner

$$I^{A\alpha\beta} = 1/\sqrt{2}\begin{pmatrix} \sqrt{2} & 0 & 0 & 0 & 0 & 0 & 0 & 0 & 0 \\ 0 & 1 & 0 & 1 & 0 & 0 & 0 & 0 & 0 \\ 0 & 0 & 1 & 0 & 0 & 0 & 1 & 0 & 0 \\ 0 & 0 & 0 & 0 & \sqrt{2} & 0 & 0 & 0 & 0 \\ 0 & 0 & 0 & 0 & 0 & 1 & 0 & 1 & 0 \\ 0 & 0 & 0 & 0 & 0 & 0 & 0 & 0 & \sqrt{2} \end{pmatrix}^{A\,\alpha\beta}. \tag{1.32}$$

The two intertwinig matrices are defined by the following relations

$$I^{A\alpha\beta} I_{\alpha\beta B} = \delta^A_B, \text{ and } I^{A\alpha\beta} I_{A\gamma\delta} = \delta^{\alpha}_{(\gamma} \delta^{\beta}_{\delta)}.$$

In the previous observer definition the inverse metric $g^{\alpha\beta}$ is used for the canonical geometry, but the intertwiners are chosen equally with index positions adjusted accordingly.
The kinematic input coefficient $p^{\#\,\alpha\beta}(\varphi) \coloneqq \left(p^{\#-1}\right)^{\alpha\beta}(\varphi)$ is then given by the inverse of the hypersurface metric $g_{\alpha\beta}(\varphi)$ expressed in terms of the configuration variables, while the tangential deformation coefficient $F^A{}_{\mu}{}^{\gamma}$ is defined via the Lie derivative of the metric

$$\frac{\partial \hat{\varphi}}{\partial g_{\alpha\beta}} \left(\mathcal{L}_{\vec{N}} \hat{g}(\varphi)\right)_{\alpha\beta} =: N^{\mu} \partial_{\mu} \varphi^A - \left(\partial_{\gamma} N^{\mu}\right) F^A{}_{\mu}{}^{\gamma}.$$

The $M^{A\gamma}$-coefficient identically vanishes in this case due to the annihilation condition, because

$$\begin{aligned} M^{A\gamma} &= \frac{\partial \hat{\varphi}^A}{\partial g_{\alpha\beta}} e^a_0 \frac{\partial \boldsymbol{g}_{\alpha\beta}}{\partial \left(\partial_{\gamma} X^a\right)} \\ &= I^{A\alpha\beta} e^a_0 g_{cd} \frac{\partial}{\partial \left(\partial_{\gamma} X^a\right)} \left(e^c_{\alpha} e^d_{\beta}\right) = 2 I^{A\gamma\alpha} g_{\alpha 0} = 0. \end{aligned}$$

In the previous observer definition, the input coefficients were defined with respect to the inverse field $g^{\alpha\beta}(\varphi)$, such that $p^{\alpha\beta}(\varphi) = g^{\alpha\beta}(\varphi)$, the $F^A{}_{\mu}{}^{\gamma}$-coefficient had a different sign and was transposed in μ and γ, while also there the $M^{A\gamma}$-coefficient vanished. As discussed in more detail by [Dü+18]; [Due20]; [Wol22], the vanishing $M^{A\gamma}$-coefficient is very important for the analytical solvability of the closure equations (see Appendix A) for metric geometry: On the one hand, the odd ($C_{A_1 \ldots A_{2N+1}}$ with $N \geq 0$) and even ($C_{A_0 \ldots A_{2N}}$ with $N \geq 0$) output coefficients decouple in the closure equations, what simplifies them a lot. On the other hand coefficients starting from fourth order C_{ABC} vanish identically in the gravitational Lagrangian. This can be shown by successive application of ($C16_{N\geq 2}$), as discussed for instance by [Due20]; [Wol22]. Also, it turns out that in the metric case the first construction coefficient C will depend at most on second derivatives of the configuration fields $\partial^2 \varphi^A$, i.e. $C\left(\varphi, \partial\varphi, \partial^2\varphi\right)$. This can be derived by application of ($C19_{N\geq 2}$) and the weak assumption that C should depend on some finite maximum derivative order of φ^A (see [Due20]; [Wol22]). Furthermore, as shown by [Wol22], the second output coefficient C_A, which can still depend on the derivatives of the configuration field to arbitrary order can generally be written as a bounday term $C_A\left[\varphi(x)\right] = \delta\Lambda\left[\varphi\right]/\delta\varphi^A(x)$ if the $M^{A\gamma}$-coefficient vanishes identically, and is thus dynamically irrelevant. Thus, the Lagrangian will finally only be constructed by $C\left(\varphi, \partial\varphi, \partial^2\varphi\right)$ and $C_{AB}(\varphi)$ (see for instance [Due20]).

The solution of these output coefficient via the gravitational closure program will eventually lead to the Einstein-Hilbert action in 3 + 1-form, which can then be recast again into the spacetime form

$$S_{\text{geo}} = \frac{c^4}{16\pi G} \int \mathrm{d}^4x \sqrt{-g}\,(R - 2\Lambda)\,,$$

with R as the Ricci scalar, Λ the cosmological constant and G the gravitational constant. So, by starting from a metric structure within the matter theory, one can thus construct general relativity, as demonstrated by [Dü+18]; [Due20]; [Wol22]. This confirms the previous derivation of the Einstein-Hilbert action by [HKT76] under more generalized conditions. Since the structure of the closure equations does in principle not change (see [Wol22]; [Wie18] in either observer definition, the results by [Dü+18]; [Due20]; [Wol22] still hold for the construction of general relativity in the alternative observer definition based on [Sch20]; [Wol22]; [Wie18]. In section 2 the steps laid out by [Due20] will be followed to solve the closure equations for a spherically symmetric, possibly stationary, metric spacetime using the alternative observer definition. Different solutions in either Schwarzschild coordinates, or Painlevé-Gullstrand coordinates will be constructed directly from the closure equations - without ever employing the Einstein field equations.

1.5 Example: General linear electrodynamics

General linear electrodynamics, which is described in more detail in [HO03]; [HO06]; [OR02]; [Rub02] and references therein, and also summarized in [Wit14]; [Due20]; [Wol22], is the simplest generalization of Maxwell electrodynamics. With a set of axioms, amongst them, as discussed in more detail in [HO06], conservation of magnetic fluxes and electric charges, locality and linearity one can set up a generalized theory of electrodynamics. In this theory the field strength tensors are coupled via the area-metric with

$$S_{\text{GLED}}[A; G) = -\frac{1}{8} \int d^4x\, \omega_{G^{-1}} G^{abcd} F_{ab} F_{cd}.$$

Here, $G^{abcd}(x)$ is the 4-rank (inverse) area-metric tensor, which possesses the same symmetries as the Riemann tensor, while $\omega_{G^{-1}} d^4x$ is the according volume measure in this kind of spacetime, instead of $\sqrt{-\det g} d^4x$ as for metric spacetime. The scalar density factor is defined as

$$\omega_{G^{-1}} = 24 \left(\epsilon_{abcd} G^{abcd}\right)^{-1}.$$

The area-metric is a genuine measure of area instead of length, unlike the metric. It is constructed as the linear constitutional relation between the electromagnetic fields $\boldsymbol{E}$ and $\boldsymbol{B}$ to the

excitations $\boldsymbol{D}$ and $\boldsymbol{H}$ via the spacetime geometry. This is similar to linear response theory (see [HO06] for more details), for electrodynamics in possibly anisotropic matter, where the vacuum fields couple to the field excitations via a constitutional relation as well. But since G^{abcd} is now part of the spacetime structure, this electrodynamic theory would consequenlty allow for effects like vacuum birefringence in principle. Interestingly, one can recover Maxwell electrodynamics when choosing a metric induced area-metric according to

$$G^{abcd} = \sqrt{-\det g}\left(g^{a[c}\, g^{d]b}\right)\psi + \phi\epsilon^{abcd},$$

with ψ and ϕ as scalar functions.
The principal polynomial as appropriate dispersion relation is now given by

$$P(k,k,k,k) = P^{abcd}k_a k_b k_c k_d = -\frac{1}{24}\omega^2_{G^{-1}}\epsilon_{uvpq}\epsilon_{rstu}G^{uvr(a}G^{b|ps|c}G^{d)qtu}k_a k_b k_c k_d,$$

with co-vector k_a, as for example discussed in [Rub02]; [Iti09]. The corresponding dual prinicpal polynomial is given by

$$P^{\#}(v,v,v,v) = P^{\#}_{abcd}v^a v^b v^c v^d = -\frac{1}{24}\omega^2_G\epsilon^{mnpq}\epsilon^{rstu}G_{mnr(a}G_{b|ps|c}G_{d)qtu}v^a v^b v^c v^d,$$

with vector v^a. The prinicpal tensor P^{abcd}, and dual principal tensor $P^{\#}_{abcd}$ are totally symmetric 4-rank objects, which are also referred to as Fresnel tensors.
Now, one needs to perform a 3 + 1-decomposition of this area-metric spacetime. The corresponding induced hypersurface fields can be defined similarly to [Wit14]; [Due20]; [Wol22] via the area-metric, but now with different index positions to adjust for the change of the observer definition and the Legendre map as:

$$\bar{\boldsymbol{g}}_{\alpha\beta} = -\bar{G}\left(\partial_0,\partial_\alpha,\partial_0,\partial_\beta\right) = -\bar{G}_{0\,\alpha\,0\beta}, \tag{1.33}$$

$$\bar{\bar{\boldsymbol{g}}}^{\alpha\beta} = \frac{1}{4}\frac{1}{\det\bar{\boldsymbol{g}}}\epsilon^{\alpha\mu\nu}\epsilon^{\beta\rho\sigma}\bar{G}\left(\partial_\mu,\partial_\nu,\partial_\rho,\partial_\sigma\right) = \frac{1}{4}\frac{1}{\det\bar{\boldsymbol{g}}}\epsilon^{\alpha\mu\nu}\epsilon^{\beta\rho\sigma}\bar{G}_{\mu\,\nu\,\rho\,\sigma}, \tag{1.34}$$

$$\bar{\bar{\boldsymbol{g}}}^{\alpha}_{\beta} = \frac{1}{2}\frac{1}{\sqrt{\det\bar{g}}}\epsilon^{\alpha\delta\sigma}\bar{G}\left(\partial_0,\partial_\beta,\partial_\delta,\partial_\sigma\right) - \delta^\alpha_\beta = \frac{1}{2}\frac{1}{\sqrt{\det\bar{\boldsymbol{g}}}}\epsilon^{\alpha\delta\sigma}\bar{G}_{0\,\beta\,\delta\,\sigma} - \delta^\alpha_\beta. \tag{1.35}$$

with effective hypersurface metric field $\bar{\boldsymbol{g}}_{\alpha\beta}$, and determinant $\det\bar{\boldsymbol{g}}$. The field $\bar{\bar{\boldsymbol{g}}}^{\gamma}_{\beta}$ is considered as traceless and $\bar{\bar{\boldsymbol{g}}}^{\alpha\beta}$ is given by

$$\bar{\bar{\boldsymbol{g}}}^{\alpha\beta} = \left(\bar{\boldsymbol{g}}^{-1}\right)^{\beta\gamma}\bar{\bar{\boldsymbol{g}}}^{\alpha}_{\gamma}.$$

The non-linear frame conditions lead to [Wol22]; [Due20]

$$P^{\#}_{0000} = P^{\#} = 1, \qquad \rightarrow \quad \bar{\boldsymbol{g}}_{\alpha\beta}\bar{\bar{\boldsymbol{g}}}^{\alpha\beta} = 0, \tag{1.36}$$

$$P^{\#}_{\alpha 000} = P^{\#}_{\alpha} = 0, \qquad \rightarrow \quad \bar{\bar{\boldsymbol{g}}}^{[\alpha\beta]} = 0, \tag{1.37}$$

in the new observer definition. Importantly, these hypersurface fields are just a specific choice for expressing the degrees of freedom of the area-metric as induced geometry. Different field definitions can be found as demonstrated by [Wol22]; [Due20] for example.
In the previous observer definition based on [RRS11], the hypersurface fields, as well as the annihilation and normalization condition were defined similarly, however with dualized indices [Wol22]; [Due20]; [Dü+18].

In the spacetime description (*divine view*) the induced hypersurface tensor fields $\bar{\boldsymbol{g}}_{\alpha\beta}$, $\bar{\bar{\boldsymbol{g}}}^{\alpha\beta}$ and $\bar{\bar{\boldsymbol{g}}}^{\alpha}_{\beta}$ are derived from the area-metric G as fundamental geometry. Now, one switches to the canonical description (*human view*), where the dynamics are fundamentally set by the tensor fields $\bar{g}_{\alpha\beta}(\sigma, t)$, $\bar{\bar{g}}^{\alpha\beta}(\sigma, t)$ and $\bar{\bar{g}}^{\alpha}_{\beta}(\sigma, t)$ directly defined on the hypersurface Σ_t as one-parameter families.
The non-linear constraints have to be reimposed for the canonical geometry with $\bar{g}_{\alpha\beta}\bar{\bar{g}}^{\alpha\beta} = 0$ and $\bar{\bar{g}}^{[\alpha\beta]} = 0$, and also $\bar{g}_{[\alpha\beta]} = 0$ and $\bar{\bar{g}}^{[\alpha\beta]} = 0$. As discussed by [Due20]; [Wol22]; [Dü+18] this reduces the 27 degrees of freedom of the canonical tensor fields to 17. These degrees of freedom can be expressed via $F = 17$ configuration field variables

$$\varphi \coloneqq \left(\bar{\varphi}^1, \cdots, \bar{\varphi}^6, \bar{\bar{\varphi}}^1, \cdots, \bar{\bar{\varphi}}^6, \bar{\bar{\bar{\varphi}}}^1, \cdots, \bar{\bar{\bar{\varphi}}}^5\right),$$

with F indexing the single configuration fields φ^F, which are, as shown in detail by [Due20]; [Wol22]; [Dü+18] related to the canonical hypersurface fields via the following non-linear relations

$$\hat{\bar{g}}_{\alpha\beta} = I_{\alpha\beta A}\bar{\varphi}^A, \;\; \hat{\bar{\bar{g}}}^{\alpha\beta} = I^{A\alpha\beta}\Delta_{AB}\bar{\bar{\varphi}}^B \text{ and } \hat{\bar{\bar{\bar{g}}}}^{\alpha\beta} = I^{A\alpha\beta}\left(\delta^B_A - \frac{n_A\bar{\varphi}^B}{n_C\bar{\varphi}^C}\right)\epsilon_{(m)B}\bar{\bar{\bar{\varphi}}}^m,$$

with the parameterization maps $\hat{\bar{g}}_{\alpha\beta}(\varphi)$,$\hat{\bar{\bar{g}}}^{\alpha\beta}(\varphi)$ and $\hat{\bar{\bar{\bar{g}}}}^{\alpha\beta}(\varphi)$ and captial letters A,B running from 1 to 6, and small letters m from 1 to 5 [Due20]; [Wol22]; [Dü+18]. Here Δ_{AB} denotes a 6×6 identity matrix

$$(\Delta_{AB})_{A=1,\cdots 6;B=1,\cdots 6} = \mathbb{1}_6,$$

while the constant intertwining matrices $I^{A\alpha\beta}$ and $I_{\alpha\beta A}$ are given by (1.32) and (1.31).

Demanding that the 3×3 matrix

$$\left(I^{A\alpha\beta}\Delta_{AB}t^B\right)_{\alpha=1,2,3;\beta=1,2,3}$$

is positive definite, [Due20]; [Wol22]; [Dü+18] can construct an $\mathbb{R}^6$-orthonormal basis with

$$t = \left(\frac{1}{\sqrt{3}}, 0, 0, \frac{1}{\sqrt{3}}, 0, \frac{1}{\sqrt{3}}\right),\ e^{(1)} = \left(\frac{\sqrt{2}}{\sqrt{3}}, 0, 0, -\frac{1}{\sqrt{6}}, 0, -\frac{1}{\sqrt{6}}\right),\ e^{(2)} = (0, 1, 0, 0, 0, 0)\,,$$
$$e^{(3)} = \left(0, 0, \frac{\sqrt{2}}{\sqrt{3}}, \frac{1}{\sqrt{6}}, 0, -\frac{1}{\sqrt{6}}\right),\ e^{(4)} = (0, 0, 0, 0, 1, 0)\,,\ e^{(5)} = \left(0, 0, \frac{1}{\sqrt{3}}, -\frac{1}{\sqrt{3}}, 0, \frac{1}{\sqrt{3}}\right),$$

and components t^A and $e^{(m)A}$. Accordingly, the co-vector basis required to set up the parameterization map $\overset{\hat{=}}{\hat{g}}{}^{\alpha\beta}(\varphi)$ is given in terms of the orthonormal basis as $n_A \coloneqq \Delta_{AB}t^B$ and $\epsilon_{(m)A} \coloneqq \Delta_{AB}e^{(m)B}$. As discussed by [Due20]; [Wol22]; [Dü+18], it can be confirmed, that the non-linear constraints on the canonical geometry are fulfilled with the according inverse parameterization maps $\hat{\varphi}(g)$ given as

$$\hat{\overset{\circ}{\varphi}}{}^A = I^{A\alpha\beta}\overset{\circ}{g}_{\alpha\beta},\ \hat{\overset{\circ}{\varphi}}{}^A = \Delta^{AB}I_{\alpha\beta B}\overset{\equiv}{\overset{\circ}{g}}{}^{\alpha\beta},\ \hat{\overset{\equiv}{\overset{\circ}{\varphi}}}{}^m = I_{\alpha\beta A}e^{(m)A}\overset{\equiv}{\overset{\circ}{g}}{}^{\alpha\beta}. \tag{1.38}$$

Now, one needs to find the kinematic input coefficients for the gravitational theory: First, there is $p^{\#}_{\alpha\beta}$ representing the α-β-0-0 components of the dual principal polynomial $P^{\#}_{\alpha\beta}$ expressed in terms of the canonical geometry. Then, $F^A\mu^\gamma$ as the hypersurface projection of the tangential deformation coefficient, and finally $M^{A\gamma}$ as the hypersurface projection of the non-local normal deformation need to be found. The coefficient $p^{\#}_{\alpha\beta}$ has the same structure as in [Due20]; [Wol22]; [Dü+18] with

$$p^{\#}_{\alpha\beta} = \frac{1}{6}\left(\hat{\overset{\circ}{g}}_{\alpha\gamma}\hat{\overset{\circ}{g}}_{\beta\delta}\hat{\overset{\equiv}{\overset{\circ}{g}}}{}^{\gamma\delta} - \hat{\overset{\circ}{g}}_{\alpha\beta}\hat{\overset{\circ}{g}}_{\gamma\delta}\hat{\overset{\equiv}{\overset{\circ}{g}}}{}^{\gamma\delta} - 2\hat{\overset{\circ}{g}}_{\alpha\beta}\hat{\overset{\circ}{g}}_{\gamma\nu}\hat{\overset{\equiv}{\overset{\circ}{g}}}{}^{\gamma\nu}\hat{\overset{\equiv}{\overset{\circ}{g}}}{}^{\delta\nu} + 3\hat{\overset{\circ}{g}}_{\gamma\delta}\hat{\overset{\circ}{g}}_{\alpha\mu}\hat{\overset{\equiv}{\overset{\circ}{g}}}{}^{\gamma\mu}\hat{\overset{\equiv}{\overset{\circ}{g}}}{}^{\delta\nu}\right).$$

However, it needs to be inverted accordingly to find the input coefficient [Wie18]; [Wol22]

$$p^{\#\,\alpha\beta} \coloneqq \left(p^{\#-1}\right)^{\alpha\beta},$$

what is not necessary in the previous observer definition used in [Dü+18]. The explicit shape of the other two kinetic input coefficients $F^A{}_\mu{}^\gamma$ and $M^{A\gamma}$ is similar to [Due20]; [Dü+18] when evaluating these for the dualized hypersurface fields in the alternative, new observer definition, with only small changes in their explicit shape.

For the $F^{A}_{\ \mu}{}^{\gamma}$-coefficient the Lie derivative of the canonical geometries $\bar{g}_{\alpha\beta}$, $\bar{\bar{g}}^{\alpha\beta}$ and $\bar{\bar{g}}^{\alpha}_{\beta}$ according to the general definition (1.23) leads to

$$\begin{aligned}
&\frac{\partial\hat{\varphi}}{\partial\bar{g}_{\alpha\beta}}\left(\mathcal{L}_{\vec{N}}\hat{\bar{\bar{g}}}(\varphi)\right)_{\alpha\beta} && \Rightarrow F^{\bar{A}}_{\ \mu}{}^{\gamma} = -2I^{A\gamma\sigma}I_{\mu\sigma B}\bar{\varphi}^{B},\\
&\frac{\partial\hat{\varphi}}{\partial\bar{\bar{g}}^{\alpha\beta}}\left(\mathcal{L}_{\vec{N}}\hat{\bar{\bar{g}}}(\varphi)\right)^{\alpha\beta} && \Rightarrow F^{\bar{\bar{A}}}_{\ \mu}{}^{\gamma} = 2\Delta^{AB}\Delta_{CD}I^{C\gamma\sigma}I_{\mu\sigma B}\bar{\bar{\varphi}}^{D},\\
&\frac{\partial\hat{\varphi}}{\partial\bar{\bar{g}}^{\alpha\beta}}\left(\mathcal{L}_{\vec{N}}\hat{\bar{\bar{g}}}(\varphi)\right)^{\alpha\beta} && \Rightarrow F^{\bar{\bar{m}}}_{\ \mu}{}^{\gamma} = 2I_{\mu\sigma A}\frac{\partial\hat{\bar{\bar{g}}}^{\gamma\sigma}}{\partial\bar{\bar{\varphi}}^{n}}\bar{\bar{\varphi}}^{n}e^{(m)A},
\end{aligned} \tag{1.39}$$

with

$$\frac{\partial\hat{\bar{\bar{g}}}^{\gamma\sigma}}{\partial\bar{\bar{\varphi}}^{n}} = I^{B\gamma\sigma}\left(\delta^{C}_{B} - \frac{n_{B}\bar{\varphi}^{C}}{n_{D}\bar{\varphi}^{D}}\right)\epsilon_{(n)C}.$$

Thus, the $F^{A}_{\ \mu}{}^{\gamma}$-coefficients in the new obsever definition have different signs and are transposed in μ and γ compared to the ones in the previous definition used by [Dü+18]; [Due20]. For the $M^{A\gamma}$-coefficients the general definition (1.26) is applied and the derivatives of the frame fields (1.12) are used. For the first coefficient $M^{\bar{A}\gamma}$ one then obtains the following explicit expressions after various steps of calculation omitted here:

$$\begin{aligned}
M^{\bar{A}\gamma} &= \frac{\partial\hat{\bar{\varphi}}^{A}}{\partial\bar{\boldsymbol{g}}_{\alpha\beta}}e^{a}_{0}\frac{\partial\bar{g}_{\alpha\beta}}{\partial\left(\partial_{\gamma}X^{a}\right)} = -I^{A\alpha\beta}e^{a}_{0}\frac{\partial G\left(e_{0},e_{\alpha},e_{0},e_{\beta}\right)}{\partial\left(\partial_{\gamma}X^{a}\right)}\\
&= -I^{A\alpha\beta}e^{a}_{0}G_{ebcd}\frac{\partial\left(e^{e}_{0}\,e^{b}_{\alpha}\,e^{c}_{0}\,e^{d}_{\beta}\right)}{\partial\left(\partial_{\gamma}X^{a}\right)} = \frac{2}{3}I^{A\alpha\beta}\sqrt{\det\bar{g}}I_{\alpha\delta B}\epsilon_{\varepsilon\sigma\beta}\frac{\partial\hat{\bar{\bar{g}}}^{\delta\varepsilon}}{\partial\bar{\bar{\varphi}}^{m}}p^{\#\sigma\gamma}\bar{\varphi}^{B}\bar{\bar{\varphi}}^{m}.
\end{aligned} \tag{1.40}$$

The second coefficients $M^{\bar{\bar{A}}\gamma}$ yields

$$\begin{aligned}
M^{\bar{\bar{A}}\gamma} &= \frac{\partial\hat{\bar{\bar{\varphi}}}^{A}}{\partial\bar{\bar{\boldsymbol{g}}}^{\alpha\beta}}e^{a}_{0}\frac{\partial\bar{\bar{g}}^{\alpha\beta}}{\partial\left(\partial_{\gamma}X^{a}\right)} = \Delta^{AB}I_{\alpha\beta B}e^{a}_{0}\frac{\partial\left(1/4\,(\det\bar{g})^{-1}\,\epsilon^{\alpha\mu\nu}\epsilon^{\beta\rho\sigma}G\left(e_{\mu},e_{\nu},e_{\rho},e_{\sigma}\right)\right)}{\partial\left(\partial_{\gamma}X^{a}\right)}\\
&= \Delta^{AB}I_{\alpha\beta B}e^{a}_{0}\frac{1}{4\det\bar{g}}\epsilon^{\alpha\mu\nu}\epsilon^{\beta\rho\sigma}G_{ebcd}\frac{\partial\left(\left(e^{e}_{\mu}\,e^{b}_{\nu}\,e^{c}_{\rho}\,e^{d}_{\sigma}\right)\right)}{\partial\left(\partial_{\gamma}X^{a}\right)}\\
&= 2\Delta^{AB}I_{\alpha\beta B}\,(\det\bar{g})^{-1/2}\,\epsilon^{\alpha\gamma\nu}\frac{\partial\hat{\bar{\bar{g}}}^{\beta\varepsilon}}{\partial\bar{\bar{\varphi}}^{m}}I_{\varepsilon\nu C}\bar{\bar{\varphi}}^{m}\bar{\varphi}^{C},
\end{aligned} \tag{1.41}$$

where one used that

$$e^{a}_{0}\frac{\partial\,(\det\bar{g})^{-1}}{\partial\left(\partial_{\gamma}X^{a}\right)} = 0.$$

At last the third coefficient $M^{\bar{\bar{m}}\gamma}$ is given by

$$
\begin{aligned}
M^{\bar{\bar{m}}\gamma} &= \frac{\partial \hat{\bar{\bar{\varphi}}}^m}{\partial \bar{\bar{g}}^{\alpha\beta}} e_0^a \frac{\partial \bar{\bar{\boldsymbol{g}}}^{\alpha\beta}}{\partial \left(\partial_\gamma X^a\right)} \\
&= I_{\alpha\beta A} e^{(m)A} e_0^a \frac{\partial}{\partial \left(\partial_\gamma X^a\right)} \left(\frac{1}{2\sqrt{\det \bar{g}}} \epsilon^{\alpha\delta\sigma} G\left(e_0, e_\rho, e_\delta, e_\sigma\right) \left(\bar{g}^{-1}\right)^{\rho\beta} - \left(\bar{g}^{-1}\right)^{\alpha\beta} \right) \qquad (1.42) \\
&= -I_{\alpha\beta A} e^{(m)A} \frac{p^{\#\omega\gamma}}{3} \left(\bar{g}^{-1}\right)^{\rho\beta} \sqrt{\det \bar{g}} \epsilon_{\varphi\omega\rho} \left(I_{\psi\eta B} \bar{\varphi}^B \frac{\partial \hat{\bar{\bar{g}}}^{\varphi\psi}}{\partial \bar{\bar{\varphi}}^n} \frac{\partial \hat{\bar{\bar{g}}}^{\alpha\eta}}{\partial \bar{\bar{\varphi}}^l} \bar{\bar{\varphi}}^n \bar{\bar{\varphi}}^l + \Delta_{CB} I^{C\alpha\varphi} \bar{\bar{\varphi}}^B \right).
\end{aligned}
$$

In the previous calculation it was additionally used that

$$
\frac{\partial \left(\bar{g}^{-1}\right)^{\rho\beta}}{\partial \left(\partial_\gamma X^a\right)} \bar{g}_{\beta\epsilon} = -\left(\bar{g}^{-1}\right)^{\rho\beta} \frac{\partial \bar{g}_{\beta\epsilon}}{\partial \left(\partial_\gamma X^a\right)}.
$$

In the previous observer definition based on [RRS11], and used by [Dü+18]; [Due20] the $M^{A\gamma}$-coefficients look very similar, however they all posses an overall additional prefactor 3, and the first and third coefficient are not contracted with the according coefficient $p^{\sigma\gamma}$, while the second one is.

These kinematic input coefficients (and their respective derivatives) serve as input for the gravitational closure equations. As discussed by [Dü+18]; [Wol22]; [Due20] these can, as of now, not be solved in general for the construction of the corresponding gravitational theory. However, perturbative solutions [Wol22]; [Sch+17]; [Wie18] and flat FLRW solutions for cosmology [Due20]; [Fis17] could already be derived successfully from the constructive gravity program.

2 Spherically symmetric metric spacetimes in Constructive Gravity

After having introduced the basic concepts of gravitational closure, the following chapter aims at demonstrating a toy example on how to construct a gravitational action in practice. The construction of this action is done for a spherically symmetric, stationary, metric, spacetime, thereby closely following the derivation of previous works by [Due20]; [Dü+20]; [Fis17]. There this derivativon was explicitly demonstrated for a cosmological model for the Legendre map L_x based on the observer definition introduced by [RRS11].
Although, no change of result is expected within the alternative definition of the Legendre map ℓ_x in the metric case, it still serves as a useful consistency check to show this. Also it was stated in [Due20] how one can find the Schwarzschild solution for specific coordinate assumptions, which are elaborated here in more detail. Additionally, it is shown how the Painlevé-Gullstrand solution can be derived with different coordinate assumptions.
Importantly, as discussed by [Due20], there are cases where the initial application of symmetries on the gravitational closure equation and subsequent solution of these to ultimately find the gravitational equations of motion, commutes with the construction of a general action and corresponding equations of motion, which are only evaluated on symmetries at the very end. While finding the general solution first, and only then applying symmetries is commonly much harder, the contrary can turn out to be more feasible.
The symmetries mentioned here are generally continuous and are mathematically defined via the Killing equation

$$\mathcal{L}_K G = 0,$$

which states that the Lie derivative of the geometric field G along the so-called Killing vector field K should vanish. Thus, the Killing vector fields encode continuous symmetries of the spacetime geometry.
Now, there are cases where the application of a symmetry reduction on the level of the action, from which, in turn, symmetry reduced equations of motions are derived, leads to the same result as the application of these symmetries on the general equations of motion. This is called the principle of symmetric criticality (see [FT02]), which allows to first evaluate the gravitational closure equations, similarly to [Due20]; [Dü+20]; [Fis17], on spherically symmetric, stationary configurations, and then solve them afterwards.

Coordinate choices concerning the radial parameter and the notion of staticity do, however, not follow the principle of symmetric criticality. They can only be implemented on the level of equations of motion, which will be derived for this special case in the following section. Using a point-mass as source of the gravitational field will also fix the integration constant of the vacuum Schwarzschild solution. Even though the following discussion will mainly reproduce well-known results from general relativity, it serves to demonstrate the practical use of the constructive gravity program.

2.1 Equations of motion in a spherically symmetric, stationary metric spacetime

This section deals with finding the solution for a spherically symmetric metric spacetime in the constructive gravity program. This was initially also discussed by [Due20] for the previous observer definition based on [RRS11]. Now, the derivation steps, outlined in [Dü+20]; [Due20]; [Fis17] are repeated here using the alternative observer definition by [Wie18]; [Sch20]; [Wol22] to show that both definitions lead to consistent results in the metric case as expected.
An ansatz for the metric in a spherically symmetric, stationary spacetime is generally given by

$$g = A(r)\mathrm{d}t^2 - 2B(r)\mathrm{d}t\mathrm{d}r - C(r)\mathrm{d}r^2 - D(r)\left(\mathrm{d}\theta^2 + \sin^2\theta\mathrm{d}\phi^2\right), \tag{2.1}$$

with $A(r)$, $B(r)$, $C(r)$ and $D(r)$ representing some unknown functions of r, as can be confirmed in standard literature (see [Ryd09]) for instance). This ansatz can be derived by solving the Killing equation

$$(\mathcal{L}_{K_i} g)_{ab} = K_i^c \partial_c g_{ab} + \partial_a K_i^c g_{cb} + \partial_b K_i^c g_{ac} = 0,$$

for a metric with the following Killing vector fields

$$K_1 = \sin\phi\partial_\theta + \cot\theta\cos\phi\partial_\phi,\ \ K_2 = -\cos\phi\partial_\theta + \cot\theta\sin\phi\partial_\phi,\ \ K_3 = \partial_\phi,$$

representing isotropy and

$$K_0 = \partial_t,$$

to express stationarity. This is similar to the ansatz by [Fis17]; [Due20], who considered isotropy and homogeneity for an FLRW solution.

Performing a 3 + 1-split of the metric by insertion of

$$\partial_t = Ne_0 + N^\alpha e_\alpha,$$

and $\partial_\alpha = e_\alpha$, one can thus find the corresponding hypersurface projections $h_{\alpha\beta} > 0$ of the metric and identify, which of the unknown functions correspond to the lapse $N(r)$ and the shift $N^\alpha(r)$. Since spherical symmetry leads to vanishing components $g_{\theta t} = 0$ and $g_{\phi t} = 0$, the shift components N^θ and N^ϕ are zero. Only the radial shift component needs to be considered. The 3 + 1-split of the metric is then given by [Str13]

$$\begin{aligned}
&g_{tt} = A(r) = N^2 g_{00} + N^r N^r g_{rr} = N^2 - (N^r)^2 h_{rr} = N^2 - (N^r)^2 C(r),\\
&g_{rt} = N^r g_{rr} = -N^r h_{rr} = -N^r C(r),\ \ g_{rr} = -h_{rr} = -C(r),\\
&g_{\theta\theta} = -h_{\theta\theta} = -D(r),\ \ g_{\phi\phi} = -h_{\phi\phi} = -D(r)\sin^2\theta,
\end{aligned} \tag{2.2}$$

where $g_{00} = 1$ and $g_{\alpha 0} = 0$ are used.
The configuration fields φ^A used to parameterize the hypersurface degrees of freedom in a canonical way thus become

$$\varphi^A = I^{A\alpha\beta} g_{\alpha\beta} = \left(-C(r), 0, 0, -D(r), 0 - D(r)\sin^2\theta\right)^A \tag{2.3}$$

after contraction with the intertwiner (1.32). This means, that generally φ^1, φ^4 and φ^6 do not vanish, and thus

$$g_{\alpha\beta} = \mathrm{diag}\left(\varphi^1(r), \varphi^4(r), \varphi^6(r,\theta)\right)_{\alpha\beta}.$$

For generality, this notation will be kept in the following discussion. The functions $A(r)$, $B(r)$, $C(r)$ and $D(r)$ will be reinserted, when solving the equations of motion later on.
Hence, the according kinematic input coefficients $p^{\alpha\beta} = \left(g^{-1}\right)^{\alpha\beta}$ after evaluation on symmetric configuration are given by[1]

$$p^{rr} = \frac{1}{\varphi^1(r)},\ \ p^{\theta\theta} = \frac{1}{\varphi^4(r)},\ \ p^{\phi\phi}\frac{1}{\varphi^6(r,\theta)}.$$

[1] In the observer definition applied by [Due20], where the dualized hypersurface field $g^{\alpha\beta}$ is considered, the corresponding values of $p^{\alpha\beta}$ are inverted.

The coefficient $F^{A}{}_{\mu}{}^{\gamma}$ is given[2] by

$$F^{A}{}_{\mu}{}^{\gamma} = -2\,\varphi^{1}\left(\delta^{A}_{1}\delta^{r}_{\mu}\delta^{\gamma}_{r} + \sqrt{2}\left(\delta^{A}_{2}\delta^{r}_{\mu}\delta^{\gamma}_{\theta} + \delta^{A}_{3}\delta^{r}_{\mu}\delta^{\gamma}_{\phi}\right)\right) - 2\,\varphi^{4}\left(\delta^{A}_{4}\delta^{\theta}_{\mu}\delta^{\gamma}_{\theta} + \sqrt{2}\left(\delta^{A}_{2}\delta^{\theta}_{\mu}\delta^{\gamma}_{r} + \delta^{A}_{5}\delta^{\theta}_{\mu}\delta^{\gamma}_{\phi}\right)\right)$$
$$- 2\,\varphi^{6}\left(\delta^{A}_{6}\delta^{\phi}_{\mu}\delta^{\gamma}_{\phi} + \sqrt{2}\left(\delta^{A}_{3}\delta^{\phi}_{\mu}\delta^{\gamma}_{r} + \delta^{A}_{5}\delta^{\phi}_{\mu}\delta^{\gamma}_{\theta}\right)\right),$$

and $M^{A\gamma} = 0$ identically. The non-vanishing components of the generalized velocities k^{A}, as stated in (1.29), are then given by

$$k^{1} = \frac{-N^{r}(r)\,\partial_{r}\varphi^{1}(r) - 2\,\partial_{r}N^{r}(r)\,\varphi^{1}(r)}{N(r)},\; k^{4} = \frac{-N^{r}(r)\,\partial_{r}\varphi^{4}(r)}{N(r)},\; k^{6} = \frac{-N^{r}(r)\,\partial_{r}\varphi^{6}(r)}{N(r)}. \tag{2.4}$$

With these input coefficients, the symmetry reduced closure equations are now solved by following the exact steps laid out in detail in [Due20], and sketched here. The explicit calculations are omitted here, but are performed with *Mathematica*, where the script by [Fis17] served as inspiration.

A further remark is that, as already mentioned in section 1.4, only the coefficient functions C and C_{AB} need to be evaluated explicitly to set up the gravitational Lagrangian. For terms with $C_{A_1\cdots A_N}$ with $N \geq 3$ vanish in the metric case, and C_A is only a boundary term. Additionally, the coefficient C only depends on spatial derivatives of φ up to second order.

Firstly, equation $(C8_3)$ is solved, and expressions for the non-vanishing components $C_{:A}{}^{\alpha\beta}\big|_{\text{sym}}$ are found. These are derivatives of C with respect to $\partial^2\varphi$ evaluated on spherically symmetric, stationary configurations. Accordingly, the common short hand notation

$$C_{:A}{}^{\alpha_1\cdots\alpha_n} \equiv \frac{\partial C}{\partial \varphi^{A}_{,\alpha_1\cdots\alpha_n}},$$

with

$$\varphi^{A}_{,\alpha_1\cdots\alpha_n} \equiv \frac{\partial^n \varphi^{A}}{\partial_{\alpha_1}\cdots\partial_{\alpha_n}},$$

is used from now on. With these relations, equation $(C8_2)$ can be evaluated. This leads to componentwise relations between the derivatives of C with respect to first spatial derivatives of the configuration fields, i.e. $C_{:A}{}^{\alpha}\big|_{\text{sym}}$ and the according non-vanishing components $C_{:A}{}^{\alpha\beta}\big|_{\text{sym}}$. With $(C1)$ one can then subsequently find explicit expressions for the derivatives of C with respect to the configuration fields $C_{:A}|_{\text{sym}}$, the componentwise relations $C_{:A}{}^{\alpha\beta}\big|_{\text{sym}}$ and the still unknown $C|_{\text{sym}} \equiv C^{\text{sym}}$. Next, $(C3)$ is evaluated such that the coefficients $C_{AB}|_{\text{sym}}$

[2] In the observer definition based on [RRS11] and applied by [Due20] the $F^{A}{}_{\mu}{}^{\gamma}$-coefficient looks similar, but has a different sign and is transposed in μ and γ. It is the $F^{A}{}_{\mu}{}^{\gamma}$-coefficient corresponding to the Lie derivative of the dualized field $g^{\alpha\beta}$.

can be related to $C_{:A}{}^{\alpha\beta}\big|_{\text{sym}}$. This also shows which of the explicit components $C_{AB}|_{\text{sym}}$ are independent. Six[3] independent components are obtained:

$$C_{14}|_{\text{sym}}\,,\ C_{15}|_{\text{sym}}\,,\ C_{16}|_{\text{sym}}\,,\ C_{34}|_{\text{sym}}\,,\ C_{36}|_{\text{sym}}\,,\ C_{46}|_{\text{sym}}\,.$$

Now, subsequently inserting these into the symmetry reduced equation ($C10_2$), reduces the amount of non-vanishing components of C_{AB} even more. It is shown that there is actually only one independent component $C_{14}^{\text{sym}} \equiv C_{14}|_{\text{sym}}$ for notational simplicity, similarly to what [Due20] found. One is left with

$$\begin{aligned} &C_{14}^{\text{sym}},\ C_{16}^{\text{sym}} = \frac{C_{14}^{\text{sym}}\varphi^4(r)}{\varphi^6(r,\theta)},\ C_{22}^{\text{sym}} = -C_{14}^{\text{sym}}, \\ &C_{33}^{\text{sym}} = -\frac{C_{14}^{\text{sym}}\varphi^4(r)}{\varphi^6(r,\theta)},\ C_{46}^{\text{sym}} = \frac{C_{14}^{\text{sym}}\varphi^4(r)}{\varphi^6(r,\theta)},\ C_{55}^{\text{sym}} = -\frac{C_{14}^{\text{sym}}\varphi^4(r)}{\varphi^6(r,\theta)}. \end{aligned} \tag{2.5}$$

Furthermore, ($C10_2$) establishes a relation between the single independent component C_{14}^{sym} and its derivatives with respect to the configuration fields $C_{14:C}|_{\text{sym}}$, given by the non-vanishing components

$$C_{14:1}|_{\text{sym}} = -\frac{C_{14}^{\text{sym}}}{2\,\varphi^1(r)}, \tag{2.6}$$

$$C_{14:4}|_{\text{sym}} = -\frac{C_{14}^{\text{sym}}}{2\,\varphi^4(r)}, \tag{2.7}$$

$$C_{14:6}|_{\text{sym}} = \frac{C_{14}^{\text{sym}}}{2\,\varphi^6(r,\theta)}. \tag{2.8}$$

This is - up to some prefactors - consistent with the result by [Due20].
Finally, the non-vanishing components of $C_{:A}{}^{\alpha\beta}\big|_{\text{sym}}$ can be further reduced, when reevaluating ($C3$) by using the components (2.5) expressed in terms of C_{14}^{sym}. Importantly, the non-vanshing components received in this step can all be expressed through three independent derivative components of $C_{:A}{}^{\alpha\beta}\big|_{\text{sym}}$.

[3] In the observer definition based on [RRS11] and used by [Due20] only five non-vanishing components can be found in this evaluation step.

These are given by

$$C_{:4}{}^{rr}\big|_{\text{sym}} = -4\, C_{14}^{\text{sym}}, \tag{2.9}$$

$$C_{:6}{}^{rr}\big|_{\text{sym}} = -\frac{4\, C_{14}^{\text{sym}} \varphi^4(r)}{\varphi^6(r,\theta)}, \tag{2.10}$$

$$C_{:6}{}^{\theta\theta}\big|_{\text{sym}} = -\frac{4\, C_{14}^{\text{sym}} \varphi^1(r)}{\varphi^6(r,\theta)}, \tag{2.11}$$

similar to what [Due20] receives. The results for $C_{:A}{}^{\alpha\beta}\big|_{\text{sym}}$ can now be used in $(C8_2)$ once more to futher simplify $C_{:A}{}^{\alpha}\big|_{\text{sym}}$.
In the later discussion the following components of $C_{:A}{}^{\alpha}\big|_{\text{sym}}$ are required for the solution and are thus stated here:

$$C_{:1}{}^{r}\big|_{\text{sym}} = \frac{2\, C_{14}^{\text{sym}} \left(\partial_r \varphi^4(r)\, \varphi^6(r,\theta) + \varphi^4(r)\, \partial_r \varphi^6(r,\theta)\right)}{\varphi^1(r)\varphi^6(r,\theta)}, \tag{2.12}$$

$$C_{:4}{}^{r}\big|_{\text{sym}} = -\frac{2\, C_{14}^{\text{sym}}\, \partial_r \varphi^6(r,\theta)}{\varphi^6(r,\theta)} + \frac{2\, C_{14}^{\text{sym}}\, \partial_r \varphi^1(r)}{\varphi^1(r)} + \frac{4\, C_{14}^{\text{sym}}\, \partial_r \varphi^4(r)}{\varphi^4(r)}, \tag{2.13}$$

$$C_{:6}{}^{r}\big|_{\text{sym}} = \frac{2\, C_{14}^{\text{sym}} \varphi^4(r)\, \partial_r \varphi^1(r)}{\varphi^1(r)\varphi^6(r,\theta)} - \frac{2\, C_{14}^{\text{sym}}\, \partial_r \varphi^4(r)}{\varphi^6(r,\theta)} + \frac{4\, C_{14}^{\text{sym}} \varphi^4(r)\, \partial_r \varphi^6(r,\theta)}{\varphi^6(r,\theta)^2}, \tag{2.14}$$

$$C_{:6}{}^{\theta}\big|_{\text{sym}} = \frac{4\, C_{14}^{\text{sym}} \varphi^1(r)\, \partial_\theta \varphi^6(r,\theta)}{\varphi^6(r,\theta)^2}. \tag{2.15}$$

At last, the previous findings for $C_{:A}{}^{\alpha\beta}\big|_{\text{sym}}$ and $C_{:A}{}^{\alpha}\big|_{\text{sym}}$ can in turn be inserted into $(C1)$ to find the derivatives of $C_{:A}|_{\text{sym}}$ written in terms of the coefficients C^{sym}, C_{14}^{sym}, the configuration fields and their derivatives. The derivative components $C_{:1}|_{\text{sym}}$, $C_{:2}|_{\text{sym}}$, $C_{:4}|_{\text{sym}}$ and $C_{:6}|_{\text{sym}}$ then turn out to be non-vanishing.
For the construction of the solution the following derivatives are especially important, namely

$$\begin{aligned} C_{:1}|_{\text{sym}} =& \frac{C^{\text{sym}}}{2\,\varphi^1(r)} - \frac{4\, C_{14}^{\text{sym}} \varphi^4(r)\, \partial_r \varphi^1(r)\, \partial_r \varphi^6(r,\theta)}{\varphi^1(r)^2 \varphi^6(r,\theta)} + \frac{2\, C_{14}^{\text{sym}}\, \partial_r \varphi^4(r)\, \partial_r \varphi^6(r,\theta)}{\varphi^1(r)\varphi^6(r,\theta)} \\ & - \frac{2\, C_{14}^{\text{sym}} \varphi^4(r) \left(\partial_r \varphi^6(r,\theta)\right)^2}{\varphi^1(r)\varphi^6(r,\theta)^2} - \frac{4\, C_{14}^{\text{sym}}\, \partial_r \varphi^1(r)\, \partial_r \varphi^4(r)}{\varphi^1(r)^2} - \frac{2\, C_{14}^{\text{sym}} \left(\partial_r \varphi^4(r)\right)^2}{\varphi^1(r)\varphi^4(r)} \\ & + \frac{4\, C_{14}^{\text{sym}} \partial_r^2 \varphi^4(r)}{\varphi^1(r)} + \frac{4\, C_{14}^{\text{sym}} \varphi^4(r)\, \partial_r^2 \varphi^6(r,\theta)}{\varphi^1(r)\varphi^6(r,\theta)}, \end{aligned} \tag{2.16}$$

and

$$C_{:4}|_{\mathrm{sym}} = \frac{C^{\mathrm{sym}}}{2\,\varphi^4(r)} + \frac{4\,C_{14}^{\mathrm{sym}}\varphi^1(r)\,\partial_\theta^2\varphi^6(r,\theta)}{\varphi^4(r)\varphi^6(r,\theta)} - \frac{2\,C_{14}^{\mathrm{sym}}\varphi^1(r)\left(\partial_\theta\varphi^6(r,\theta)\right)^2}{\varphi^4(r)\varphi^6(r,\theta)^2} + \frac{4\,C_{14}^{\mathrm{sym}}\,\partial_r^2\varphi^4(r)}{\varphi^4(r)} \tag{2.17}$$

$$+ \frac{2\,C_{14}^{\mathrm{sym}}\,\partial_r\varphi^4(r)\,\partial_r\varphi^6(r,\theta)}{\varphi^4(r)\varphi^6(r,\theta)} - \frac{2\,C_{14}^{\mathrm{sym}}\,\partial_r\varphi^1(r)\,\partial_r\varphi^4(r)}{\varphi^1(r)\varphi^4(r)} - \frac{4\,C_{14}^{\mathrm{sym}}\left(\partial_r\varphi^4(r)\right)^2}{\varphi^4(r)^2}, \tag{2.18}$$

$$C_{:6}|_{\mathrm{sym}} = \frac{C^{\mathrm{sym}}}{2\,\varphi^6(r,\theta)} - \frac{2\,C_{14}^{\mathrm{sym}}\varphi^4(r)\,\partial_r\varphi^1(r)\,\partial_r\varphi^6(r,\theta)}{\varphi^1(r)\varphi^6(r,\theta)^2} - \frac{4\,C_{14}^{\mathrm{sym}}\varphi^1(r)\left(\partial_\theta\varphi^6(r,\theta)\right)^2}{\varphi^6(r,\theta)^3}$$
$$+ \frac{4\,C_{14}^{\mathrm{sym}}\varphi^1(r)\partial_\theta^2\varphi^6(r,\theta)}{\varphi^6(r,\theta)^2} + \frac{2\,C_{14}^{\mathrm{sym}}\,\partial_r\varphi^4(r)\,\partial_r\varphi^6(r,\theta)}{\varphi^6(r,\theta)^2} + \frac{4\,C_{14}^{\mathrm{sym}}\varphi^4(r)\,\partial_r^2\varphi^6(r,\theta)}{\varphi^6(r,\theta)^2}$$
$$- \frac{4\,C_{14}^{\mathrm{sym}}\varphi^4(r)\left(\partial_r\varphi^6(r,\theta)\right)^2}{\varphi^6(r,\theta)^3}. \tag{2.19}$$

Next, the equations (2.6) to (2.8) are direclty solved to find the solution for C_{14}^{sym}, and due to (2.5) also for C_{16}^{sym} and for C_{46}^{sym}, which are relevant for the construction.
This leads to

$$C_{14}^{\mathrm{sym}} = \kappa\frac{\sqrt{-\varphi^1(r)\,\varphi^4(r)\,\varphi^6(r,\theta)}}{\varphi^1(r)\,\varphi^4(r)}, \tag{2.20}$$

where κ is an integration constant. Now, as in the derivation of [Due20] one can read off from the chain rule equations

$$\frac{\partial C^{\mathrm{sym}}}{\partial r} = C_{:1}|_{\mathrm{sym}}\,\partial_r\varphi^1(r) + C_{:4}|_{\mathrm{sym}}\,\partial_r\varphi^4(r) + C_{:6}|_{\mathrm{sym}}\,\partial_r\varphi^6(r,\theta) + C_{:1}{}^{r}\big|_{\mathrm{sym}}\,\partial_r^2\varphi^1(r)$$
$$+ C_{:4}{}^{r}\big|_{\mathrm{sym}}\,\partial_r^2\varphi^4(r) + C_{:6}{}^{r}\big|_{\mathrm{sym}}\,\partial_r^2\varphi^6(r,\theta) + C_{:6}{}^{\theta}\big|_{\mathrm{sym}}\,\partial_r\partial_\theta\varphi^6(r,\theta)$$
$$+ C_{:4}{}^{rr}\big|_{\mathrm{sym}}\,\partial_r^3\varphi^4(r) + C_{:6}{}^{rr}\big|_{\mathrm{sym}}\,\partial_r^3\varphi^6(r,\theta) + C_{:6}{}^{\theta\theta}\big|_{\mathrm{sym}}\,\partial_\theta^2\partial_r\varphi^6(r,\theta),$$

and

$$\frac{\partial C^{\mathrm{sym}}}{\partial \theta} = C_{:6}|_{\mathrm{sym}}\,\partial_\theta\varphi^6(r,\theta) + C_{:6}{}^{\theta}\big|_{\mathrm{sym}}\,\partial_\theta^2\varphi^6(r,\theta) + C_{:6}{}^{\theta\theta}\big|_{\mathrm{sym}}\,\partial_\theta^3\varphi^6(r,\theta),$$

which components of $C_{:A}{}^{\alpha\beta}\big|_{\mathrm{sym}}$, $C_{:A}{}^{\alpha}\big|_{\mathrm{sym}}$ and $C_{:A}|_{\mathrm{sym}}$ are required to construct the solution for C. Then, successive integration of equations (2.9)-(2.11) leads to explicit solutions for the components $C_{:A}{}^{\alpha\beta}\big|_{\mathrm{sym}}$, while integration of equations (2.12)-(2.15) solves $C_{:A}{}^{\alpha}\big|_{\mathrm{sym}}$ and finally from the equations (2.16)-(2.19) the solution for $C_{:A}|_{\mathrm{sym}}$ is found, similarly to [Due20]. Consequently, the C coefficient in the alternative observer definition, as introduced by [Wie18];

[Sch20]; [Wol22], becomes

$$C^{\mathrm{sym}} = 4\kappa\sqrt{-\varphi^1(r)\,\varphi^4(r)\,\varphi^6(r,\theta)}\Bigg(-\frac{\partial_r^2\varphi^4(r)}{\varphi^1(r)\varphi^4(r)} - \frac{\partial_r^2\varphi^6(r,\theta)}{\varphi^1(r)\varphi^6(r,\theta)} - \frac{\partial_\theta^2\varphi^6(r,\theta)}{\varphi^4(r)\varphi^6(r,\theta)} + \frac{1}{2}\frac{\partial_r\varphi^4(r)\,\partial_r\varphi^1(r)}{\varphi^1(r)^2\varphi^4(r)} + \frac{1}{2}\frac{\partial_r\varphi^6(r,\theta)\,\partial_r\varphi^1(r)}{\varphi^1(r)^2\varphi^6(r,\theta)} + \frac{1}{2}\frac{\left(\partial_r\varphi^4(r)\right)^2}{\varphi^1(r)\varphi^4(r)^2} - \frac{1}{2}\frac{\partial_r\varphi^6(r,\theta)\,\partial_r\varphi^4(r)}{\varphi^1(r)\varphi^4(r)\varphi^6(r,\theta)} + \frac{1}{2}\frac{\left(\partial_r\varphi^6(r,\theta)\right)^2}{\varphi^1(r)\varphi^6(r,\theta)^2} + \frac{1}{2}\frac{\left(\partial_\theta\varphi^6(r,\theta)\right)^2}{\varphi^4(r)\varphi^6(r,\theta)^2} + \frac{1}{4}\lambda\Bigg), \tag{2.21}$$

where λ is a further integration constant. The gravitational action for a spherically symmetric, stationary spacetime, is then generally given by

$$S_{\mathrm{geo}} = \int \mathrm{d}t \int \mathrm{d}^3x \left(NC^{\mathrm{sym}} + 2N\left(C_{14}^{\mathrm{sym}}k^1k^4 + C_{16}^{\mathrm{sym}}k^1k^6 + C_{46}^{\mathrm{sym}}k^4k^6\right)\right), \tag{2.22}$$

with C^{sym} as given in (2.21), C_{14}^{sym} as given in (2.20) and finally the generalized velocities k^1, k^4 and k^6 according to (2.4).

A consistency check, where the configuration fields φ^A are replaced by $1/\varphi^A$ in the action, then yields the same result as [Due20] found for the observer definition based on [RRS11]. The author [Due20] constructed the solution for the dualized hypersurface field $g^{\alpha\beta}$, instead of $g_{\alpha\beta}$, and studied them for cosmological symmetries.

Finally, the integration constants are fixed to

$$\kappa = \frac{1}{64\pi G},\ \lambda = 8\Lambda.$$

Now inserting the unknown functions $C(r)$ and $D(r)$ as in (2.3) for the configuration fields results in the following action for the geometry, and thus gravity:

$$S_{\mathrm{geo}} = \int \mathrm{d}t \int \mathrm{d}^3x \left(-\frac{\sin(\theta)N(r)\,\partial_r D(r)\,\partial_r C(r)}{16\pi G C(r)^{3/2}} + \frac{\sin(\theta)N^r(r)^2\partial_r D(r)\,\partial_r C(r)}{16\pi G\sqrt{C(r)}N(r)} - \frac{\sin(\theta)N(r)\left(\partial_r D(r)\right)^2}{32\pi G D(r)\sqrt{C(r)}} + \frac{\sin(\theta)\sqrt{C(r)}N^r(r)\,\partial_r D(r)\,\partial_r N^r(r)}{8\pi G N(r)} + \frac{\sin(\theta)\sqrt{C(r)}N^r(r)^2\left(\partial_r D(r)\right)^2}{32\pi G D(r)N(r)} + \frac{\sin(\theta)N(r)\partial_r^2 D(r)}{8\pi G\sqrt{C(r)}} + \frac{\Lambda\sin(\theta)D(r)\sqrt{C(r)}N(r)}{8\pi G} - \frac{\sin(\theta)\sqrt{C(r)}N(r)}{8\pi G}\right).$$

Finally, the equations of motion are derived by variation of the total actions $S = S_{\mathrm{geo}} + S_{\mathrm{matter}}$ with respect to shift $N^r(r')$, lapse $N(r')$ (constraint equations) and the two unknown functions

$C(r')$, $D(r')$, such that

$$\frac{\delta S_{\text{geo}}}{\delta N(r')} = -\frac{\delta S_{\text{matter}}}{\delta N(r')}, \frac{\delta S_{\text{geo}}}{\delta N^r(r')} = -\frac{\delta S_{\text{matter}}}{\delta N^r(r')}, \frac{\delta S_{\text{geo}}}{\delta C(r')} = -\frac{\delta S_{\text{matter}}}{\delta C(r')}, \frac{\delta S_{\text{geom}}}{\delta D(r')} = -\frac{\delta S_{\text{matter}}}{\delta D(r')}, \tag{2.23}$$

and setting $r' = r$ after variation. Naturally, the right-hand sides of these equations are zero for vacuum solutions. The detailed expressions for the geometric parts of the equations of motion are omitted here, but can be explicitly evaluated with *Mathematica*. They have a very involved and coupled structure, such that one can not solve them straightforwardly, as already mentioned by [Due20]. They possess, however, all possible solutions for a spherically symmetric, stationary spacetime, which can be extracted for specific coordinate choices in the next sections. There, the equations of motion for the matter part will be specified, too.

2.2 Solutions in spherically symmetric, metric spacetimes

After having obtained general equations of motion for a spherically symmetric spacetime, these will be evaluated for specific coordinate choices in the following section. Special focus lies on the Schwarzschild coordinates, as well as the Painlevé-Gullstrand coordinates. Furthermore, the Reissner-Nordström solution will be considered, and the Birkhoff Theorem will be confirmed for the metric case from the constructed equations of motion. While this will confirm standard results from general relativity, the Einstein field equations in their usual form are not used here.

2.2.1 Metric Schwarzschild spacetimes

At first, the Schwarzschild solution is derived from the previously constructed equations of motion. As already remarked by [Due20], this is only possible by setting $N^r = 0$ and $D(r) = r^2$ and thus gauge fixing[4], i.e. choosing specific coordinates. Since this does not fulfill symmetric criticality, one can only impose the conditions for the equations of motion, and not on the level of the action and thus the closure equations (see also [FT02]).
It is important to understand, how the specific choices of coordinates can be imposed as well-defined conditions to be generalized to area-metric spacetimes later on. This generalization must be independent of the corresponding physical interpretation in metric spacetime, which might not hold anymore, or in a different way for other spacetime structures.
First of all, by setting $D(r) = r^2$, the radial coordinate r is chosen in such a way, that the

[4]The necessity of choosing a specific gauge was also discussed in [Wit14].

submanifold defined by the angular part of the line element (2.1) corresponds to

$$\mathrm{d}s^2_{\mathrm{ang}} = g_{\mathrm{sub},\alpha\beta}\mathrm{d}x^\alpha \mathrm{d}x^\beta = r^2\left(\mathrm{d}\theta^2 + \sin^2\theta \mathrm{d}\phi^2\right),$$

of the sphere (see [Str13]). The infinitesimal area-element, given as metric volume element with

$$\mathrm{d}A = \sqrt{\det g_{\mathrm{sub}}}\,\mathrm{d}\theta\,\mathrm{d}\phi = r^2\sin\theta\,\mathrm{d}\theta\,\mathrm{d}\phi,$$

thus defines the radial parameter r, such that these areas on the θ-ϕ submanifold scale with r^2. However, r is not a radial distance in the euclidean sense. How this choice for the parameter r can be generalized to area-metric spacetime is discussed in section 3.1.
Choosing $N^r = 0$ is related to a notion of staticity of spacetime - at least in the metric case - as discussed for instance in [Ryd09]; [Wal84]; [Str13]; [Bar19b]).
However, it can naturally also be understood by requiring hypersurface orthogonality of the timelike Killing vector field K which enforces stationarity: One demands that the corresponding co-vector $\omega = K^\flat$ of this Killing vector fulfills the so-called **Frobenius condition**

$$\omega \wedge \mathrm{d}\omega = 0,$$

such that the spatial hypersurfaces with $t = \text{const}$ are integrable. Then the corresponding time-coordinate can be written as exact differential $\mathrm{d}t$. A brief summary of the definition of the Frobenius condition is given in Appendix B.
As discussed in detail in [Str13] for instance, staticity corresponds to a discrete time-reflection symmetry $t \to -t$ in the metric case. Thus, one finds that $g_{rt} = 0$, and hence $N^r = 0$ due to the 3 + 1-decomposition of the metric. This in turn implies the fulfillment of the Frobenius condition as shown by [Str13].
On the other hand, if one starts with the Frobenius condition it can be shown, that it is always possible to find a coordinate system where the shift N^r vanishes, i.e. hypersurface orthogonality is established. Then the off-diagonal element of the metric g_{rt} vanishes in this specific coordinate system, what is generally interpreted as staticity.
The according proof for these statements is given for instance by [Str13] and the steps of the proof are applied and further interpreted in section 3.3 for the area-metric case.
The equations of motion (2.23) are now evaluated for these coordinate choices. One finds that

$$\left.\frac{\delta S_{\mathrm{geo}}}{\delta N(r)}\right|_{N^r=0,D=r^2} = -\frac{r\sin(\theta)\,\partial_r C(r)}{8\pi G C(r)^{3/2}} + \frac{\Lambda r^2\sin(\theta)\sqrt{C(r)}}{8\pi G} - \frac{\sin(\theta)\sqrt{C(r)}}{8\pi G} + \frac{\sin(\theta)}{8\pi G\sqrt{C(r)}} = 0, \tag{2.24}$$

and

$$\left.\frac{\delta S_{\text{geo}}}{\delta N^r(r)}\right|_{N^r=0,D=r^2} = 0, \tag{2.25}$$

$$\left.\frac{\delta S_{\text{geo}}}{\delta C(r)}\right|_{N^r=0,D=r^2} = \frac{r\sin(\theta)\,\partial_r N(r)}{8\pi G C(r)^{3/2}} + \frac{\Lambda r^2 \sin(\theta) N(r)}{16\pi G\sqrt{C(r)}} + \frac{\sin(\theta)N(r)}{16\pi G C(r)^{3/2}} - \frac{\sin(\theta)N(r)}{16\pi G\sqrt{C(r)}}, \tag{2.26}$$

$$\left.\frac{\delta S_{\text{geo}}}{\delta D(r)}\right|_{N^r=0,D=r^2} = -\frac{\sin(\theta)\,\partial_r C(r)\,\partial_r N(r)}{16\pi G C(r)^{3/2}} - \frac{\sin(\theta)N(r)\,\partial_r C(r)}{16\pi G r C(r)^{3/2}} + \frac{\sin(\theta)\,\partial_r N(r)}{8\pi G r\sqrt{C(r)}} = 0,$$

$$+ \frac{\sin(\theta)\,\partial_r^2 N(r)}{8\pi G\sqrt{C(r)}} + \frac{\Lambda\sin(\theta)\sqrt{C(r)}\,N(r)}{8\pi G} = 0, \tag{2.27}$$

for vacuum solutions, i.e. if the total action is given by the gravitational action only, such that its variation gives zero. In total this leads to the following solutions:

- Solving (2.24) results in
$$C(r) = \left(1 - \frac{r^2\Lambda}{3} + \frac{K}{r}\right)^{-1}. \tag{2.28}$$
Here, K is an integration constant, which still needs to be fixed.

- Equation (2.25) is fulfilled identically.

- Equation (2.26) leads to
$$N(r) = \sqrt{1 - \frac{r^2\Lambda}{3} + \frac{K}{r}},$$
for the lapse function, given (2.28) is fulfilled.

- At last (2.27) is identically fulfilled when inserting the solutions for $C(r)$ and $N(r)$.

Now, the integration constant K can be fixed by the following simplified assumption, that the source of the gravitational field is given by a point mass [5]. Similarly to [Ale20a], one hereby considers an energy-momentum tensor with $T^0_0 = \rho = M\delta^3(\boldsymbol{r} - \boldsymbol{r}_0)$.
A variation of the matter action S_{matter} with respect to the degrees of freedom $N(r)$, $N^r(r)$, $C(r)$ and $D(r)$ is then performed. Afterwards, these need to be related to the according variations of the gravitational action. With the definition of the gravitational source tensor S^{ab}, i.e. the Hilbert-stress-energy momentum tensor in the metric case, the variation of the matter action is generally given by

$$\delta S_{\text{matter}} = \frac{\sqrt{-\det g}}{2} S^{ab}\delta g_{ab} = \frac{\sqrt{-\det g}}{2} T^a_c g^{cb}\delta g_{ab}.$$

[5] For an extended mass the solution outside of this mass would be equivalent to the point mass solution.

In the metric case the energy-momentum tensor and the source tensor are related via $T^0_0 = g_{00}S^{00} \equiv T^{00}$. Thus, since $g_{00} = 1$ and $g_{0\alpha} = 0$, it follows that $T^{00} = M\delta^3(\boldsymbol{r} - \boldsymbol{r}_0)$. All other components of the source tensor vanish in the foliation frame. Similar to [Gou07] this corresponds to the pressureless source tensor of an ideal fluid, comoving with the flow generated the by timelike hypersurface normal vector field e_0

$$T^{ab} = \rho u^a u^b = \rho u^0 u^0 = M\delta^3(\boldsymbol{r} - \boldsymbol{r}_0).$$

Here, the energy density ρ is given in terms of $\rho = M\delta^3(\boldsymbol{r} - \boldsymbol{r}_0)$ and 4-velocity of the point mass $\boldsymbol{u} = e_0$ with $u^0 = 1$, such that the point-mass is at rest in the spatial hypersurface in the 0-α-frame.
Now, the according right-hand sides of the equations of motion (2.23) generally become:

$$\frac{\delta S_{\text{matter}}}{\delta N} = \frac{\delta S_{\text{matter}}}{\delta g_{ab}}\frac{\partial g_{ab}}{\partial N} = \frac{\sqrt{-\det g}}{2}T^a_c g^{cb}\frac{\partial g_{ab}}{\partial N} = \frac{\sqrt{-\det g}}{2}\left(T^{tt}\frac{\partial g_{tt}}{\partial N} + 2T^{tr}\frac{\partial g_{tr}}{\partial N} + T^{\alpha\beta}\frac{\partial g_{\alpha\beta}}{\partial N}\right) \tag{2.29}$$

$$= \frac{\sqrt{-\det g}}{2}T^{tt}2N = \sqrt{-\det g}\frac{T^{00}}{N} = \sin\theta\sqrt{C(r)}D(r)M\delta^3(\boldsymbol{r} - \boldsymbol{r}_0), \tag{2.30}$$

where the 3 + 1-split of the spherically symmetric, stationary metric in (2.2) was inserted. Furthermore, the following 3 + 1-decompositions for the source tensor can be given in terms of the dual basis $\left(\epsilon^0, \epsilon^\beta\right)$ as

$$\begin{aligned}
T^{tt} =& T(\mathrm{d}t, \mathrm{d}t) = T^{ab}\epsilon^0_a\epsilon^0_b\frac{1}{N^2} = T^{00}\frac{1}{N^2},\\
T^{t\alpha} =& T(\mathrm{d}t, \mathrm{d}x^\alpha) = T^{ab}\epsilon^0_a\left(-N^\alpha\frac{\epsilon^0_b}{N} + \epsilon^\alpha_b\right) = -T^{00}\frac{N^\alpha}{N^2} + \frac{T^{0\alpha}}{N},\\
T^{\alpha\beta} =& T\left(\mathrm{d}x^\alpha, \mathrm{d}x^\beta\right) = T^{ab}\left(-N^\alpha\frac{\epsilon^0_a}{N} + \epsilon^\alpha_a\right)\left(-N^\alpha\frac{\epsilon^0_b}{N} + \epsilon^\beta_b\right) = \frac{N^\alpha N^\beta}{N^2}T^{00} - 2\frac{N^\alpha}{N}T^{0\beta} + T\left(\epsilon^\alpha, \epsilon^\beta\right),
\end{aligned} \tag{2.31}$$

by insertion of the co-frame (1.7). This frame simplifies here, since $N^\alpha = N^r$, $T^{0\alpha} = 0$ and $T\left(\epsilon^\alpha, \epsilon^\beta\right) = 0$.
Likewise, one finds

$$\begin{aligned}
\frac{\delta S_{\text{matter}}}{\delta N^r(r)} &= \frac{1}{2}\sqrt{C(r)}D(r)N\sin\theta\left(T^{tt}\frac{\partial g_{tt}}{\partial N^r} + 2T^{tr}\frac{\partial g_{tr}}{\partial N^r} + T^{rr}\frac{\partial g_{rr}}{\partial N^r}\right)\\
&= \frac{1}{2}\sqrt{C(r)}D(r)N\sin\theta\left(T^{00}\frac{1}{N^2}(-C(r)2N^r) + 2(-C(r))\frac{-T^{00}N^r}{N^2}\right) = 0,
\end{aligned} \tag{2.32}$$

as well as,

$$\begin{aligned}\frac{\delta S_{\text{matter}}}{\delta C(r)} &= \frac{1}{2}\sqrt{C(r)}D(r)N\sin\theta\left(T^{tt}\frac{\partial g_{tt}}{\partial C(r)} + 2T^{tr}\frac{\partial g_{tr}}{\partial C(r)} + T^{rr}\frac{\partial g_{rr}}{\partial C(r)}\right)\\ &= \frac{1}{2}\sqrt{C(r)}D(r)N\sin\theta\left(-T^{00}\frac{(N^r)^2}{N^2} + 2\frac{-T^{00}N^r}{N^2}(-N^r) - \frac{(N^r)^2}{N^2}T^{00}\right) = 0, \qquad (2.33)\end{aligned}$$

and finally

$$\frac{\delta S_{\text{matter}}}{\delta D(r)} = 0. \qquad (2.34)$$

Furthermore, solving

$$\begin{aligned}&\frac{\delta S_{\text{geo}}}{\delta N(r)}\bigg|_{N^r=0,D=r^2} = -\frac{\delta S_{\text{matter}}}{\delta N}\bigg|_{N^r=0,D=r^2},\\ \Rightarrow\ &-\frac{r\sin(\theta)\,\partial_r C(r)}{8\pi G C(r)^{3/2}} + \frac{\Lambda r^2\sin(\theta)\sqrt{C(r)}}{8\pi G} - \frac{\sin(\theta)\sqrt{C(r)}}{8\pi G} + \frac{\sin(\theta)}{8\pi G\sqrt{C(r)}}\\ &= -\sin\theta\sqrt{C(r)}r^2 M\frac{\delta(r)\delta(\theta)\delta(\phi)}{r^2\sin^2\theta},\\ \Rightarrow\ &-M\delta(r)\,\delta(\theta)\,\delta(\phi) = \frac{\sin\theta}{8\pi G C(r)} - \frac{\sin\theta}{8\pi G} + \frac{r^2\Lambda\sin\theta}{8\pi G} - \frac{r\sin\theta\,\partial_r C(r)}{8\pi G C(r)^2},\end{aligned}$$

with $\delta^3(\boldsymbol{r}-\boldsymbol{r}_0) = \delta(r)\,\delta(\theta)\,\delta(\phi)/(r^2\sin^2\theta)$ in spherical (polar) coordinates fixes the integration constant K for the Schwarzschild coordinates.
Now, an integration around the point mass, inspired by [NO12], within the intervall $r \in (-R, R)$, $\phi \in [0, \pi)$ and $\theta \in [0, \phi)$, in spherical polar coordinates [AW05] is performed. Using that outside the point mass, i.e. for $r \neq 0$, $|R| > r$, the solution for $C(r)$ is given by

$$C(r) = \left(1 - \frac{|r|^2\Lambda}{3} + \frac{K}{|r|}\right)^{-1},$$

one thus finds

$$\begin{aligned}&\int_{-R}^{R}\mathrm{d}r\int_0^{\pi}\mathrm{d}\phi\int_0^{\pi}\mathrm{d}\theta\,8\pi GM\delta(r)\,\delta(\theta)\,\delta(\phi) = \int_{-R}^{R}\mathrm{d}r\int_0^{\pi}\mathrm{d}\phi\int_0^{\pi}\mathrm{d}\theta\left(-\sin\theta\partial_r\left(\frac{r}{C(r)}\right) - \sin\theta\left(r^2\Lambda - 1\right)\right),\\ &\Rightarrow\ 8\pi GM = -2\pi\frac{r}{C(r)}\bigg|_{-R}^{R} - 2\pi\left(\frac{r^3\Lambda}{3} - r\right)\bigg|_{-R}^{R},\\ &\Rightarrow\ K = -2GM.\end{aligned}$$

This is exactly the integration constant required for the metric Schwarzschild (de-Sitter) so-

lution. The difference to the conventional derivation of this solution in standard books on general relativity (see for instance [Ryd09]; [Str13]) is, that one did not employ the Newtonian limit solution here to derive the integration constant, but instead fixed it by sourcing the gravitational field direclty with a point mass. This method is always useful whenever the weak field limit is not necessarily known, for instance for non-metric theories.

Reissner-Nordström Solution

As a consistency check one can also derive the Reissner-Nordstroem solution for a charged black hole via the equations of motion derived from gravitational closure. Variation of the Maxwell action with respect to the geometry consequenlty leads to the source tensor T^{ab}_{em} of the electromagnetic field as standard result (see [Str13]) with

$$T^{ab}_{\text{em}} = \frac{1}{4\pi}\left(F^{bd}F^{ac}g_{cd} - \frac{1}{4}g^{ab}F^{mn}F_{mn}\right).$$

For a point charge q this leads to

$$F_{0r} = -\frac{q}{r^2},\ F^{0r} = -\frac{q}{r^2}\frac{1}{N^2C(r)},$$

such that the equations of motion for the matter part - also including the point mass (pm), as was discussed before - evaluated on the Schwarzschild parameterization become

$$\begin{aligned}\left.\frac{\delta S_{\text{matter, em}}}{\delta N}\right|_{N^r=0,D=r^2} + \left.\frac{\delta S_{\text{matter, pm}}}{\delta N}\right|_{N^r=0,D=r^2} &= \left.\frac{1}{2}\sqrt{-\det g}T^{ab}_{\text{em}}\frac{\partial g_{ab}}{\partial N}\right|_{N^r=0,D=r^2} + \left.\frac{\delta S_{\text{matter, pm}}}{\delta N}\right|_{N^r=0,D=r^2} \\ &= -\frac{\sin\theta}{8\pi}\frac{q^2}{N^2r^2}\frac{1}{\sqrt{C(r)}} + \left.\frac{\delta S_{\text{matter, pm}}}{\delta N}\right|_{N^r=0,D=r^2},\end{aligned}$$

and similarly, omitting the detailed steps

$$\begin{aligned}\left.\frac{\delta S_{\text{matter, em}}}{\delta N^r}\right|_{N^r=0,D=r^2} &= 0, \\ \left.\frac{\delta S_{\text{matter, em}}}{\delta C(r)}\right|_{N^r=0,D=r^2} &= -\frac{1}{2}\sin\theta\frac{q^2}{8\pi r^2N}\left(C(r)\right)^{-3/2}, \\ \left.\frac{\delta S_{\text{matter, em}}}{\delta D(r)}\right|_{N^r=0,D=r^2} &= \frac{1}{8\pi}\frac{q^2}{r^4}\sin\theta\frac{1}{N\sqrt{C(r)}}.\end{aligned}$$

Thus, using the equations of motion for $r \neq 0$ with

$$-\left.\frac{\delta S_{\text{matter, em}}}{\delta N}\right|_{N^r=0,D=r^2} = \left.\frac{\delta S_{\text{geo}}}{\delta N}\right|_{N^r=0,D=r^2}\ (I), \quad -\left.\frac{\delta S_{\text{matter, em}}}{\delta C(r)}\right|_{N^r=0,D=r^2} = \left.\frac{\delta S_{\text{geo}}}{\delta C(r)}\right|_{N^r=0,D=r^2}\ (II),$$

and relating the corresponding expressions by subracting (II) from (I), one finds that the lapse is given by

$$N^2 = \frac{K_2}{C(r)}.$$

Here K_2 is a further integration constant, which can be set to 1. With this relation between lapse and $C(r)$ the equation

$$-\left.\frac{\delta S_{\text{matter, em}}}{\delta N}\right|_{N^r=0,D=r^2} = \left.\frac{\delta S_{\text{geo}}}{\delta N}\right|_{N^r=0,D=r^2},$$

can be solved outside the point source to find the following result:

$$C(r) = \left(1 - \frac{\Lambda r^2}{3} + \frac{K}{r} - \frac{Gq}{r^2}\right)^{-1}.$$

Then, the integration constant K can be fixed again by integrating around the point mass in spherical polar coordinates, as discussed previously. Again, this leads to $K = -2GM$, as expected for the Reisser-Nordström solution. Finally, it can be confirmed by explicitly inserting this solutions that

$$-\left.\frac{\delta S_{\text{matter, em}}}{\delta D(r)}\right|_{N^r=0,D=r^2} = \left.\frac{\delta S_{\text{geo}}}{\delta D(r)}\right|_{N^r=0,D=r^2},$$

is fulfilled identically.

Birkhoff Theorem

If stationarity as symmetry condition is not demanded in in the first place, an explicit time-dependence in the spherically symmetric metric is left. However, it is a well-known fact (see for instance [Ryd09]) that even in this case one can still find an explicit parameterisation, where this time-dependence can be absorbed within the time-parameter t' of the metric. It only needs to be ensured that $\mathrm{d}t'$ can be written as perfect differential in a specific coordinate system, such that the Frobenius condition, and thus hypersurface orthogonality for this time-parameter holds. The Schwarzschild solution, i.e. a spherically symmetric, stationary and static spacetime for vacuum, can then be recovered. This is the so-called Birkhoff Theorem (see also [Str13] for more details).

This theorem can also be derived easily from the gravitational action constructed in (2.22), with only the slight change, that the configuration fields $\varphi^1, \cdots, \varphi^6$, and thus the unkown functions $C(r,t)$ and $D(r,t)$, as well as the shift $N^r(r,t)$ and the lapse $N(r,t)$ may now also explicitly depend on the time parameter t. Furthermore, the generalized velocities, which

need to be inserted into the action, are now given by

$$
\begin{aligned}
k^1 &= \partial_t \varphi^1(r,t) - \frac{N^r(r,t)\,\partial_r \varphi^1(r,t) - 2\,\partial_r N^r(r,t)\,\varphi^1(r,t)}{N(r,t)}, \\
k^4 &= \partial_t \varphi^4(r,t) - \frac{N^r(r,t)\,\partial_r \varphi^4(r,t)}{N(r,t)}, \\
k^6 &= \partial_t \varphi^6(r,t) - \frac{N^r(r,t)\,\partial_r \varphi^6(r,t)}{N(r,t)}.
\end{aligned}
$$

Variation of the corresponding action with respect to the unknown functions $C(r,t)$, $D(r,t)$, $N^r(r,t)$ and $N(r,t)$ is a tedious task which can however be performed with *Mathematica*. The resulting equations of motion in vacuum

$$
\frac{\delta S_{\text{geo}}}{\delta N(r,t)} = 0,\ \frac{\delta S_{\text{geo}}}{\delta N^r(r,t)} = 0,\ \frac{\delta S_{\text{geo}}}{\delta C(r,t)} = 0,\ \frac{\delta S_{\text{geom}}}{\delta D(r,t)} = 0,
$$

are have a very involved structure, and are thus omitted here. But they can again be simplified enourmously by fixing the gauge via $N^r(r,t) = 0$ and $D(r,t) = r^2$. This leads to the following equations of motion

$$
\begin{aligned}
\left.\frac{\delta S_{\text{geo}}}{\delta N(r,t)}\right|_{N^r=0,D=r^2} =& -\frac{r\sin(\theta)\,\partial_r C(r,t)}{8\pi G C(r,t)^{3/2}} + \frac{\Lambda r^2 \sin(\theta)\sqrt{C(r,t)}}{8\pi G} - \frac{\sin(\theta)\sqrt{C(r,t)}}{8\pi G} \\
&+ \frac{\sin(\theta)}{8\pi G\sqrt{C(r,t)}} = 0, \qquad (2.35) \\
\left.\frac{\delta S_{\text{geo}}}{\delta N^r(r,t)}\right|_{N^r=0,D=r^2} =& -\frac{r\sin(\theta)\,\partial_t C(r,t)}{8\pi G\sqrt{C(r,t)}N(r,t)} = 0, \qquad (2.36)
\end{aligned}
$$

$$
\begin{aligned}
\left.\frac{\delta S_{\text{geo}}}{\delta C(r,t)}\right|_{N^r=0,D=r^2} =& \frac{r\sin(\theta)\,\partial_r N(r,t)}{8\pi G C(r,t)^{3/2}} + \frac{\Lambda r^2 \sin(\theta) N(r,t)}{16\pi G\sqrt{C(r,t)}} + \frac{\sin(\theta)N(r,t)}{16\pi G C(r,t)^{3/2}} \\
&- \frac{\sin(\theta)N(r,t)}{16\pi G\sqrt{C(r,t)}} = 0, \qquad (2.37) \\
\left.\frac{\delta S_{\text{geo}}}{\delta D(r,t)}\right|_{N^r=0,D=r^2} =& \frac{\sin(\theta)\,\partial_t C(r,t)\,\partial_t N(r,t)}{16\pi G\sqrt{C(r,t)}N(r,t)^2} - \frac{\sin(\theta)\,\partial_r C(r,t)\,\partial_r N(r,t)}{16\pi G C(r,t)^{3/2}} + \frac{\sin(\theta)\,(\partial_t C(r,t))^2}{32\pi G C(r,t)^{3/2}N(r,t)} \\
&- \frac{\sin(\theta)\,\partial_r C(r,t)\,N(r,t)}{16\pi G r C(r,t)^{3/2}} - \frac{\sin(\theta)\partial_t^2 C(r,t)}{16\pi G\sqrt{C(r,t)}N(r,t)} + \frac{\sin(\theta)\partial_r N(r,t)}{8\pi G r\sqrt{C(r,t)}} \\
&+ \frac{\sin(\theta)\partial_r^2 N(r,t)}{8\pi G\sqrt{C(r,t)}} + \frac{\Lambda\sin(\theta)\sqrt{C(r,t)}N(r,t)}{8\pi G} = 0. \qquad (2.38)
\end{aligned}
$$

From (2.36) it can be read-off, that the explicit time-dependence of $C(r,t) = C(r)$ vanishes. Thus, one can solve (2.35) to receive

$$C(r) = \left(1 - \frac{r^2\Lambda}{3} + \frac{K}{r}\right)^{-1},$$

as for the time-independent case (2.28) with integration constant K. With this result (2.37) can in turn be solved, what leads to

$$N(r,t) = f(t)\sqrt{1 - \frac{r^2\Lambda}{3} + \frac{K}{r}},$$

where $f(t)$ is some unknown function of t. Finally, with the given solutions for $C(r)$ and $N(r,t)$ equation (2.38) is identically fulfilled. At last, the integration constant is again fixed to $K = -2GM$, as previously discussed for the time-independent case. Thus, for the final metric g outside the mass distribution one receives

$$g = f(t)^2\left(1 - \frac{r^2\Lambda}{3} - \frac{2GM}{r}\right)\mathrm{d}t^2 - \left(1 - \frac{r^2\Lambda}{3} - \frac{2GM}{r}\right)^{-1}\mathrm{d}r^2 - r^2\left(\mathrm{d}\theta^2 + \sin^2\theta\mathrm{d}\phi^2\right),$$

where the time-parameter can now be replaced by $t' = \int f(t)\mathrm{d}t$ to absorb the unknown function (see for instance [Ryd09]). This takes us back to the stationary case, what confirms the Birkhoff theorem for a metric spacetime structure.

2.2.2 Painlevé-Gullstrand solution

Next, using the general equations of motion (2.23) it is shown how to derive different types of solutions for spherically, symmetric spacetimes, like the solution in Painlevé-Gullstrand coordinates. In the metric case these are chosen such that the spatial hypersurfaces are flat (see for instance [Bla20]) in the sense that

$$g = \left(N^2 - (N^r)^2\right)\mathrm{d}t^2 - 2N^r\mathrm{d}t\mathrm{d}r - \mathrm{d}r^2 - r^2\left(\mathrm{d}\theta^2 + \sin^2\theta\mathrm{d}\phi^2\right),$$

and all spacetime curvature effects are encoded in the lapse N and the shift N^r instead.
Evaluated on $C(r) = 1$ and $D(r) = r^2$ the variations of the gravity-part of the action then become

$$\left.\frac{\delta S_{\text{geo}}}{\delta N(r)}\right|_{C=1,D=r^2} = -\frac{r\sin(\theta)N^r(r)\,\partial_r N^r(r)}{4\pi G N(r)^2} - \frac{\sin(\theta)N^r(r)^2}{8\pi G N(r)^2} + \frac{\Lambda r^2\sin(\theta)}{8\pi G} = 0, \tag{2.39}$$

and

$$\left.\frac{\delta S_{\text{geo}}}{\delta N^r(r)}\right|_{C=1,D=r^2} = \frac{r\sin(\theta)N^r(r)\,\partial_r N(r)}{4\pi G N(r)^2} = 0, \tag{2.40}$$

$$\begin{aligned}\left.\frac{\delta S_{\text{geo}}}{\delta C(r)}\right|_{C=1,D=r^2} =& \frac{r\sin(\theta)\,\partial_r N(r)}{8\pi G} + \frac{r\sin(\theta)N^r(r)^2\,\partial_r N(r)}{8\pi G N(r)^2} + \frac{\Lambda r^2\sin(\theta)N(r)}{16\pi G} \\ &- \frac{r\sin(\theta)N^r(r)\,\partial_r N^r(r)}{8\pi G N(r)} - \frac{\sin(\theta)N^r(r)^2}{16\pi G N(r)} = 0,\end{aligned} \tag{2.41}$$

$$\begin{aligned}\left.\frac{\delta S_{\text{geo}}}{\delta D(r)}\right|_{C=1,D=r^2} =& \frac{\sin(\theta)\,\partial_r N(r)}{8\pi G r} + \frac{\sin(\theta)\partial_r^2 N(r)}{8\pi G} + \frac{\sin(\theta)N^r(r)\,\partial_r N(r)\,\partial_r N^r(r)}{8\pi G N(r)^2} \\ &+ \frac{\Lambda\sin(\theta)N(r)}{8\pi G} - \frac{\sin(\theta)N^r(r)\,\partial_r N^r(r)}{4\pi G r N(r)} - \frac{\sin(\theta)\,(\partial_r N^r(r))^2}{8\pi G N(r)} \\ &+ \frac{\sin(\theta)N^r(r)^2\partial_r N(r)}{8\pi G r N(r)^2} - \frac{\sin(\theta)N^r(r)\partial_r^2 N^r(r)}{8\pi G N(r)} = 0,\end{aligned} \tag{2.42}$$

outside of the source. From equation (2.40) it can now be read off, that the lapse should be contant in r, i.e. $N(r) = \text{const.}$, what simplifies the other three equations significantly.
Now, by choosing $N(r) = 1$ in the following, equation(2.39) can be solved for the shift to yield

$$N^r(r) = \sqrt{\frac{K}{r} + \frac{r^2\Lambda}{3}}.$$

With these solutions for the lapse and the shift the equations (2.41) and (2.42) are fulfilled identically. Similarly to the Schwarzschild case, one can now fix the integration constant K by sourcing the gravitational field with a point mass according to $T^{00} = M\delta^3(\boldsymbol{r} - \boldsymbol{r}_0)$ in the $\left(\epsilon^0, \epsilon^\beta\right)$-frame.
The variations of S_{matter} with respect to the degrees of freedom $N(r)$, $N^r(r)$, $C(r)$ and $D(r)$ are then in general again given by (2.30), (2.32), (2.33), (2.34), and need to be evaluated on the Painlevé-Gullstrand parameterization. While the latter three variations are trivial and the equations of motion (2.40)-(2.42) are consequently fulfilled identically,

$$\left.\frac{\delta S_{\text{geo}}}{\delta N(r)}\right|_{C=1,D=r^2} = -\left.\frac{\delta S_{\text{matter}}}{\delta N(r)}\right|_{C=1,D=r^2}$$

yields a condition to fix the integration constant K. The corresponding result is given by

$$\begin{aligned}&-\frac{r\sin(\theta)N^r(r)\partial_r N^r(r)}{4\pi G} - \frac{\sin(\theta)N^r(r)^2}{8\pi G} + \frac{\Lambda r^2\sin(\theta)}{8\pi G} = -\sin\theta r^2 M\delta(r)\delta(\theta)\delta(\phi)/(r^2\sin^2\theta), \\ \Rightarrow &M\delta(r)\delta(\theta)\delta(\phi = -\frac{\partial_r\left(r\,(N^r)^2\right)\sin\theta}{8\pi G} + \frac{r^2\Lambda\sin\theta}{8\pi G}.\end{aligned}$$

This can then be solved by integrating around the source mass in spherical polar coordinates with $r \in (-R, R)$, $\phi \in [0, \pi)$ and $\theta \in [0, \phi)$. When performing the integration, one uses that for $r \neq 0$ the solution of the shift in these coordinates can be written as

$$N^r(r) = \sqrt{\frac{K}{|r|} + \frac{r^2\Lambda}{3}}.$$

The parameter r is again replaced by the absolute value $|r|$ in the solution $N^r(r)$, since the scope of the spherical polar coordinates also allows for negative values of r, which then needs to be compensated.
Consequently, the integration constant becomes $K = 2GM$, such that the full metric can be written as

$$g = \left(1 - \frac{2GM}{r^2} - \frac{r^2\Lambda}{3}\right)\mathrm{d}t^2 - 2\sqrt{\frac{2GM}{r^2} + \frac{r^2\Lambda}{3}}\mathrm{d}t\mathrm{d}r - \mathrm{d}r^2 - r^2\left(\mathrm{d}\theta^2 + \sin^2\theta\mathrm{d}\phi^2\right),$$

as expected for the Painlevé-Gullstrand coordinates. Interestingly, they have the common interpretation (see also [Bla20]) of spacetime flowing towards the point mass. Though only in these coordinates the source tensor of the point mass itself - besides the energy density term T^{tt} - also containts momentum densities T^{tr} and pressure terms T^{rr}, as can be seen by (2.31) due to the non-vanishing shift. Thus, the interpretation of the dynamics in these specific coordinates is the following: Spacetime flows towards the point-mass along some specific shift field, but this point-mass also needs to - in a sense - flow with the same rate and direction to ensure overall stationarity.

2.3 Summary

To summarize, it was shown in this chapter how to construct the equations of motion for a spherically symmetric, possibly stationary spacetime sourced by a point mass. The corresponding equations of motion have a coupled structure. That makes it hard to solve them explicitly, without choosing specific coordinates or gauges, which are not connected to Killing symmetries. It was possible to confirm the Schwarzschild solution, Reissner-Nordström solution, as well as the Birkhoff theorem in a metric spacetime with the constructed gravity action, and also the Painlevé-Gullstrand solution in a different parameterization. As a further example one might have also considered isotropic coordinates (see [Ryd09]), however the solution principle stays the same.
These findings are, of course, not surprising, since these are standard results in general relativity, which itself can also be more generally derived with gravitational closure (see [Dü+18];

[Due20]; [Wol22]). The objective of this whole discussion was to understand how it is possible to derive Schwarzschild-type solutions for non-metric spacetime geometries, and how to generalize specific coordinate choices in these cases. This will, however, prove to be a challenge already for area-metric spacetimes, as discussed in the next chapter.

3 Spherically symmetric area-metric spacetimes

In this section it will be discussed how the Killing symmetries of a spherically symmetric, stationary area-metric spacetime will result in the according symmetry reduced kinematic input-coefficients for the gravitational closure equations. The overarching goal of this discussion would be to eventually use these coefficients as input to solve the gravitational closure equations for a spherically symmetric, stationary area-metric case. This is, however, highly non-trivial, and is open to further research. It is also elaborated, how the hypersurface orthogonality condition is described in an area-metric setting, and it will be clarifed what staticity in the sense of a discrete time-reflection symmetry means in this case. Furthermore, it is shown, how a spherically symmetric, stationary area-metric spacetime can in general posses birefringence, what recapitulates the former result by [PWS09]; [SWW10]. Finally, it will also be discussed which challenges one faces when trying to solve the gravitational closure equations for this case. These challenges are - so far - obstructive to find a solution in the general case.

3.1 Symmetry reduction and kinematic set-up

The first step in the symmetry reduction is - similar to [Due20]; [Fis17] - to solve the Killing equations for a spherically symmmetric, stationary area-metric spacetime via:

$$(\mathcal{L}_{K_i} G)_{abcd} = 0 \qquad \text{for } i = 0, \dots, 3\,. \tag{3.1}$$

It is important to note that imposing stationarity and spherical symmetry as symmetry conditions is mathematically well-defined due to application of the Killing condition. Hence, this ansatz can be generalized from the metric to the area-metric case. It will mainly reproduce the ansatz for spherical symmetry already worked out by [PWS09]; [SWW10].
Here $K_0 = \partial_t$ must be timelike in the sense that its respective co-vector shall be in the interior of the hyperbolicity cone,

$$\ell(K_0) \in C, \tag{3.2}$$

where the interior needs to be of constant sign. Though this sign can be chosen arbitrarily by appropriate rescaling as discussed in [Dü+18] one chooses

$$P(x, C_x) > 0,$$

here, as in [Dü+18]. The spatial Killing vector fields implying spherical symmetry are then again given by

$$\begin{aligned} K_1 &= \sin\phi\partial_\theta + \cot\theta\cos\phi\partial_\phi, \\ K_2 &= -\cos\phi\partial_\theta + \cot\theta\sin\phi\partial_\phi, \\ K_3 &= \partial_\phi, \end{aligned}$$

while the following othogonality conditions of the Killing vector field can be imposed as

$$\ell(K_0)(K_1) = 0\,, \qquad \ell(K_0)(K_2) = 0\,, \qquad \ell(K_0)(K_3) = 0\,. \tag{3.3}$$

Then, the according principal polynomial P, as well as the dual polynomial $P^\#$, have to be calculated from the area-metric G_{abcd} and its inverse G^{abcd}, which are received from the Killing equations. With the corresponding Legendre map ℓ_x given as

$$\ell(Z)(X) = \frac{P^\#(X,Z,Z,Z)}{P^\#(Z,Z,Z,Z)}\,. \tag{3.4}$$

in the alternative observer definition, one can consequently evaluate the orthogonality conditions for the space-like Killig vectors (3.3) spanning a spatial θ-ϕ-hypersurface.
Next, sign conditions for the surviving degrees of freedom of the area-metric will be derived. They follow from the bihyperbolicity condition for $P^\#$ and P, and finally from the timelike condition (3.2) for K_0.
Now, the previously described steps of this strategy will be applied in the remainder of this section to find the area-metric compatible with the above discussed conditions.
Evaluation of the Killing conditions for spherical symmetry and stationarity (3.1) leads to the following area-metric with 7 unknown functions of r in Petrov representation G_{MN} with index pairs $M,N = tr, t\theta, t\phi, r\theta, r\phi, \theta\phi$:

$$\mathrm{Pet}\,(G) = \begin{pmatrix} c_1(r) & 0 & 0 & 0 & 0 & \sin(\theta)c_2(r) \\ 0 & c_5(r) & 0 & c_4(r) & \sin(\theta)c_3(r) & 0 \\ 0 & 0 & \sin^2(\theta)c_5(r) & -\sin(\theta)c_3(r) & \sin^2(\theta)c_4(r) & 0 \\ 0 & c_4(r) & -\sin(\theta)c_3(r) & c_6(r) & 0 & 0 \\ 0 & \sin(\theta)c_3(r) & \sin^2(\theta)c_4(r) & 0 & \sin^2(\theta)c_6(r) & 0 \\ \sin(\theta)c_2(r) & 0 & 0 & 0 & 0 & \sin^2(\theta)c_7(r) \end{pmatrix}. \tag{3.5}$$

This result looks similar to the one by [PWS09]; [SWW10]. However, while [PWS09]; [SWW10] presented an area-metric with $G_{t\theta r\theta} = 0$ and $G_{t\theta r\theta} = 0$, this is not the case here: Applying the Killing symmetries does in general result in the area-metric components $G_{t\theta r\theta} = c_4(r)$ and $G_{t\phi r\phi} = \sin^2(\theta)c_4(r)$. But still, special coordinates can be chosen such, that these

area-metric components vanish to arrive at the result of [PWS09]. What this implies for the principal polynomial will be discussed in section 3.3.
Also the area-metric component $G_{\theta\phi\theta\phi} = \sin^2(\theta)c_7(r)$ is not specified by the Killing conditions. However, [PWS09] set this component to $G_{\theta\phi\theta\phi} = \sin^2(\theta)r^4$. This can be motivated by choosing the so-called radial Schwarzschild coordinate r defined by the surface area $A = 4\pi r^2$ of the sphere, i.e. the spatial θ-ϕ-hypersurface with solid angle $\mathrm{d}\Omega$ on the sphere, such that

$$\mathrm{d}A = \mathrm{d}\Omega r^2 = \sin\theta r^2 \mathrm{d}\theta\mathrm{d}\phi.$$

Then $G_{\theta\phi\theta\phi}$ as area measure on this θ-ϕ-hypersurface can be set to

$$G_{\theta\phi\theta\phi}\mathrm{d}\theta\mathrm{d}\phi\mathrm{d}\theta\mathrm{d}\phi = \mathrm{d}A^2 = r^4 \sin^2\theta \mathrm{d}\theta\mathrm{d}\phi\mathrm{d}\theta\mathrm{d}\phi.$$

That defines the radial parameter, which should however be clearly distinguished from the Euclidean radius r. This is actually similar to the choice of the radial parameter in the metric case (see 2.2.1), and can hence be seen as generalization to area-metric spacetimes.
Again, it should be highlighted that application of the Killing condition does fulfill symmetric criticality, while coordinate choices do not. Consequently, the general form (3.5) of the area-metric will be used for the following calculations of this section.
One can now perform a reparameterization of (3.5) motivated from the area-metric inverse volume measure

$$\omega_G = 24\left(\epsilon^{abcd}G_{abcd}\right)^{-1}, \tag{3.6}$$

and the fact, that, according to [Gie+12], the area-metric can be as written as

$$G_{abcd} = G_{Cabcd} + \omega_G^{-1}\epsilon_{abcd}, \tag{3.7}$$

with the cyclic term $G_{Ca[bcd]} = 0$ and a totally antisymmetric term $\omega_G^{-1}\epsilon_{abcd}$.
First of all evaluation of (3.6) leads to

$$\omega_G^2 = \frac{9\sin^{-2}(\theta)}{(c_2(r) - 2c_3(r))^2} \equiv \frac{\sin^{-2}(\theta)}{T(r)^2}, \tag{3.8}$$

with the parameterizations $c_2(r) \equiv T(r) + 2S(r)$ and $c_3(r) \equiv S(r) - T(r)$, as also chosen by [PWS09] to display the volume form in a more compact way.

Thus, the area-metric can be displayed according to relation (3.7) as

$$\mathrm{Pet}\,(G) = \begin{pmatrix} c_1(r) & 0 & 0 & 0 & 0 & s(T(r)+2S(r)) \\ 0 & c_5(r) & 0 & c_4(r) & s(S(r)-T(r)) & 0 \\ 0 & 0 & s^2c_5(r) & s(T(r)-S(r)) & s^2c_4(r) & 0 \\ 0 & c_4(r) & s(T(r)-S(r)) & c_6(r) & 0 & 0 \\ 0 & s(S(r)-T(r)) & s^2c_4(r) & 0 & s^2c_6(r) & 0 \\ s(T(r)+2S(r)) & 0 & 0 & 0 & 0 & s^2c_7(r) \end{pmatrix}, \quad (3.9)$$

and hence looks more similar to the area-metric derived by [PWS09] with $s \equiv \sin(\theta)$ for a compact notation.

The dual principal polynomial can now be evaluated using *Mathematica* scripts based on [Dü+20]; [Fis17] and results in

$$\begin{aligned} P^{\#}(p,p,p,p) &= -\frac{1}{24}\omega_G^2 \epsilon^{mnpq}\epsilon^{rstu} G_{mnr(a}G_{b|ps|c}G_{d)qtu}p^a p^b p^c p^d \\ &= -\frac{1}{T(r)^2}\Big[-9S(r)^2\left(\sin^2(\theta)p^{\phi 2}+p^{\theta 2}\right)\left(-2p^r p^t c_4(r)+p^{t2}c_5(r)+p^{r2}c_6(r)\right) \\ &\quad +\Big(-2p^r p^t c_1(r)c_4(r)+p^{t2}c_1(r)c_5(r)-\left((c_4(r))^2-c_5(r)c_6(r)\right)\Big(\sin^2(\theta)p^{\phi 2} \\ &\quad +p^{\theta 2}\Big)+p^{r2}c_1(r)c_6(r)\Big) \\ &\quad \left(-2p^r p^t c_4(r)+p^{t2}c_5(r)+c_7(r)\left(\sin^2(\theta)p^{\phi 2}+p^{\theta 2}\right)+p^{r2}c_6(r)\right)\Big], \end{aligned}$$

with an arbitrary vector p given by $p = \left(p^t, p^r, p^\theta, p^\phi\right)$. This dual principal polynomial presented is generally birefringent, since it is not possible to express it in a metric induced way. However, guided by the ansatz given by [PWS09]; [SWW10] the dual principal polynomial can be rewritten such, that it is induced by a bi-metric structure:

The following definitions

$$\begin{aligned} w &:= \sin^2\theta p^{\phi 2}+p^{\theta 2}, \\ u &:= -2p^t p^r c_4(r)+p^{t2}c_5(r)+p^{r2}c_6(r), \\ q &:= c_4(r)^2-c_5(r)c_6(r), \end{aligned}$$

are introduced to simplify notation.

Then, one finds that

$$\begin{aligned}\Rightarrow P^{\#}(p,p,p,p) &= \frac{-1}{T(r)^2}\left[c_1(r)u^2 + \left(c_1(r)c_7(r) - q - 9S(r)^2\right)uw - c_7(r)qw^2\right] \\ &= \frac{-c_1(r)}{T(r)^2}\left(u - \zeta^+ w\right)\left(u - \zeta^- w\right) \\ &= \frac{-c_1(r)}{T(r)^2} g^+(p,p)\, g^-(p,p)\,.\end{aligned} \tag{3.10}$$

Here the two functions $\zeta^+(r)$ and $\zeta^-(r)$ are given by

$$\zeta^{+/-}(r) := \frac{-\left(c_1(r)c_7(r) - q - 9S(r)^2\right) \pm \sqrt{\left(c_1(r)c_7(r) - q - 9S(r)^2\right)^2 + 4c_1(r)c_7(r)q}}{2c_1(r)}. \tag{3.11}$$

The two metrics, which directly lead to a double light-cone structure, are given by

$$\begin{aligned} g^+ &= c_5(r)\mathrm{d}t^2 - 2c_4(r)\mathrm{d}t\mathrm{d}r + c_6(r)\mathrm{d}r^2 - \zeta^+\left(\mathrm{d}\theta^2 + \sin^2\theta\mathrm{d}\phi^2\right), \\ g^- &= c_5(r)\mathrm{d}t^2 - 2c_4(r)\mathrm{d}t\mathrm{d}r + c_6(r)\mathrm{d}r^2 - \zeta^-\left(\mathrm{d}\theta^2 + \sin^2\theta\mathrm{d}\phi^2\right).\end{aligned}$$

As discussed by [PWS09] this will in general lead to a polarisation split. But, as also pointed out by [PWS09], the area-metric and the dual principal polynomial can be considered as metric induced, if $\zeta^+(r) = \zeta^-(\mathrm{r})$. This holds if

$$\begin{aligned} &\left(c_1(r)c_7(r) - q - 9S(r)^2\right)^2 = -4c_1(r)c_7(r)q, \\ \Rightarrow\quad &4c_1(r)c_7(r) < 0 \quad \text{for} \quad c_1(r)c_7(r) - q - 9S(r)^2 \in \mathbb{R}, \\ \Rightarrow\quad &-9S(r)^2 = 2\sqrt{|c_1(r)c_7(r)|q} + q + |c_1(r)c_7(r)| = \left(\sqrt{|c_1(r)c_7(r)|} + \sqrt{q}\right)^2.\end{aligned} \tag{3.12}$$

From this follows that $S(r)$ is either complex valued or zero, thus reproducing the result by [PWS09]. Also this shows that $c_1(r)$ and $c_7(r)$ need to have opposite signs to reproduce the metric limit case. For $S(r) = 0$ it would then follow that

$$c_1(r) = \frac{-q}{c_7(r)} = \frac{c_5(r)c_6(r) - c_4(r)^2}{c_7(r)},$$

to receive a metric induced dual principal polynomial. Consequenlty , as first pointed out by [PWS09], small deviations like $S(r)/\sqrt{q} = \sigma(r) \ll 1$ with nth derivative $\sigma(r)^{(n)} \ll 1$ and

$$c_1(r) = -(1 + \epsilon(r))q/c_7(r),$$

with nth derivative $\epsilon(r)^{(n)} \ll 1$ already introduce weak birefringence.

As a side remark, it can be observed that for $S(r) = 0$, i.e. when excluding birefringence, the ansatz for the two metrics becomes

$$g = c_5(r)\mathrm{d}t^2 - 2c_4(r)\mathrm{d}t\mathrm{d}r + c_6(r)\mathrm{d}r^2 + c_7(r)\left(\mathrm{d}\theta^2 + \sin^2\theta\mathrm{d}\phi^2\right),$$

recovering the symmetry reduced ansaz (2.1) for the purely metric case. When excluding birefringence, the area-metric should then be metric induced (see for instance [LH04]) with g as the according metric.

Now, using the Legendre map as defined in (3.4) it becomes obvious that

$$\ell(K_0)(K_0) = 1,$$

such that

$$P^{\#}(K_0, K_0, K_0, K_0) = P^{\#}_{tttt} = \frac{-c_1(r)(c_5(r))^2}{T(r)^2} \neq 0 \quad \Rightarrow c_1(r) \neq 0\,, c_5(r) \neq 0.$$

Now, the relations (3.3) are evaluated to understand whether orthogonality of K_0 with respect to the vector fields K_1, K_2, and K_3 contains any new information about the area-metric, starting with K_3:

$$\begin{aligned} &\ell(K_0)(K_3) \stackrel{!}{=} 0 \\ &\frac{P^{\#}(K_0, K_0, K_0, K_3)}{P^{\#}(K_0, K_0, K_0, K_0)} \stackrel{!}{=} 0 \\ &\frac{T(r)^2}{c_1(r)(c_5(r))^2} P^{\#}_{ttt\phi} \stackrel{!}{=} 0 \end{aligned} \tag{3.13}$$

But explicit evaluation of $P^{\#}_{ttt\phi}$ with respect to the symmetry reduced area-metric shows that

$$P^{\#}_{ttt\phi} = 0$$

already, so equation (3.13) is trivially fulfilled. Hence, orthogonality of K_0 with respect to K_3 is basically already enforced by the Killing symmetries. Also explicit evaluation of $P^{\#}_{ttt\theta}$ built from the symmetry reduced area-metric shows that this component of the principal tensor field vanishes:

$$P^{\#}_{ttt\theta} = 0.$$

Consequently, also the orthogonality of K_0 with respect to K_1 and K_2 is trivially fulfilled:

$$\begin{aligned}\ell(K_0)(K_1) =& \frac{P^\#(K_0, K_0, K_0, K_1)}{P^\#(K_0, K_0, K_0, K_0)} \\ =& \frac{T(r)^2}{c_1(r)(c_5(r))^2}\left(\cot\theta\cos\phi P^\#_{ttt\phi} + \sin\phi P^\#_{ttt\theta}\right) = 0,\end{aligned}$$

$$\begin{aligned}\ell(K_0)(K_2) =& \frac{P^\#(K_0, K_0, K_0, K_2)}{P^\#(K_0, K_0, K_0, K_0)} \\ =& \frac{T(r)^2}{c_1(r)(c_5(r))^2}\left(\cot\theta\sin\phi P^\#_{ttt\phi} - \cos\phi P^\#_{ttt\theta}\right) = 0.\end{aligned}$$

To conclude the Killing symmetries already enforce orthogonality of the timelike vector field K_0 with respect to the orbits of SO(3), i.e. the spatial θ-ϕ-hypersurface, similar to the metric case [Str13]. This orthogonality does however not hold in general for vector fields $X = \partial_r$ in radial direction r, as can be seen by the following calculation:

$$\begin{aligned}\ell(K_0)(X) =& \frac{P^\#(K_0, K_0, K_0, X)}{P^\#(K_0, K_0, K_0, K_0)} \\ =& \frac{T(r)^2}{-c_1(r)(c_5(r))^2} P^\#_{tttr} \\ =& -\frac{T(r)^2}{-c_1(r)(c_5(r))^2}\frac{c_1(r)c_4(r)c_5(r)}{T(r)^2} = \frac{c_4(r)}{c_5(r)}.\end{aligned}$$

One can, however, try to find a coordinate system where $c_4(r)$ vanishes similarly to the discussion in [Str13] by employing the Frobenius integrability theorem, as will be discussed in section 3.3.

Next, sign relations between the unknown functions in the ansatz for the area-metric are derived by demanding hyperbolicity of the dual prinicpal polynomial $P^\#$ and the principal polynomial P. This is now different from the ansätze in [PWS09]; [SWW10], where the signs were fixed such to consistently receive the metric limiting case, while the necessary kinematics in space-times with generally non-metric geometries were presented in later works [RRS11] and given in [Sch20]; [Wie18]; [Wol22] in the new, alternative observer definition. According to [RRS11]; [Gie+12]; [Due20]; [Wol22], and also summarized in section 1.2, the dual principal polynomial is hyperbolic, if there exists one vector field $p(x)$ with $P^\#(h) \neq 0$, such that for every vector field $q(x)$ the roots $\lambda(x)$ of

$$P^\#\left(x, q(x) + \lambda(x)p(x)\right) = 0$$

are real functions.

Additionally, if a polynomial is reducible into n factors of lower order polynomials as

$$P^{\#}(x) = P_1^{\#}(x)P_2^{\#}(x)...P_n^{\#}(x),$$

each factor must already be hyperbolic [RRS11]; [Due20]. With these conditions the sign relations between the unknown functions in (3.10) can be fixed. Since the dual principal polynomial splits up in a bi-metric way, one needs to ensure that each of the lower order polynomials $g^+(p,p)$ and $g^-(p,p)$ is already hyperbolic. This hints at a Lorentzian signature for both of the metrics as already discussed in [PWS09] for instance. This can be shown with the following calculation for $g^+(p,p)$, which will be analogous for $g^-(p,p)$. As an explicit example the vector $p = \{p^t, 0, 0, 0\}$, for which it holds that $g^+(p,p) = c_5(r)p^t p^t \neq 0$, may be considered, and some vector $q = \{q^t, q^r, q^\theta, q^\phi\}$.
Consequently, one finds

$$\begin{aligned}
& g^+(q+\lambda p, q+\lambda p) = 0, \\
\Rightarrow\quad & c_5(r)\left(q^t q^t + \lambda^2 p^t p^t + 2\lambda q^t p^t\right) - 2c_4(r)\left(\lambda p^t q^r + q^t q^r\right) \\
& + c_6(r)q^r q^r - \zeta^+ q^\theta q^\theta - \zeta^+ \sin^2(\theta) q^\phi q^\phi = 0, \\
\Rightarrow\quad & g^+(q,q) + \lambda^2 c_5(r)p^t p^t + 2\lambda\left(-c_4(r)p^t q^t + c_5(r)p^t q^t\right) = 0,
\end{aligned} \tag{3.14}$$

The roots of this quadratic equation in λ can be derived easily. Then, it can be checked whether these roots are real by evaluation of the discriminant

$$\begin{aligned}
& 4\left(-c_4(r)p^t q^r + c_5(r)p^t q^t\right)^2 - 4c_5(r)p^t p^t g^+(q,q) > 0, \\
\Rightarrow & \left(-c_4(r)p^t q^r\right)^2 - c_5(r)p^t p^t\left(c_6(r)q^r q^r - \zeta^+(q^\theta q^\theta + \sin^2(\theta)q^\phi q^\phi)\right) > 0.
\end{aligned}$$

Since this needs to hold for every q, two cases are now distinguished to simplify the discussion: First, consider the case $q^r = 0$, $q^\theta \neq 0$, $q^\phi \neq 0$ what leads to

$$-c_5(r)p^t p^t\left(-\zeta^+(q^\theta q^\theta + \sin^2(\theta)q^\phi q^\phi)\right) > 0, \quad \Rightarrow\ c_5(r)\zeta^+ > 0.$$

Thus, $c_5(r)$ and ζ^+ have the same sign.
Next, consider $q^r \neq 0$, $q^\theta = 0$, $q^\phi = 0$ with

$$\left(-c_4(r)p^t q^r\right)^2 - c_5(r)p^t p^t c_6(r)q^r q^r > 0, \quad \Rightarrow\ q = c_4(r)^2 - c_5(r)c_6(r) > 0.$$

So, in general it is concluded that $c_4(r)^2 > c_5(r)c_6(r)$, but this needs to hold in any coordinate system, and thus, also in coordinate systems where the off-diagonal element vanishes locally.

This hints at $c_5(r)c_6(r) < 0$ with opposite signs for $c_5(r)$ and $c_6(r)$, and consequently also opposite signs for $c_6(r)$ and ζ^+.
Evaluation of $g^-(p,p)$ in a similar manner also results in

$$c_5(r)\zeta^- > 0, \tag{3.15}$$

such that $c_5(r)$ needs to have the same sign as ζ^-. Consequently, considering ζ^- as given in relation (3.11) and the fact that $c_1(r)$ and $c_7(r)$ have opposite sign it becomes clear, that $c_1(r)\zeta^- > 0$. Hence, these two functions have the same signature, as well as for $c_1(r)\zeta^+ > 0$.
To summarize the former discussion, the following sign conditions for the hyperbolicity of the dual principal polynomial were derived:

$$\begin{aligned} &c_1(r)\zeta^+ > 0,\ c_1(r)\zeta^- > 0,\ c_1(r)c_5(r) > 0, \\ &c_1(r)c_7(r) < 0,\ c_1(r)c_6(r) < 0,\ c_6(r)c_7(r) > 0, \end{aligned} \tag{3.16}$$

This shows that the two metrics g^+ and g^- must be of Lorentzian signature as expected. Next, the hyperbolicity condition for the principal polynomial P also has to be ensured. The principle polynomial is derived similary to the dual polynomial with the inverse area-metric G^{abcd} instead, where the inversion condition is stated by [PWS09] as

$$G^{abpq}G_{pqcd} = 2\left(\delta^a_c\delta^b_d - \delta^a_d\delta^b_q\right). \tag{3.17}$$

The principal polynomial is then given by

$$P(n,n,n,n) = -\frac{1}{24}\omega^2_{G^{-1}}\epsilon_{uvpq}\epsilon_{rstu}G^{uvr(a}G^{b|ps|c}G^{d)qtu}n_an_bn_cn_d,$$

with scalar density factor

$$\omega_{G^{-1}} = 24\left(\epsilon_{abcd}G^{abcd}\right)^{-1}.$$

Applying the Killing conditions to the inverse area-metric leads to a similar results as for the area-metric, however it is in general parametrized by a different set of unknown functions of r denoted as

$$\mathrm{Pet}\left(G^{-1}\right) = \begin{pmatrix} \tilde{c}_1(r) & 0 & 0 & 0 & 0 & c(2\tilde{S}(r)+\tilde{T}(r)) \\ 0 & \tilde{c}_5(r) & 0 & \tilde{c}_4(r) & c(\tilde{S}(r)-\tilde{T}(r)) & 0 \\ 0 & 0 & c^2\tilde{c}_5(r) & c(\tilde{T}(r)-\tilde{S}(r)) & c^2\tilde{c}_4(r) & 0 \\ 0 & \tilde{c}_4(r) & c(\tilde{T}(r)-\tilde{S}(r)) & \tilde{c}_6(r) & 0 & 0 \\ 0 & c(\tilde{S}(r)-\tilde{T}(r)) & c^2\tilde{c}_4(r) & 0 & c^2\tilde{c}_6(r) & 0 \\ c(2\tilde{S}(r)+\tilde{T}(r)) & 0 & 0 & 0 & 0 & c^2\tilde{c}_7(r) \end{pmatrix},$$

where $c \equiv \csc(\theta)$ is introduced as short notation.

Then, the principal polynomial has the following form

$$\begin{aligned} P(n,n,n,n) = \frac{-1}{\tilde{T}(r)^2}\Big[&-9\tilde{S}(r)^2\left(\csc^2(\theta)n_\phi^2 + n_\theta^2\right)\left(-2n_r n_t\tilde{c}_4(r) + n_t^2\tilde{c}_5(r) + n_r^2\tilde{c}_6(r)\right) \\ &+ \Big(-\left((\tilde{c}_4(r))^2 - \tilde{c}_5(r)\tilde{c}_6(r)\right)\left(\csc^2(\theta)n_\phi^2 + n_\theta^2\right) \\ &-2n_r n_t\tilde{c}_1(r)\tilde{c}_4(r) + n_t^2\tilde{c}_1(r)\tilde{c}_5(r) + n_r^2\tilde{c}_1(r)\tilde{c}_6(r)\Big) \\ &\left(\tilde{c}_7(r)\left(\csc^2(\theta)n_\phi^2 + n_\theta^2\right) - 2n_r n_t\tilde{c}_4(r) + n_t^2\tilde{c}_5(r) + n_r^2\tilde{c}_6(r)\right)\Big] \\ &= \frac{-\tilde{c}_1(r)}{\tilde{T}(r)^2}\tilde{g}^+(n,n)\,\tilde{g}^-(n,n)\,. \end{aligned} \tag{3.18}$$

It is also of bi-metric structure with the lower order polynomials of degree 2 given by

$$\begin{aligned} \tilde{g}^+(n,n) &= \tilde{c}_5(r)n_t^2 - 2\tilde{c}_4(r)n_t n_r + \tilde{c}_6(r)n_r^2 - \tilde{\zeta}^+\left(n_\theta^2 + \csc^2\theta n_\phi^2\right), \\ \tilde{g}^-(n,n) &= \tilde{c}_5(r)n_t^2 - 2\tilde{c}_4(r)n_t n_r + \tilde{c}_6(r)n_r^2 - \tilde{\zeta}^-\left(n_\theta^2 + \csc^2\theta n_\phi^2\right), \end{aligned}$$

and the following abbreviations

$$\begin{aligned} &\tilde{q} = \tilde{c}_4^2(r) - \tilde{c}_5(r)\tilde{c}_6(r), \\ &\tilde{\zeta}^{+/-} := \frac{-\left(\tilde{c}_1(r)\tilde{c}_7(r) - \tilde{q} - 9\tilde{S}(r)^2\right) \pm \sqrt{\left(\tilde{c}_1(r)\tilde{c}_7(r) - \tilde{q} - 9\tilde{S}(r)^2\right)^2 + 4\tilde{c}_1(r)\tilde{c}_7(r)\tilde{q}}}{2\tilde{c}_1(r)}. \end{aligned}$$

The hyperbolicity of P was defined in section 1.2 - similary to $P^\#$ - as the requirement that there exists a co-vector field $n(x)$ with $P(n) \neq 0$ such, that the roots $\mu(x)$ of

$$P\left(x, m(x) + \mu(x)n(x)\right) = 0$$

are real functions for any co-vector field $m(x)$ [RRS11]; [Gie+12]. Additionally, if the principal polynomial is reducible in the sense that it can be expressed as a product of n lower order polynomials as

$$P(x) = P_1(x)P_2(x)...P_n(x),$$

then each of them must already be hyperbolic [RRS11]; [Due20]. A calculation similar to (3.14)-(3.15) leads to the following sign conditions for the degrees of freedom of the inverse area-metric:

$$\begin{aligned} &\tilde{c}_1(r)\tilde{\zeta}^+ > 0,\ \tilde{c}_1(r)\tilde{\zeta}^- > 0,\ \tilde{c}_1(r)\tilde{c}_5(r) > 0, \\ &\tilde{c}_1(r)\tilde{c}_7(r) < 0,\ \tilde{c}_1(r)\tilde{c}_6(r) < 0,\ \tilde{c}_6(r)\tilde{c}_7(r) > 0. \end{aligned} \tag{3.19}$$

Now, using the inversion relation (3.17) and *Mathematica* scripts based on [Fis17] the unknown functions of the inverse area-metric are expressed in terms of the unknown functions of the area-metric:

$$\tilde{c}_1(r) = \frac{-c_7(r)}{(2S(r)+T(r))^2 - c_1(r)c_7(r)}, \tag{3.20}$$

$$\tilde{c}_5(r) = \frac{-c_6(r)}{(S(r)-T(r))^2 + c_4(r)^2 - c_5(r)c_6(r)}, \tag{3.21}$$

$$\tilde{c}_6(r) = \frac{-c_5(r)}{(S(r)-T(r))^2 + c_4(r)^2 - c_5(r)c_6(r)}, \tag{3.22}$$

$$\tilde{c}_7(r) = \frac{-c_1(r)}{(2S(r)+T(r))^2 - c_1(r)c_7(r)}, \tag{3.23}$$

$$\tilde{c}_4(r) = \frac{c_4(r)}{(c_4(r))^2 - c_5(r)c_6(r) + (S(r)-T(r))^2}, \tag{3.24}$$

$$\tilde{T}(r) = \frac{1}{3}\left(\frac{2S(r)+T(r)}{(2S(r)+T(r))^2 - c_1(r)c_7(r)} + \frac{2T(r)-2S(r)}{(c_4(r))^2 - c_5(r)c_6(r) + (S(r)-T(r))^2}\right), \tag{3.25}$$

$$\tilde{S}(r) = \frac{1}{3}\left(\frac{S(r)-T(r)}{(c_4(r))^2 - c_5(r)c_6(r) + (S(r)-T(r))^2} + \frac{2S(r)+T(r)}{(2S(r)+T(r))^2 - c_1(r)c_7(r)}\right). \tag{3.26}$$

These expressions also verify the sign conditions (3.27): Since $\tilde{c}_1(r)$ and $\tilde{c}_7(r)$ need to be of opposite sign, this should also hold for $c_1(r)$ and $c_7(r)$, and thus confirms the previous result (3.12). Similarly, the opposite sign of $c_5(r)$ and $c_6(r)$ is confirmed by (3.21) and (3.22).
So to summarize the entire discussion, bi-hyperbolicity eventually implies the following sign condition for the unknown functions in the area-metric:

$$c_1(r)c_5(r) > 0,\ c_1(r)c_7(r) < 0,\ c_1(r)c_6(r) < 0,\ c_6(r)c_7(r) > 0, \tag{3.27}$$

With the requirement that K_0 should be timelike, in the sense that its respective co-vector lies in the interior of the hyperbolicity cone C via equation (3.2) with $P(x, C_x) > 0$, one can also conclude further sign conditions for the unknown functions. In the metric case this definition for a timelike vector K^a with respective co-vector n_a actually translates to the conventional requirement that

$$g^{ab}n_a n_b = g^{ab}g_{ac}g_{bd}K^cK^d = K^b g_{bd}K^d = n(K) > 0,$$

for a $\{+,-,-,-\}$-signature.
In the area-metric case the co-vector $n = K^\flat$ is instead given by

$$n_a = (\ell(K_0))_a = \frac{P^{\#}_{abcd}K_0^bK_0^cK_0^d}{P^{\#}(K_0,K_0,K_0,K_0)} = \frac{P^{\#}_{attt}K_0^tK_0^tK_0^t}{P^{\#}_{tttt}},$$

where the Legendre map and $K_0^t = 1$ were used.
This requirement becomes

$$P(n,n,n,n) = P^{abcd} n_a n_b n_c n_d = \frac{P^{abcd} P^{\#}_{attt} P^{\#}_{bttt} P^{\#}_{cttt} P^{\#}_{dttt} (K_0^t)^4}{\left(P^{\#}_{tttt}\right)^4} > 0.$$

Explicitly inserting the expressions for the components of P and $P^{\#}$ in terms of the unknown functions of the area-metric leads to the condition $c_7(r) > 0$.
Thus, together with (3.16), the final results for the sign relations of the unknown functions are given by the following inequalities:

$$c_7(r) > 0,\ c_6(r) > 0,\ c_1(r) < 0,\ c_5(r) < 0.$$

To summarize, this section has shown how the Killing conditions for spherical symmetry and stationarity reduce the degrees of freedom of an area-metric spacetime to seven unknown functions of r. Employing kinematic requirements like bi-hyperbolicity and the fact that the Killing vector K_0 should be timelike in the sense that its respective co-vector should lie within the forward hyperbolicity cone C, sign relations for the unknown functions were derived.
As mentioned in the beginning of this section one should be aware that stationarity and spherical symmetry can be imposed in a well-defined way via their according Killing vectors. Because of that they are no misleading notions, and can generalized from the metric to the area-metric case. However, are has to be taken of the hypersurface orthogonality condition of the timelike vector field, as will be discussed in more detail in section 3.3. While in the metric case this condition implies staticity in the sense of a discrete time-reflection symmetry, it is unclear whether or how this still holds in the area-metric case [Scha]. Nevertheless, one can still impose hypersurface orthogonality as a well-defined requirement using the Frobenius condtion, and find more conditions for the degrees of freedom of the area-metric.
But first, a 3 + 1-split of this spherically symmetric, stationary area-metric spacetime is performed in the next section. The goal is to find the induced geometric fields on the spatial hypersurfaces. Furthermore, a parameterization for the shift N^α and the lapse fields N is needed to set up the input coeffcients for the symmetry reduced closure equations.

3.2 3+1-split of an area-metric, spherically symmetric stationary spacetime

Using various contractions of the area-metric one can define for instance 3 spatial hypersurface fields in a 3 + 1-split of spacetime based on standard methods [ADW08]; [Gou07] for the metric case. The fields are similar to [Due20], but they are built from the dualized area-metric

to match the new observer definition in the t-α-frame with basis vectors $(\partial_t, \partial_\alpha)$ and $\alpha = 1, 2, 3$ denoting the spatial indices:

$$\tilde{\boldsymbol{g}}_{\alpha\beta} = -G\left(\partial_t, \partial_\alpha, \partial_t, \partial_\beta\right) = -G_{t\,\alpha\,t\beta}, \tag{3.28}$$

$$\tilde{\bar{\boldsymbol{g}}}^{\alpha\beta} = \frac{1}{4}\frac{1}{\det\tilde{\boldsymbol{g}}}\epsilon^{\alpha\mu\nu}\epsilon^{\beta\rho\sigma}G\left(\partial_\mu, \partial_\nu, \partial_\rho, \partial_\sigma\right) = \frac{1}{4}\frac{1}{\det\tilde{\boldsymbol{g}}}\epsilon^{\alpha\mu\nu}\epsilon^{\beta\rho\sigma}G_{\mu\,\nu\,\rho\,\sigma}, \tag{3.29}$$

$$\tilde{\bar{\bar{\boldsymbol{g}}}}^{\alpha}_{\beta} = \frac{1}{2}\frac{1}{\sqrt{\det\tilde{\boldsymbol{g}}}}\epsilon^{\alpha\delta\sigma}G\left(\partial_t, \partial_\beta, \partial_\delta, \partial_\sigma\right) = \frac{1}{2}\frac{1}{\sqrt{\det\tilde{\boldsymbol{g}}}}\epsilon^{\alpha\delta\sigma}G_{t\,\beta\,\delta\,\sigma}. \tag{3.30}$$

Here, $\det\tilde{\boldsymbol{g}}$ is the determinant of an effective hypersurface metric $\tilde{\boldsymbol{g}}_{\alpha\beta}$. The field $\tilde{\bar{\bar{\boldsymbol{g}}}}^{\alpha}_{\beta}$ is not traceless, unlike the analogous relation (1.35), and $\tilde{\bar{\bar{\boldsymbol{g}}}}^{\alpha\beta} = \left(\tilde{\boldsymbol{g}}^{-1}\right)^{\beta\gamma}\tilde{\bar{\bar{\boldsymbol{g}}}}^{\alpha}_{\gamma}$. The expressions (3.28)-(3.30) can be related to the hypersurface fields (1.33)-(1.35) in the 0-α-foliation frame via insertion of $\partial_t = Ne_0 + N^\alpha e_\alpha$ and $\partial_\alpha = e_\alpha$.
Thus, the area-metric components $\bar{G}_{....}$ in the foliation frame can be related to the components $G_{....}$ in the t-α-coordinate-frame, as will be shown in the following paragraph. For the purely spatial part it holds that

$$\bar{G}_{\mu\nu\rho\sigma} = \det\bar{\boldsymbol{g}}\epsilon_{\alpha\mu\nu}\epsilon_{\beta\rho\sigma}\bar{\bar{\boldsymbol{g}}}^{\alpha\beta} = \det\tilde{\boldsymbol{g}}\epsilon_{\alpha\mu\nu}\epsilon_{\beta\rho\sigma}\tilde{\bar{\bar{\boldsymbol{g}}}}^{\alpha\beta} = G_{\mu\nu\rho\sigma},$$

and thus

$$\left(\det\bar{\boldsymbol{g}}\right)\bar{\bar{\boldsymbol{g}}}^{\alpha\beta} = \left(\det\tilde{\boldsymbol{g}}\right)\tilde{\bar{\bar{\boldsymbol{g}}}}^{\alpha\beta}. \tag{3.31}$$

For the component $G_{t\beta\delta\sigma}$ one finds

$$G_{t\beta\delta\sigma} = N\bar{G}_{0\beta\delta\sigma} + N^\alpha\bar{G}_{\alpha\beta\delta\sigma} = N\sqrt{\bar{g}}\left(\bar{\bar{g}}^{\alpha}_{\gamma} + \delta^\alpha_\beta\right)\epsilon_{\alpha\delta\sigma} + N^\alpha\bar{G}_{\alpha\beta\delta\sigma},$$

and consequently

$$\tilde{\bar{\bar{\boldsymbol{g}}}}^{\alpha}_{\beta} = \frac{\sqrt{\bar{\boldsymbol{g}}}}{\sqrt{\tilde{\boldsymbol{g}}}}N\left(\bar{\bar{\boldsymbol{g}}}^{\alpha}_{\beta} + \delta^\alpha_\beta\right) + \sqrt{\det\tilde{\boldsymbol{g}}}\tilde{\bar{\bar{\boldsymbol{g}}}}^{\gamma\alpha}\epsilon_{\gamma\delta\beta}N^\delta. \tag{3.32}$$

Finally, $G_{t\,\alpha\,t\beta}$ and consequently $\det\tilde{\boldsymbol{g}}$ can be expressed via the components of $\bar{G}$ in the foliation frame as

$$\begin{aligned}\tilde{\boldsymbol{g}}_{\alpha\beta} =& -G_{t\,\alpha\,t\beta} = -N^2\bar{G}_{0\,\alpha\,0\beta} - NN^\gamma\bar{G}_{\gamma\,\alpha\,0\beta} - NN^\delta\bar{G}_{0\,\alpha\,\delta\beta} - N^\gamma N^\delta\bar{G}_{\gamma\,\alpha\,\delta\beta}\\ =& N^2\bar{\boldsymbol{g}}_{\alpha\beta} - NN^\gamma\sqrt{\det\bar{\boldsymbol{g}}}\left(\bar{\bar{\boldsymbol{g}}}^{\sigma}_{\beta} + \delta^\sigma_\beta\right)\epsilon_{\sigma\gamma\alpha} - NN^\delta\sqrt{\det\bar{\boldsymbol{g}}}\left(\bar{\bar{\boldsymbol{g}}}^{\sigma}_{\alpha} + \delta^\sigma_\alpha\right)\epsilon_{\sigma\delta\beta}\\ &- N^\gamma N^\delta\det\tilde{\boldsymbol{g}}\tilde{\bar{\bar{\boldsymbol{g}}}}^{\sigma\rho}\epsilon_{\sigma\gamma\alpha}\epsilon_{\rho\delta\beta}.\end{aligned} \tag{3.33}$$

Now, explicit evaluation of the expressions (3.28)-(3.30) with the components of the area-metric for a spherically symmetric, stationary spacetime as displayed in (3.9) leads to the

following non-vanishing components for the hypersurface fields in the t-α-frame:

$$\tilde{\boldsymbol{g}}_{\alpha\beta}: \quad \tilde{\boldsymbol{g}}_{rr} = -c_1(r),\ \tilde{\boldsymbol{g}}_{\theta\theta} = -c_5(r),\ \tilde{\boldsymbol{g}}_{\phi\phi} = -c_5(r)\sin(\theta)^2,$$
$$\det\tilde{\boldsymbol{g}} = -c_1(r)c_5(r)^2\sin(\theta)^2, \tag{3.34}$$

$$\tilde{\tilde{\boldsymbol{g}}}^{\alpha\beta}: \quad \tilde{\tilde{\boldsymbol{g}}}^{rr} = \frac{-c_7(r)}{c_1(r)c_5(r)^2},\ \tilde{\tilde{\boldsymbol{g}}}^{\theta\theta} = \frac{-c_6(r)}{c_1(r)c_5(r)^2},\ \tilde{\tilde{\boldsymbol{g}}}^{\phi\phi} = \frac{-c_6(r)}{c_1(r)c_5(r)^2\sin(\theta)^2}, \tag{3.35}$$

$$\tilde{\tilde{\boldsymbol{g}}}^{\alpha}_{\beta}: \quad \tilde{\tilde{\boldsymbol{g}}}^{r}_{r} = \frac{-2S(r)-T(r)}{\sqrt{-c_1(r)c_5(r)^2}},\ \tilde{\tilde{\boldsymbol{g}}}^{\theta}_{\theta} = \frac{-T(r)+S(r)}{\sqrt{-c_1(r)c_5(r)^2}},\ \tilde{\tilde{\boldsymbol{g}}}^{\phi}_{\phi} = \frac{-T(r)+S(r)}{\sqrt{-c_1(r)c_5(r)^2}},$$
$$\tilde{\tilde{\boldsymbol{g}}}^{\theta}_{\phi} = -\frac{\sin(\theta)\,c_4(r)}{\sqrt{-c_1(r)c_5(r)^2}},\ \tilde{\tilde{\boldsymbol{g}}}^{\phi}_{\theta} = -\frac{c_4(r)}{\sin(\theta)\sqrt{-c_1(r)c_5(r)^2}}, \tag{3.36}$$

By comparison of the results for $\tilde{\tilde{\boldsymbol{g}}}^{\phi}_{\theta}$ and $\tilde{\tilde{\boldsymbol{g}}}^{\theta}_{\phi}$ with equation (3.32) one can read off, that

$$\tilde{\tilde{\boldsymbol{g}}}^{\phi}_{\theta} = \tilde{\tilde{\boldsymbol{g}}}^{\theta}_{\phi} = 0,$$

and finds a radial component of the shift vector N^r:

$$N^r(r) = \frac{c_4(r)}{c_6(r)} \propto G_{trt\theta}. \tag{3.37}$$

Furthermore, since the terms $\tilde{\tilde{\boldsymbol{g}}}^{\theta}_{r}$, $\tilde{\tilde{\boldsymbol{g}}}^{r}_{\theta}$, $\tilde{\tilde{\boldsymbol{g}}}^{\phi}_{r}$, $\tilde{\tilde{\boldsymbol{g}}}^{r}_{\phi}$ vanish, it is concluded from (3.32) that the other parts of the shift vector field, namely N^θ and N^ϕ, are also zero.
This result (3.37) for the shift vector field can also be confirmed by the 3 + 1-decomposition of the $P^{\#}_{\alpha ttt}$-component of the dual prinicipal tensor. It can be expressed in terms of the shift vector field N^α and its other components $P^{\#}_{\alpha\beta tt}$, $P^{\#}_{\alpha\beta\gamma t}$, $P^{\#}_{\alpha\beta\gamma\delta}$ as

$$\begin{aligned} P^{\#}_{\alpha ttt} &= P^{\#}_{abcd}e^a_\alpha\left(Ne^b_0 + e^b_\beta N^\beta\right)\left(Ne^c_0 + e^c_\gamma N^\gamma\right)\left(Ne^d_0 + e^d_\delta N^\delta\right) \\ &= N^3P^{\#}_{\alpha 000} + 3N^2N^\beta P^{\#}_{\alpha\beta 00} + 3NN^\beta N^\gamma P^{\#}_{\alpha\beta\gamma 0} + N^\beta N^\gamma N^\delta P^{\#}_{\alpha\beta\gamma\delta} \\ &= 3N^\beta P^{\#}_{\alpha\beta tt} - 3N^\beta N^\gamma P^{\#}_{\alpha\beta\gamma t} + N^\beta N^\gamma N^\delta P^{\#}_{\alpha\beta\gamma\delta}, \end{aligned} \tag{3.38}$$

by insertion of $\partial_t = Ne_0 + N^\alpha e_\alpha$, as well as successive application of the expressions

$$\begin{aligned} P^{\#}_{\alpha\beta\gamma 0} &= \frac{P^{\#}_{\alpha\beta\gamma t} - N^\delta P^{\#}_{\alpha\beta\gamma\delta}}{N}, \\ P^{\#}_{\alpha\beta 00} &= \frac{P^{\#}_{\alpha\beta tt} - 2N^\gamma N P^{\#}_{\alpha\beta\gamma 0} - N^\gamma N^\delta P^{\#}_{\alpha\beta\gamma\delta}}{N^2} \\ &= \frac{P^{\#}_{\alpha\beta tt} - 2N^\gamma P^{\#}_{\alpha\beta\gamma t} + N^\gamma N^\delta P^{\#}_{\alpha\beta\gamma\delta}}{N^2}, \end{aligned}$$

and the annihilation condition

$$P^{\#}(e_\alpha, e_0, e_0, e_0) = P^{\#}_{\alpha 000} = 0.$$

Since $P^{\#}_{\theta ttt} = 0$, $P^{\#}_{\phi ttt} = 0$, $N^\theta = 0$ and $N^\phi = 0$ hold, equation (3.38) simplifies to

$$P^{\#}_{rttt} = 3N^r P^{\#}_{rrtt} - 3N^r N^r P^{\#}_{rrrt} + N^r N^r N^r P^{\#}_{rrrr},$$

which is identically fulfilled for $N^r = c_4(r)/c_6(r)$ and

$$\begin{aligned} P^{\#}_{rttt} &= -\frac{c_1(r)c_5(r)c_4(r)}{T(r)^2}, \quad P^{\#}_{rrtt} = -\frac{c_1(r)\left(2c_4(r)^2 + c_5(r)c_6(r)\right)}{T(r)^2}, \\ P^{\#}_{rrrt} &= -\frac{c_1(r)c_4(r)c_6(r)}{T(r)^2}, \quad P^{\#}_{rrrr} = -\frac{c_1(r)c_6(r)^2}{T(r)^2}. \end{aligned}$$

These results of the components of the principal tensor were also found by explicit evaluation of $P^{\#}_{abcd}$ in the t-α-frame with *Mathematica*.
Comparing the explicit expressions $\tilde{\tilde{\boldsymbol{g}}}^r_r$, $\tilde{\tilde{\boldsymbol{g}}}^\theta_\theta$, $\tilde{\tilde{\boldsymbol{g}}}^\phi_\phi$ given in (3.36) with the decomposition (3.32) one can additionally conclude that the lapse function $N(r)$ is related to the unknown free function $T(r)$ via

$$T(r)\sin(\theta) = N(r)\sqrt{\det \bar{\boldsymbol{g}}} = \omega_{G^{-1}}, \tag{3.39}$$

with density factor $\omega_{G^{-1}}$, while the non-vanishing components of $\bar{\bar{\boldsymbol{g}}}$ are given by

$$\begin{aligned} \bar{\bar{\boldsymbol{g}}}^r_r &= \frac{2S(r)}{T(r)} \coloneqq 2\mathcal{S}(r), \\ \bar{\bar{\boldsymbol{g}}}^\theta_\theta &= \frac{-S(r)}{T(r)} \coloneqq -\mathcal{S}(r), \\ \bar{\bar{\boldsymbol{g}}}^\phi_\phi &= \frac{-S(r)}{T(r)} \coloneqq -\mathcal{S}(r), \end{aligned} \tag{3.40}$$

with reparameterization $\mathcal{S}(r) \coloneqq S(r)/T(r)$.
Next, using the relation (3.31) between the components of $\tilde{\tilde{\boldsymbol{g}}}$ and $\bar{\bar{\boldsymbol{g}}}$, as well as the explicit expressions (3.34) and (3.35), one finds that the non-vanishing components of $\bar{\bar{\boldsymbol{g}}}$ are given by

$$\begin{aligned} \bar{\bar{\boldsymbol{g}}}^{rr} &= \frac{c_7(r)\sin(\theta)^2}{\det \bar{\boldsymbol{g}}} \coloneqq C_7(r), \\ \bar{\bar{\boldsymbol{g}}}^{\theta\theta} &= \frac{c_6(r)\sin(\theta)^2}{\det \bar{\boldsymbol{g}}} \coloneqq C_6(r), \\ \bar{\bar{\boldsymbol{g}}}^{\phi\phi} &= \frac{c_6(r)}{\det \bar{\boldsymbol{g}}} \coloneqq \frac{C_6(r)}{\sin(\theta)^2}, \end{aligned} \tag{3.41}$$

with reparameterizations $C_7(r) \coloneqq c_7(r)\sin(\theta)^2/\det\bar{\boldsymbol{g}}$ and $C_6(r) \coloneqq c_6(r)\sin(\theta)^2/\det\bar{\boldsymbol{g}}$.
At last, the non-vanishing components of $\bar{\boldsymbol{g}}$ are determined by relation (3.33) and the explicit terms in (3.34) to be

$$\begin{aligned}
\bar{\boldsymbol{g}}_{rr} &= -\frac{c_1(r)}{N^2(r)} \coloneqq -C_1(r),\\
\bar{\boldsymbol{g}}_{\theta\theta} &= \frac{1}{N^2(r)}\left(-c_5(r) + \frac{c_4(r)^2}{c_6(r)}\right) \coloneqq -C_5(r),\\
\bar{\boldsymbol{g}}_{\phi\phi} &= \frac{1}{N^2(r)}\left(-c_5(r) + \frac{c_4(r)^2}{c_6(r)}\right)\sin(\theta)^2 \coloneqq -C_5(r)\sin(\theta)^2,
\end{aligned} \tag{3.42}$$

with reparameterizations $C_1(r) \coloneqq c_1(r)/N(r)^2$ and $C_5(r) \coloneqq 1/N(r)^2\left(c_5(r) - c_4(r)^2/c_6(r)\right)$. Thus, the square root of the determinant $\sqrt{\bar{\boldsymbol{g}}}$ is given by

$$\sqrt{\det\bar{\boldsymbol{g}}} = \sqrt{-C_1(r)C_5(r)^2}\sin(\theta) = \frac{1}{N(r)^3}\sqrt{-c_1(r)\left(c_5(r) - \frac{c_4(r)^2}{c_6(r)}\right)^2}\sin(\theta),$$

such that with (3.39) it follows that the lapse can be expressed in terms of the unknown degrees of freedom as

$$N(r)^2 = \frac{1}{T(r)}\sqrt{-c_1(r)c_5(r)^2 + 2\frac{c_1(r)c_5(r)c_4(r)^2}{c_6(r)} - \frac{c_1(r)c_4(r)^2}{c_6(r)^2}}. \tag{3.43}$$

This expression for the lapse $N(r)$ can be confirmed by the 3 + 1-decomposition of the $P^{\#}_{tttt}$-component of the dual principal tensor field via the following steps: At first this component is explicitly evaluated, what results in

$$\begin{aligned}
P^{\#}_{tttt} &= P^{\#}_{a\,b\,c\,d}\left(Ne^a_0 + e^a_\alpha N^\alpha\right)\left(Ne^b_0 + e^b_\beta N^\beta\right)\left(Ne^c_0 + e^c_\gamma N^\gamma\right)\left(Ne^d_0 + e^d_\delta N^\delta\right)\\
&= N^4 P^{\#}_{0000} + 4N^3 N P^{\#}_{\alpha 000} + 6N^2 N^\alpha N^\beta P^{\#}_{\alpha\beta 00} + 4NN^\alpha N^\beta N^\gamma P^{\#}_{\alpha\beta\gamma 0}\\
&\quad + N^\alpha N^\beta N^\gamma N^\delta P^{\#}_{\alpha\beta\gamma\delta}\\
&= N^4 + 6N^\alpha N^\beta P^{\#}_{\alpha\beta tt} - 8N^\alpha N^\beta N^\gamma P^{\#}_{\alpha\beta\gamma t} + 3N^\alpha N^\beta N^\gamma N^\delta P^{\#}_{\alpha\beta\gamma\delta}.
\end{aligned} \tag{3.44}$$

Then, using the normalization condition $P^{\#}_{0000} = 1$, the annihilation condition $P^{\#}_{\alpha 000} = 0$, the expressions for $P^{\#}_{rrrr}$, $P^{\#}_{rrtt}$, $P^{\#}_{rttt}$ and $P^{\#}_{tttt} = -c_1(r)c_5(r)^2/T(r)^2$, as well as $N^r = c_4(r)/c_6(r)$, $N^\theta = 0$, $N^\phi = 0$ the lapse $N(r)$ can be extracted from (3.44) as

$$\begin{aligned}
N(r)^4 &= P^{\#}_{tttt} - 6(N^r(r))^2 P^{\#}_{rrtt} + 8(N^r(r))^3 P^{\#}_{rrrt} - 3(N^r(r))^4 P^{\#}_{rrrr}\\
&= -\frac{c_1(r)c_5(r)^2}{T(r)^2} + 2\frac{c_1(r)c_5(r)c_4(r)^2}{c_6(t)T(r)^2} - \frac{c_1(r)c_4(r)^4}{c_6(r)^2T(r)^2},
\end{aligned}$$

in accordance with the previous result (3.43).

To summarize, the seven unknown degrees of freedom of the area-metric of a spherically symmetric, stationary spacetime $c_1(r)$, $S(r)$, $T(r)$, $c_4(r)$, $c_5(r)$, $c_6(r)$ and $c_7(r)$ were reparameterized using a 3 + 1-decomposition into lapse $N(r)$, radial shift $N^r(r)$, and five degrees of freedom $C_1(r)$, $C_5(r)$, $C_6(r)$, $C_7(r)$ and $\mathcal{S}(r)$ for the three hypersurface fields $\bar{\boldsymbol{g}}$, $\bar{\bar{\boldsymbol{g}}}$ and $\bar{\bar{\bar{\boldsymbol{g}}}}$. This decomposition is in general required to derive the symmetry reduced input coefficients to set up the symmetry reduced closure equation in section 3.4.
However, before discussing this, it will now be elaborated how the notion of hypersurface orthogonality due to the Frobenius integrability theorem - which corresponds to a specific coordinate choice motivated by time reflection symmetry in the metric case [Str13]; [Wal84] - can be understood in the context of an area-metric spacetime. It will therefore be shown how a parametrization is chosen such, that the shift vector field vanishes. If one was able to derive the gravitational action for an area-metric, spherically symmetric and stationary spacetime - as would be interesting for future research - the final equations of motion could then also be simplified, similarly as in the metric case in Chapter 2.

3.3 Discussion on staticity in area-metric spacetime

In standard literature (see for instance [Wal84]) staticity is associated to a discrete time-reflection symmetry $t \to -t$. In case of a Lorentzian geometry (M, g) this corresponds to a vanishing off-diagnoal element of the metric $g_{t\alpha} = 0$, which is in this case both the fundamental geometry and the principal tensor field.
As briefly mentioned in section 2.2.1 there is a one to one correspondence between the notion of staticity $g_{t\alpha} = 0$ of a spherically symmetric, stationary, metric spacetime and hypersurface orthogonality of the timelike Killing vector field $X = \partial_t$. This means that a specific coordinate frame, where spatial hypersurfaces are defined by $t = \text{const.}$, can be found. Then, the radial shift N^r vanishes, i.e. $N^r = 0$.
However, the concept of staticity in the sense of time-reflection symmetry can not be adapted so straightforwardly for an area-metric spacetime. Especially, there is the area-metric G_{abcd} as basic geometric field on the one hand, and the according dual principal tensor field $P^{\#}_{abcd}$ on the other hand. Now, the question arises to which of these fields the time-reflection symmetry - if at all - applies. If the time-reflection symmetry was to apply to G_{abcd}, this would also follow for $P^{\#}_{abcd}$, but not necessarily the other way round. Additionally, if all terms $G_{\alpha\beta\gamma t}$ vanished, then ω_G would not be well-defined, what is also problematic. At this point, it is still unclear how the notion of staticity as a discrete time-reflection symmetry can be applied to

make any statements about the area-metric spacetime.
Instead, as already discussed in 2.2.1, one needs to retreat to a mathematically more well-defined concept, such as the **Frobenius condition**

$$\omega \wedge \mathrm{d}\omega = 0. \tag{3.45}$$

If it holds, this ensures that the spacelike hypersurfaces of the spacetime foliation are integrable, and the co-vector ω corresponding to the timelike Killing vector field of the stationary spacetime is hence hypersurface orthogonal in a specific coordinate frame.
This is possible, since the Frobenius condition itself does not rely on a metric structure, but employs more general concepts like differential forms and one-forms in a dual space which can be easily found by application of the Legendre map. Of course, these concepts also exist for a spacetime manifold with area-metric structure.
Thus, the following discussion of integrability in spherically symmetric, stationary area-metric spacetime closely follows the steps made in [Str13], but now for an area-metric geometry. The idea is to show at first that, assuming a coordinate system with a hypersurface orthogonal timelike Killing vector, the Frobenius follows. Vice versa the Frobenius condition should also implies that one can choose a coordinate system in the spherically symmetric case, where the timelike Killing vector field becomes hypersurface orthogonal.

The starting point is the assumption that the timelike Killing vector field denoted by $K = \partial_\tau$, which implies stationartiy of the spacetime [Str13], is hypersurface orthogonal to a specific choice of spatial sections with τ = const. as the corresponding coordinate. In a 3 + 1-split the timelike Killing vector ∂_t field is generally given by

$$\partial_t = Ne_0 + N^\alpha e_\alpha,$$

where e_0 is the vector orthogonal to the hypersurfaces, so that $\partial_\tau \propto e_0$, and hence $N^\alpha_\tau = 0$ in this specific frame, i.e.

$$K = \partial_\tau = N_\tau e_0,$$

with N_τ as the corresponding lapse. In Section 3.2 it was shown that the radial shift vector field N^r is generally proportional to the component $c_4(r) = G_{t\theta r\theta}(r)$ one receives by symmetry reduction of the area-metric in the t-α-coordinates. Consequently, a vanishing shift N^α_τ in the τ-α-coordinates corresponds to $G_{\tau\theta r\theta} = 0$ in these coordinates.

Now, the one-form $\omega = K^\flat$ can be derived via the Legendre map $\ell(K) \in \Omega^1(M)$ defined by (3.4):

$$\begin{aligned} \ell(K) &= \frac{P^\#(K,K,K,\cdot)}{P^\#(K,K,K,K)}, \\ \Rightarrow \quad \omega &= \ell(K)P^\#(K,K,K,K) = \ell(K)\omega(K) = P^\#(K,K,K,\cdot) \end{aligned}$$

where $\cdot$ denotes an open slot and $\omega(K) = P^\#(K,K,K,K)$ is a normalization factor.
In explicit components this is equivalent to

$$\omega_a = P^\#_{abcd}K^bK^cK^d = P^\#_{a\tau\tau\tau}.$$

For spatial indices $a = \alpha$ the 3 + 1-decomposition of $P^\#_{\alpha ttt}$ was given by (3.38) in a general t-α-frame. Now, this component vanishes for a hypersurface orthogonal timelike Killing vector field $K = \partial_\tau$ due to the vanishing shift vector field in this special frame. Then ω simplifies to

$$\omega = P^\#_{\tau\tau\tau\tau}\mathrm{d}\tau,$$

where $P^\#_{\tau\tau\tau\tau}(r)$ is a function of r in spherically symmetric, stationary space-time. This expression fulfills the Frobenius condition since

$$\begin{aligned} \omega \wedge \mathrm{d}\omega =& P^\#_{\tau\tau\tau\tau}\mathrm{d}\tau \wedge \mathrm{d}\left(P^\#_{\tau\tau\tau\tau}\mathrm{d}\tau\right) \\ =& P^\#_{\tau\tau\tau\tau}\mathrm{d}\tau \wedge \partial_r P^\#_{\tau\tau\tau\tau} \wedge \mathrm{d}r \wedge \mathrm{d}\tau \\ =& 0, \end{aligned}$$

due to the antisymmetry of the wedge product.
So to summarize, the assumption of hypersurface orthogonality of the timelike Killing vector field leads to the fulfillment of the Frobenius condition, similar to the metric case, but now for an area-metric geometry.

Next, the other direction has to be shown: The Frobenius condition should imply that there is a frame, where the timelike Killing vector field is hypersurface orthogonal, even for an area-metric geometry. Furthermore, the transformation of the components of the symmetry reduced area-metric (3.9) in such a frame is investigated.
This part of the proof only works under the condition that K is actually a timelike Killing vector field, as for example discussed by [Str13]; [Ryd09]. To see this, one first applies, as also done in [Str13], the interior product $i_K : \Omega^r(M) \to \Omega^{r-1}(M)$ ([Nak03]) onto (3.45), what

leads to

$$0 = i_K(\omega \wedge \mathrm{d}\omega) = \omega(K)\mathrm{d}\omega - \omega \wedge i_K(\mathrm{d}\omega).$$

Next, application of Cartan's formula [Str13]; [Nak03]

$$\mathcal{L}_K\omega = \mathrm{d}\omega(K) + i_K(\mathrm{d}\omega),$$

with $\mathcal{L}_K\omega$ as Lie derivative of ω along the flow generated by K leads to

$$0 = \omega(K)\,\mathrm{d}\omega - \omega \wedge (\mathcal{L}_K\omega - \mathrm{d}\omega(K)). \tag{3.46}$$

Following the steps in [Str13] it must now be shown that $\mathcal{L}_K\omega$ vanishes, under the condition that K is a Killing vector field. Care has to be taken here, since the Killing symmetry condition actually applies to the area-metric in this case, i.e.

$$\mathcal{L}_K G = 0.$$

But since the dual principal polynomial $P^{\#}$, required for the Legendre map to derive $\omega = K^\flat$, is built up from the area-metric according to

$$P^{\#}_{abcd} = -\frac{1}{24}\omega_G^2 \epsilon^{mnpq}\epsilon^{rstu} G_{mnr(a}G_{b|ps|c}G_{d)qtu},$$

it follows that the symmetries of G are also symmetries of $P^{\#}$, i.e.

$$\mathcal{L}_K P^{\#} = 0,$$
$$\text{in coordinates: } K^b\partial_b P^{\#}_{apqr} + \partial_a K^b P^{\#}_{bpqr} + \partial_p K^b P^{\#}_{abqr} + \partial_q K^b P^{\#}_{apbr} + \partial_r K^b P^{\#}_{apqb} = 0.$$

Appendix C elaborates this in more detail.
Thus, the Lie derivative of $\omega = K^\flat$ with respect to K indeed vanishes, because

$$\begin{aligned}\mathcal{L}_K\omega &= K^b(\partial_b\omega_a) + \partial_a K^b\omega_b \\ &= K^b\partial_b\left(P^{\#}_{apqr}K^pK^qK^r\right) + \left(\partial_a K^b\right)P^{\#}_{bpqr}K^pK^qK^r \\ &= 0,\end{aligned}$$

when inserting the Killing condition for the dual principal polynomial.
Therefore, the exact same arguments made by [Str13] apply, such that (3.46) can be rewritten as

$$\mathrm{d}\left(\frac{\omega}{\omega(K)}\right),$$

with $\omega/\omega(K)$ being a closed form. It is also exact with

$$\omega = \omega(K)\ell(K) = \omega(K)\mathrm{d}\tau,$$

due to the Poincaré-Lemma, provided a star domain is considered. This expression is orthogonal to the spatial hypersurfaces defined by constant τ, which parameterizes time, i.e.

$$\omega(X) = \omega(K)\mathrm{d}\tau(X) = 0,$$

for X being a hypersurface tangential vector field as in [Str13]. This orthogonality condition allows to choose specific coordinates, similarly to [Ryd09], who discussed how the orthogonality leads to a special choice of coordinates in the metric case. For the area-metric case the calculations are analogous:
The time coordinate τ defining the integrable hypersurfaces can be related to annother t-α'-coordinate system with

$$\tau(x'^{\alpha}, t),$$

such that

$$\omega = \omega(K)\mathrm{d}\tau = \omega(K)\left(\frac{\partial\tau}{\partial r}\mathrm{d}r + \frac{\partial\tau}{\partial t}\mathrm{d}t\right). \tag{3.47}$$

Here, $\omega(K)$ is the actual norm of the timelike Killing vector field which is a scalar, and hence a coordinate invariant. So, in the$t$-α'-frame one can choose $K' = \partial_t$ with non-vanishing component $K'^t = 1$ and corresponding one-form $\omega'_a = P^{\#'}_{abcd}K'^b K'^c K'^d$.
The norm $\omega(K)$ becomes

$$\begin{aligned}\omega(K) = P^{\#}(K,K,K,K) &= P^{\#}_{abcd}K^a K^b K^d K^c \\ &= P^{\#'}_{defg}K'^d K'^e K'^f K'^g = P^{\#'}_{tttt} = \omega(\partial_t).\end{aligned}$$

On the other hand, direct application of (3.47) to ∂_t leads to

$$\omega(\partial_t) = \omega(K)\left(\partial_t\tau\mathrm{d}t(\partial_t) + \partial_r\tau\mathrm{d}r(\partial_t)\right) = \omega(K)\partial_t\tau = P^{\#'}_{tttt}\partial_t\tau,$$

and thus $\partial_t\tau = 1$ holds. Next, application of (3.47) on $\partial/\partial x^{\alpha'} \equiv \partial_{\alpha'}$ leads to

$$\omega(\partial_{\alpha'}) = P^{\#'}_{ttt\alpha'} = P^{\#'}_{tttt}\partial_{\alpha'}\tau = P^{\#'}_{tttt}\partial_{\alpha'}h, \tag{3.48}$$

where $h(x^{\alpha'})$ is a function of the spatial coordinates.

Consequently, τ is given by

$$\tau(t, x^{'\alpha}) = t + h(x^{\alpha'}),$$

and thus

$$t(\tau, x^{\alpha}) = \tau - h(x^{\alpha}), \tag{3.49}$$

while the spatial coordinates of the t-α'-frame and the τ-α-frame are connected by $x^{\alpha'} = x^{\alpha}$ as also stated in [Ryd09].
While the transformation from t-coordinate to τ-coordinate does not affect the timelike Killing vector field [Ryd09], as well as the component

$$P^{\#}_{\tau\tau\tau\tau} = P'^{\#}_{abcd}\frac{\partial x^{'a}}{\partial\tau}\frac{\partial x^{'b}}{\partial\tau}\frac{\partial x^{'c}}{\partial\tau}\frac{\partial x^{'d}}{\partial\tau} = P'^{\#}_{tttt},$$

one finds the following for the $P^{\#}_{\tau\tau\tau\alpha}$-component

$$P^{\#}_{\tau\tau\tau\alpha} = P'^{\#}_{abcd}\frac{\partial x^{'a}}{\partial\tau}\frac{\partial x^{'b}}{\partial\tau}\frac{\partial x^{'c}}{\partial\tau}\frac{\partial x^{'d}}{\partial x^{\alpha}} = -P'^{\#}_{tttt}\partial_{\alpha}h + P'^{\#}_{ttt\alpha} = 0,$$

due to (3.48). For an area-metric reduced by spherical symmetry and stationarity as discussed in the previous section, the corresponding principal tensor components $P'^{\#}_{ttt\theta} = P'^{\#}_{ttt\phi}$ are zero. Thus, it holds that $\partial_{\theta}h = \partial_{\phi}h = 0$ in this case, so $h(r)$ only depends on the radial parameter. Using the explicit expressions for $P'^{\#}_{tttr}$ and $P'^{\#}_{tttt}$ in the t-α-system results in

$$\partial_r h = \frac{P'^{\#}_{tttr}}{P'^{\#}_{tttt}} = \frac{c_4(r)}{c_5(r)} = N^r(r)\frac{c_6(r)}{c_5(r)}.$$

With this expression for $\partial_r h$ the chart transformation of the area-metric component

$$G_{abcd} = G'_{efgh}\frac{\partial x^{'e}}{\partial x^{a}}\frac{\partial x^{'f}}{\partial x^{b}}\frac{\partial x^{'g}}{\partial x^{c}}\frac{\partial x^{'h}}{\partial x^{d}},$$

when going from the t-α-frame to the τ-α-frame is evaluated: Due to equation (3.49) almost all components of the area-metric G (3.9) are unchanged in the τ-α-frame, except two components, namely $G_{\tau\theta r\theta}$ and $G_{\tau\phi r\phi}$ with

$$G_{\tau\theta r\theta} = G'_{efgh}\frac{\partial x^{'e}}{\partial\tau}\frac{\partial x^{'f}}{\partial\theta}\frac{\partial x^{'g}}{\partial r}\frac{\partial x^{'h}}{\partial\theta} = G'_{t\theta t\theta}\frac{\partial t}{\partial r} + G'_{t\theta r\theta}\frac{\partial r}{\partial r} = -c_5(r)\partial_r h(r) + c_4(r) = 0,$$

and similarly for $G_{\tau\phi r\phi}$. The area-metric components $G_{\tau\theta r\theta}$ and $G_{\tau\phi r\phi}$ in the τ-α-frame are then again proportional to the radial shift vector $N^r_{\tau}(r)$ which vanishes in this frame. This is thus the coordinate system with a hypersurface orthogonal timelike Killing vector field.

By choosing a time parameterisation τ where $G_{\tau\theta r\theta} = c_4(r) = 0$, the Frobenius condition is identically fulfilled. Interestingly, the components $P^{\tau\alpha\beta\gamma}$ and $P^{\tau\tau\tau\alpha}$ of the principal tensor field, as well as their correspoding duals $P^{\#}_{\tau\alpha\beta\gamma}$ and $P^{\#}_{\tau\tau\tau\alpha}$ also vanish in this case. Hence, the according principal polynomial $P(n)$ in (3.18), as well as its dual $P^{\#}(p)$ in (3.10) actually become time-reflection symmetric in these coordiates with $\tau \to -\tau$. This is similar to the metric case where the components $g_{\tau\alpha}$ and $g^{\tau\alpha}$ are zero. Consequently, also the actions for massless particles (1.2) and massive particles (1.6) in area-metric geometry, and thus the associated geodesics need to be time-reflection symmetric. The original notion of staticity is hence regained.

In the first instance, it seemed unclear at first, whether time-reflection symmetry applies already to the area-metric, or only to the principal polynomial. But the Frobenius condition enables a choice of coordinates such, that the notion of staticity in the sense of time-reflection symmetry still applies for the principal polynomial and its dual, but generally not for the area-metric itself. This is possible, since the shift vanishes in this frame.

That in turn is actually not suprising, given that according to [BS03] and also mentioned in [Wol22] there always exists a global diffeomorphism between a hyperbolic spacetime manifold M and $\mathbb{R} \times S$, where S is a smooth Cauchy hypersurface. This means that one can always find a coordinate frame, where the shift becomes identically zero, but never the lapse. Thus, using the Frobenius condition to find the coordinate frame with vanishing shift rather serves as an explicit confirmation of the general findings by [BS03]. Unfortunately, these special coordinate choices do not fulfill symmetric criticality [FT02] in general. Hence, they can only be imposed on the level of the equations of motion. If one was to find those for the area-metric case, this could however help in finding according Schwarzschild type solutions for this spacetime structure.

The first step in the construction of an area-metric Schwarzschild solution is to find the input coefficients for the closure equations similar to [Dü+20], what will be done in the next section. Then it will also be discussed why it is still obstructive to find a general Schwarzschild solution for these spacetimes and how these issues can be addressed in future research.

3.4 Symmetry reduced input coefficients

The gravitational closure equations given in Appendix A are set up via the input coefficients $p^{\#\alpha\beta}$, $F^{A}{}_{\mu}{}^{\gamma}$ and $M^{A\gamma}$. In an area-metric geometry their general structure is given in section 1.5. These input coefficient - which encapsulate the essential kinematical information about the causal structure of area-metric geometry - need to be inserted into the gravitational closure

equation. Then the according gravitational dynamics need to be derived by solving for the output coefficients C, C_A, C_{AB} and $C_{A_1\dots A_N}$ with $N \geq 2$ in the corresponding Lagrangian.
If the spacetime possesses Killing symmetries, the principle of symmetric criticality [FT02] allows to perform a symmetry reduction at the level of the gravitational closure equations, before solving their simplified versions. So, the first step is to find the input coefficients evaluated on spherical symmetry and stationarity. This task can be performed with *Mathematica* for instance. Then, inserting these into the closure equations simplifies their general structure. This was also demonstrated very successfully by [Due20] for FLRW symmetries. The goal is to find corresponding output coefficients for a spherically symmetric, stationary area-metric spacetime. This is, however, still a mathematically highly sophisticated task, even if symmetry reduction is applied. The challenges arising in the solvability in this context will then be discussed at the end of this section.

From the explicit components of the hypersurface fields evaluated on spherical symmetry and stationarity (3.40)-(3.42), and (1.38), one finds the corresponding configuration fields $\varphi^F\big|_{\text{sym}}$ evaluated on symmetries:

$$\begin{aligned}
\bar{\varphi}^A &= \Big(-C_1(r), 0, 0, -C_5(r), 0, -\sin^2(\theta)C_5(r)\Big)^A, \\
\bar{\bar{\varphi}}^A &= \Big(C_7(r), 0, 0, C_6(r), 0, \csc^2(\theta)C_6(r)\Big)^A, \\
\bar{\bar{\bar{\varphi}}}^m &= \left(-\frac{\mathcal{S}(r)\Big(\big(\csc^2(\theta)+1\big)C_1(r)+4C_5(r)\Big)}{\sqrt{6}C_1(r)C_5(r)}, 0, -\frac{\cot(\theta)^2\mathcal{S}(r)}{\sqrt{6}C_5(r)}, 0, \frac{\cot(\theta)^2\mathcal{S}(r)}{\sqrt{3}C_5(r)}\right)^m.
\end{aligned}$$

The non-vanishing components of the coefficient $p^{\#\alpha\beta} = \left(p^{\#-1}\right)^{\alpha\beta}$ are then given by

$$\begin{aligned}
p^{\#rr} &= -\frac{3}{C_1(r)C_5(r)C_6(r)}, \\
p^{\#\theta\theta} &= -\frac{6}{C_5(r)\left(C_5(r)C_6(r)+C_1(r)C_7(r)-9\mathcal{S}(r)^2\right)}, \\
p^{\#\phi\phi} &= \csc^2(\theta)p^{\#\phi\phi}.
\end{aligned}$$

The tangential deformation coefficients $F^{A}{}_{\mu}{}^{\gamma}\big|_{\text{sym}}$ as given in (1.39) and evaluated on symmetric configurations are then given by

$$\begin{aligned}
F^{\bar{A}}{}_{\mu}{}^{\gamma} = {}& \sqrt{2}C_1(r)\Big(\sqrt{2}\delta^{\bar{A}}_1\delta^r_\mu\delta^\gamma_r + \delta^{\bar{A}}_2\delta^r_\mu\delta^\gamma_\theta + \delta^{\bar{A}}_3\delta^r_\mu\delta^\gamma_\phi\Big) + \sqrt{2}C_5(r)\Big(\sqrt{2}\delta^{\bar{A}}_4\delta^\theta_\mu\delta^\gamma_\theta + \delta^{\bar{A}}_2\delta^\theta_\mu\delta^\gamma_r + \delta^{\bar{A}}_5\delta^\theta_\mu\delta^\gamma_\phi\Big) \\
&+ \sqrt{2}\sin^2(\theta)C_5(r)\Big(\sqrt{2}\delta^{\bar{A}}_6\delta^\phi_\mu\delta^\gamma_\phi + \delta^{\bar{A}}_3\delta^\phi_\mu\delta^\gamma_r + \delta^{\bar{A}}_5\delta^\phi_\mu\delta^\gamma_\theta\Big),
\end{aligned}$$

$$
\begin{aligned}
F^{\bar{\bar{A}}\ \gamma}_{\ \mu} &= \sqrt{2}C_7(r)\left(\sqrt{2}\delta_1^{\bar{\bar{A}}}\delta_\mu^r\delta_r^\gamma + \delta_2^{\bar{\bar{A}}}\delta_\mu^\theta\delta_r^\gamma + \delta_3^{\bar{\bar{A}}}\delta_\mu^\phi\delta_r^\gamma\right) + \sqrt{2}C_6(r)\left(\sqrt{2}\delta_4^{\bar{\bar{A}}}\delta_\mu^\theta\delta_\theta^\gamma + \delta_2^{\bar{\bar{A}}}\delta_\mu^r\delta_\theta^\gamma + \delta_5^{\bar{\bar{A}}}\delta_\mu^\phi\delta_\theta^\gamma\right) \\
&\quad + \sqrt{2}\csc^2(\theta)C_6(r)\left(\sqrt{2}\delta_6^{\bar{\bar{A}}}\delta_\mu^\phi\delta_\phi^\gamma + \delta_3^{\bar{\bar{A}}}\delta_\mu^r\delta_\phi^\gamma + \delta_5^{\bar{\bar{A}}}\delta_\mu^\theta\delta_\phi^\gamma\right), \\
F^{\bar{\bar{\bar{m}}}\ \gamma}_{\ \mu} &= -\frac{\mathcal{S}(r)}{C_1(r)}\left(4\sqrt{\frac{2}{3}}\delta_1^{\bar{\bar{\bar{m}}}}\delta_\mu^r\delta_r^\gamma + 2\sqrt{2}\delta_2^{\bar{\bar{\bar{m}}}}\delta_\mu^\theta\delta_r^\gamma + \frac{4}{\sqrt{3}}\delta_3^{\bar{\bar{\bar{m}}}}\delta_\mu^\phi\delta_r^\gamma + 2\sqrt{\frac{2}{3}}\delta_5^{\bar{\bar{\bar{m}}}}\delta_\mu^\phi\delta_r^\gamma\right) \\
&\quad - \frac{\mathcal{S}(r)}{C_5(r)}\left(\sqrt{\frac{2}{3}}\delta_1^{\bar{\bar{\bar{m}}}}\delta_\mu^\theta\delta_\theta^\gamma - \sqrt{2}\delta_2^{\bar{\bar{\bar{m}}}}\delta_\mu^r\delta_\theta^\gamma - \sqrt{\frac{2}{3}}\delta_3^{\bar{\bar{\bar{m}}}}\delta_\mu^\theta\delta_\theta^\gamma - \sqrt{2}\delta_4^{\bar{\bar{\bar{m}}}}\delta_\mu^\phi\delta_\theta^\gamma + \frac{2}{\sqrt{3}}\delta_5^{\bar{\bar{\bar{m}}}}\delta_\mu^\theta\delta_\theta^\gamma\right) \\
&\quad - \frac{\csc^2(\theta)\mathcal{S}(r)}{C_5(r)}\left(\sqrt{\frac{2}{3}}\delta_1^{\bar{\bar{\bar{m}}}}\delta_\mu^\phi\delta_\phi^\gamma - \frac{2}{\sqrt{3}}\delta_3^{\bar{\bar{\bar{m}}}}\delta_\mu^r\delta_\phi^\gamma + \sqrt{\frac{2}{3}}\delta_3^{\bar{\bar{\bar{m}}}}\delta_\mu^\phi\delta_\phi^\gamma - \sqrt{2}\delta_4^{\bar{\bar{\bar{m}}}}\delta_\mu^\theta\delta_\phi^\gamma\right. \\
&\qquad\qquad \left. - \sqrt{\frac{2}{3}}\delta_5^{\bar{\bar{\bar{m}}}}\delta_\mu^r\delta_\phi^\gamma - \frac{2}{\sqrt{3}}\delta_5^{\bar{\bar{\bar{m}}}}\delta_\mu^\phi\delta_\phi^\gamma\right).
\end{aligned}
$$

At last, the normal deformation coefficients $M^{A\gamma}\big|_{\text{sym}}$, given by (1.40), (1.41) and (1.42), need to be evaluated on symmetric configurations, what leads to the following non-vanishing contributions

$$
\begin{aligned}
M^{\bar{A}\gamma} &= \frac{6\sqrt{2}\mathcal{S}(r)\sqrt{-\sin^2(\theta)C_1(r)C_5(r)^2}}{C_5(r)\left(C_5(r)C_6(r) + C_1(r)C_7(r) - 9\mathcal{S}(r)^2\right)}\left(\csc^2(\theta)\delta_2^{\bar{A}}\delta_\phi^\gamma - \delta_3^{\bar{A}}\delta_\theta^\gamma\right), \\
M^{\bar{\bar{A}}\gamma} &= \frac{3\sqrt{2}\mathcal{S}(r)}{\sqrt{-\sin^2(\theta)C_1(r)C_5(r)^2}}\left(\delta_2^{\bar{\bar{A}}}\delta_\phi^\gamma - \delta_3^{\bar{\bar{A}}}\delta_\theta^\gamma\right), \\
M^{\bar{\bar{\bar{m}}}\gamma} &= \frac{\left(C_5(r)C_6(r) - C_1(r)C_7(r) + 3\mathcal{S}(r)^2\right)}{\left(C_5(r)C_6(r) + C_1(r)C_7(r) - 9\mathcal{S}(r)^2\right)\sqrt{-\sin^2(\theta)C_1(r)C_5(r)^2}} \\
&\qquad \times\left(\sqrt{2}\delta_2^{\bar{\bar{\bar{m}}}}\delta_\phi^\gamma - \frac{2}{\sqrt{3}}\delta_3^{\bar{\bar{\bar{m}}}}\delta_\theta^\gamma - \sqrt{\frac{2}{3}}\delta_5^{\bar{\bar{\bar{m}}}}\delta_\theta^\gamma\right).
\end{aligned}
$$

Now, as discussed by [Due20] one also needs to evaluate derivatives of the input coefficients with respect to the configuration fields, and only after derivation they may be evaluated on symmetric configurations. These terms are, however, omitted here.

As a side remark, Section 3.1 has discussed that, if the free function $S(r)$, and thus $\mathcal{S}(r)$ as defined in Section 3.2, was identically zero with

$$
S(r) = \mathcal{S}(r) = 0,
$$

the is no birefringence. The reason is that the principal polynomial and its dual are of metric-induced shape in this case, and the area-metric is also metric induced. As discussed in Section

3.1 the function $c_1(r)$ is then given by

$$c_1(r) = \frac{c_5(r)c_6(r) - c_4(r)^2}{c_7(r)},$$

such that

$$C_1(r) = \frac{1}{N(r)^2}\frac{c_5(r)c_6(r) - c_4(r)^2}{c_7(r)}.$$

Furthermore, inserting the explicit definitions $C_5(r) = \left(c_5(r)c_6(r) - c_4(r)^2\right)/N(r)^2$, $C_6(r) = c_6(r)\sin(\theta)^2/\det\bar{\boldsymbol{g}}$ and $C_7(r) = c_7(r)\sin(\theta)^2/\det\bar{\boldsymbol{g}}$ discussed in Section 3.2, leads to

$$C_5(r)C_6(r) - C_1(r)C_7(r) = 0.$$

Thus, the configuration fields and input coefficients evaluated on symmetric configurations simplify even further: The third field $\bar{\bar{\bar{\varphi}}}^m$, and consequently the third $F^A{}_\mu{}^\gamma$-coefficient, as well as all three $M^{A\gamma}$-coefficients vanish on symmetric configurations with

$$\bar{\bar{\bar{\varphi}}}^m\big|_{\text{sym}} = 0, \;\; F^{\bar{\bar{\bar{m}}}}{}_\mu{}^\gamma\Big|_{\text{sym}} = 0, \;\text{ and }\; M^{A\gamma}\big|_{\text{sym}} = 0.$$

Still, their derivatives evaluated on symmetric configurations do not vanish in general. This is similar to an ansatz with cosmological symmetries for arbitrary spatial curvature K, as discussed by [Due20]; [Fis17]. For FLRW symmetries the free function $\mathcal{S}(r)$ already vanishes on symmetric configurations due to homogeneity, even though there is still a time dependence in the unknown functions.

Now, the main problem in solving the closure equations for spherically symmetric spacetimes, including cosmological spacetimes for $K \neq 0$, is that the non-local deformation $M^{A\gamma}$ coefficient does not vanish identically, unlike in the metric case. Even if it vanishes on specific symmetric configurations, its derivatives generally do not vanish, what leads to a more complicated structure of the equations. Especially equation $(C19_{N\geq 2})$ leads, once $M^{A\gamma}$ and all of its spatial derivatives vanish, to the collapse of the dependency of $C\left(\varphi, \partial\varphi, \cdots \partial^n\varphi\right)$ to second spatial derivative order in the configuration fields $C\left(\varphi, \partial\varphi, \partial^2\varphi\right)$, as shown by [Dü+18]; [Due20]; [Wol22]. Unfortunately, this does not hold in the case considered here. So, due to the collapse problem it is generally unclear up to which derivative order C_A maximally depends. Even in the metric case this is not restricted, but that does not pose a problem there, since C_A then becomes a boundary term (see [Wol22] for a thorough discussion). However, for the area-metric case these conclusions cannot be drawn in general. Only for flat FLRW spacetime in area-metric geometry [Due20]; [Fis17] the collapse problem can be circumvented, because

the configuration fields φ^F do not depend on spatial coordinates in this case. Consequently, contractions with derivative terms like $C_{:A}{}^{\gamma\alpha_1\ldots\alpha_K}$ and $C_{B:A}{}^{\gamma\alpha_1\ldots\alpha_K}$ with K unknown but finite, drop out of the closure equations, such that they are simplified significantly. But since this does not work in general, the collapse problem makes it still unclear how to continue with the solution scheme. However, possible outlooks to this problem will be given in the next section. If the collapse problem was fixed, the closure equations would still have a harder structure compared to the flat FLRW case, but might then be solvable.

3.5 Summary and outlook

In this section the spherically symmetric, stationary area-metric ansatz made by [PWS09], as well as the according dispersion relations and their implications on light propagation, were reproduced. Then the $3+1$-split of the area-metric spacetime was studied, and the connection between the Frobenius condition and staticity were discussed. Additionally, the symmetry reduced kinematic input coefficients for the closure equations were evaluated, and the general problems in solving these equations were discussed.

The greatest difficulty in the solution scheme arises due to the missing collapse to known derivative order $\partial^n\varphi$ for the dependencies of the output coefficients C and C_A. However, one might only be interested in a subset of solutions for which at most $C(\varphi, \partial\varphi, \partial^2\varphi)$ and $C_A(\varphi, \partial\varphi, \partial^2\varphi)$, though it is unclear, if there is also interesting physical information in higher order derivative terms. Hence, before making the effort in solving the very involved structure of closure equations, it needs to be clarified whether or why it would even be possible to make assumptions on the dependencies of the output coefficients.

As discussed by [Wol22], the collapse problem may be addressed by directly demanding that the principal polynomial $P_{\text{matter}}(x,k)$ of the matter theory is equal to the principal polynomial $P_{\text{gravity}}(x,k)$ of the gravity theory. This is a very reasonable assumption given that one wants to ensure a consistent co-evolution of the initial hypersurface data for matter fields and the gravitational field: [Wol22] mentions that for matter theories the equations of motion generally contain the same number of temporal and spatial derivatives, which would not be the case for the equations of motion of a gravity theory, given that the output coefficients C and C_A can depend on arbitrary derivative order $\partial^n\varphi$. But then, according to [Wol22], $\mathrm{d}t$ is a characteristic co-vector for the geometric symbol, and thus also for the principal polynomial of the gravity action. Contrary $\mathrm{d}t$ is a timelike co-vector for the principal polynomial of the matter action. Hence, this hints at the fact that a compatibility condition between these principal polynomials needs to be found to fix the collapse problem. However, even if a rigorous mathematical proof is still missing, this argument already implies that a collpase of the dependencies of C and

C_A to lower order derivative order, as for instance $\partial^2\varphi$, needs to occur. The higher derivative order dependencies of the coefficients C and C_A would then only appear as boundary terms [Wol22]. These are dynamically irrelevant, and do not affect the causality structure set by the principal polynomial.
All in all, the solution to the collapse problem is the bottleneck for finding specific solutions for the gravitational closure equations: If this problem was fixed, the gravitational dynamics could then possibly be found, for instance with methods explained by [Wol22] in more detail.

4 Intrinsic and extrinsic gravitational flexions

The results on intrinsic flexions presented in section 4.4.1 of this chapter, and parts of section 4.2 indicated therein have been published in
E. S. Giesel, B. Ghosh and B. M. Schäfer,
Monthly Notices of the Royal Astronomical Society (December 2021), 510, 2773–2789,
Intrinsic and extrinsic gravitational flexions.
Further discussion concerning details on the numerical value of the alignment parameter and updated plots have been updated on *ArXiv* arXiv:2107.09000v3.

After having discussed basic ideas about constructive gravity and its set-up for symmetries in spherically symmetric spacetime, the following chapter will introduce and investiagte an entirely different topic, namely intrinsic alignment and intrinsic flexions in classical gravity. Intrinsic alignment describes how galaxies orient themselves and deform inside tidal fields in their surroundings. In turn, intrinsic flexion describe this deformation due to gradients of the tidal fields. While these concepts seem to be unconnected to the first part of this thesis, the ideas laid out in the following chapter concerning the modelling of linear alignments, as well as the machinery summarized to calculate lensing spectra will become important in Chapter 5. There, the ideas of intrinsic alignment and lensing on the one hand, and solutions of the constructive gravity program in weakly birefringent spacetimes on the other hand, will be combined to study how area-metric refinements will affect observable quantities in lensing.
This chapter is structures as follows: After giving a short introduction to basic ideas on gravitational lensing as a summary of [BS01]; [Bar10]; [BM17]; [SEF92] and the gravitational lensing flexion, one will further develop the linear alignment model for elliptical galaxies discussed in [GDS21] to intrinsic flexions. Afterwards the observability of this effect will be discussed for a survey like *Euclid*.

4.1 Introduction to gravitational lensing: General description of image distortions

In gravitational lensing [BS01] the light reaching the observer from far away galaxies is deflected at the position of a gravitational lens, which could be a galaxy cluster or a large-scale distribution of dark matter for instance. Mathematically, this is described by the lens or ray

tracing equation [BS01]; [SEF92]

$$\boldsymbol{\beta} = \boldsymbol{\theta} - \boldsymbol{\alpha}(\boldsymbol{\theta}),$$

where $\boldsymbol{\beta}$ is the actual angular position of the source on the sky and $\boldsymbol{\theta}$ is the angular postion of the image on the sky, i.e. the position where the observer sees the source. The reduced deflection angle $\boldsymbol{\alpha} = D_{\mathrm{ds}}/D_{\mathrm{s}}\,\hat{\boldsymbol{\alpha}}$ is defined by the deflection angle $\hat{\boldsymbol{\alpha}}$ times the ratio of the angular diameter distances between the lens and the source D_{ds} and between the observer and the source D_{s}, as depicted in 4.1. One way to derive this lens equation in the frame-

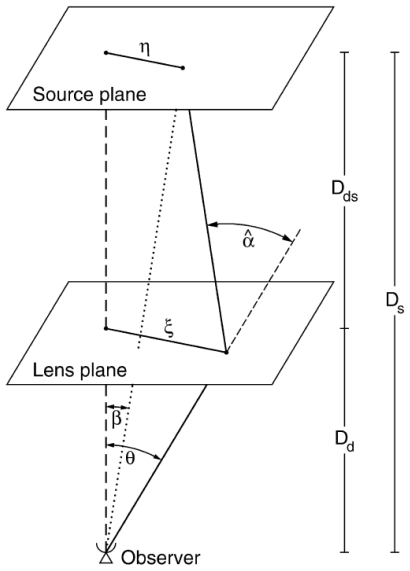

Figure 4.1: **Depiction of the lens-system**: For the observer the source appears under an angle $\boldsymbol{\theta}$ due to light deflection in the lens-plane with angular diameter distance D_{d} from the observer. If there was no gravitational lens, the source would appear under the true angle $\boldsymbol{\beta}$, so the light is deflected by the deflection angle $\hat{\boldsymbol{\alpha}}$. With the distance from the source to the observer D_{s} and the distance from the lens-plane to the source plane D_{ds} it is possible to convert the deflection angle $\hat{\boldsymbol{\alpha}}$ to the reduced deflection angle as the difference between $\boldsymbol{\theta}$ and $\boldsymbol{\beta}$. The figure is taken from [BS01].

work of general relativity is by solving, for instance, the geodesic deviation equation which describes the relative deflection of infinitesimally distant light rays as they propagate to the observer through a spacetime perturbed by a Newtonian gravitational potential Φ/c^2 of the lens [Bar19a]; [Bar19b].
Alternatively, one can derive an index of refraction $n = c'/c = 1 - 2\Phi/c^2$ from the weak field line-element, i.e.

$$\mathrm{d}s^2 = c^2\left(1 + 2\Phi/c^2\right)\mathrm{d}t^2 - \left(1 - 2\Phi/c^2\right)\mathrm{d}x_\alpha \mathrm{d}x^\alpha,$$

and then extremize the optical path of the light ray from the source to the observer using Fermat's principle, as is for instance discussed in [SEF92]; [BS01] [1]. This will lead to the following expression for the reduced deflection angle

$$\boldsymbol{\alpha} = \boldsymbol{\nabla}_{\perp} \frac{2}{c^2} \frac{D_{\mathrm{ds}}}{D_{\mathrm{s}}} \int \Phi \, \mathrm{d}z \,, \tag{4.1}$$

where the gradient of the potential perpendicular to the line-of-sight is integrated along the latter, i.e. from the observer to the source. At this point of the derivation Born's approximation [Bar19a] is used by integrating along the straight, unperturbed line-of-sight, instead of the actual light path. This simplification applies, since the magnitude of the deflection angles is often much smaller compared to the length of the integration path. Lensing effects for the case where Born's approximation does not hold are for instance discussed in [Sch+12]. For cosmological lensing the derivation is similar because the FLRW-line element perturbed with a Newtonian potential is used, as discussed in [SEF92]. The result will be very similar due to the conformal flatness of FLRW spacetime, so light-propagation works similar to flat Minkowskian spacetime. The distances D_{ds} and D_{s} denote the angular diameter distances which are defined by the ratio between the cross section area δA of an object and the solid angle $\delta\Omega$ under which it appears [Bar19a]. They are generally different from the euclidean distance in a non-flat geometry like FLRW spacetime.
Now, as for example stated in [BM17], the perpendicular gradient $\boldsymbol{\nabla}_{\perp}$ can be expressed in terms of a gradient $\boldsymbol{\nabla}_{\theta} = D_{\mathrm{d}}^{-1} \boldsymbol{\nabla}_{\theta}$ with respect to the apparent angular position $\boldsymbol{\theta}$, where D_{d} is the angular diameter distance from lens to observer. Subsequently, the reduced deflection angle $\boldsymbol{\alpha}$ from equation (4.1) can be written as the angular gradient of the *lensing potential* Ψ, via

$$\begin{aligned} \boldsymbol{\alpha} &= \boldsymbol{\nabla}_{\theta} \Psi \,, \\ \Psi &:= \frac{2}{c^2} \frac{D_{\mathrm{ds}}}{D_{\mathrm{s}} D_{\mathrm{d}}} \int \Phi \mathrm{d}z \,, \end{aligned}$$

such that the ray tracing equation becomes[2]

$$\boldsymbol{\beta} = \boldsymbol{\theta} - \boldsymbol{\nabla} \psi \,. \tag{4.2}$$

[1] Conerning notation Greek letters α are used to denote spatial indices running from 1 to 3, even though the conventional notation would be to use Latin indices here instead. However, since in the Chapters 1 to 3 the notation by [Dü+18] was adopted, Greek letters were used for spatial indices, and Latin letters for spacetime indices, one will stick to this unconventional notation here, to be consistent with the previous chapters.
[2] To simplify notation the subscript θ of the angular gradient $\boldsymbol{\nabla}_{\theta}$ is dropped in the remainder of this chapter.

Since the actual size of the source $\delta\boldsymbol{\beta}$ is generally much smaller compared to changes in the deflection angle $\delta\boldsymbol{\theta}$ [BM17] one can approximate the ray tracing equation (4.2) by a first order Taylor expansion in $\boldsymbol{\theta}$ as

$$\delta\beta_i \approx \frac{\partial\beta_i}{\partial\theta_j}\delta\theta_j = \mathcal{A}_{ij}\delta\theta_j = \left(\delta_{ij} - \Psi_{ij}\right)\delta\theta_j \text{ with } \Psi_{ij} \coloneqq \frac{\partial^2\Psi}{\partial\theta_i\partial\theta_j}\,. \tag{4.3}$$

In this so-called lens map (4.3), the Jacobian $\mathcal{A}$, is a symmetric tensor in two dimensions[3] - provided that Schwarz's rule[4] applies for Ψ_{ij}. Then, it has three degrees of freedom, denoted by the convergence

$$a_0 \coloneqq \kappa = \frac{1}{2}\left(\Psi_{00} + \Psi_{11}\right)\,, \tag{4.4}$$

which leads to an effective distortion in the size of the image, and the two shear components

$$a_3 \coloneqq \gamma_+ = \frac{1}{2}\left(\Psi_{00} - \Psi_{11}\right) \quad \text{and} \quad a_1 \coloneqq \gamma_\times = \Psi_{01} = \Psi_{10}\,. \tag{4.5}$$

which lead to a distortion in the shape of the image. Hence, $\mathcal{A}$ acquires the following shape [SEF92]:

$$\mathcal{A} = \begin{pmatrix} 1-\kappa-\gamma_+ & -\gamma_\times \\ -\gamma_\times & 1-\kappa+\gamma_+ \end{pmatrix} = \mathbb{1} - \kappa\sigma^{(0)} - \gamma_+\sigma^{(3)} - \gamma_\times\sigma^{(1)} = \sum_{k=0}^{k=3} a_k\sigma^{(k)}. \tag{4.6}$$

Since it has three independent components, a basis decomposition of the Jacobian in equation (4.6) into the three Pauli matrices

$$\sigma^{(0)} = \begin{pmatrix} 1 & 0 \\ 0 & 1 \end{pmatrix},\ \sigma^{(1)} = \begin{pmatrix} 0 & 1 \\ 1 & 0 \end{pmatrix},\ \sigma^{(3)} = \begin{pmatrix} 1 & 0 \\ 0 & -1 \end{pmatrix},$$

as described in [Sch+12] makes it possible to extract the various effects of image distortion due to lensing. As a side remark, the second Pauli matrix

$$\sigma^{(2)} = \begin{pmatrix} 0 & -\mathrm{i} \\ \mathrm{i} & 0 \end{pmatrix},$$

measuring image rotations is antisymmetric, and since the Jacobian is supposed to be symmetric there is in fact no contribution from $\sigma^{(2)}$. Finally, the convergence and the two shear

[3] In gravitational lensing one explicitly considers images projected on a two dimensional screen, hence the indices i and j run from 0 to 1.

[4] If the Born approximation is dropped, for instance, the Jacobian $\mathcal{A}$ is generally not symmetric in higher order correction terms, what is discussed in more detail in [Sch+12].

components can be recovered by projecting

$$a_k = \frac{1}{2}\mathrm{Tr}\left((\mathbb{1} - \mathcal{A})\,\sigma^{(k)}\right),$$

using the properties $\sigma^{(i)}\sigma^{(j)} = \mathbb{1}\delta_{ij} + \mathrm{i}\epsilon_{ijk}\sigma^{(k)}$ and $\mathrm{Tr}\left(\sigma^{(k)}\right) = 0$ with $k > 0$ of the Pauli matrices [Sch+12].

Since for weak lensing, the image of a source is projected into a two-dimensional plane, it is convenient to describe lensing effects using a complex number representation [Bac+06]. With the complex gradient operator ∂ and its complex conjugate

$$\partial = \partial_0 + \mathrm{i}\partial_1, \quad \text{and} \quad \partial^* = \partial_0 - \mathrm{i}\partial_1\,, \tag{4.7}$$

one can define the deflection angle from the scalar lensing potential Ψ as a vector valued quantity $\alpha = \partial\psi$ with spin 1. As such it has the required transformation behaviour for the operator ∂ transforms as $\partial \to \partial \exp(\mathrm{i}\phi)$ under rotation with angle ϕ. The convergence κ can then be derived in the complex notation as

$$\kappa = \frac{1}{2}\partial^*\alpha = \frac{1}{2}\partial^*\partial\Psi\,,$$

which is again a scalar, and hence a spin-0 quantity. The operator ∂ is to be understood as a spin raising operator, while ∂^* acts as a spin lowering operator [Bac+06]. The complex shear γ can then be defined as a spin-2 field with

$$\gamma = \gamma_+ + \mathrm{i}\gamma_\times = \frac{1}{2}\partial\partial\Psi\,,$$

which clearly transforms accordingly as $\gamma \to \gamma \exp(\mathrm{i}2\phi)$ with ϕ as rotation angle.

Using this complex notation simplifies the derivation of higher order lensing distortions by repeatedly applying the spin ladder operators onto the convergence and shear. For each derivative order the according spin field decomposition can be infered. This is for instance discussed in section 4.2 for the lensing flexion as the next order image distortion.

Now, one can measure the shear and size changes of the image compared to the source via the normalised quadrupole moment

$$q_{ij} = \frac{\int \mathrm{d}^2\theta\, I(\theta)\,\Delta\theta_i\Delta\theta_j}{\int \mathrm{d}^2\theta\, I(\theta)},$$

of the surface brightness distribution $I(\theta)$. Now, according to [BS01] the complex ellipticity χ is defined as

$$\chi = \frac{q_{11} - q_{22} + 2\mathrm{i}q_{12}}{q_{11} + q_{22}}\,.$$

Using the lens map (4.3) a transformation law between the source ellipticity χ^s, also called intrinsic ellipticity, and the observed, lensed ellipticity χ, can be derived, as discussed in [BS01]. In the weak lensing limit with $\kappa \ll 1$ and $|\gamma| \ll 1$ this leads to

$$\langle\chi\rangle \approx \langle\chi^s\rangle + 2\gamma,$$

as average of the observed ellipticities.
To first order approximation $\langle\chi^s\rangle$ is often assumed to vanish for large samples [BM17], but in general there is the possibility of a correction due to intrinsic alignment.

4.2 Flexions in weak lensing

In [Bac+06]; [GB05] the spin operators from equation (4.7) are applied on the comlex shear in order to derive the flexion as third order image distortion. The flexion generally measures how bent an image appears, as it might be forming for instance an arc shape. More specifically one can distinguish a spin-1 flexion field

$$\mathcal{F} = \frac{1}{2}\partial\partial^*\partial\Psi = \partial\kappa = \partial^*\gamma\,,$$

causing the galaxy center to appear shifted to the observer, illustratively speaking similar to a fried egg, and a spin-3 field

$$\mathcal{G} = \frac{1}{2}\partial\partial\partial\Psi = \partial\gamma\,,$$

which gives rise to a 3-fold symmetry of the image, analogical to a Mercedes star.
Clearly, under rotation with angle ϕ these transform as $\mathcal{F} \to \mathcal{F}\exp(\mathrm{i}\phi)$ and $\mathcal{G} \to \mathcal{G}\exp(3\mathrm{i}\phi)$.
The flexion fields may now be expressed in terms of the shear components as

$$\mathcal{F} = \mathcal{F}_1 + \mathrm{i}\mathcal{F}_2 = (\partial_0\gamma_+ + \partial_1\gamma_\times) + \mathrm{i}\,(\partial_0\gamma_\times - \partial_1\gamma_+)\,, \tag{4.8}$$

$$\mathcal{G} = \mathcal{G}_1 + \mathrm{i}\mathcal{G}_2 = (\partial_0\gamma_+ - \partial_1\gamma_\times) + \mathrm{i}\,(\partial_0\gamma_\times + \partial_1\gamma_+)\,. \tag{4.9}$$

The flexions can be related to the ray tracing equation (4.2) by expanding the latter to second order in the lensed coordinates, as discussed in [Bac+06], yielding a refined lens map

$$\delta\beta_i \approx \frac{\partial\beta_i}{\partial\theta_j}\delta\theta_j + \frac{1}{2}\frac{\partial\beta_i}{\partial\theta_j\partial\theta_k}\delta\theta_j\delta\theta_k = \mathcal{A}_{ij}\delta\theta_j + \frac{1}{2}D_{ijk}\delta\theta_j\delta\theta_k\,. \tag{4.10}$$

By fixing the index k the tensor

$$D_{ijk} \equiv \partial_k \mathcal{A}_{ij} = \mathcal{F}_{ijk} + \mathcal{G}_{ijk}$$

may then be represented as

$$\left(D_{ij0}\right)_{i=1,2;j=1,2} = \begin{pmatrix} -2\partial_0\gamma_+ - \partial_1\gamma_\times & -\partial_0\gamma_\times \\ -\partial_0\gamma_\times & \partial_1\gamma_\times \end{pmatrix} = -\frac{1}{2}\begin{pmatrix} 3\mathcal{F}_1 & \mathcal{F}_2 \\ \mathcal{F}_2 & \mathcal{F}_1 \end{pmatrix} - \frac{1}{2}\begin{pmatrix} \mathcal{G}_1 & \mathcal{G}_2 \\ \mathcal{G}_2 & -\mathcal{G}_1 \end{pmatrix}, \tag{4.11}$$

with $D_{ij0} = \mathcal{F}_{ij0} + \mathcal{G}_{ij0}$ and

$$\left(D_{ij1}\right)_{i=1,2;j=1,2} = \begin{pmatrix} -\partial_0\gamma_\times & -\partial_1\gamma_\times \\ -\partial_1\gamma_\times & 2\partial_1\gamma_+ - \partial_0\gamma_\times \end{pmatrix} = -\frac{1}{2}\begin{pmatrix} \mathcal{F}_2 & \mathcal{F}_1 \\ \mathcal{F}_1 & 3\mathcal{F}_2 \end{pmatrix} - \frac{1}{2}\begin{pmatrix} \mathcal{G}_2 & -\mathcal{G}_1 \\ -\mathcal{G}_1 & -\mathcal{G}_2 \end{pmatrix}, \tag{4.12}$$

with $D_{ij1} = \mathcal{F}_{ij1} + \mathcal{G}_{ij1}$. The derivatives of the matrix components of $\mathcal{A}$ are explicitly evaluated, and identified with the corresponding flexion expressions.

As for the Jacobian $\mathcal{A}$ it is now possible to find an orthonormal decomposition for the flexion tensor D_{ijk}: In [Sch+12] the $2 \times 2 \times 2$ flexion tensor can be rewritten in terms of a 4×4-block diagonal matrix $\mathcal{D}$ with components $(\mathcal{D})_{i+2k,j+2k} = D_{ijk}$ as

$$\mathcal{D} = \begin{pmatrix} \left(D_{ij0}\right)_{i=1,2;j=1,2} & 0 \\ 0 & \left(D_{ij1}\right)_{i=1,2;j=1,2} \end{pmatrix}.$$

This can then be decomposed into a set of 4×4-Dirac matrices as a generalisation of the Pauli matrices and in [Sch+12] one finds for instance 6 distinct Dirac matrices with

$$\tilde{\Delta}^{(i)} = \begin{pmatrix} \sigma^{(i)} & 0 \\ 0 & \sigma^{(i)} \end{pmatrix} \quad \text{and} \quad \tilde{\Delta}^{(3+i)} = \begin{pmatrix} \sigma^{(i)} & 0 \\ 0 & -\sigma^{(i)} \end{pmatrix}.$$

However, in the course of this work the tensor D_{ijk} is symmetric in all its three indices, unlike in [Sch+12] where the authors explicitly consider lens-lens coupling and investigate the effect of loosening the assumption of Born's approximation. There, the corresponding rank-3 tensor D_{ijk} discussed in [Sch+12] is only symmetric in the last two indices leading to six degrees of freedom. Here, in contrast, the rank-3 tensor D_{ijk} has only 4 degrees of freedom, which reduces the number of linearly independet basis matrices. These are, however, still similar to the Dirac matrices. It is now possible to derive the proper decompostion of D_{ijk} by following

the derivation from $\mathcal{A}$ as in [Bac+06] but based on its decomposition (4.6):

$$\begin{aligned}\mathcal{D} &= \begin{pmatrix} \left(D_{ij0}\right)_{i=1,2;j=1,2} & 0 \\ 0 & \left(D_{ij1}\right)_{i=1,2;j=1,2} \end{pmatrix} = \begin{pmatrix} \partial_0 \left(\mathcal{A}_{ij}\right)_{i=1,2;j=1,2} & 0 \\ 0 & \partial_1 \left(\mathcal{A}_{ij}\right)_{i=1,2;j=1,2} \end{pmatrix} \\ &= -\begin{pmatrix} \partial_0\kappa\sigma^{(0)} + \partial_0\gamma_+\sigma^{(3)} + \partial_0\gamma_\times\sigma^{(1)} & 0 \\ 0 & \partial_1\kappa\sigma^{(0)} + \partial_1\gamma_+\sigma^{(3)} + \partial_1\gamma_\times\sigma^{(1)} \end{pmatrix}.\end{aligned}$$

Due to equations (4.4) and (4.5) it follows, that

$$\partial_0\kappa = \partial_0\gamma_+ + \partial_1\gamma_\times, \quad \text{and} \quad \partial_1\kappa = -\partial_1\gamma_+ + \partial_0\gamma_\times\,.$$

This shows, that the required four degrees of freedom of $\mathcal{D}$ can solely be expressed by derivatives of the shear components $\partial_0\gamma_+$, $\partial_1\gamma_+$, $\partial_0\gamma_\times$ and $\partial_1\gamma_\times$. It follows that

$$\begin{aligned}\mathcal{D} = &-\partial_0\gamma_+\begin{pmatrix}\sigma^{(0)}+\sigma^{(3)} & 0\\ 0 & 0\end{pmatrix} - \partial_1\gamma_+\begin{pmatrix}0 & 0\\ 0 & \sigma^{(3)}-\sigma^{(0)}\end{pmatrix} \\ &-\partial_0\gamma_\times\begin{pmatrix}\sigma^{(1)} & 0\\ 0 & \sigma^{(0)}\end{pmatrix} - \partial_1\gamma_\times\begin{pmatrix}\sigma^{(0)} & 0\\ 0 & \sigma^{(1)}\end{pmatrix}.\end{aligned}$$

Now, using the relations (4.8) and (4.9) one can combine the derivatives of the shear such, that the 4 distinct degrees of freedom may be rewritten in terms of the two distinct spin fields $\mathcal{F}$ and $\mathcal{G}$ with

$$\begin{aligned}\partial_0\gamma_+ &= \frac{\mathcal{F}_1 + \mathcal{G}_1}{2}, \quad \text{and} \quad \partial_1\gamma_+ = \frac{\mathcal{G}_2 - \mathcal{F}_2}{2}, \\ \partial_0\gamma_\times &= \frac{\mathcal{F}_2 + \mathcal{G}_2}{2}, \quad \text{and} \quad \partial_1\gamma_\times = \frac{\mathcal{F}_1 - \mathcal{G}_1}{2}.\end{aligned}$$

This leads to the following decomposition in terms of the flexion fields, consistent with the results of [Bac+06]:

$$\begin{aligned}\mathcal{D} = &-\frac{1}{2}\mathcal{F}_1\begin{pmatrix}2\sigma^{(0)}+\sigma^{(3)} & 0\\ 0 & \sigma^{(1)}\end{pmatrix} - \frac{1}{2}\mathcal{F}_2\begin{pmatrix}\sigma^{(1)} & 0\\ 0 & 2\sigma^{(0)}-\sigma^{(3)}\end{pmatrix} \\ &-\frac{1}{2}\mathcal{G}_1\begin{pmatrix}\sigma^{(3)} & 0\\ 0 & -\sigma^{(1)}\end{pmatrix} - \frac{1}{2}\mathcal{G}_2\begin{pmatrix}\sigma^{(1)} & 0\\ 0 & \sigma^{(3)}\end{pmatrix}.\end{aligned} \tag{4.13}$$

This would in principle be a valid decomposition into Dirac-type matrices, which are linearly independent by definition. That can be confirmed by contracting the various matrices in equation (4.13) with each other, using that the Pauli matrices themselves form an orthonormal basis

and are traceless. However, for the contractions

$$\frac{1}{4}\mathrm{Tr}\left(\begin{pmatrix} 2\sigma^{(0)}+\sigma^{(3)} & 0 \\ 0 & \sigma^{(1)} \end{pmatrix}\cdot\begin{pmatrix} 2\sigma^{(0)}+\sigma^{(3)} & 0 \\ 0 & \sigma^{(1)} \end{pmatrix}\right) = 3,$$
$$\frac{1}{4}\mathrm{Tr}\left(\begin{pmatrix} \sigma^{(1)} & 0 \\ 0 & 2\sigma^{(0)}-\sigma^{(3)} \end{pmatrix}\cdot\begin{pmatrix} \sigma^{(1)} & 0 \\ 0 & 2\sigma^{(0)}-\sigma^{(3)} \end{pmatrix}\right) = 3,$$

are not normalized to one, a normalization factor $1/\sqrt{3}$ is introduced in front of the basis matrices of the $\mathcal{F}$-flexion field. Then the orthonormal decomposition of D_{ijk} is given by

$$\begin{aligned}\mathcal{D} =& d_1\frac{1}{\sqrt{3}}\begin{pmatrix} 2\sigma^{(0)}+\sigma^{(3)} & 0 \\ 0 & \sigma^{(1)} \end{pmatrix} + d_2\frac{1}{\sqrt{3}}\begin{pmatrix} \sigma^{(1)} & 0 \\ 0 & 2\sigma^{(0)}-\sigma^{(3)} \end{pmatrix} \\ &+ d_3\begin{pmatrix} \sigma^{(3)} & 0 \\ 0 & -\sigma^{(1)} \end{pmatrix} + d_4\begin{pmatrix} \sigma^{(1)} & 0 \\ 0 & \sigma^{(3)} \end{pmatrix},\end{aligned} \tag{4.14}$$

where the coefficients are given by

$$d_1 \coloneqq -\frac{\sqrt{3}}{2}\mathcal{F}_1,\ d_2 \coloneqq -\frac{\sqrt{3}}{2}\mathcal{F}_2,\ d_3 \coloneqq -\frac{1}{2}\mathcal{G}_1,\ \text{and } d_4 \coloneqq -\frac{1}{2}\mathcal{G}_2.$$

The corresponding Dirac-type matrix bases for the spin-1 field $\mathcal{F}$ and the spin-3 field $\mathcal{G}$ are then given by

$$\text{spin-1-types: } \Delta^{(1)} = \frac{1}{\sqrt{3}}\begin{pmatrix} 2\sigma^{(0)}+\sigma^{(3)} & 0 \\ 0 & \sigma^{(1)} \end{pmatrix}, \tag{4.15}$$
$$\Delta^{(2)} = \frac{1}{\sqrt{3}}\begin{pmatrix} \sigma^{(1)} & 0 \\ 0 & 2\sigma^{(0)}-\sigma^{(3)} \end{pmatrix}, \tag{4.16}$$
$$\text{spin-3-types: } \Delta^{(3)} = \begin{pmatrix} \sigma^{(3)} & 0 \\ 0 & -\sigma^{(1)} \end{pmatrix}, \tag{4.17}$$
$$\Delta^{(4)} = \begin{pmatrix} \sigma^{(1)} & 0 \\ 0 & \sigma^{(3)} \end{pmatrix}. \tag{4.18}$$

Consequently, one receives the distinct degrees of freedom of the flexion field by the following projection

$$d_k = \frac{1}{4}\mathrm{Tr}\left(\mathcal{D}\cdot\Delta^{(k)}\right),$$

with $k = 1, 2, 3, 4$.

4.3 Measurement of the flexion in weak lensing

Similar to convergence and shear the flexion field is an abstract concept which can, however, be directly measured by its consequential distortion of the surface brightness distribution $I(\theta)$. While for the apparent shape and size changes due to weak lensing the quadrupole moment q_{ij} is usually considered, the flexions are quantified via the so-called Higher Order Lensing Image's Characteristics or HOLICs first introduced by [OUF07]. They combine the normalized octopole moments

$$q_{ijk} = \frac{\int \mathrm{d}^2\theta\, I(\theta)\, \Delta\theta_i \Delta\theta_j \Delta\theta_k}{\int \mathrm{d}^2\theta\, I(\theta)},$$

and the normalized hexadecapole moments

$$q_{ijkl} = \frac{\int \mathrm{d}^2\theta\, I(\theta)\, \Delta\theta_i \Delta\theta_j \Delta\theta_k \Delta\theta_l}{\int \mathrm{d}^2\theta\, I(\theta)},$$

to a spin-1 quantity which measures the $\mathcal{F}$-flexion

$$\zeta = \frac{(q_{000} + q_{011}) + \mathrm{i}\,(q_{001} + q_{111})}{\xi},$$

and a spin-3 quantity which measures the $\mathcal{G}$-flexion

$$\delta = \frac{(q_{000} - 3q_{011}) + \mathrm{i}\,(3q_{001} - q_{111})}{\xi}.$$

Here, ξ is a spin-0 normalization factor

$$\xi = q_{0000} + 2q_{0011} + q_{1111}.$$

Clearly the definition shows, that the HOLICs ζ and δ, and thus also the flexions, should be given in units of inverse angle.

[OUF07] then establish a relation between the source octopole moments q^s_{ijk} with coordinates $\boldsymbol{\theta}$ and the measured image octopole moments q_{ijk} with coordinates $\boldsymbol{\beta}$ via a higher order expansion in the lens equation (4.10) which finally leads them to the following first order relation between the observable HOLICs and the flexion fields:

$$\langle \zeta \rangle \approx \langle \zeta^s \rangle + \frac{9}{4}\mathcal{F}, \tag{4.19}$$

$$\langle \delta \rangle \approx \langle \delta^s \rangle + \frac{3}{4}\mathcal{G}. \tag{4.20}$$

Here, $\langle\zeta\rangle$ and $\langle\delta\rangle$ are the expectation values of the totally measured spin-1 and the spin-3 HOLICs, while $\langle\zeta^s\rangle$ and $\langle\delta^s\rangle$ denote the expectation values of the intrinsic source HOLICs. These will be denoted by $\langle\Delta\zeta\rangle$ and $\langle\Delta\delta\rangle$ as the intrinsic flexions of the intrinsic alignment model discussed in equations (4.39) and (4.40) in the latter course of this work. In [OUF07] one explicitly assumes that the expectation values of the intrinsic HOLICs average to zero over a sufficiently large sample. However, the necessary corrections due to intrinsic alignment - and their correlation with lensing flexions - will be quantified using a Jeans-model for the potential perturbations in section 4.4.1.
As a side remark, [OUF07] refine their relations (4.19) and (4.20) by taking a centroid shift of the true galaxy center to an apparent center due to lensing into account. This actually leads to a correction term in the prefactor of the flexion-HOLIC relation, which will, however, be neglected in the calculations of the present work. Taking it into account does, in turn, achieve higher accuracy in calculating the correlation functions.

At last, it should be stressed that neither lensing ellipticities nor flexions can simply be directly measured in particular directions, because the unlensed shape of the galaxy is unknown. Instead, different lensing quantities need to be compared at different positions on the sky [BM17]. This means that one actually needs to measure angular correlations of the lensing quantities $x(\boldsymbol{\theta})$, where the correlation function is given by

$$\zeta(\Delta\boldsymbol{\theta}) \coloneqq \langle x(\boldsymbol{\theta})\, x(\boldsymbol{\theta}+\Delta\boldsymbol{\theta})\rangle\,.$$

The brackets $\langle....\rangle$ stand for an ensemble average. For homogeneous random fields the corresponding Fourier transform of the correlation function is considered. The corresponding spectrum $C(\ell)$ is given by

$$C(\ell) = \int \mathrm{d}^2\psi\, \zeta(\psi) \exp\left(-\mathrm{i}\boldsymbol{\ell}\cdot\boldsymbol{\psi}\right),$$

where $\boldsymbol{\ell}$ is the angular wave vector corresponding to the angular separation $\Delta\boldsymbol{\theta} = \boldsymbol{\psi}$ in real space [BM17] with magnitude ℓ. More details on the power spectrum and its application in cosmology and gravitational lensing can be found in standard literature like [Bar19a]; [Dur08].

4.4 Intrinsic flexions in a linear alignment model for elliptical galaxies

After having discussed how flexions arise in weak lensing, this section is dedicated to the description of intrinsic gravitational flexions. First, basic ideas about intrinsic alignment will

be reviewed briefly, and afterwards it is shown how intrinsic flexions can be quantified and measured via a linear intrinsic alignment model. The measurability should then be evaluated for surveys like *Euclid* and compared to the measurability of weak lensing flexions.

4.4.1 Summary of basic ideas about intrinsic alignment

Intrinsic alignment of galaxies occurs if these are subject to tidal gravitational fields, for example within clusters (see [SKW06]; [Hir+04]; [Hir+07]; [HS10]; [BM17]; [GDS21]; [SCH09] for more details). The tidal interaction of foreground galaxies with the local large-scale sturcture (LSS) causes them to align accordingly and leads to intrinsic shape deformations, like intrinsic ellipticities and other types of shape and size distortions. These have to be dinstinguished from image distortion effects of background galaxies caused by gravitational lensing.
In fact, the alignment effects will generallly contaminate the weak lensing signal, thereby modifying the expected weak lensing spectrum. This will consequently lead to systematic uncertainties in weak lensing measurements of up to 10% (see [Hir+04]; [HS10]; [BM17] for more details), for instance in the determination of cosmological parameters, like $\sigma_8 = 0.8$. This parameter is a measure for the correlation of density fluctuations within cosmic structures at scales larger than $R = 8h^{-1}$Mpc, where $h = 0.7$ is the Hubble parameter. Thus, to reach higher accuracy, the weak lensing signal with angular power spectrum C_{GG} has to be corrected by an intrinsic shape or size correlation of the foreground galaxies measured by the spectrum C_{II}. Here the subscript II denotes the self-correlation of intrinsic shape distortions, while the subscript GG denotes the lensing self-correlation. Furthermore, there is a cross-correlation $C_{GI}(\ell)$ between the apparent shape change of background galaxies due to lensing as integrated effect and the actual physical shape change of foreground galaxies aligned in local tidal field. This is reasonable, for both effects are caused by the same tidal field.
Then the total angular power spectrum $\tilde{C}$ is given by

$$\tilde{C}(\ell) = C_{GG}(\ell) + C_{GI}(\ell) + C_{II}(\ell),$$

similar to [HS10]. For the totally measured power spectrum one would generally also need to add annother noise term. There is, however, no cross-correlation term $C_{IG}(\ell)$ between the intrinsic shape for a background galaxy and the lensing effect for a foreground galaxy, as intrinsic alginment only happens locally. Thus, the shape of the background galaxy is generally not affected by the tidal field of the lens deflecting light of the foreground galaxy, due to the mutual distance.
All in all, it is important to quantify the effects of intrinsic alignment and their correlation

to image distortions in lensing to reduce systematic errors in the measurement of cosmological parameters. Furthermore, intrinsic alignment can be considered as a useful tool to study possible deviation from general relativity towards modified gravity theories, as is for instance discussed by [Rei+22]. There the authors studied how intrinsic alignment in combination with gravitational lensing can be used to test Horndeski gravity, which is however restricted by the precision of the intrinsic alignment parameter D_{IA}, which will be explained in detail in the following sections. This parameter basically gives a measure for the sensitivity of the galaxies to align in the tidal fields, and its precise value is still debated upon, as discussed by [GDS21]; [Rei+22]. Values within magnitudes of $D \simeq 10^{-4}\,(\mathrm{Mpc/h})^2$ [TS18]; [Hil+17] to $D \simeq 10^{-6}\,(\mathrm{Mpc/h})^2$ [ZSH22] were found from measurements and simulations, while [GDS21] chose to set the alignment parameter to $D \simeq 10^{-5}\,(\mathrm{Mpc/h})^2$. All in all, the magnitude of the alignment parameter is thus determined up to a factor of 10, so for now its value is assumed to lie between $D \simeq 10^{-6}\,(\mathrm{Mpc/h})^2$ and $D \simeq 10^{-5}\,(\mathrm{Mpc/h})^2$. However, as will be discussed in section 4.4.3 in more detail, a rescaling of the alignment parameter will be necessary for the numerical evaluation. In this section, one will also summarize the linear alignment model specified by [GDS21] based on ideas of [Pir+17] for intrinsic ellipticities and sizes and their correlations with lensing shear and convergence. This linear description on intrinsic alignment was first introduced by [Hir+07]; [HS10]. The main goal of the next section is to extended and develop this linear alignment model further to derive the according instrinsic flexion spectra.

4.4.2 Description of intrinsic shapes and flexions

To understand the change of intrinsic ellipticity of a galaxy within a tidal field locally sourced by the surrounding LSS, the authors of [GDS21] investigate how the stellar density $\rho(r)$ within the galaxies is altered due to a second order perturbation in the Newtonian gravitational field. Assuming that this density change should result in an imediate and linear reaction of the galaxy size and shape itself [GDS21], the second order moments of the corresponding surface brightness distribution[5] $\rho(r)$ - from which the intrinsic ellipticities and shear can be infered - vary accordingly. The size of the galaxies changes because the volume element is altered due to a non-vanishing Ricci curvature such that the change in size directly scales with $\Delta\Phi$ [GDS21]. To model the unperturbed gravitational field one approximates with a virialised, self-gravitating, spherical system in steady state with constant velocity dispersion σ^2 and vanishing averaged velocity such that the Jeans-equation, as discussed in [Pir+17] applies:

$$\sigma^2 \partial_r \ln\left(\rho(r)\right) = -\partial_r \Phi\,.$$

[5]The surface brightness distribution $I(\theta)$ is clearly proportional to the stellar density such that higher order moments of the former can be directly infered from $\rho(r) \propto I(\theta)$.

Consequently, the stellar density of the unperturbed system is given by

$$\rho(r) \propto \exp\left(-\frac{\Phi(r)}{\sigma^2}\right), \tag{4.21}$$

what is maximized at the galaxy center set at $r = 0$, where the potential is minimized. Under the gravitational influence of surrounding matter one can also perturb the gravitational field to third order to receive

$$\Phi(r) \;\rightarrow\; \Phi(r) + \frac{1}{2}\partial_a\partial_b\Phi\, r^a r^b + \frac{1}{3!}\partial_a\partial_b\partial_c\Phi\, r^a r^b r^c, \tag{4.22}$$

where the - for the moment - spatial derivatives of the potential, abbreviated by $\partial_{r_a} \equiv \partial_a$, are evaluated at the center of the galaxy. As shown in [GDS21] the tidal tensor $\partial_a\partial_b\Phi$ gives rise to intrinsic ellipticities.
Now, the variation of the tidal tensor $\partial_a\partial_b\partial_c\Phi$ should give rise to intrinsic flexions, leading to bent galaxy shapes, similar to the flexion of gravitational lensing [Bac+06]. In [GDS21] it is furthermore assumed that projected quantities should be proportional to $\rho(r)$, such that it does conceptually not make a difference to consider $\rho(r)$ as the 2-dimensional projected quantity on the celestial sphere[6]. Hence, the indices a,b and c run from 0 to 1, where

$$r_0 = r\cos(\phi) \quad \text{and} \quad r_1 = r\sin(\phi)$$

are the polar coordinates for the spherically shaped, unperturbed galaxy. Next, inserting the expansion (4.22) into equation (4.21), assuming that the tidal field and its derivative are small, a first-order Taylor expansion with respect to the higher order derivatives of Φ leads to the following perturbed density profile $\rho'(r)$:

$$\rho'(r) \propto \exp\left(-\frac{\Phi(r)}{\sigma^2}\right)\left(1 - \frac{1}{2\sigma^2}\partial_a\partial_b\Phi\, r^a r^b - \frac{1}{3!\sigma^2}\partial_a\partial_b\partial_c\Phi\, r^a r^b r^c\right). \tag{4.23}$$

In [GDS21] perturbations up to second order are considered only, so the term $\partial_a\partial_b\partial_c\Phi$ is negelected there.
Under these circumstances, the second moment of the surface brightness distribution, i.e. the quadrupole

$$q_{ab} = \int \mathrm{d}^2 r\, \rho'(r) r_a r_b$$

[6] In fact one could explicitly calculate the projected quantities from the unprojected ones via an Abel transform [AW05]. This would however only account for a correction factor of order one and is hence neglected for simplicity, as in [GDS21].

would be altered in the following way [GDS21]:

$$\Delta q_{cd} = \int \mathrm{d}^2 r\, \rho(r) r_c r_d r_a r_b \, \frac{\partial_a \partial_b \Phi}{2\sigma^2} = \tilde{S}_{abcd} \Phi_{ab} \,, \tag{4.24}$$

with $\Phi_{ab} \equiv \partial_a \partial_b \Phi$ and

$$\begin{aligned}
\tilde{S}_{abcd} &\equiv \frac{1}{2\sigma^2} \int \mathrm{d}^2 r\, \rho(r) r_c r_d r_a r_b \\
&= \underbrace{\frac{1}{2\sigma^2} \int_0^\infty \mathrm{d}r\, r^5 \rho(r)}_{:= D_e} \underbrace{\int_0^{2\pi} \mathrm{d}\phi \cos(\phi)^{4-(a+b+c+d)} \sin(\phi)^{a+b+c+d}}_{:= S_{abcd}} \\
&= D_e S_{abcd},
\end{aligned}$$

where the radial integral gives rise to an (unnormalized) alignment parameter D_e, and S_{abcd} is the angular integral, also called susceptibility, which is totally symmetric in all four indices. Inclusion of the third order term $\partial_a \partial_b \partial_c \Phi$ does in fact not alter the result of [GDS21] for the second moment of the surface brightness. This can be shown by the following calculation for Δq_{ab} with $\partial_a \partial_b \partial_c \Phi \neq 0$:

$$\begin{aligned}
\Delta q_{cd} &= \int \mathrm{d}^2 r\, \rho(r) r_c r_d \left(r_a r_b \, \frac{\Phi_{ab}}{2\sigma^2} + r_a r_b r_e \, \frac{\Phi_{abe}}{6\sigma^2} \right) \\
&= D_e S_{abcd} \Phi_{ab} + \int \mathrm{d}^2 r\, \rho(r) r_c r_d r_a r_b r_e \frac{\Phi_{abe}}{6\sigma^2} \\
&= D_e S_{abcd} \Phi_{ab} + \frac{1}{6\sigma^2} \int_0^\infty \mathrm{d}r\, r^6 \rho(r) \underbrace{\int_0^{2\pi} \mathrm{d}\phi \cos^{5-(a+b+c+d+e)} \phi \sin^{a+b+c+d+e} \phi}_{:= S_{abcde}} \Phi_{abe}.
\end{aligned}$$

One can quickly verify that the angular integral S_{abcde}, which is totally symmetric, vanishes for any index combination, i.e.

$$S_{abcde} = \int_0^{2\pi} \mathrm{d}\phi \, \cos^{5-A} \phi \sin^A \phi = 0 \quad \text{for } A \text{ ranging from 0 to 5} \,,$$

where $A = a + b + c + d + e$ is the sum over the small indices, each of them ranging from 0 to 1. Thus Δq_{cd} is independent of Φ_{abe} and is only sourced by the tidal field.
However, the third order term $\partial_a \partial_b \partial_c \Phi$ gives rise to a perturbation in the third order moment of the surface brightness distribution, i.e. in the octopole moment

$$q_{abc} = \int \mathrm{d}^2 r\, \rho'(r) r_a r_b r_c \,.$$

This change of the octopole moment in turn does not depend on the tidal field $\partial_a\partial_b\Phi \equiv \Phi_{ab}$, but only its derivative $\partial_a\partial_b\partial_c\Phi \equiv \Phi_{abc}$. Now, the third moment of the brightness distribution Δq_{abc} changes according to

$$\begin{aligned}
\Delta q_{abc} =& \int \mathrm{d}^2 r\, \rho(r) r_a r_b r_c \left(r_d r_e \frac{\Phi_{de}}{2\sigma^2} + r_d r_e r_f \frac{\Phi_{def}}{6\sigma^2} \right) \\
=& \frac{1}{2\sigma^2} \int_0^\infty \mathrm{d}r\, r^6 \rho(r) \underbrace{\int_0^{2\pi} \mathrm{d}\phi\, \cos^{5-(a+b+c+d+e)}\phi \sin^{a+b+c+d+e}\phi}_{=0} \Phi_{de} \\
&+ \underbrace{\frac{1}{6\sigma^2} \int_0^\infty \mathrm{d}r\, r^7 \rho(r)}_{:=D_f} \underbrace{\int_0^{2\pi} \mathrm{d}\phi\, \cos^{6-(a+b+c+d+e+f)}\phi \sin^{a+b+c+d+e+f}\phi}_{:=S_{abcdef}} \Phi_{def} \\
=& D_f S_{abcdef} \Phi_{def} \,.
\end{aligned} \tag{4.25}$$

While the term proportional to Φ_{de} drops out because it again contains the vanishing angular integral S_{abcde}, the third derivative of the potential Φ_{def} leads to effective changes in the third order brightness moment. The radial part of the integral in equation (4.25) leads to an unnormalized linear alignment parameter D_f once more, which is however differently defined than D_e. For the angular integral S_{abcdef} one receives the following values:

$$\begin{aligned}
S_{abcdef} =& \int_0^{2\pi} \mathrm{d}\phi\, \cos^{6-(a+b+c+d+e+f)}\phi \sin^{a+b+c+d+e+f}\phi \\
=& \int_0^{2\pi} \mathrm{d}\phi\, \cos^{6-B}\phi \sin^{B}\phi \quad \text{for } B = a+b+c+d+e+f \text{ ranging from 0 to 6}\,, \\
=& \begin{cases} \frac{5\pi}{8} & \text{for } B = 0 \text{ and } B = 6\,, \\ 0 & \text{for } B = 1,\, B = 3 \text{ and } B = 5\,, \\ \frac{\pi}{8} & \text{for } B = 2 \text{ and } B = 4\,. \end{cases}
\end{aligned} \tag{4.26}$$

So for the susceptibility factor S_{abcdef} which is totally symmetric in all its indices the only non-vanishing contributions are $S_{000000} = S_{111111} = \frac{5\pi}{8}$ and $S_{000011} = S_{111100} = \frac{\pi}{8}$ and respective symmetric perturbations.

Next, an appropriate decomposition of Φ_{abc} into an orthonormal basis[7] is introduced to extract the linearly independent contributions to the third order distortions of the galaxy shape, i.e. the intrinsic flexions. In analogy to the lensing flexions discussed in Chapter 4.2 the follow-

[7] A decomposition of Φ_{ab} into a basis of Pauli matrices $\sigma^{(n)}_{ab}$, similar to the decomposition in weak lensing given by relation (4.6), is thoroughly discussed in [GDS21].

ing decomposition of Φ_{abc} into four 4×4 block-diagonal Dirac-type matrices $\Delta^{(n)}$ with the 2×2 Pauli matrices $\sigma^{(n)}$ as entries is proposed. These matrices account for intrinsic shape distortions with either spin-1 or spin-3 symmetry:

$$\text{spin 1: } \Delta^{(1)} = \frac{1}{\sqrt{3}} \begin{pmatrix} 2\sigma^{(0)} + \sigma^{(3)} & 0 \\ 0 & \sigma^{(1)} \end{pmatrix}, \; \Delta^{(2)} = \frac{1}{\sqrt{3}} \begin{pmatrix} \sigma^{(1)} & 0 \\ 0 & 2\sigma^{(0)} - \sigma^{(3)} \end{pmatrix}, \tag{4.27}$$

$$\text{spin 3: } \Delta^{(3)} = \begin{pmatrix} \sigma^{(3)} & 0 \\ 0 & -\sigma^{(1)} \end{pmatrix}, \; \Delta^{(4)} = \begin{pmatrix} \sigma^{(1)} & 0 \\ 0 & \sigma^{(3)} \end{pmatrix}. \tag{4.28}$$

As the lensing potential Ψ is sourced by the Newtonian potential Φ of the same structure responsible for the intrinsic alignment effect, íts third derivative $\partial_a \partial_b \partial_c \Psi \equiv \Psi_{abc}$ is proportional to Φ_{abc}. Consequently, the same decomposition into the Dirac-type matrices (4.27) and (4.28) for Φ_{abc} as for Ψ_{abc} in Chapter 4.2 can be used. This is also a reasonable choice since Φ_{abc} and Ψ_{abc} are symmetric in all their indices, and thus have four degrees of freedom. Hence, one can evaluate the change of the galaxy shape ζ_1 modulo D_f caused by interaction with $\Phi_{abc} \propto \Delta^{(1)}$ as

$$\zeta_1 = \frac{1}{4} \Delta q_{abc} \Delta^{(1)}_{abc} \propto \frac{1}{4} S_{abcdef} \Delta^{(1)}_{def} \Delta^{(1)}_{abc} = \frac{3\pi}{4} \,. \tag{4.29}$$

The change in shape ζ_2 modulo D_f generated by $\Phi_{abc} \propto \Delta^{(2)}$ is similarly given by

$$\zeta_2 = \frac{1}{4} \Delta q_{abc} \Delta^{(2)}_{abc} \propto \frac{1}{4} S_{abcdef} \Delta^{(2)}_{def} \Delta^{(2)}_{abc} = \frac{3\pi}{4} \,. \tag{4.30}$$

Both ζ_1 and ζ_2 measure an intrinsic centroid shift of the galaxy for they arise due to distortions with spin-1 symmetry. Similarly, the change of shape δ_1 modulo D_f due to $\Phi_{abc} \propto \Delta^{(3)}$ is received via

$$\delta_1 = \frac{1}{4} \Delta q_{abc} \Delta^{(3)}_{abc} \propto \frac{1}{4} S_{abcdef} \Delta^{(3)}_{def} \Delta^{(3)}_{abc} = \frac{\pi}{4} \,, \tag{4.31}$$

while δ_2 modulo D_f is generated by $\Phi_{abc} \propto \Delta^{(4)}$ with

$$\delta_2 = \frac{1}{4} \Delta q_{abc} \Delta^{(4)}_{abc} \propto \frac{1}{4} S_{abcdef} \Delta^{(4)}_{def} \Delta^{(4)}_{abc} = \frac{\pi}{4} \,. \tag{4.32}$$

These account for intrinsic shape distortions which cause the galaxy to establish a three-fold spin-3 symmetry. Importantly, tidal fields proportional to $\Delta^{(n)}$ will not excite distortion modes proportional to $\Delta^{(m)}$ if $n \neq m$, because the Dirac matrices form an orthonormal basis[8]. Interestingly, the observable changes in (4.31) and (4.32) due to the spin-3 field are one third of the distortions caused by the spin-1 field.

[8] A similar observation for intrinsic ellipticities and their composition into a basis of Pauli matrices is discussed in [GDS21].

As a side remark, it is sketched in the following how the values given in equations (4.29) to (4.32) can be explicitly derived. Here the $2 \times 2 \times 2$-tensorial objects Δq_{abc} should be appropriately represented as 4×4 symmetric block-diagonal matrices, so that they can be reasonably contracted with the 4×4-Dirac matrices $\Delta^{(n)}$. At first, the octopole moments of the surface brightness distribution Δq_{abc} in equations (4.29) to (4.32) may be recast into a 4×4 block diagonal matrix $\Delta\tilde{q}$ with components $\Delta\tilde{q}_{a+2c,b+2c} = \Delta q_{abc}$ such, that

$$\begin{aligned} \Delta\tilde{q} &\equiv \begin{pmatrix} (\Delta q_{ab0})_{a=1,2;b=1,2} & 0 \\ 0 & (\Delta q_{ab1})_{a=1,2;b=1,2} \end{pmatrix} \\ &= \begin{pmatrix} \left(S_{ab0def}\Delta^{(n)}_{def}\right)_{a=1,2;b=1,2} & 0 \\ 0 & \left(S_{ab1def}\Delta^{(n)}_{def}\right)_{a=1,2;b=1,2} \end{pmatrix}. \end{aligned} \tag{4.33}$$

Here $S_{ab0def}\Delta^{(n)}_{def}$ and $S_{ab1def}\Delta^{(n)}_{def}$ are components of 2×2 matrices each. Now, these components $S_{abcdef}\Delta^{(n)}_{def}$ in (4.33) which are contracted over the indices d,e and f according to Einstein's sum convention need to be computed. Therefore, the susceptibility S_{abcdef} can also be represented by a block-diagonal 4×4 matrix $\tilde{S}$ with

$$\tilde{S} \equiv \begin{pmatrix} (S_{abc\,de0})_{d=1,2;e=1,2} & 0 \\ 0 & (S_{abc\,de1})_{d=1,2;e=1,2} \end{pmatrix},$$

where $S_{abc\,de0}$ and $S_{abc\,de1}$ are in turn components of 2×2 matrices, but now with indices e and d ranging from 0 to 1. Then, the contraction $S_{abcdef}\Delta^{(n)}_{def}$ can be computed as trace over the matrix product between $\tilde{S}$ and the Dirac-type matrix $\Delta^{(n)}$. Afterwards, taking the trace over the matrix product between $\Delta\tilde{q}$ and the Dirac-type matrix $\Delta^{(n)}$ finally leads to the explicit results (4.29) to (4.32).

Next, the unnormalized alignment parameter D_f for the intrinsic flexion is analyzed. It will be related to the unnormalized alignment parameter D_e for the intrinsic ellipticities to compare the magnitude of the two alignment effects. To explicitly compute the radial integrals the projected stellar density $\rho(r)$ is now modelled by the empirical Sérsic profile [Sér63]; [GD05]; [Vau48]

$$\rho(r) \propto \exp\left(-b(n)\left[\left(\frac{r}{r_0}\right)^{n^{-1}} - 1\right]\right), \tag{4.34}$$

with

$$b(n) \approx 2n - \frac{1}{3},$$

and n being the Sérsic index. Using this profile the authors [GDS21] derived the normalized alignment parameter $\tilde{D}_e$ for the relative change of the instrinsic ellipticities as

$$\begin{aligned}\Delta\varepsilon =& \frac{\Delta q_{00} - \Delta q_{11}}{q_{00} + q_{11}} + 2\mathrm{i}\frac{\Delta q_{01}}{q_{00} + q_{11}} = \frac{\mathrm{tr}\left(\Delta q_{ab}\sigma^{(3)}_{ab}\right)}{\mathrm{tr}\left(q_{ab}\sigma^{(0)}_{ab}\right)} + \mathrm{i}\frac{\mathrm{tr}\left(\Delta q_{ab}\sigma^{(1)}_{ab}\right)}{\mathrm{tr}\left(q_{ab}\sigma^{(0)}_{ab}\right)} \\ \propto& \frac{\int_0^\infty \mathrm{d}r\,\rho(r)r^5}{\int_0^\infty \mathrm{d}r\,\rho(r)r^3} \equiv \tilde{D}_e\,.\end{aligned} \tag{4.35}$$

Here, the change in the quadrupole moments Δq_{ab} is proportional to $D_e \propto \int_0^\infty \mathrm{d}r\rho(r)r^5$, and is normalized with respect to the size s_0 of the unperturbed galaxy

$$s_0 \propto q_{00} + q_{11} = \int \mathrm{d}^2 r\,\rho(r)\left(r_0^2 + r_1^2\right) = 2\pi\int_0^\infty \mathrm{d}r\,\rho(r)r^3.$$

Inserting the Sérsic profile (5.19) into the expression (4.35) and substituting

$$x = b\left[(r/r_{\mathrm{scale}})^{n^{-1}} - 1\right] \tag{4.36}$$

into the radial integrals, the authors of [GDS21] receive

$$\tilde{D}_e = r_{\mathrm{scale}}^2\,\frac{\int_{-b}^\infty \mathrm{d}x\;(x/b+1)^{6n-1}\exp(-x)}{\int_{-b}^\infty \mathrm{d}x\;(x/b+1)^{4n-1}\exp(-x)}, \tag{4.37}$$

where r_{scale} is a scale radius for the typical size of an elliptical galaxy. Now, these integrals of type

$$\int_{-b}^\infty \mathrm{d}x\,\left(\frac{x}{b}+1\right)^{m-1}\exp(-x), \tag{4.38}$$

may be further rewritten in terms of the Gamma function $\Gamma(z)$ [GD05], generally defined by

$$\Gamma(z) = \int_0^\infty \mathrm{d}t\,t^{z-1}\exp\left(-t\right).$$

This can be done by substituting $y = x + b$ into (4.38), as shows the following calculation:

$$\begin{aligned}\int_{-b}^{\infty} \mathrm{d}x \left(\frac{x}{b}+1\right)^{m-1} \exp(-x) &= \int_{-b}^{\infty} \mathrm{d}x \left(\frac{1}{b}\right)^{m-1} (x+b)^{m-1} \exp(-x) \\ &= \int_{0}^{\infty} \mathrm{d}y \left(\frac{1}{b}\right)^{m-1} y^{m-1} \exp(-y+b) \\ &= \frac{\exp(b)}{b^{m-1}} \int_{0}^{\infty} \mathrm{d}y\, y^{m-1} \exp(-y) \\ &= \frac{\exp(b)}{b^{m-1}} \Gamma(m).\end{aligned}$$

Hence $\tilde{D}_e$ in equation (4.37) is given accordingly by

$$\tilde{D}_e = r_{\mathrm{scale}}^2 \frac{\int_{-b}^{\infty} \mathrm{d}x\ (x/b+1)^{6n-1} \exp(-x)}{\int_{-b}^{\infty} \mathrm{d}x\ (x/b+1)^{4n-1} \exp(-x)} = r_{\mathrm{scale}}^2 b^{-2n} \frac{\Gamma(6n)}{\Gamma(4n)}.$$

While the exact numerical value of the normalized alignment parameter $\tilde{D}_e$ needs to be measured or inferred from simulations, its scaling with the Sérsic index n can still be determined. Similarly one may calculate the normalized alignment parameter $\tilde{D}_f$ for the intrinsic flexions from the change of the HOLICs ([OUF07]) as introduced in section 4.3. However, in the following discussion the HOLICs should - for the moment - be defined as higher order moments of the projected stellar density distribution $\rho(r)$ in spatial coordinates. This is possible since $I(\theta) \propto \rho(r(\theta))$. In Section 4.4.4 these HOLICs will then again be rewritten as higher order moments of the surface brightness distribution. Thus, using the definitions of the quantities ζ_1, ζ_2, δ_1 and δ_2 given in equations (4.29) to (4.32) the intrinsic HOLICs can be expressed as follows:
The HOLIC with spin-1 symmetry is given by

$$\begin{aligned}\text{spin 1 HOLIC:}\quad \Delta\zeta &= \frac{4/\sqrt{3}\zeta_1 + \mathrm{i}4/\sqrt{3}\zeta_2}{\xi} = \frac{1/\sqrt{3}\left(\Delta q_{abc}\Delta^{(1)}_{abc}\right) + \mathrm{i}/\sqrt{3}\left(\Delta q_{abc}\Delta^{(2)}_{abc}\right)}{\xi} \\ &= \frac{(\Delta q_{000} + \Delta q_{011}) + \mathrm{i}\,(\Delta q_{001} + \Delta q_{111})}{\xi},\end{aligned} \tag{4.39}$$

while for the HOLIC with spin-3 symmetry one finds

$$\begin{aligned}\text{spin 3 HOLIC:}\quad \Delta\delta &= \frac{4\delta_1 + \mathrm{i}4\delta_2}{\xi} = \frac{\left(\Delta q_{abc}\Delta^{(3)}_{abc}\right) + \mathrm{i}\left(\Delta q_{abc}\Delta^{(4)}_{abc}\right)}{\xi} \\ &= \frac{(\Delta q_{000} - 3\Delta q_{011}) + \mathrm{i}\,(3\Delta q_{001} - \Delta q_{111})}{\xi}.\end{aligned} \tag{4.40}$$

Here, the normalization factor $\xi = q_{0000} + 2q_{0011} + q_{1111}$ which has zero spin is given by the trace over the unperturbed hexadecapole moment $q_{abcd} = \int \mathrm{d}^2 r\, \rho(r) r_a r_b r_c r_d$. It can be explicitly calculated via its representation as a 4×4 matrix $\tilde{q}$ with components $\tilde{q}_{a+2c,b+2d} = q_{abcd}$ such that

$$\tilde{q} \equiv \begin{pmatrix} (q_{ab00})_{a=1,2;b=1,2} & (q_{ab01})_{a=1,2;b=1,2} \\ (q_{ab10})_{a=1,2;b=1,2} & (q_{ab11})_{a=1,2;b=1,2} \end{pmatrix}.$$

This is analogous to equation (4.33), but now there are also 2×2-block matrices in the off-diagonal part. As a side remark, one will find a different basis decompostion into Dirac-type matrices for fourth order perturbations in the field Φ_{abcd}, which relates to the various changes to the hexadecapole moment. In that context, the trace of this higher-order moment would just be a spin-0 distortion, while there would also be distortions of type spin-2 and spin-4 (see also [OUF07]).

As shown by relation (4.25), the changes in the octopole moments of the brightness distribution Δq_{abc} are proportional to $D_f \propto \int_0^\infty \mathrm{d}r\, \rho(r) r^7$, while for the normalization factor ξ of the unperturbed distribution one now receives

$$\begin{aligned}\xi &= q_{0000} + 2q_{0011} + q_{1111} = \int \mathrm{d}^2 r\, \rho(r) \left(r_0^4 + 2r_0^2 r_1^2 + r_1^4\right) \\ &= \int \mathrm{d}^2 r\, \rho(r) r^4 = 2\pi \int_0^\infty \mathrm{d}r\, \rho(r) r^5.\end{aligned}$$

Hence, the normalized alignment parameter $\tilde{D}_f$ for the intrinsic flexions is given by

$$\begin{aligned}\Delta\zeta, \Delta\delta \propto \tilde{D}_f &\equiv \frac{\int_0^\infty \mathrm{d}r\, \rho(r) r^7}{\int_0^\infty \mathrm{d}r\, \rho(r) r^5} \\ &= r_{\mathrm{scale}}^2 \frac{\int_{-b}^\infty \mathrm{d}x\ (x/b+1)^{8n-1} \exp(-x)}{\int_{-b}^\infty \mathrm{d}x\ (x/b+1)^{6n-1} \exp(-x)} \\ &= r_{\mathrm{scale}}^2 b^{-2n} \frac{\Gamma(8n)}{\Gamma(6n)},\end{aligned} \tag{4.41}$$

for the Sérsic profile.
Here, the same substitution as given in equation (4.36) was inserted and r_{scale} is, as before, the scaling radius for the galaxy size. Next, it may be shown how the ratio of these different normalized alignment parameters $\tilde{D}_e$ and $\tilde{D}_f$ scales with varying Sérsic index n as

$$\frac{\tilde{D}_f}{\tilde{D}_e} = \frac{\Gamma(8n)\Gamma(4n)}{\Gamma(6n)^2}. \tag{4.42}$$

This susceptibility ratio is illustrated in Figure 4.2 for different values of the Sérsic index n, together with the scalings of the susceptibility for intrinsic ellipticities proportional to $\tilde{D}_e$, and for the intrinsic flexions proportional to $\tilde{D}_f$ for arbitrary scale radius. While both $\tilde{D}_e$ and $\tilde{D}_f$ grow by several orders of magnitude with increasing Sérsic index, the susceptibility ratio grows significantly less in comparison. Especially for small Sérsic indices the susceptibillity ratio implies that both the intrinsic flexions and intrinsic ellipticities are of the same order of magnitude. For $n = 1$ (exponential profile) a ratio of $\tilde{D}_f/\tilde{D}_e = 2.1$ is received, while for the other extreme choice of $n = 4$ (de Vaucouleurs-profile) the ratio is given by $\tilde{D}_f/\tilde{D}_e = 16.1$. Higher Sérsic indices than $n = 4$ occur very rarely and are consequently irrelevant for the discussion here.

4.4.3 Relations between intrinsic flexions and intrinsic sizes and shapes

In [GDS21] the intrinsic size caused by the tidal field $\partial_a\partial_b\Phi = \Phi_{ab}$ is shown to be given by the Laplacian of the potential $\Delta\Phi$ due to

$$\begin{aligned}
s =& \frac{1}{2}\Delta q_{cd}\sigma^{(0)}_{cd} = \frac{1}{2}\int \mathrm{d}^2r\,\rho(r) r_a r_b \frac{\Phi_{ab}}{2\sigma^2} \underbrace{r_c r_d \sigma^{(0)}_{cd}}_{r_0^2+r_1^2=r^2} \\
=& \frac{1}{2}\int \mathrm{d}^2r\,\rho(r) r^2 \frac{1}{2}\left(r_a r_b \frac{\Phi_{ab}}{2\sigma^2}\right) = \frac{1}{2}\int \mathrm{d}^2r\,\rho(r) r^2 \frac{1}{2\sigma^2}\left(r_0^2\Phi_{00} + 2r_0r_1\Phi_{01} + r_1^2\Phi_{11}\right) \\
=& \int_0^{2\pi} \mathrm{d}\phi \int \mathrm{d}r\, r^5 \rho(r) \frac{1}{4\sigma^2}\left(\cos^2(\phi)\,\partial_0^2\Phi + 2\cos(\phi)\sin(\phi)\,\partial_0\partial_1\Phi + \sin^2(\phi)\,\partial_1^2\Phi\right) \\
=& \frac{\pi}{2} D_e \left(\partial_0^2\Phi + \partial_1^2\right)\Phi = \frac{\pi}{2} D_e \Delta\Phi.
\end{aligned} \tag{4.43}$$

Next, with the relations (4.29) and (4.30) it will be shown how changes in the intrinsic size s can be related to the intrinisc spin-1 flexion field. The terms ζ_1 and ζ_2 are explicitly calculated in terms of third order derivatives of the potential $\partial_a\partial_b\partial_c\Phi \equiv \Phi_{abc}$, and the resulting

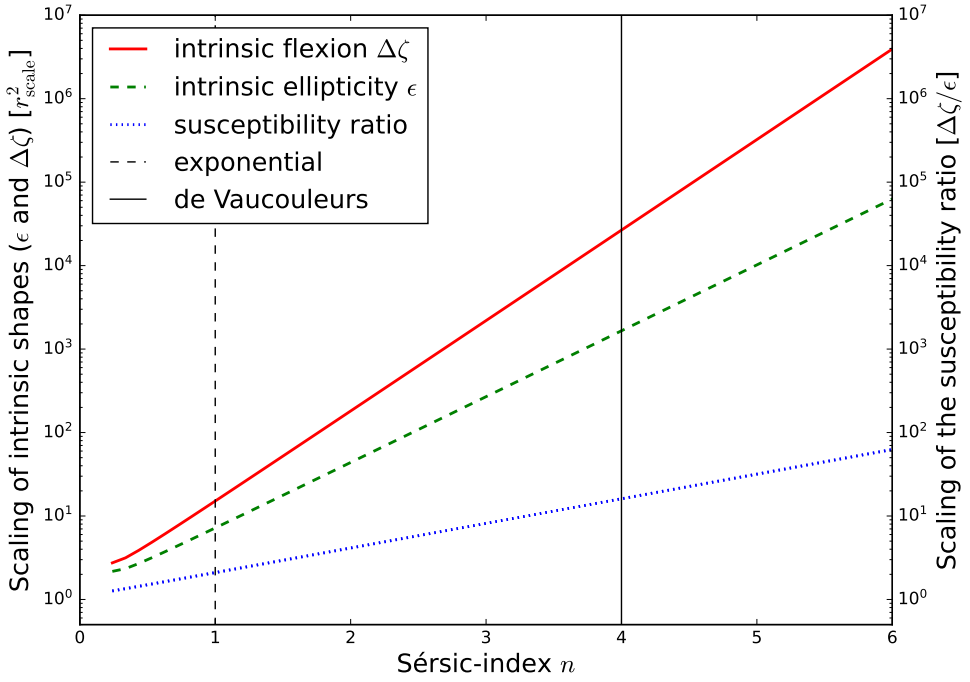

Figure 4.2: **Scaling of the alignment parameters for intrinsic shapes and their ratio with different Sérsic indices:** The scaling of the alignment parameters (with magnitude given on the left axis) for both intrinsic ellipticities $\tilde{D}_e$ (depicted as ε on the green curve) and flexions $\tilde{D}_f$ (depicted as $\Delta\zeta$ on the red curve) grow by several orders of magnitude for increasing Sérsic index n, while their ratio (depicted as blue curve with magnitude given on the right axis) grows at a much lower rate and is still at order 10^1 for $n = 4$ corresponding to de Vaucouleurs profiles. For exponential profiles ($n = 1$) the ratio is of order 10^0.

expression are related to $\partial s \propto \partial\Delta\Phi$:

$$
\begin{aligned}
\zeta_1 =& \frac{1}{4}\Delta q_{abc}\Delta^{(1)}_{abc} = \frac{1}{4}\int \mathrm{d}^2r\,\rho(r)\frac{\Phi_{efg}}{6\sigma^2}r_e r_f r_g \underbrace{r_a r_b r_c \Delta^{(1)}_{abc}}_{\sqrt{3}(r_0^3+r_0r_1^2)} \\
=& \frac{1}{4}\int \mathrm{d}^2r\,\rho(r)\,\sqrt{3}r^3\left(\cos^3(\phi)+\cos(\phi)\sin^2(\phi)\right)\frac{1}{6\sigma^2}\Phi_{efg}\,r_e r_f r_g \\
=& \frac{1}{4}\int \mathrm{d}^2r\,\rho(r)\,\sqrt{3}r^3\left(\cos^3(\phi)+\cos(\phi)\sin^2(\phi)\right)\frac{1}{6\sigma^2} \\
&\times\left(\Phi_{000}r_0^3+3\Phi_{001}r_0^2r_1+3\Phi_{011}r_1^2r_0+\Phi_{111}r_1^3\right) \\
=& \frac{\sqrt{3}}{4}\int_0^{2\pi}\mathrm{d}\phi\int \mathrm{d}r\,\rho(r)r^7\left(\cos^3(\phi)+\cos(\phi)\sin^2(\phi)\right) \\
&\times\frac{1}{6\sigma^2}\left(\Phi_{000}\cos^3(\phi)+3\Phi_{001}\cos^2(\phi)\sin(\phi)+3\Phi_{011}\cos(\phi)\sin^2(\phi)+\Phi_{111}\sin^3(\phi)\right) \\
=& \frac{\sqrt{3}}{4}D_f\frac{3\pi}{4}\partial_0\Delta\Phi.
\end{aligned}
\tag{4.44}
$$

In a similar calculation ζ_2 can be determined as

$$\zeta_2 = \frac{1}{4}\Delta q_{abc}\Delta^{(2)}_{abc} = \frac{\sqrt{3}}{4}D_f\frac{3\pi}{4}\partial_1\Delta\Phi\,. \tag{4.45}$$

In total, this yields the following relation between the intrinsic size, as it is given in relation (4.43), and the complex intrinsic spin-1 type flexion field

$$\zeta_1 + \mathrm{i}\zeta_2 = \frac{\sqrt{3}}{4}D_f\frac{3\pi}{4}\left(\partial_0 + \mathrm{i}\partial_1\right)\Delta\Phi = \frac{3}{8}\frac{\sqrt{3}}{}\frac{D_f}{D_e}\partial s \propto \partial s. \tag{4.46}$$

The complex derivative operator $\partial = (\partial_0 + \mathrm{i}\partial_1)$ is now defined with respect to the spatial coordinates $\partial_r = \partial_{r_0} + \mathrm{i}\partial_{r_1}$.
The ratio of the unnormalized alignment parameters for flexion D_f and ellipticity D_e is given by

$$\frac{D_f}{D_e} = \frac{1}{3}r^2_{\mathrm{scale}}b^{-2n}\frac{\Gamma(8n)}{\Gamma(6n)}.$$

The factor $1/3$ in the ratio arises because the unnormalized alignment parameter D_f for the intrinsic flexion is defined with a factor $1/(6\sigma^2)$, since the intrinsic flexion arises as third order correction in the Jeans-Model of the stellar density (4.25). In contrast, for the intrinsic ellipticity and size this factor is given by $1/(2\sigma^2)$ in the definition of D_e in (4.24).
The relation (4.46) can further be simplified in terms of the spin-1 HOLIC $\Delta\zeta$ as given in equation (4.39). One finds

$$\Delta\zeta = \frac{3}{2}\frac{D_f}{D_e}\frac{s_0}{\xi}\partial\left(\frac{s}{s_0}\right) = \frac{3}{2}\frac{\tilde{D}_f}{3\tilde{D}_e}\partial\Delta s\,, \tag{4.47}$$

where $\Delta s = s/s_0$ is the relative size change of the perturbed galaxy compared to the size of the unperturbed one. Additionally, the ratio $\tilde{D}_f/\tilde{D}_e$ of normalized alignment parameters only depends on the Sérsic index n according to (4.42).
This result is to be compared to the corresponding definition of the spin-1 flexion field $\mathcal{F}$ of weak lensing which is given by

$$\mathcal{F} = \mathcal{F}_1 + \mathrm{i}\mathcal{F}_2 = \partial\kappa.$$

The convergence κ measures the apparent size change of the image due to lensing, and the complex derivative operator is defined with respect to the angular coordinates θ, i.e $\partial \equiv \partial_\theta$. It is apparent that the definition of the weak lensing quantities is very similar to the results of the intrinsic fields.

Analogously to the previous discussion one can now explicitly calculate the intrinsic ellip-

ticities ϵ_+ and $\epsilon_\times$ from their definition given in [GDS21]. Then, they are related to the intrinsic spin-3 type flexions δ_1 and δ_2. For the ellipticity component ϵ_+ one receives

$$\epsilon_+ = \frac{1}{2}\Delta q_{cd}\sigma^{(3)}_{cd} = \frac{\pi}{2}D_e\frac{1}{2}\left(\partial_0^2\Phi - \partial_1^2\Phi\right), \tag{4.48}$$

while $\epsilon_\times$ can be written as

$$\epsilon_\times = \frac{1}{2}\Delta q_{cd}\sigma^{(1)}_{cd} = \frac{\pi}{2}D_e\partial_0\partial_1\Phi. \tag{4.49}$$

Consequently, for the the complex ellipticity ϵ it holds, that

$$\epsilon = \epsilon_+ + \mathrm{i}\epsilon_\times = \frac{\pi}{2}D_e\left(\frac{1}{2}\left(\partial_0^2\Phi - \partial_1^2\Phi\right) + \mathrm{i}\partial_0\partial_1\Phi\right),$$

while the complex derivative $\partial\epsilon$ with respect to the spatial coordinates $\partial \equiv \partial_r$ is given by

$$\begin{aligned}\partial\epsilon =& \frac{\pi}{2}D_e\left(\partial_0 + \mathrm{i}\partial_1\right)\left(\frac{1}{2}\left(\partial_0^2\Phi - \partial_1^2\Phi\right) + \mathrm{i}\partial_0\partial_1\Phi\right)\\ =& \frac{\pi}{2}D_e\frac{1}{2}\left(\partial_0^3\Phi - 3\partial_0\partial_1^2\Phi + \mathrm{i}\left(3\partial_1\partial_0^2\Phi - \partial_1^3\Phi\right)\right).\end{aligned} \tag{4.50}$$

The spin-3 type intrinsic flexion quantity δ_1 is explicitly written as

$$\delta_1 = \frac{1}{4}\Delta q_{abc}\Delta^{(3)}_{abc} = \frac{1}{4}D_f\frac{\pi}{4}\left(\partial_0^3\Phi - 3\partial_0\partial_1^2\Phi\right), \tag{4.51}$$

while δ_2 is expressed by

$$\delta_2 = \frac{1}{4}\Delta q_{abc}\Delta^{(4)}_{abc} = \frac{1}{4}D_f\frac{\pi}{4}\left(3\partial_0^2\partial_1\Phi - \partial_1^3\Phi\right). \tag{4.52}$$

Hence, by virtue of relation (4.50), the complex intrinsic spin-3 type flexion becomes

$$\delta_1 + \mathrm{i}\delta_2 = \frac{1}{4}\frac{D_f}{D_e}\partial\epsilon,$$

such that the spin-3 HOLIC (4.40) $\Delta\delta$ can be related to the relative ellipticity change $\Delta\epsilon = \epsilon/s_0$ defined in (4.35) via

$$\Delta\delta = \frac{D_f}{D_e}\frac{s_0}{\xi}\partial\Delta\epsilon = \frac{\tilde{D}_f}{3\tilde{D}_e}\partial\Delta\epsilon. \tag{4.53}$$

This result is analogous to the $\mathcal{G}$ flexion of weak lensing given by

$$\mathcal{G} = \mathcal{G}_1 + \mathrm{i}\mathcal{G}_2 = \partial\gamma.$$

Here $\partial\gamma \equiv \partial_\theta\gamma$ denotes the change of the complex shear γ with respect to the angular coordinates of the image. The shear is responsible for apparent ellipticity changes in the lensed image, while the intrinsic ellipticity ϵ actually influences the physical shape of the galaxy.
To summarize, the analogy between the intrinsic HOLIC $\Delta\zeta$ to the spin-1 lensing flexion $\mathcal{F}$, and between $\Delta\delta$ to the spin-3 lensing flexion $\mathcal{G}$ shows that it is natural to identify these quantities with the intrinsic spin-1 and spin-3 flexion.
Furthermore, there is a numerical factor of $3/2$ in result (4.47) for $\Delta\zeta$ compared to the result (4.53) for $\Delta\delta$. This factor arises since the galaxy distortions due to the intrinsic spin-1 field are thrice as strong as for the spin-3 field with $|\Delta\zeta| \propto 3\,|\Delta\delta|$ as shown in (4.29)-(4.32). Beyond that, the factor $1/2$ appears for the intrinsic size changes twice as much under the influence of the tidal field as the intrinsic ellipticites $|\Delta s| \propto 2\,|\Delta\epsilon|$ as previously shown by [GDS21]. Hence, this leads to a different numerical prefactor for the two HOLIC relations (4.47) and (4.53).

Now, according to relation (4.41) the normalized alignment parameter $\tilde{D}_f \propto r_{\text{scale}}^2$ scales with squared length. The parameter $\tilde{D}_f$ is introduced the proportionality constant between the intrinsic flexion and the third order derivative in the Newtonian potential Φ. Besides the parameter $\tilde{D}_f$ there is also the angular integral[9] S_{abcdef} in relation (4.25), which is part of the proportionality constant. For simplicity these two constants can be combined to the total alignment parameter $D_{IA,3}$ for flexions to describe the proportionality between the shape distortion of a galaxy due to variations in the tidal field. Thus, one finds that the constant, relating the intrinsic flexions $\Delta\zeta$ respectively $\Delta\delta$ to third order derivative terms $\partial_a\partial_b\partial_c\Phi/c^2$, can be estimated by

$$\Delta\delta \propto \underbrace{\frac{c^2}{6\sigma^2}\frac{\int \mathrm{d}^2r\,\rho(r)r^6}{\int \mathrm{d}^2r\,\rho(r)r^4}}_{\equiv D_{IA,3}}\frac{\partial_a\partial_b\partial_c\Phi}{c^2}.$$

While the intrinsic flexion $\Delta\delta$ should scale with inverse length, the third order derivative of the potential scales with r_{scale}^{-3}. Hence, the proportionality constant $D_{IA,3}$ scales as expected from relation (4.41) with length squared r_{scale}^2 in units of comoving length $(\text{Mpc/h})^2$. This result is similar to the alignment parameter

$$D_{IA,2} = \frac{c^2}{2\sigma^2}\frac{\int \mathrm{d}^2r\,\rho(r)r^4}{\int \mathrm{d}^2r\,\rho(r)r^2} \propto \frac{c^2}{2\sigma^2}\tilde{D}_e S_{abcd} \propto r_{\text{scale}}^2,$$

found in [GDS21] for the intrinsic ellipticities and sizes which also scales with length squared. In fact, the two alignment parameters $D_{IA,3}$ for intrinsic flexions and $D_{IA,2}$ for intrinsic ellip-

[9] Here the notation is meant such that S_{abcdef} denotes any of the non-vanishing angular integrals explicitly discussed in equation (4.26).

ticities only differ by a numerical prefactor which can be estimated as

$$\frac{D_{IA,3}}{D_{IA,2}} = \frac{2\sigma^2}{6\sigma^2}\frac{\tilde{D}_f\pi/4}{\tilde{D}_e\pi/2} = \frac{1}{6}\frac{\Gamma(8n)\Gamma(4n)}{\Gamma(6n)^2}.$$

Here, the intrinsic δ flexion[10] scales with $\pi/4$ due to the angular integration, while the intrinsic ellipticites scale with $\pi/2$ as shown by [GDS21]. Hence, for small Sérsic indices around $n \leq 4$ the ratio of the two different alignment parameters is less than 10^0 (see also Figure 4.2).
Now, concerning the value of the alignment parameter used for numerical evaluation of the intrinsic flexion spectra in Section 4.4.5, a subtlety has to be taken into account. First of all, the magnitude of the alignment parameter was set to be between $D \simeq 10^{-5}\,(\mathrm{Mpc/h})^2$ to $D \simeq 10^{-6}\,(\mathrm{Mpc/h})^2$ for a galaxy with Sérsic radius of scale $r_{\mathrm{scale}} \simeq 1\mathrm{kpc}$. For the Milky Way this accounts to $r_{\mathrm{scale}} \simeq 2\mathrm{kpc}$. However, in the linear alignment model based on a virialised system, where D_{IA} is supposed to scale with the inverse of the velocity disperion σ^2 instead of the orbital speed typical for Sérsic type galaxies, the typical length scale is actually given by $r_{\mathrm{vir}} \simeq 10^2\mathrm{kpc}$. For the Milky Way this corresponds to $r_{\mathrm{vir}} \simeq 200\mathrm{kpc}$. Thus, since the alignment parameter scales with $D_{\mathrm{IA}} \propto r^2_{\mathrm{scale}}$ the following rescaling is necessary:

$$D' \simeq \frac{r^2_{\mathrm{vir}}}{r^2_{\mathrm{scale}}} D = 10^4 D \simeq 10^{-2}\,(\mathrm{Mpc/h})^2\,,$$

for $D \simeq 10^{-6}\,(\mathrm{Mpc/h})^2$. Thus, also taking a velocity dispersion of $\sigma = 100\mathrm{km/s}$ for systems like the Milky Way into account the final alignment parameter - modulo a Sérsic index dependent prefactor - used for the numerical evaluation is given by

$$D_{\mathrm{IA}} \simeq \frac{c^2}{\sigma^2} 10^{-2}\,(\mathrm{Mpc/h})^2\,.$$

Next, using the alignment parameters $D_{IA,3}$ and $D_{IA,2}$ the relations (4.47) and (4.53) can be expressed as

$$\Delta\zeta = 3\frac{D_{IA,3}}{D_{IA,2}}\partial\Delta s, \tag{4.54}$$

$$\Delta\delta = 2\frac{D_{IA,3}}{D_{IA,2}}\partial\Delta\epsilon. \tag{4.55}$$

[10] For the ζ flexion an additional prefactor 3 is required.

Furthermore, the intrinsic flexion can be related to variations in the cosmic density contrast δ. In this context the Poisson equation

$$\frac{\Delta\Phi}{c^2} = \frac{3}{2}\frac{\Omega_m}{\chi_{\mathrm{H}}^2}\delta, \tag{4.56}$$

yields, as shown in [GDS21], the following proportinality between intrinsic size Δs and density contrast

$$\Delta s \propto D_{IA,2}\frac{3}{2}\frac{\Omega_m}{\chi_{\mathrm{H}}^2}\delta \propto \delta,$$

Due to (4.54) one thus finds

$$\Delta\zeta \propto D_{IA,3}\frac{3}{2}\frac{\Omega_m}{\chi_{\mathrm{H}}^2}\partial\delta \propto \partial\delta.$$

Here, $\Omega_m = 0.3$ is the matter density parameter in accordance with ΛCDM.
In the subsequent section it is discussed how the intrinsic flexions are statistically correlated, and tomographic methods are applied to derive the power spectrum of the intrinsic flexions. Also the correlation to weak lensing flexions is evaluated, and the amplitude of the lensing flexion signal is compared to the amplitude of the intrinsic flexion signal.

4.4.4 Tomographic analysis

When it comes to measuring the magnitude of the intrinsic flexions it is not reasonable to do so for single galaxies. It is rather required to average the intrinsic alignment effect over various galaxies. For the intrinsic flexions this can be done by tomographic redshift bins, similarly to [GDS21], where this is method is applied for the intrinisc ellipticities.
An average over the intrinsic quantities like ellipticities or flexions over localized redshift bins is performed. In the weak lensing approach the tomographic binning [Hu02; JT03; HW05; AR07; TW04; MCK14] has the advantage that, compared to an average over the full line-of-sight, higher sensitivities to determine possible non-linear redshift dependencies of cosmological parameters are achieved, as stated by [SH11].
In the following discussion the intrinsic flexion spectra will be directly compared to the weak flexion lensing spectra: One will hereby follow the approach of [GDS21] and weight the intrinisc alignment quantities by a normalized redshift distribution of galaxies as proposed by *Euclid* [Lau+11]

$$p(z) = \frac{\beta}{z_0\Gamma\left((\alpha+1)/\beta\right)}\left(\frac{z}{z_0}\right)^{\alpha}\exp\left(-\left(\frac{z}{z_0}\right)^{\beta}\right) \propto \left(\frac{z}{z_0}\right)^{2}\exp\left[-\left(\frac{z}{z_0}\right)^{\beta}\right],$$

with $\beta = 3/2$ and $z_0 = 0.64$. Next, a line-of-sight integral between the redshifts z_A and $z_{\mathrm{A}+1}$ limiting a specific redshift bin A is performed. According to [SSR20] the bin boundaries can be chosen such, that the number of galaxies in each bin is equal, leading to the same Poissonian error in each bin.

Consider first the normalized spin-3 HOLIC component δ_1/ξ. Its according tomographic average should be written in angular coordinates, i.e. in terms of θ. Here $r = \theta\chi$ is the physical separation of different points, while θ is the respective angular separation, and χ denotes the comoving distance between the galaxy and the observer. One can confirm that the spatial expression $\delta_1/\xi \equiv \delta_1/\xi_r$ has units of inverse comoving length with

$$\left(\frac{\delta_1}{\xi}\right)_r \propto \frac{\Delta q_{abd}}{q_{abcd}} \propto \frac{\int \mathrm{d}^2 r\, \rho(r) r_a r_b r_c}{\int \mathrm{d}^2 r\, \rho_0(r) r_a r_b r_c r_d} \propto \frac{\chi^3}{\chi^4} \frac{\int \mathrm{d}^2\theta\, \rho(\theta)\theta_a\theta_b\theta_c}{\int \mathrm{d}^2\theta\, \rho_0(\theta)\theta_a\theta_b\theta_c\theta_d} \propto \left(\frac{1}{\chi}\frac{\delta_1}{\xi}\right)_\theta,$$

while the according angular HOLIC δ_1/ξ_θ needs to be in units of inverse angle. In the above calculation the invariance of the volume element

$$\mathrm{d}^2 r\, \rho(r) = \mathrm{d}^2\theta\, \rho(\theta),$$

needs to be taken into account, since the projected stellar density as measure for the surface brightness scales with inverse length squared, such that the expression for the volume element does not depend on the comoving distance. In terms of relation (4.29) the angular spin-3 HOLIC component $(\delta_1/\xi)_\theta$ is thus given by

$$\begin{aligned}\left(\frac{\delta_1}{\xi}\right)_\theta &= \chi\left(\frac{\delta_1}{\xi}\right)_r = \frac{1}{4}\chi D_{IA,3}\, \partial_{r_a}\partial_{r_b}\partial_{r_c}\frac{\Phi}{c^2}\Delta^{(3)}_{abc} \\ &= \frac{1}{4}\chi D_{IA,3}\, \frac{1}{\chi^3}\partial_a\partial_b\partial_c\frac{\Phi}{c^2}\Delta^{(3)}_{abc} = \frac{1}{4} D_{IA,3}\, \frac{1}{\chi^2}\partial_a\partial_b\partial_c\frac{\Phi}{c^2}\Delta^{(3)}_{abc}.\end{aligned} \tag{4.57}$$

Here, $\partial_a \equiv \partial_{\theta_a}$ denotes the angular derivative which is related to the spatial derivative by $\partial_{r_a}\chi \equiv \partial_{\theta_a}$. As the alignment parameter is proportional to comoving length squared the expression (4.57) does not scale with length. Now, the angular HOLIC component $\left(\bar{\delta}_1/\xi\right)_\theta \equiv \bar{\delta}_1/\xi_A$ averaged over one tomographic A bin is given by

$$\begin{aligned}\frac{\bar{\delta_1}}{\xi}_A &= \int_{z_\mathrm{A}}^{z_{\mathrm{A}+1}} \mathrm{d}z\; p(z)\, \frac{1}{4} D_{IA,3}\, \frac{D_+(a)}{a}\, \frac{1}{\chi^2}\partial_a\partial_b\partial_c\frac{\Phi}{c^2}\Delta^{(3)}_{abc} \\ &= \int_{\chi_\mathrm{A}}^{\chi_{\mathrm{A}+1}} \mathrm{d}\chi\; p(\chi)\; \mathrm{H}(\chi)\frac{1}{4} D_{IA,3}\, \frac{D_+(a)}{a}\, \frac{1}{\chi^2}\partial_a\partial_b\partial_c\frac{\Phi}{c^2}\Delta^{(3)}_{abc} \\ &= \frac{1}{4}\frac{D_{IA,3}}{D_{IA,2}}\partial_a\partial_b\partial_c\varphi_A\Delta^{(3)}_{abc}.\end{aligned} \tag{4.58}$$

Here, φ_A can be considered as a line-of-sight averaged alignment potential which has the same form as in [GDS21] for the intrinsic ellipticites and sizes, namely

$$\varphi_A = \int_{\chi_\mathrm{A}}^{\chi_\mathrm{A+1}} \mathrm{d}\chi\, p(\chi) \frac{H(\chi)}{c} D_{IA,2}\, \frac{D_+(a)}{a} \frac{1}{\chi^2} \frac{\Phi}{c^2} = \int \mathrm{d}\chi\, W_{\varphi,A}\,(\chi)\, \frac{\Phi}{c^2},$$

with weighting function

$$\begin{aligned} W_{\varphi,A} &= p_A(\chi) \frac{H(\chi)}{c} D_{IA,2}\, \frac{D_+(a)}{a} \frac{1}{\chi^2}, \\ \text{and} \quad p_A(\chi) &= p(\chi) \Theta\,(\chi - \chi_\mathrm{A})\, \Theta\,(\chi_\mathrm{A+1} - \chi)\,, \end{aligned} \tag{4.59}$$

where the Heaviside-functions Θ ensure that the alignment effect is restricted to one localized bin A. As in [GDS21] the Hubble law was inserted here with $-\mathrm{d}\chi\, \mathrm{H}(\chi) = c\mathrm{d}z$ and Hubble function $\mathrm{H}(\chi(z))$. Furthermore, the potential must be corrected by a linear growth factor $D_+(a)/a$ which arises in the theory of linear sturcture growth [Bar19a]. It takes into account how the density contrast and hence - by virtue of the Poisson equation - the sourced gravitational potential changes due to the cosmic expansion.
The other HOLIC components can then be expressed accordingly by

$$\frac{\bar{\delta}_2}{\xi}_A = \frac{1}{4} \frac{D_{IA,3}}{D_{IA,2}} \partial_a \partial_b \partial_c \varphi_A \Delta^{(4)}_{abc}, \tag{4.60}$$

$$\frac{\bar{\zeta}_1}{\xi}_A = \frac{3}{4} \frac{D_{IA,3}}{D_{IA,2}} \partial_a \partial_b \partial_c \varphi_A \Delta^{(1)}_{abc}, \tag{4.61}$$

$$\frac{\bar{\zeta}_2}{\xi}_A = \frac{3}{4} \frac{D_{IA,3}}{D_{IA,2}} \partial_a \partial_b \partial_c \varphi_A \Delta^{(2)}_{abc}, \tag{4.62}$$

where the factor 3 in the expressions for the spin-1 HOLIC takes into account, that the intrinsic centroid shift is thrice as strong as the three-fold symmetric shape changes δ_1 and δ_2 as shown by the previous results (4.29) and (4.30). Hence, the third derivative of the line-of sight projected intrinsic alignment potential φ_A can be decomposed in terms of the Dirac-type matrices similarly to the lensing flexions as

$$\partial_a \partial_b \partial_c \varphi_A = \frac{D_{IA,2}}{D_{IA,3}} \left(\frac{1}{3} \frac{\bar{\zeta}_1}{\xi}_A \Delta^{(1)}_{abc} + \frac{1}{3} \frac{\bar{\zeta}_2}{\xi}_A \Delta^{(2)}_{abc} + \frac{\bar{\delta}_1}{\xi}_A \Delta^{(3)}_{abc} + \frac{\bar{\delta}_2}{\xi}_A \Delta^{(4)}_{abc} \right).$$

These results are similar to [GDS21], where a similar decompostion of the intrinsic size and ellipticities in terms of the Pauli matrices and the same intrinsic alignment potential φ_A is

stated as

$$\bar{s}_A = \frac{1}{2}\partial_a\partial_b\varphi_A\sigma^{(0)}_{ab},$$
$$\bar{\epsilon}_{+_A} = \frac{1}{2}\partial_a\partial_b\varphi_A\sigma^{(3)}_{ab},$$
$$\bar{\epsilon}_{\times_A} = \frac{1}{2}\partial_a\partial_b\varphi_A\sigma^{(1)}_{ab}.$$

Additionally, there is a factor 2 between the intrinsic size and shape as shown in [GDS21]. Consequently, the relations (4.54) and (4.55) between the HOLICs and the changes in size and ellipticity also hold consistently for the averaged quantities

$$\Delta\bar{\zeta}_A = 3\frac{D_{IA,3}}{D_{IA,2}}\partial\Delta\bar{s}_A,$$
$$\Delta\bar{\delta}_A = 2\frac{D_{IA,3}}{D_{IA,2}}\partial\Delta\bar{\epsilon}_A,$$

and hence must be sourced by the same potential φ_A.
For the weak lensing flexions the lensing potential Ψ_B within a tomographic bin B is usually given by (see also [SH11]; [MCK14] for instance)

$$\Psi_B = \int \mathrm{d}\chi\, W_{\Psi,B}(\chi)\,\frac{\Phi}{c^2},$$
$$\text{with } W_{\Psi,B} = \frac{2}{\chi}\frac{D_+(a)}{a}\int_{\max(\chi,\chi_B)}^{\chi_{B+1}} \mathrm{d}\chi'\, p(\chi')\,\frac{\mathrm{d}z}{\mathrm{d}\chi'}\left(1-\frac{\chi}{\chi'}\right).$$

As in [GDS21] the weak lensing efficiency $W_{\Psi,B}$ can be taken as a weighting function. Unlike the efficiency function for the intrinisc alignment $W_{\varphi,A}$ the weak lensing efficiency function is non-zero from $\chi = 0$ to χ_{B+1}, what takes the lensing effect along the whole line-of-sight from the observer to the according bin edge into account. Intrinsic alignment on the other hand only takes place within the specific bin chosen, and alignments in different bins should be uncorrelated. Analogously to the intrinsic flexions, the decomposition of the weak lensing flexion within the tomographic bins is given by

$$\partial_a\partial_b\partial_c\Psi_B = -\frac{\sqrt{3}}{2}\mathcal{F}_{1,B}\Delta^{(1)}_{abc} - \frac{\sqrt{3}}{2}\mathcal{F}_{2,B}\Delta^{(2)}_{abc} - \frac{1}{2}\mathcal{G}_{1,B}\Delta^{(3)}_{abc} - \frac{1}{2}\mathcal{G}_{2,B}\Delta^{(4)}_{abc},$$

such that the relations

$$-\frac{\sqrt{3}}{2}\mathcal{F}_{1,B} = \frac{1}{4}\partial_a\partial_b\partial_c\Psi_B\Delta^{(1)}_{abc}, \tag{4.63}$$

$$-\frac{\sqrt{3}}{2}\mathcal{F}_{2,B} = \frac{1}{4}\partial_a\partial_b\partial_c\Psi_B\Delta^{(2)}_{abc}, \tag{4.64}$$

$$-\frac{1}{2}\mathcal{G}_{1,B} = \frac{1}{4}\partial_a\partial_b\partial_c\Psi_B\Delta^{(3)}_{abc}, \tag{4.65}$$

$$-\frac{1}{2}\mathcal{G}_{2,B} = \frac{1}{4}\partial_a\partial_b\partial_c\Psi_B\Delta^{(4)}_{abc}, \tag{4.66}$$

hold.

4.4.5 Flexion power spectra

Next, the power spectra for the intrinsic flexions, as well as the according cross-correlations with the lensing flexions will be derived. The statistical fluctuations in the density variations and hence potential variations are typically assumed to be described by homogeneous and isotropic gaussian random fields on the sphere [Dur08]; [Bar19a]. Furthermore, a flat sky approximation which allows to apply Limber's equation [BS01]; [Lim54]; [Sch11] is used. Consequently, the intrinsic self-correlation, i.e. the II-correlation of the alignment potential φ_A becomes

$$\left\langle \varphi_{A,abc}\left(\ell\right)\varphi^*_{B,def}\left(\ell'\right)\right\rangle = (2\pi)^2\,\delta_D\left(\ell-\ell'\right)C^{\varphi_A\varphi_B}_{abcdef}, \tag{4.67}$$

with

$$\begin{aligned} C^{\varphi_A\varphi_B}_{abcdef} &= \ell_a\ell_b\ell_c\ell_d\ell_e\ell_f\left\langle\int \mathrm{d}\chi\, W_{\varphi_A}\frac{\Phi}{c^2}\left(k=\ell/\chi,\chi\right)\int \mathrm{d}\chi'\, W_{\varphi_B}\frac{\Phi}{c^2}\left(k'=\ell'/\chi',\chi'\right)\right\rangle \\ &\underbrace{=}_{\text{Limber}}\ell_a\ell_b\ell_c\ell_d\ell_e\ell_f\int \mathrm{d}\chi\,\frac{W_{\varphi_A}W_{\varphi_B}}{\chi^2}P_{\Phi\Phi}\left(k=\ell/\chi,\chi\right) \\ &= \ell_a\ell_b\ell_c\ell_d\ell_e\ell_f C^{\varphi_A\varphi_B}(\ell), \end{aligned}$$

in Fourier space, where the angular derivatives ∂_a become the reciprocal wave vector modes via $-\mathrm{i}\ell_a$. This result is similar to [GDS21] for the II-spectra of second order derivatives of the alignment potential. The short hand notation $\varphi_{A,abc}$ denotes $\partial_a\partial_b\partial_c\varphi_A$, while $P_{\Phi\Phi} = \left\langle\frac{\Phi}{c^2}\frac{\Phi'}{c^2}\right\rangle$ is the power spectrum of the potential fluctuations sourced from the fluctuations in the cosmic density field [Bar19a]. Due to the Poisson equation in Fourier space (4.56) the linear power spectrum for the potential fluctuations is given in terms of the linear power spectrum of the

density fluctuations $P_{\delta\delta}$ - normalized to σ_8 - as (see also [SH11])

$$P_{\Phi\Phi} = \left(\frac{3\Omega_m}{2\chi_{\rm H}}\right)^2 k^{-4} P_{\delta\delta} \propto k^{n_s-4} T(k)^2.$$

Here, $T(k)$ is the transfer function obtained from n-Body simulation fits for linear structure formation by [Bar+86], while $P_{\delta\delta} \propto k^{n_s}$ with spectral index $n_s \leq 1$ (here $n_s = 0.96$) as predicted by standard inflational theory of structure formation (see [Bar19a] for more details). For a non-linear description of structure formation on small scales one can consider, as in [GDS21], the halo model established by [Smi+03]. For the numerical evaluation of the power spectra for the intrinisc alignment contribution a Gaussian smoothing of the potential Φ is introduced to suppress scales smaller than the size of a typical elliptical galaxy, as discussed by [GDS21].
The cross-correlation of intrinsic alignment with weak gravitational lensing, i.e the *GI*-term, are given by

$$\left\langle \psi_{A,abc}(\ell)\, \varphi^*_{B,def}(\ell') \right\rangle = (2\pi)^2\, \delta_D(\ell - \ell')\, C^{\psi_A\varphi_B}_{abcdef},$$

with

$$\begin{aligned} C^{\psi_A\varphi_B}_{abcdef} =& \ell_a\ell_b\ell_c\ell_d\ell_e\ell_f \int {\rm d}\chi\, \frac{W_{\psi_A} W_{\varphi_B}}{\chi^2} P_{\Phi\Phi}(k = \ell/\chi, \chi) \\ =& \ell_a\ell_b\ell_c\ell_d\ell_e\ell_f C^{\psi_A\varphi_B}(\ell), \end{aligned}$$

similarly to equations (4.67). Finally, the auto-correlation of the lensing potential, i.e. the *GG*-term, can be expressed as

$$\left\langle \psi_{A,abc}(\ell)\, \psi^*_{B,def}(\ell') \right\rangle = (2\pi)^2\, \delta_D(\ell - \ell')\, C^{\psi_A\psi_B}_{abcdef}, \tag{4.68}$$

with

$$\begin{aligned} C^{\psi_A\psi_B}_{abcdef} =& \ell_a\ell_b\ell_c\ell_d\ell_e\ell_f \int {\rm d}\chi\, \frac{W_{\psi_A} W_{\psi_B}}{\chi^2} P_{\Phi\Phi}(k = \ell/\chi, \chi) \\ =& \ell_a\ell_b\ell_c\ell_d\ell_e\ell_f C^{\psi_A\psi_B}(\ell). \end{aligned}$$

Besides the auto-correlators $\left\langle \varphi_{A,abc}(\ell)\, \varphi^*_{B,def}(\ell') \right\rangle$, $\left\langle \psi_{A,abc}(\ell)\, \psi^*_{B,def}(\ell') \right\rangle$ and the cross-correlator $\left\langle \psi_{A,abc}(\ell)\, \psi^*_{B,def}(\ell') \right\rangle$ there may generally also be non-vanishing cross-correlations between third order derivatives of the alignment potential, or lensing potential, and their second order derivatives. This is for example also specifically evaluated in [Bac+06] for the cross-

correlation between lensing convergence and the lensing $\mathcal{F}$ flexion. Thus, there are actually also be the following correlators:

$$
\begin{aligned}
&II\text{: } \left\langle \varphi_{A,abc}(\ell)\, \varphi^*_{B,de}(\ell') \right\rangle, \\
&GI\text{: } \left\langle \psi_{A,abc}(\ell)\, \varphi^*_{B,de}(\ell') \right\rangle \ , \left\langle \psi_{A,ab}(\ell)\, \varphi^*_{B,cde}(\ell') \right\rangle, \\
&GG\text{: } \left\langle \psi_{A,abc}(\ell)\, \psi^*_{B,de}(\ell') \right\rangle.
\end{aligned}
$$

These would result in cross-correlations between both lensing and intrinsic flexions with shear, convergence, intrinsic size and intrinsic ellipticities. However, in this thesis only the information contained in the pure flexion correlations is considered, even though there might also be interesting information contained in the cross-correlations between third and second order derivatives of the potential. These are not elaborated here, but could be considered in further research.

Using the decompostions (4.58) and (4.60)-(4.62) for the intrinsic flexion components in terms of the Dirac-type matrices the II-correlations for the flexions can now be derived explicitly. For the spin-1 field component $\bar{\zeta}_1/\xi$ one receives the following auto-correlation:

$$
\left\langle \frac{\bar{\zeta}_1}{\xi}_A(\ell)\ \frac{\bar{\zeta}_1}{\xi}^*_B(\ell') \right\rangle = (2\pi)^2\, \delta(\ell - \ell')\, C_{AB}^{\frac{\bar{\zeta}_1}{\xi}\frac{\bar{\zeta}_1}{\xi}}(\ell),
$$

with

$$
C_{AB}^{\frac{\bar{\zeta}_1}{\xi}\frac{\bar{\zeta}_1}{\xi}}(\ell) = \frac{9}{16}\frac{D^2_{IA,3}}{D^2_{IA,2}} \Delta^{(1)}_{abc}\Delta^{(1)}_{def}\ell_a\ell_b\ell_c\ell_d\ell_e\ell_f C^{\varphi_A\varphi_B}(\ell).
$$

For evaluating the contraction of $\ell_a\ell_b\ell_c\ell_d\ell_e\ell_f$ with $\Delta^{(1)}_{abc}\Delta^{(1)}_{def}$ it is useful to write $\ell_a\ell_b\ell_c$ decomposed into the orthonormal set of Dirac matrices. This is done similarly to [GDS21], where $\ell_a\ell_b$ is decomposed in terms of Pauli matrices. For $\ell_a\ell_b\ell_c$ one thus finds the following result

$$
\ell_a\ell_b\ell_c = \frac{1}{4}\Big[\sqrt{3}\ell^3\cos\phi\Delta^{(1)}_{abc} + \sqrt{3}\ell^3\sin\phi\Delta^{(2)}_{abc} + \ell^3\cos(3\phi)\,\Delta^{(3)}_{abc} + \ell^3\sin(3\phi)\,\Delta^{(4)}_{abc}\Big], \quad (4.69)
$$

with $\ell_0 = \ell\cos\phi$ and $\ell_1 = \ell\sin\phi$. This result also confirms the different spins of the flexion fields: While the contractions of the Dirac matrices $\Delta^{(1)}$ and $\Delta^{(2)}$ with $\ell_a\ell_b\ell_c$ have spin-1 symmetry, the according contractions of $\ell_a\ell_b\ell_c$ with the Dirac matrices corresponding to the intrinsic flexion with spin-3 are invariant under $2\pi/3$ rotations. Due to the assumed isotropy of the random field, the angle $\phi = 0$ is fixed, similar to [GDS21], which leaves the correlators

invariant, but simplifies expression (4.69) to

$$\ell_a\ell_b\ell_c = \frac{1}{4}\left[\sqrt{3}\ell^3\Delta^{(1)}_{abc} + \ell^3\Delta^{(3)}_{abc}\right] \text{ for } \phi = 0\,.$$

Thus, one only needs to evaluate the $\bar{\zeta}_1/\xi$-component for the intrinsic spin-1 flexion $\Delta\zeta$ and $\bar{\delta}_1/\xi$ for the intrinsic spin 3 flexion $\Delta\delta$. The power spectrum for $\Delta\zeta$ consequently becomes

$$C^{\Delta\zeta\Delta\zeta}_{AB}(\ell) = C^{\frac{4}{\sqrt{3}}\frac{\bar{\zeta}_1}{\xi}\frac{4}{\sqrt{3}}\frac{\bar{\zeta}_1}{\xi}}_{AB}(\ell) = 9\frac{D^2_{IA,3}}{D^2_{IA,2}}\ell^6 C^{\varphi_A\varphi_B}(\ell),$$

where the additional factor $4/\sqrt{3}$ comes from relation (4.39).
Analogously the power spectrum for $\Delta\delta$ is given by

$$C^{\Delta\delta\Delta\delta}_{AB}(\ell) = C^{4\frac{\bar{\delta}_1}{\xi}4\frac{\bar{\delta}_1}{\xi}}_{AB}(\ell) = \frac{D^2_{IA,3}}{D^2_{IA,2}}\ell^6 C^{\varphi_A\varphi_B}(\ell),$$

while the cross-correlated power spectrum becomes

$$C^{\Delta\zeta\Delta\delta}_{AB}(\ell) = C^{\frac{4}{\sqrt{3}}\frac{\bar{\zeta}_1}{\xi}4\frac{\bar{\delta}_1}{\xi}}_{AB}(\ell) = 3\frac{D^2_{IA,3}}{D^2_{IA,2}}\ell^6 C^{\varphi_A\varphi_B}(\ell)\,.$$

Now, multiplication of the intrinsic flexion fields with the prefactor $4/9$ for the intrinsic spin-1 flexion $\Delta\zeta$, respectively with the factor $4/3$ for the intrinsic spin-3 flexion $\Delta\delta$, directly relates the magnitude of the intrinsic flexion fields to the lensing flexion fields, because of the approximate results (4.19) and (4.20) from [OUF07] discussed in section 4.3. One thus finds the following *II* spectra:

$$\Delta\zeta\Delta\zeta\text{: } C^{\frac{4}{9}\Delta\zeta\frac{4}{9}\Delta\zeta}_{AB}(\ell) = \frac{16}{9}\frac{D^2_{IA,3}}{D^2_{IA,2}}\ell^6 C^{\varphi_A\varphi_B}(\ell),$$

$$\Delta\delta\Delta\delta\text{: } C^{\frac{4}{3}\Delta\delta\frac{4}{3}\Delta\delta}_{AB}(\ell) = \frac{16}{9}\frac{D^2_{IA,3}}{D^2_{IA,2}}\ell^6 C^{\varphi_A\varphi_B}(\ell),$$

$$\Delta\zeta\Delta\delta\text{: } C^{\frac{4}{9}\Delta\zeta\frac{4}{3}\Delta\delta}_{AB}(\ell) = \frac{16}{9}\frac{D^2_{IA,3}}{D^2_{IA,2}}\ell^6 C^{\varphi_A\varphi_B}(\ell).$$

Equation (4.69) can then also be applied to calculate the *GG*-spectra of the weak lensing flexions $\mathcal{F}$ and $\mathcal{G}$, as well as the according cross-correlations *GI*. By inserting the expressions

(4.63) and (4.65) into (4.68) the following GG-spectra are obtained:

$$\mathcal{FF}\colon C_{AB}^{\mathcal{FF}}(\ell) = \frac{1}{16}\left(\frac{-2}{\sqrt{3}}\right)^2 \Delta_{abc}^{(1)}\Delta_{def}^{(1)}\ell_a\ell_b\ell_c\ell_d\ell_e\ell_f C^{\psi_A\psi_B}(\ell) = \frac{1}{4}\ell^6 C^{\psi_A\psi_B}(\ell),$$
$$\mathcal{GG}\colon C_{AB}^{\mathcal{GG}}(\ell) = \frac{1}{16}(-2)^2\,\Delta_{abc}^{(3)}\Delta_{def}^{(3)}\ell_a\ell_b\ell_c\ell_d\ell_e\ell_f C^{\psi_A\psi_B}(\ell) = \frac{1}{4}\ell^6 C^{\psi_A\psi_B}(\ell),$$
$$\mathcal{FG}\colon C_{AB}^{\mathcal{FG}}(\ell) = \frac{1}{16}\frac{(-2)^2}{\sqrt{3}}\Delta_{abc}^{(1)}\Delta_{def}^{(3)}\ell_a\ell_b\ell_c\ell_d\ell_e\ell_f C^{\psi_A\psi_B}(\ell) = \frac{1}{4}\ell^6 C^{\psi_A\psi_B}(\ell).$$

Finally, the GI-spectra which correlate the intrinsic flexion with the weak lensing flexion $\mathcal{F}$ are given by

$$\mathcal{F}\Delta\zeta\colon C_{AB}^{\mathcal{F}\frac{4}{9}\Delta\zeta}(\ell) = \frac{-2}{9}\frac{D_{IA,3}}{D_{IA,2}}\Delta_{abc}^{(1)}\Delta_{def}^{(1)}\ell_a\ell_b\ell_c\ell_d\ell_e\ell_f C^{\psi_A\varphi_B}(\ell) = -\frac{2}{3}\frac{D_{IA,3}}{D_{IA,2}}\ell^6 C^{\psi_A\varphi_B}(\ell),$$

$$\mathcal{F}\Delta\delta\colon C_{AB}^{\mathcal{F}\frac{4}{3}\Delta\delta}(\ell) = \frac{-2}{3\sqrt{3}}\frac{D_{IA,3}}{D_{IA,2}}\Delta_{abc}^{(1)}\Delta_{def}^{(3)}\ell_a\ell_b\ell_c\ell_d\ell_e\ell_f C^{\psi_A\varphi_B}(\ell) = -\frac{2}{3}\frac{D_{IA,3}}{D_{IA,2}}\ell^6 C^{\psi_A\varphi_B}(\ell).$$

The according GI-spectra which relate the intrinsic flexions with the weak lensing flexion $\mathcal{G}$ are expressed as

$$\mathcal{G}\Delta\zeta\colon C_{AB}^{\mathcal{G}\frac{4}{9}\Delta\zeta}(\ell) = \frac{-2}{3\sqrt{3}}\frac{D_{IA,3}}{D_{IA,2}}\Delta_{abc}^{(3)}\Delta_{def}^{(1)}\ell_a\ell_b\ell_c\ell_d\ell_e\ell_f C^{\psi_A\varphi_B}(\ell) = -\frac{2}{3}\frac{D_{IA,3}}{D_{IA,2}}\ell^6 C^{\psi_A\varphi_B}(\ell),$$

$$\mathcal{G}\Delta\delta\colon C_{AB}^{\mathcal{G}\frac{4}{3}\Delta\delta}(\ell) = \frac{-2}{3}\frac{D_{IA,3}}{D_{IA,2}}\Delta_{abc}^{(3)}\Delta_{def}^{(3)}\ell_a\ell_b\ell_c\ell_d\ell_e\ell_f C^{\psi_A\varphi_B}(\ell) = -\frac{2}{3}\frac{D_{IA,3}}{D_{IA,2}}\ell^6 C^{\psi_A\varphi_B}(\ell).$$

The negative sign of the cross-correlation spectra shows that the intrinsic alignment effect and weak lensing are actually anti-correlated. The physical meaning of this is generally the following: For an overdense region the background galaxies are magnified due to lensing, while the foreground galaxies actually get smaller due to intrinsic alignment. For an underdense region the opposite is the case as discussed in [GDS21].
A measure for the degree of anti-correlation between the intrinisc flexion and the weak lensing flexion is the Pearson-correlation coefficient $r_{\mathcal{F}\,4/9\Delta\zeta} \equiv r_{\mathcal{F}\Delta\zeta'}$, where $4/9\Delta\zeta = \Delta\zeta'$ is introduced to simplify notation. It turns out to be identical to the Pearon-correlation coefficient $r_{\gamma\epsilon}$ derived by [GDS21] for the anti-correlation of intrinsic shapes and shear. This holds because the coefficient is actually an expression for the correlation between the intrinsic alignment

potential and lensing potential as shown by the following calculation:

$$
\begin{aligned}
r_{\mathcal{F}\Delta\zeta'} &= \frac{C_{AA}^{\mathcal{F}\Delta\zeta'}}{\sqrt{C_{AA}^{\mathcal{F}\mathcal{F}}\, C_{AA}^{\Delta\zeta'\Delta\zeta'}}} = \frac{-2/3 D_{IA,3}/D_{IA,2} l^6 C^{\psi_A\varphi_A}(l)}{\sqrt{4/9\, D_{IA,3}^2/D_{IA,2}^2\, l^6 C^{\psi_A\psi_A}(l)\, l^6 C^{\varphi_A\varphi_A}(l)}} \\
&= -\frac{C^{\psi_A\varphi_A}(l)}{\sqrt{C^{\psi_A\psi_A}(l)\, C^{\varphi_A\varphi_A}(l)}}.
\end{aligned}
\tag{4.70}
$$

For the Pearson-correlation coefficient $r_{\mathcal{G}\Delta\delta'}$, with $\Delta\delta' \equiv 4/3\Delta\delta$, the same result is obtained. Due to the Cauchy-Schwarz inequality $\left(C_{AA}^{\mathcal{F}\Delta\zeta'}\right)^2 \leq C_{AA}^{\mathcal{F}\mathcal{F}} C_{AA}^{\Delta\zeta'\Delta\zeta'}$ the correlation coefficient is bounded between -1 (perfect anti-correlation) and 1 (perfect correlation) as stated in [GDS21]. A value of zero would account for statistical independence of intrinsic flexion from weak lensing flexion. Like in [GDS21] only values $C_{AA}^{\Delta\zeta'\Delta\zeta'}$ within the same bin can be accounted for. The correlation proportional to $C_{AB}^{\Delta\zeta'\Delta\zeta'} = 0$ vanishes for different bins $A \neq B$, because the tidal field in one bin does generally not affect the galaxies in another bin, for their mutual distance is too large. The Pearson-correlation coefficient is depicted in Figure 4.3 for low, intermediate and high redshift bins. One can see, that in all three cases the correlation coefficients based on a model of linear structure formation differ from the coefficients based on a non-linear model of structure formation for higher multipole order, and thus smaller structures. The reason for this are the different amplitudes of the spectra based on a non-linear power spectrum, what will also be specified in the following paragraph.

When making predictions about the observed flexion power spectrum, which includes GG, GI and II terms one also has to take a Poissonian noise term N_{noise} into account [SCH09]. It quantifies the uncertainity in the HOLIC measurement for the auto-correlations $C_{AB}^{\zeta\zeta}$ and $C_{AB}^{\delta\delta}$. In [OUF07] the dispersion for the intrinsic HOLICs is estimated to be $\sigma_{\Delta\zeta} = \sigma_{\Delta\delta} = 0.02\,\text{arcsec}^{-1}$ per galaxy. Using the relative scaling factors of $9/4$ between the spin-1 HOLIC and the $\mathcal{F}$-flexion, respectively $3/4$ between the spin-3 HOLIC and the $\mathcal{G}$-flexion, derived in [OUF07], the flexion dispersions are given by $\sigma_{\mathcal{F}} = 0.009\,\text{arcsec}^{-1}$ per galaxy and $\sigma_{\mathcal{G}} = 0.027\,\text{arcsec}^{-1}$ per galaxy. However, the noise terms stated by [OUF07] are highly optimistic, and in most cases the flexion dispersions are much higher. There are a lot of challenges in their estimation as addressed in detail by [Row+13], where the authors discuss various uncertainties in estimating the lensing flexions from pixel data using Hubble space telescope Ultra Deep Field data. Amongst them are finite photon numbers in the detectors, systematic errors due to centroid shifts, or the specific choice of point spread function to model effects of the measurement devices on the measurement, for instance. Also, concrete methods in data evaluation like deblending of the pixel data, and calibrations for measuring flexions via shapelet decompositions

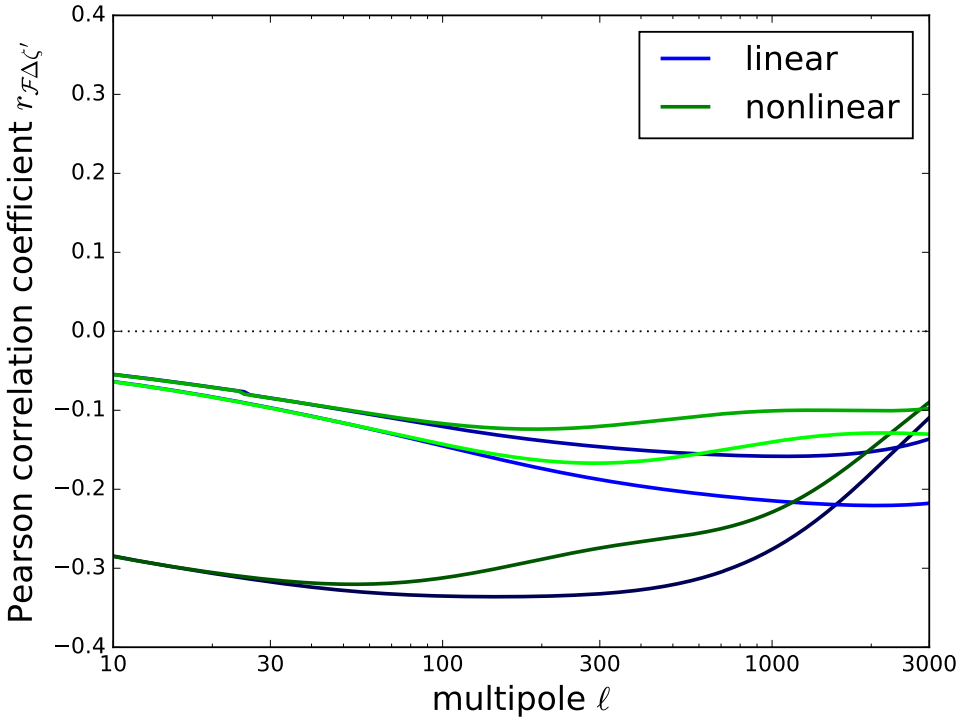

Figure 4.3: **Pearson correlation coefficient $r_{\mathcal{F}\Delta\zeta'}$ versus multipole oder l for three different redshift bins:** The coefficient for the the correlation between intrinsic flexion of spin 1 and lensing flexion $\mathcal{F}$ is identical as in [GDS21] for intrinsic shape and shear, as shown by (4.70). The scheme is as follows: Low redshift bins: Lower two dark curves, Intermediate redshift bins: upper pair of curves, High redshift bins: intermediate pair of bright curves.

introduce further sources of error. The authors [Row+13] also showed, that the uncertaintiy of the lensing flexion scales with a steeply falling power law

$$\sigma_{\mathcal{F}} = 0.33 \left(\frac{\mathrm{SNR}}{100} \right)^{-0.83} \ \mathrm{arcsec}^{-1},$$

depending on the signal-to-noise ratio (SNR) of the observed galaxies. Thus, according to this power law an optimistic value of $\sigma_{\mathcal{F}} = 0.009\,\mathrm{arcsec}^{-1}$ from [OUF07] corresponds to a very high SNR of about SNR $\approx$ 7700 for very bright sources. More realistic, but still optimistic values of $\sigma_{\mathcal{F}} = 0.04\,\mathrm{arcsec}^{-1}$ as estimated by [GB05] imply SNR $\approx$ 1300 what is still a high value. For lower, but actually realistic SNR of fainter sources, like for instance SNR = 100 the dispersion would amount to $\sigma_{\mathcal{F}} = 0.33\,\mathrm{arcsec}^{-1}$ [Row+13]. In this thesis, one chooses to evaluate the spectra for all of these dispersions, what will become especially important

in the numerical evaluation of the attainable cumulated signal-to noise-ratios, as well as the Fisher-analysis in the following Section 4.4.6. It will be estimated for which noise value an observation of the intrinsic flexions would actually be possible in a *Euclid*-like survey, and which cumulated signal-to-noise ratios might in fact be more realistic with the dipersions stated by [GB05] and [Row+13].
Now, the total noise contribution for the spectra is given by a Poissonian error with

$$(N_{\text{noise},\mathcal{F}})_{AB} = \sigma^2_{\mathcal{F}} \frac{n_{\text{tomo}}}{\bar{n}} \delta_{AB}, \tag{4.71}$$

and accordingly for the $\mathcal{G}$ flexions. Here n_{tomo} denotes the number of tomographic bins under consideration. Furthermore, the baseline value of $\bar{n} = 3.545 \times 10^8 \text{sr}^{-1} = 30\,\text{arcmin}^{-2}$ is chosen for the observable galaxy number density in reach of *Euclid* (see [Lau+11]), noting that previous studies by [GDS21] used the stretch goal value of $\bar{n} = 4.727 \times 10^8 \text{sr}^{-1} = 40\,\text{arcmin}^{-2}$. The noise term (4.71) is diagonal, where δ_{AB} is the Kronecker delta. This means that only an error on auto-correlations for the observed HOLICs is considered in the same bin. Also, the error measurement of the spin-1 flexion and the spin-3 flexion are statistically independent. In the further discussion only contributions from the spin-1 flexion are considered, since the error for these flexion types is only a third of the uncertainty for spin-3 flexions.
Figures 4.4 and 4.5 depict the *GG*, *GI* and *II* spectra for the spin-1 flexions for different Sérsic indices to present two extreme cases. For an exponential galaxy profile the magnitude expected for the pure lensing spectrum is much larger than for the *GG* and *GI* correlations, while the contributions of these two spectra rise significantly for a de Vaucouleurs profile, since the susceptibility ratio $\tilde{D}_f/\tilde{D}_e$ between third and second order corrections in intrinsic alignment grows at least by an order of magnitude between $n = 1$ and $n = 4$. Also the Poissonian uncertainties of spin-1 type flexions for different multipole orders are shown for the three flexion dispersion discussed previously. They are several orders of magnitude larger than the signal: For a dispersion of $\sigma_{\mathcal{F}} = 0.09\,\text{arcsec}^{-1}$ the noise exceeds the signal by two orders of magnitude for high multipole order, for $\sigma_{\mathcal{F}} = 0.04\,\text{arcsec}^{-1}$ by three to four orders of mangitude and for $\sigma_{\mathcal{F}} = 0.33\,\text{arcsec}^{-1}$ by six to seven orders of magnitude.

4.4.6 Fisher-analysis and signal-to-noise ratio

Next, it will be determined whether one can measure the intrinsic flexions via evaluation of the cumulative signal-to-noise ratio, and also whether one can reasonably constrain the matter density parameter Ω_m and equation of state parameter w via a Fisher-analysis using the total flexion signal. For the numerical evaluation in the wCDM-cosmology the following fiducial values for the cosmological parameters are taken: The dark enery equation of state parameter

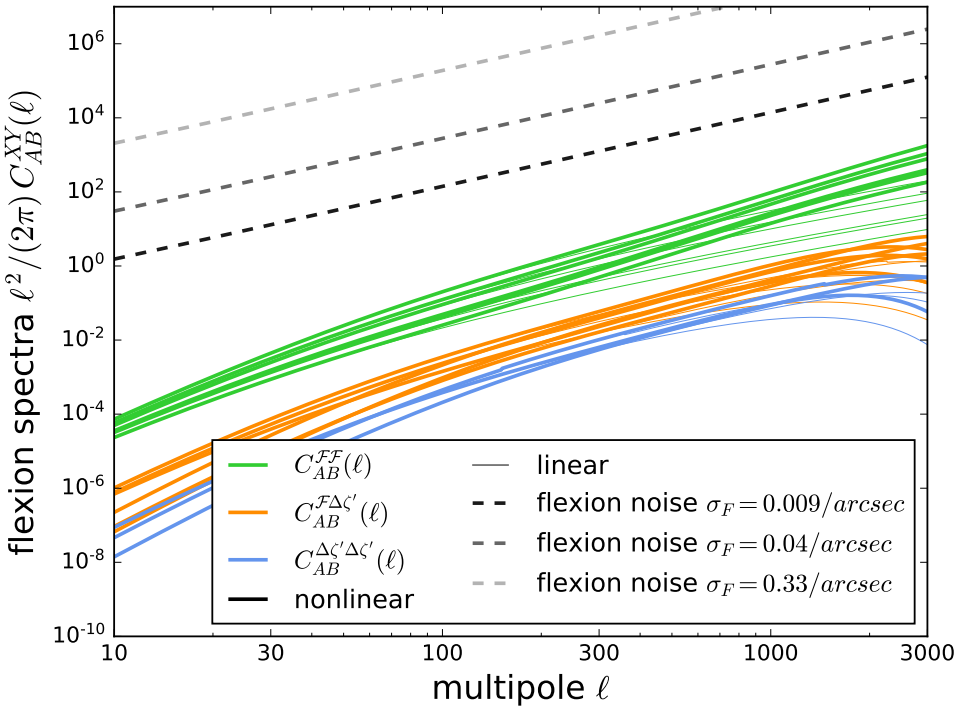

Figure 4.4: **Flexion spectra for elliptical galaxies for Sérsic index $n = 1$:** The signal strength is presented for the different spin-1 flexion spectra for a linear structure growth model (thin curves), and a non-linear model (bold curves) for a three bin tomography is depicted for an exponential galaxy profile. The *GG*-spectrum for the lensing flexion $\mathcal{F}$ is shown in green, the cross-correlation *GI* with intrinsic flexion $\Delta\zeta' = 4/9\Delta\zeta$ in orange and the *II*-spectrum for the intrinsic flexion in blue. The different noise contributions for different flexion dispersions are depicted as dashed lines.

is set to $w = -0.9$ for numerical reasons, but is actually close to -1, the matter density parameter to $\Omega_m = 0.3$, while the σ_8-parameter is set to $\sigma_8 = 0.8$, the Hubble parameter to $h = 0.7$, and finally the scalar spectral index is given by $n_S = 0.96$.

Now, similar to [GDS21] a multivariate likelihood ansatz is made. The first is hereby to set up the covariance matrix $C_{ij} = \left\langle x_i(\ell) x_j^*(\ell') \right\rangle$ from the measured spectra for the spin-1 flexion. It estimates the correlations of various cosmological parameters via the Fisher approximation (see for instance [TTH97]; [HT99]; [SH11]; [SR16] for applications). This method is generally used to find the parameter set θ^μ of a physical model from the measured data set $x_i(\ell)$ by

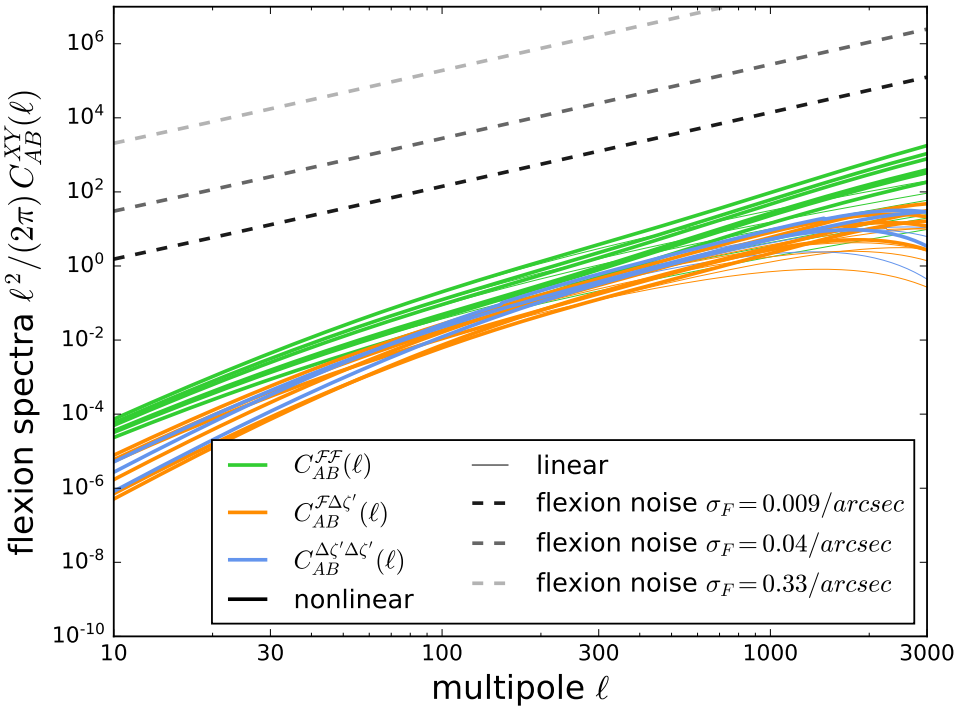

Figure 4.5: **Flexion spectra for elliptical galaxies for Sérsic index $n = 4$:** The signal strength is presented for the different spin-1 flexion spectra for a linear structure growth model (thin curves), and a non-linear model (bold curves) for a three bin tomography is depicted for a de Vaucouleurs galaxy profile. Due to the increase of the susceptibility ratio in the alignment model the signal strength of the *GI*- and *II*-spectra is one to two orders of magnitude larger compared to the exponential profile.

mapping from a Gaussian likelihood function

$$\mathcal{L}(x_i(\ell)|\theta^\mu) = \frac{1}{\sqrt{(2\pi)^N \det(C)}} \exp\left(-\frac{1}{2} x_i(\ell)\, C_{ij}^{-1}(\ell,\ell')\, x_i^*(\ell')\right) \propto \exp\left(-\frac{\chi^2}{2}\right),$$

with

$$\chi^2 = \sum_\ell \mathrm{tr}\left[\ln C + C^{-1} D\right], \text{and data matrix } D_{ij} = x_i(\ell) x_j^*(\ell'),$$

for the observed data given the model to a multivariate Gaussian distribution in the model parameters given information on the data. This yields a possible approximation of the posterior

$$P \propto \exp\left(-\frac{1}{2}\Delta\theta^\mu F_{\mu\nu} \Delta\theta^\nu\right).$$

Here, the Fisher information matrix [SH11]; [SR16]; [GDS21]

$$F_{\mu\nu} \equiv -\left\langle \frac{\partial^2}{\partial\theta^\mu \partial\theta^\nu} \frac{\chi^2}{2} \right\rangle = \sum_\ell \frac{2l+1}{2} \mathrm{tr}\left(\frac{\partial C}{\partial\theta^\mu} C^{-1} \frac{\partial C}{\partial\theta^\nu} C^{-1} \right),$$

evaluated at best fit with multiplicity $m = 2\ell + 1$ corresponds to an inverse parameter covariance. Now, the covariance matrix C, with components C_{AB} and A, B as redshift bin indices, formed from the measured flexion modes $\mathcal{F}_{lm}$ (lensing flexion) and $\Delta\zeta'_{lm}$ (intrinsic flexion) is given by

$$\begin{aligned} C_{AB}(\ell) =& C_{AB}^{\mathcal{F}\mathcal{F}}(\ell) + C_{AB}^{\Delta\zeta'\Delta\zeta'}(\ell) + C_{AB}^{\mathcal{F}\Delta\zeta'}(\ell) + C_{AB}^{\Delta\zeta'\mathcal{F}}(\ell) + \sigma_{\mathcal{F}}^2 \frac{n_{\mathrm{tomo}}}{\bar{n}} \delta_{AB} \\ =& \ell^6 \left[\frac{1}{4} C^{\psi_A\psi_B}(\ell) + \frac{4^2}{9} \frac{D_{IA,3}^2}{D_{IA,2}^2} C^{\varphi_A\varphi_B}(\ell) - \frac{2}{3} \frac{D_{IA,3}}{D_{IA,2}} \left(C^{\psi_A\varphi_B}(\ell) + C^{\varphi_A\psi_B}(\ell) \right) \right] \\ &+ \sigma_{\mathcal{F}}^2 \frac{n_{\mathrm{tomo}}}{\bar{n}} \delta_{AB}, \end{aligned}$$

such that it is symmetric in A and B as required by definition. The Cauchy-Schwarz inequality

$$C_{AA}^{\mathcal{F}\Delta\zeta'\,2} \leq C_{AA}^{\mathcal{F}\mathcal{F}} C_{AA}^{\Delta\zeta'\Delta\zeta'}$$

ensures that the diagonal elements are always positive definite, since

$$\left| C_{AA}^{\mathcal{F}\Delta\zeta'} \right| \leq C_{AA}^{\mathcal{F}\mathcal{F}} > 0, \text{ if } C_{AA}^{\mathcal{F}\mathcal{F}} > C_{AA}^{\Delta\zeta'\Delta\zeta'},$$

while it holds that

$$\left| C_{AA}^{\mathcal{F}\Delta\zeta'} \right| \leq C_{AA}^{\Delta\zeta'\Delta\zeta'} > 0, \text{ for } C_{AA}^{\Delta\zeta'\Delta\zeta'} > C_{AA}^{\mathcal{F}\mathcal{F}}.$$

As discussed earlier, there are also no *IG* correlations, since terms like $C_{AB}^{\Delta\zeta'\mathcal{F}}$ should be zero for $A > B$ while $C_{AB}^{\mathcal{F}\Delta\zeta'} = 0$ for $B > A$, because lensing in lower redshift bins cannot be correlated with intrinsic alignment in higher redshift bins.

Evaluation of the Fisher matrix for the dark energy equation of state parameter w and the matter density parameter Ω_m for the given covariance of the measured flexion modes then leads to the typical 1-σ ellipsoidal confidence contours. These are depicted in Figure (4.6) for the highly optimistic dispersion of $\sigma_{\mathcal{F}} = 0.009\,\mathrm{arcsec}^{-1}$, and in Figure (4.7) for dispersion of $\sigma_{\mathcal{F}} = 0.04\,\mathrm{arcsec}^{-1}$ which is also still optimistic. Additionally, the two extreme choices of Sérsic indices $n = 1$ and $n = 4$, i.e. the exponential and the de Vaucouleurs galaxy profile are compared in these figures. The Fisher ellipses for the dispersion of $\sigma_{\mathcal{F}} = 0.33\,\mathrm{arcsec}^{-1}$ are not depicted. They are not constraining at all for Ω_m and w, for they would contain a vast amount of the parameter space becuase the uncertainty is too high compared to the signal strength.

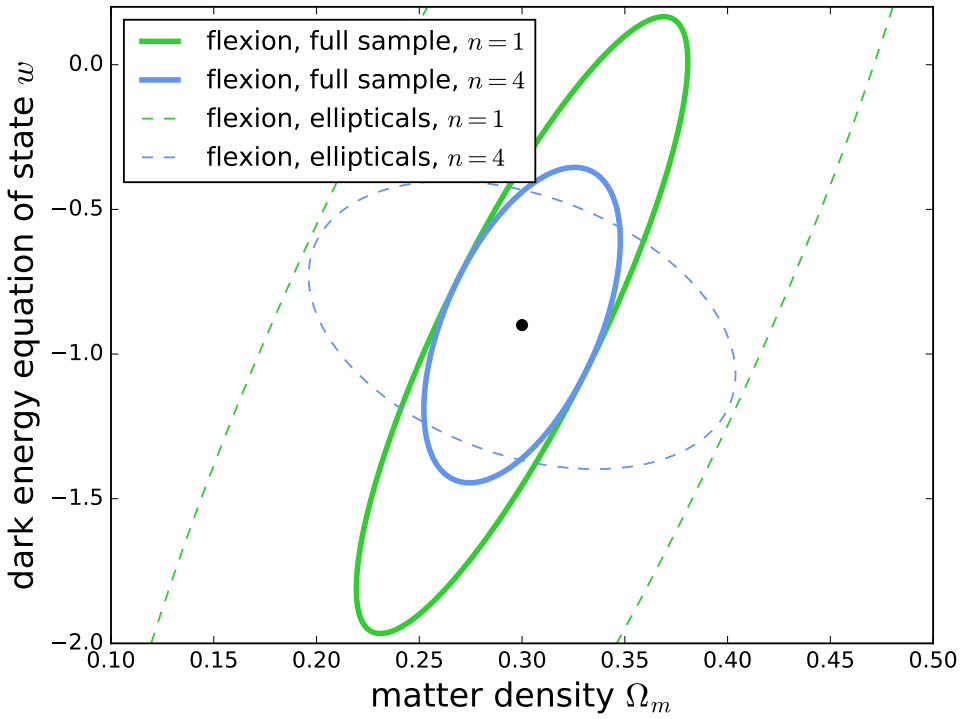

Figure 4.6: **Fisher ellipses in the w-Ω_m-plane:** Similar to [GDS21] the Fisher ellipses generated from the full flexion spectra for a wCDM cosmology, with $\Omega_m = 0.3$ and $w = -0.9$ as fiducial values, are shown. Especially for $n = 1$, ellipticals only, the 1-σ confidence contour is not very constraining, with large errors, which are reduced for the full galaxy sample. If one considers a de Vaucouleurs profile with $n = 4$ the 1-σ contour gets even more constraining, since the signal strength is increased with the susceptibility ratio. The flexion noise was chosen as $\sigma_{\mathcal{F}} = 0.009\,\text{arcsec}^{-1}$.

Here, as in [GDS21], two selection modes are considered: On the one hand, the full survey can be evaluated for the measurement of flexions, also including spiral galaxies which are sensitive to lensing, but are assumed not be sensitive to the linear alignment model worked out for intrinsic flexions. So, as done in [GDS21] for the intrinsic sizes and shapes, the *GI*-flexion-spectrum signal is weighted by a factor of $1/3$. The *II*-flexion-spectrum singal is reduced by a factor of $1/9$, since only a third of all galaxies are assumed to be elliptical and hence sensitive to the model. On the other hand, when choosing only elliptical galaxies, the signal size is not affected, since then all galaxies in the sample would be sensitive of the intrinsic flexion. However, in this case the Poissonian noise term would be increased by a factor of 3 since the whole sample size is reduced to $1/3$ of the full sample.

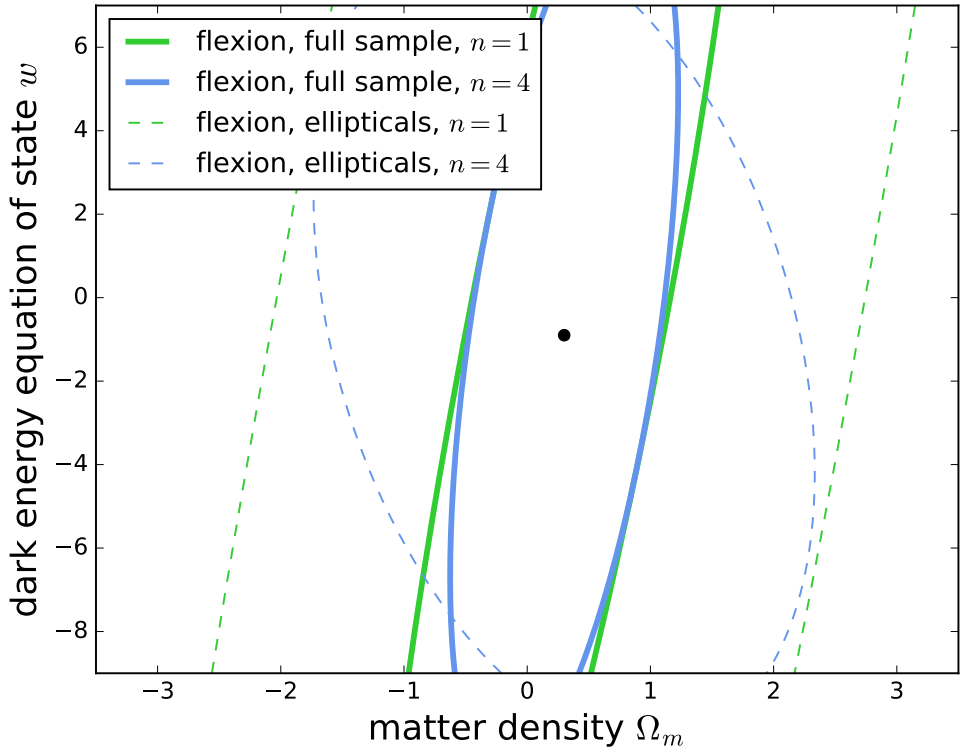

Figure 4.7: **Fisher ellipses in the w-Ω_m-plane:** This plot is similar to Figure 4.6, however here a higher noise of $\sigma_{\mathcal{F}} = 0.04\,\mathrm{arcsec}^{-1}$ was chosen. Thus, the confidence contours are even less constraining.

Thus, the Fisher ellipses in Figure (4.6) for the full galaxy sample (bold lines) are smaller than for the case, where only the elliptical galaxies are selected (dashed lines). However, for an exponential galaxy profile with $n = 1$ the 1-σ-contours in the w-Ω_m-plane derived from the flexion covariance are still less constraining compared to the 1-σ-contours for the ellipticities [GDS21], since the relative uncertainity in determining the flexions is much larger. Choosing a de Vaucouleurs profile with $n = 4$ increases the signal strength for the intrinsic flexion correlation and the according cross-correlation with the lensing flexion. This leads to less extended 1-σ-contours, giving tighter contraints on the correlation of the two parameters w and Ω_m. Since the dispersion by [OUF07] is, however, too optimistic and thus likely underestimates the uncertainty for flexion measurements, the Fisher constraints depicted in Figure 4.7 seem to be more realisitic, even though the noise level is still very optimistic. They are even an order of magnitude less constraining that the ellipses in Figure 4.6. Hence it can be concluded that the cosmological parameters can hardly be reasonably constrained with flexion measurements.

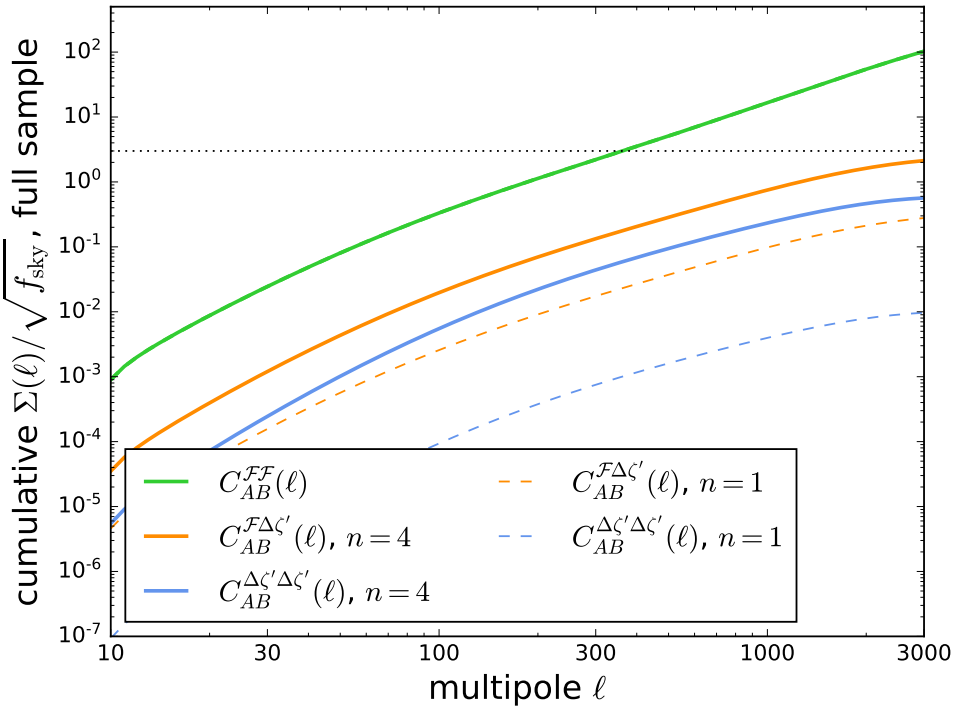

Figure 4.8: **Cumulative signal-to-noise ratios for flexion spectra for the full galaxy sample:** The flexion noise was chosen to be $\sigma_{\mathcal{F}} = 0.009\,\mathrm{arcsec}^{-1}$ according to [OUF07]. The *GI* (depicted in orange) and *II* correlations (depicted in blue) are in general not measurable, neither for exponential (dashed lines) nor de Vaucouleurs profiles (bold lines) for they do not exceed the critical mark of $\Sigma(\ell) \geq 3$ in the presented range of multipole orders. In case of a de Vaucouleurs profile the attainable cumulated signal-to-noise ratio goes up to at least $\Sigma(\ell) \geq 2$ for high multipole orders. It exceeds the values for the exponential profiles since a lager Sérsic index increases the effective alignment parameter. The lensing flexion spectra (shown in green) is measurable very well, with cumulated signal to noise rations of about $\Sigma(\ell) \geq 100$ for $\ell \geq 3000$. The *GI* spectra are futher weighted by a factor $q = 1/3$, while the *II* spectra are weighted by a factor q^2.

The effect on the measurability of the flexions for different flexion dispersions will also become clearer when considering the cumulated signal-to-noise ratios Σ (see [TTH97]; [HT99] and also [SH11] for applications). They estimate whether the intrinsic flexion signals can be detected by surveys like *Euclid*

$$\Sigma^2 = \sum_l \frac{2l+1}{2} \mathrm{tr}\left(C^{-1}S\,C^{-1}S\right),$$

where C is again the covariance matrix, and S the signal matrix under consideration. Thus, the cumulated signal-to-noise ratio for the *GG*, *GI* and *II*-flexion spectra can be evaluated for either selection modes, previously discussed, namely by choosing the full galaxy sample, or by only considering the elliptical galaxies. With the cumulative signal-to-noise ratio it is estimated, whether the intrinsic flexion signals might be detectable by *Euclid*, assuming a 5-bin tomography and full sky coverage ($f_{\rm sky} = 1$), similar to the analysis by [GDS21], to ensure statistical independence between the different modes. For incomplete sky coverage one then needs to rescale with the factor $f_{\rm sky}$ accordingly.

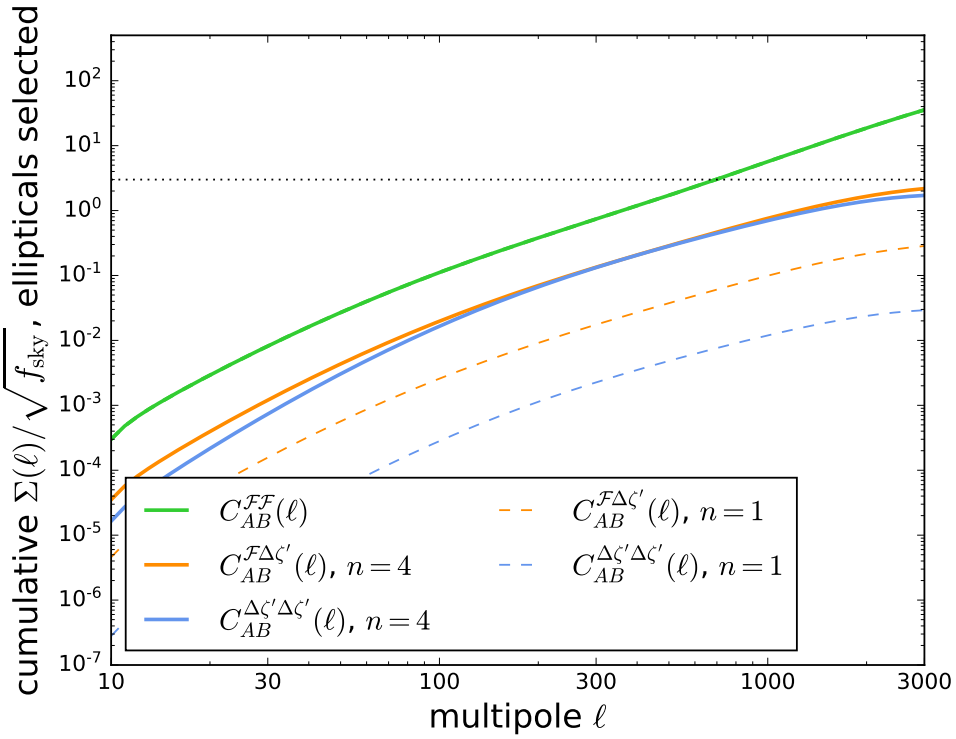

Figure 4.9: **Cumulative signal to noise ratios for flexion spectra for choosing only elliptical galaxies:** This plot is similar to Figure 4.8 with the dispersion of $\sigma_{\mathcal{F}} = 0.009\,\mathrm{arcsec}^{-1}$, but here only the elliptical galaxies were selected, such that the alignment spectra are not suppressed. The noise, however, is generally increased by a factor of 3 due to the smaller sample size. Thus, the *GG* signal is decreased, though it is still being measurable quite well with $\Sigma(\ell) \geq 40$ for $\ell \geq 3000$. Neither the *GI* nor the *II* spectra would be measurable with $\Sigma(\ell) \geq 2$ for $n = 4$ for high multipole orders, and even less than $\Sigma(\ell) \leq 1$ (*GI*) and $\Sigma(\ell) \leq 10^{-1}$ (*II*) for $n = 1$.

The according signal-to-noise ratios, for both ellitpcals only and the full galaxy sample, are depicted in Figures (4.8) and (4.9) for the highly optimistic dispersion of $\sigma_{\mathcal{F}} = 0.009\,\mathrm{arcsec}^{-1}$, as well as in (4.10) respectively (4.10) for the still optimistic but more realistic dispersion of $\sigma_{\mathcal{F}} = 0.04\,\mathrm{arcsec}^{-1}$. Finally, the same is depicted for the error value of $\sigma_{\mathcal{F}} = 0.33\,\mathrm{arcsec}^{-1}$ in (4.12) and (4.12).

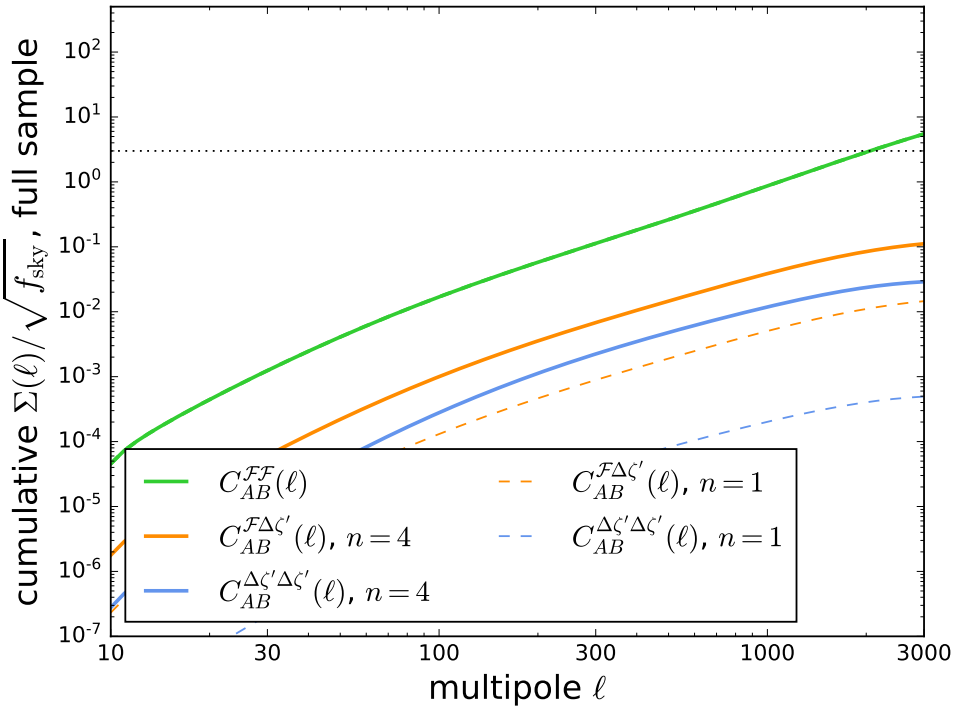

Figure 4.10: **Cumulative signal-to-noise ratios for flexion spectra for the full galaxy sample:** This plot is similar to Figure 4.8, however with a higher dispersion of $\sigma_{\mathcal{F}} = 0.04\,\mathrm{arcsec}^{-1}$. Hence, the cumulated signal-to-noise ratios are generally decreased. The lensing flexion would still be measurable with $\Sigma(\ell) \geq 5$ for $\ell \geq 3000$.

When only choosing elliptical galaxies the cumulated signal-to-noise ratio for the *GG*-signal is lowered compared to selecting all galaxies due to the larger Poissonian error, which is scaled by a factor of 3. However, the signal-to-noise ratio for the intrinsic flexions and cross-correlations with the lensing flexions is increased, compared to the full galaxy sample selection mode. For this mode extra suppression factors are multiplied with the spectra ($1/3$ for *GI*, $1/9$ for *II*), to ensure that only the galaxies sensitive to the Jeans-model are considered.

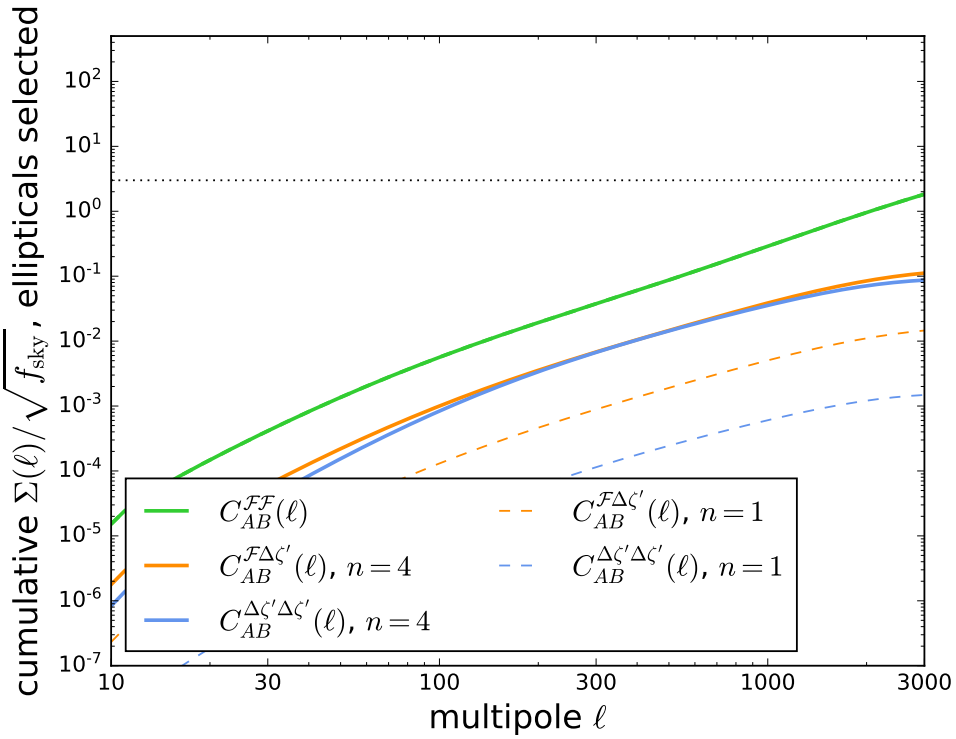

Figure 4.11: **Cumulative signal-to-noise ratios for flexion spectra for elliptical galaxies:** This plot is similar to Figure 4.9, however with a higher dispersion of $\sigma_{\mathcal{F}} = 0.04\,\mathrm{arcsec}^{-1}$ such that the cumulated signal-to-noise ratios are generally decreased. The lensing flexion is not measurable anymore with only $\Sigma(\ell) \geq 2$ for $\ell \geq 3000$. The *GG* and *GI* spectra are increased compared to 4.10, however still not measurable.

Figures 4.8-4.11 show that the intrinsic flexion signals are not even measurable for optimistic choices of noise. Only for the lowest noise level and for the extreme choice of $n = 4$ for a de Vaucouleurs profile one finds a cumulative signal to noise ratio of $\Sigma(\ell) \approx 2$ for very high multipole orders for the *GI* spectrum in both selction modes, and for the *II* spectrum in elliptical selection mode. Contrary, the observability of the lensing flexion is guaranteed at least for the dispersion of $\sigma_{\mathcal{F}} = 0.009\,\mathrm{arcsec}^{-1}$ and for $\sigma_{\mathcal{F}} = 0.04\,\mathrm{arcsec}^{-1}$ for ellipticals only. Still, these dispersions are too optimistic choices for the noise. For more realistical dispersions like $\sigma_{\mathcal{F}} = 0.33\,\mathrm{arcsec}^{-1}$ neither lensing nor intrinsic flexions can be observed anymore as shown in Figures 4.12 and 4.13. Thus, an attainable flexion signal cannot be received at all for these cases. Consequently, a Fisher estimation does not lead to sufficient results to contrain w or Ω_m. This is why only the Fisher ellipses for the two smaller flexion errors were presented. Even for

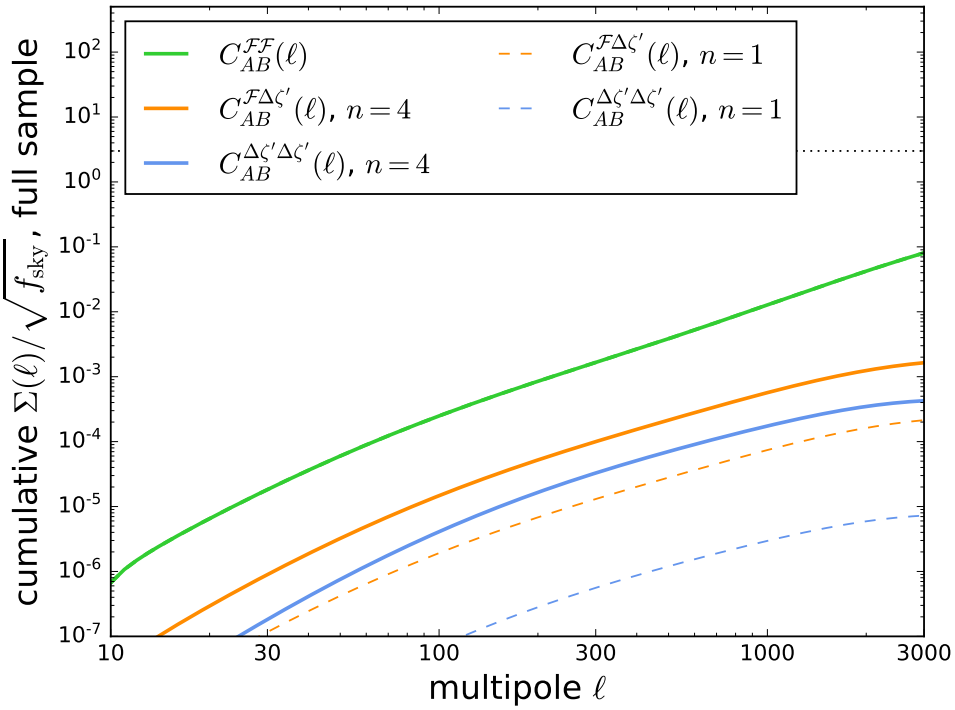

Figure 4.12: **Cumulative signal-to-noise ratios for flexion spectra for the full galaxy sample:** This plot is similar to Figures 4.8 and 4.10, but with a higher dispersion of $\sigma_{\mathcal{F}} = 0.33\,\mathrm{arcsec}^{-1}$, such that the cumulated signal-to-noise ratios are decreased even futher. The lensing flexion dominating all other signals is still strongly suppressed with $\Sigma(\ell) \leq 10^{-1}$ for $\ell \geq 3000$.

these cases, the Fisher ellipses do not have comparatively constraining power as those shown by [GDS21]. These are about one order of magnitude more constraining.

4.5 Summary and outlook

In this chapter basic ideas about weak gravitational lensing [BS01]; [Bar10]; [BM17]; [SEF92], weak lensing flexion [Bac+06]; [GB05] and later intrinsic alignment [SKW06]; [BM17]; [SCH09] were summarized. Then, the linear alignment model [11] was further developed inspired from previous work by [GDS21], to study intrinsic flexions. These were derived from the octopole moments of the surface brightness distribution, which arise due to third order perturbations of the gravitational potential. Additionally, the corresponding intrinsic flexion spectra, derived from a tomographic analysis, were compared to the spectra of flexions in weak lensing via the HOLICs formalism established by [OUF07]; [OUF08]. Furthermore, the

[11] See also [Hir+04]; [Hir+07]; [HS10]; [Pir+17] for more details on linear alignment.

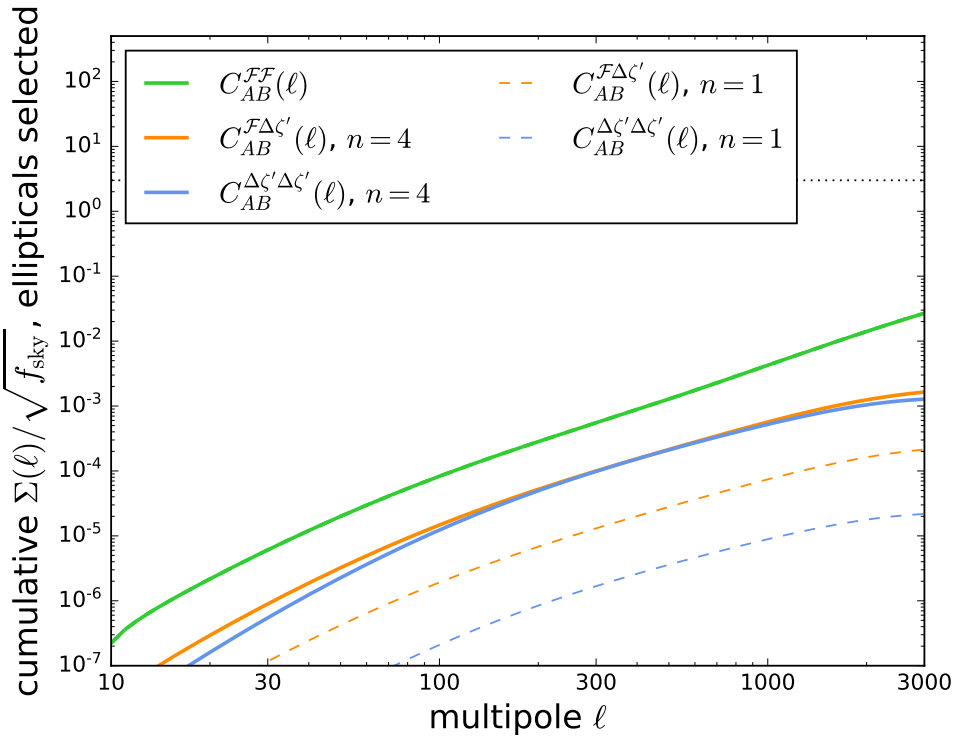

Figure 4.13: **Cumulative signal-to-noise ratios for flexion spectra for elliptical galaxies:** This plot is similar to Figures 4.9 and 4.11, however with a higher dispersion of $\sigma_{\mathcal{F}} = 0.33\,\mathrm{arcsec}^{-1}$ such that the cumulated signal-to-noise ratios are generally decreased. Since the Poissonian noise is increased for selecting ellipticals only, the lensing flexion drops to $\Sigma(\ell) \geq 10^{-2}$ for $\ell \geq 3000$ compared to Figure 4.12.

matching signal-to-noise ratios were estimated for a *Euclid*-like survey and a Fisher-analysis was performed for three different flexion noises ($\sigma_{\mathcal{F}} = 0.009\,\mathrm{arcsec}^{-1}$, $\sigma_{\mathcal{F}} = 0.04\,\mathrm{arcsec}^{-1}$ and $\sigma_{\mathcal{F}} = 0.33\,\mathrm{arcsec}^{-1}$) and two extreme choices of Sérsic indices.
The result was that for optimistic noise values the intrinsic lensing flexion can we observed well with *Euclid*, but this does not hold for the cross-correlations between lensing and intrinsic flexion and the intrinsic auto-correlations. Since the attainable flexion signals are quite low compared to the noise the Fisher-analysis does not sufficiently constrain cosmological parameters like w and Ω_m. All in all, intrinsic flexions are hardly measurable in upcoming surveys like *Euclid*.

As possible outlook one could thus further investigate cross-correlation of the intrinsic flexion with intrinsic ellipticities, intrinsic sizes or weak lensing ellipticities and convergences in future studies. As the amplitude for these effects is larger, the according cross-correlations could

lead to larger signal strengths, possibly enabling to find signatures of the intrinsic flexions in the flexion-ellipticity spectra.

The statistical methods used in weak lensing and summarized here, are now further applied in the following Chapter 5, where tests of the Etherington distance duality violation, and thus surface brightness conservation violation in area-metric lensing will be invesitgated. Furthermore, one will see that surface brightness fluctuations can also arise in classical astrophysical applications like intrinsic alignment. The aim of the next chapter is to compare these two effects quantitatively, and to study their measurability. To achieve this, statistical spectra of these intrinsic surface brightness fluctuations will be derived in the further course of this thesis. They then need to be compared to surface brightness fluctuation spectra based on area-metric refinements of gravity. At last, other observational lensing quantities like the magnification bias shall also be investigated in regards with these refinements.

5 Testing the modified Etherington distance duality in area-metric spacetimes

The results discussed in sections 5.3 and 5.4 of this chapter are also published as
E. S. Giesel, B. Ghosh and B. M. Schäfer,
ArXiv: arXiv:2208.07197, *(August 2022)*
Etherington duality breaking: gravitational lensing in non-metric spacetimes versus intrinsic alignments.
and submitted to the *Monthly Notices of the Royal Astronomical Society*.

Gravitational lensing is a powerful tool to study the phenomenology of modifications to general relativity, since the way light is deflected is directly affected. Consequenlty, this translates to the modifications in the well-known image distortions of sources, like shear or convergence in weak lensing. Another important observable quantity is the Etherington distance duality, which relates the luminosity distance and the angular diameter distance. Since it is universal for metric spacetimes in general relativity, and for photon conserving particle theories, it is the perfect observable to probe any modifications of these theories. Thus, based on the results by [SW17], who predicted a modification of this duality in weakly birefringet spacetimes, it will be discussed further how this can affect other lensing observables like surface brightness or the magnification bias. This is the main objective of this chaper, which is structured as follows: First it is repeated, based on [GM01] and summarized for instance in [Wit14]; [Due20]; [Fis17], how the concept of covariant energy-momentum conservation can be generalized from metric spacetimes to area-metric geometries. In the weakly birefingent case, this generalized concept of covariant energy-momentum conservation results in the photon currents of sources to be conserved with respect to a different volume measure, as expected from metric spacetimes via $\mathrm{d}^4x\sqrt{-\det g}$. This leads to the Etherington distance duality modifications as given in [SW17]. Next, a summary is given on how light propagates in weakly birefringent spacetime, and how this affects image distortion measures like the effective convergence. Next, it will be described how intrinsic surface brightness fluctuations arise in general relativity due to intrinsic alignment. The phenomenology of this intrinsic effect turns out to be similar to a real violation of the conservation of surface brightness in weakly birefingent spacetimes. Finally, modifications of the magnification bias factor in area-metric weak lensing will be discussed and numerically quantified.

5.1 Introduction: Energy-momentum conservation in weakly birefringent spacetimes

General linear electrodynamics, which is reviewed in more detail in [HO03]; [OR02]; [Rub02], and is defined by the according action

$$S_{\text{matter}}[A;G) = -\frac{1}{8}\int d^4x\, \omega_{G^{-1}}(x) G^{abcd}(x) F_{ab}(x) F_{cd}(x), \tag{5.1}$$

allows for surprising effects as vacuum birefringence. Going from this birefringent electrodynamics to a suitable set of gravitational field equations via the gravitational closure program as generally introduced in Chapter 1 has, so far, notably been possible for highly symmetric spacetimes as in [Due20], or in the weak field limit [Sch+17]; [Wol22]. In thia limit weak birefringence is stipulated in the sense that one considers a Minkowskian metric induced area-metric background geometry with a purely area-metric perturbation. Then the input coefficients in this perturbative treatment are derived to find the corresponding perturbed closure equations. These need to be solved to find a a set of linearized gravitational field equations in this set-up. The according gravitational Lagrangian is stated in [Sch+17]; [Wol22] in its general form. After appropriate gauge fixing this finally leads to a set of equations of motion as stated in [Sch+17]; [Wol22], which are concretized further, if the gravitational field is sourced by a point-mass, as shown by [Ale20b]; [Ale22]. Then the gravitational dynamics can be solved explicitly. The according consequences of this weakly area-metric solution on observables in lensing will be recapitulated and further discussed in the following section. Special focus will be put on the modification of the Etherington distance duality as predicted by [SW17]. It relates the angular diameter distance D_A and luminosity distance D_L via

$$D_L = (1+z)^2 D_A, \tag{5.2}$$

and is an important observable for the fundamental geometric structure of spacetime. For a metric, Lorentzian spacetime it is always given by (5.2), independent of the choice of metric as shown in [SEF92]. Also in case of a purely Minkowski metric induced area-metric, which implies non-birefringence [LH04] and is, as already mentioned in Section 1.5, given by

$$G^{abcd} = \sqrt{-\det g}\left(g^{a[c}\, g^{d]b}\right)\psi + \phi\epsilon^{abcd},$$

with ψ as dilaton field, and ϕ as axion field, the authors [Mor+16] find that the Etherington distance duality is not changed. This is to be expected because the background geometry is, after all, metric induced.

Thus, as soon as one deviates from metric geometry, it becomes possible to find imprints on this observable quantity, even thouh this always needs to be proven explicitly by caluclation first. In case of weak birefringence the Etherington distance duality is ultimately changed due to a modification in the energy-momentum conservation law on an area-metric geometry [SW17]. This will be described in more detail in the following paragraph, summarizing the discussions in [Wit14]; [Due20]; [Fis17]; [SW17]:
In classical general relavity the $(1,1)$ energy-momentum tensor T^a_b is given by

$$T^a_b = g^{ac} S_{cb} = -\frac{2}{\sqrt{-\det g}} g^{ac} \frac{\delta S_{\text{matter}}}{\delta g^{cb}},$$

with the Hilbert-stress energy tensor as the source tensor S_{cb}. It describes how matter reacts to variations in the spacetime geometry. Now, in an area-metric geometry going from the $(1,1)$ energy momentum tensor T^a_b to a $(0,2)$ source tensor S_{ab} is not straightforward at all, since indices cannot simply be lowered and raised by using a metric [Wit14]. However, following [GM01] it is still possible to properly define the so-called Gotay-Mardsen energy-momentum tensor density for generalized spacetime geometries $G^{\mathcal{A}}$ as

$$\tilde{T}^a_b = C^{\mathcal{A}a}{}_b \frac{\delta S_{\text{matter}}}{\delta G^{\mathcal{A}}}.$$

Here, a de-densitization factor $f(G)^{-1}$, which depends on the specific geometry, can be introduced according to [Fis17]. Then, the tensor density $\tilde{T}^a_b$ is related to the corresponding tensor T^a_b by

$$T^a_b = f(G)^{-1} \tilde{T}^a_b.$$

Furthermore, the coefficient $C^{\mathcal{A}a}{}_b$ is defined via the Lie derivative

$$(\mathcal{L}_X G)^{\mathcal{A}} = X^a \partial_a G^{\mathcal{A}} - C^{\mathcal{A}a}{}_b \partial_a X^b.$$

The source tensor density $\tilde{S}_{\mathcal{A}}$ is then given by a variation of the matter action with respect to the spacetime geometry with

$$\tilde{S}_{\mathcal{A}} = -\text{rank} G \frac{\delta S_{\text{matter}}}{\delta G^{\mathcal{A}}},$$

which can also be written as a tensor by mulitplication with the de-densitization factor [Fis17]. In area-metric geometry the Gotay-Marsden energy momentum tensor specializes to [Due20]

$$T^a_b = -\frac{4}{\omega_{G^{-1}}} G^{ampq} \frac{\delta S_{\text{matter}}}{\delta G^{bmpq}}. \tag{5.3}$$

Here, $1/\omega_{G^{-1}}$ is the de-densitization factor. In [GM01] it is also shown how a covariant energy-momentum tensor density conservation law can be established on a generalized geometry as

$$0 = \partial_a \left(\tilde{T}^a_b \right) - \frac{\delta S_{\text{matter}}}{\delta G^{\mathcal{A}}} \partial_b G^{\mathcal{A}},$$

similar to the notation by [Fis17]. While in the metric case this becomes the usual local energy-momentum conservation with respect to the covariant derivative [Fis17]

$$\begin{aligned} &\partial_a \left(\sqrt{-\text{det}g} T^a_b \right) + \frac{1}{2} \sqrt{-\text{det}g} T^c_d g_{ca} \partial_b g^{ad} = 0, \\ \Rightarrow\ &\nabla_a T^a_b = 0, \end{aligned}$$

the local covariant energy-momentum conservation in the area-metric case is given by [SW17]

$$\partial_a \left(\omega_{G^{-1}} T^a_b \right) - \frac{\delta S_{\text{matter}}}{\delta G^{cdef}} \partial_b G^{cdef} = 0.$$

Thus, from (5.3) it can be infered that variation of the action 5.1 with respect to the area-metric leads to the Gotay-Mardsen energy momentum tensor for area-metric electrodynamics [Fis17]

$$T^a_b = \frac{1}{2} G^{paqr} \left(F_{pb} F_{qr} - \frac{\omega_{G^{-1}}}{24} \epsilon_{pbqr} G^{cdef} F_{cd} F_{ef} \right).$$

By subsequent insertion of a WKB ansatz for the field strength F_{ab} one can further derive the period of oscillation averaged Gotay-Mardsen energy momentum tensor density for propagating light accordig to the steps laid out in [SW17]; [Fis17], which are based on general ideas from [SEF92]. Here, conditions like $G^{abcd} k_b k_c A_d = 0$ have to be applied on the electromagnetic potential A_p, where k_b is the wave co-vector. This condition may be derived by insertion of the WKB ansatz into the Maxwell equations of area-metric electrodynamics. These are given by [Fis17]

$$\begin{aligned} &\partial_{[b} F_{cd]} = 0, \\ &\frac{1}{2} \frac{1}{\omega_{G^{-1}}} \partial_b \left(\omega_{G^{-1}} G^{abcd} F_{cd} \right) = 0. \end{aligned}$$

The according derivation steps are discussed in more detail in [SW17]; [Fis17], and hence omitted here.

The authors [SW17] finally find that the averaged energy-momentum tensor density is given by

$$\omega_{G^{-1}} \left\langle T^a_b \right\rangle = -\frac{1}{4} \omega_{G^{-1}} G^{paqr} \left(A_p A^*_q + A^*_p A_q \right) k_r k_b \coloneqq \tilde{N}^a k_b,$$

with photon current density $\tilde{N}^a$. Hence, the according covariant energy-momentum conservation law becomes

$$\partial_b \tilde{N}^b = \partial_b \left(\omega_{G^{-1}} N^b \right) = 0.$$

This is different from the covariant conservation law in metric geometry which is given by

$$\frac{1}{\sqrt{-\det g}} \partial_b \left(\sqrt{-\det g} N^b \right) = 0, \quad \Rightarrow \ \nabla_a N^a = 0,$$

for it is defined with respect to a different density factor $\sqrt{-\det g}$ instead of $\omega_{G^{-1}}$. Here, N^a is the photon current vector.
In a weakly birefringent setting the photon geodesic can actually described by an effective metric to first order, what will be further discussed in Section 5.2. Contrary, the covariant consevation law is non-metric, what will lead to a surprising results: The covariant derivative of the photon current vector with respect to the effective metric is non-vanishing $\nabla_a N^a \neq 0$, such that line-of sight integration of the photon current from the source to the observer leads to a photon excess, as shown in [SW17] for instance. The implications thereof on the Etherington distance duality and other observables like surface brightness and the magnification bias in lensing will be summarized and further developed in this chapter.

5.2 Light propagation and lensing in area-metric spacetimes

In this section basic ideas about light propagation in weakly birefringent spacetimes should be recapitulated based on works by [Dü+18]; [Sch+17]; [Wol22]; [SW17]; [Ale20b]. Afterwards, the weak lensing spectra in such spacetimes should be derived following the steps discussed in [SEF92]; [BS01]; [Bar10]; [BM17] for instance.

On a flat background with a small perturbation H^{abcd} an ansatz for the area-metric can be generally given by [SW17]; [Sch+17]; [Ale20b]; [Lic17]

$$G^{abcd} = \eta^{ac}\eta^{bd} - \eta^{ad}\eta^{bc} - \sqrt{-\det\eta}\epsilon^{abcd} + H^{abcd}.$$

The components are specified as

$$\begin{aligned}
G^{t\alpha t\beta} &= -\gamma^{\alpha\beta} + H^{t\alpha t\beta} = -\gamma^{\alpha\beta} + (2A - 1/2U + 1/2V)\,\gamma^{\alpha\beta}, \\
G^{t\beta\gamma\delta} &= \epsilon^{\beta\gamma\delta} + H^{t\beta\gamma\delta} = \epsilon^{\beta\gamma\delta} + \left(\frac{3}{4}U - \frac{3}{4}V - A \right) \epsilon^{\beta\gamma\delta}, \\
G^{\alpha\beta\gamma\delta} &= \gamma^{\alpha\gamma} - \gamma^{\beta\delta} - \gamma^{\alpha\delta}\gamma^{\beta\gamma} + H^{\alpha\beta\gamma\delta} = (1 + 2U - V)\left(\gamma^{\alpha\gamma} - \gamma^{\beta\delta} \right),
\end{aligned}$$

where $\gamma^{\alpha\beta}$ is an euclidean metric in spatial three space and a and b are the spacetime indices. The split of the area-metric components into the functions $U(r)$, $V(r)$ and $A(r)$ is purely kinematic. The according dynamics, and thus explicit solutions for these functions, can be derived again from the gravitational closure equations[1] in the weak field limit for a point mass M as source of the gravitational field. The according solutions are Yukawa refinements of the Newtonian potential which are given by

$$\begin{aligned} A(r) &= -\frac{M}{4\pi r}\left(\kappa - \kappa\sigma\delta\exp\left(-\eta r\right)\right), \\ U(r) &= -\frac{M}{4\pi r}\kappa\delta\exp\left(-\eta r\right), \\ V(r) &= \frac{M}{4\pi r}\left(4\kappa - \tau\kappa\exp\left(-\eta r\right)\right), \end{aligned}$$

as stated for instance in [SW17]; [Sch+17]; [Ale20b]; [Lic17] with $r = |\boldsymbol{r} - \boldsymbol{r}_M|$ as the radial distance from the point-like source, and integration constants κ, δ, η, σ and τ. These are not specified by the constructive gravity program though, so they need to be determined by experiments. For abbreviation [SW17] introduce the following definitions

$$\zeta = \frac{1}{24}\epsilon_{abcd}H^{abcd} = \omega_G^{-1} - 1, \quad H^{ab} = H^{manb}\eta_{mn}, \quad H = H^{ab}\eta_{ab},$$

such that the prinicpal polynomial P^{abcd} and its dual $P^{\#}_{abcd}$ are approximately given by [SW17]; [Lic17]

$$\begin{aligned} P^{abcd} &\propto P^{(ab}P^{cd)} + O\left(H^2\right) \text{ with } P^{ab} = \eta^{ab} + \frac{1}{2}H^{ab} - \zeta\eta^{ab}, \\ P^{\#}_{abcd} &\propto P^{\#}_{(ab}P^{\#}_{cd)} + O\left(H^2\right) \text{ with } P^{\#}_{ab} = \eta_{ab} + \frac{1}{2}H_{ab} - \zeta\eta_{ab}, \\ P^{\#}_{00} &= (1 + 2A), \quad P^{\#}_{\alpha\beta} = -\gamma_{\alpha\beta}\left(1 + \frac{1}{2}\left(V - 3U\right)\right), \end{aligned}$$

to first order in the perturbation H. Here, $P^{\#}_{ab}$ is the effective metric for light propagation [SW17]. To first order the Legendre-map also becomes proportional to the Minkowski metric, which can thus be used for raising and lowering indices as one is used to in weak field general relativity [SW17]; [Lic17].

However, for cosmological lensing care has to be taken for the background geometry is actually not given by a Minkowski metric induced area-metric. Fortunately, as shown by [Due20]; [Fis17] the area-metric for a spatially flat universe ($k = 0$) is induced by the inverse FLRW-

[1] As a side remark, the results reviewed here were derived in the observer definition by [RRS11] based on the Legendre map L_x.

metric

$$g^{ab}\left(a(t)\right) = \mathrm{diag}\left(1, a^{-2}(t), a^{-2}(t), a^{-2}(t)\right),$$

depending on the scale factors $a(t)$ such that

$$G^{abcd} = c(t)^2 g^{ac}\left(a(t)\right) g^{bd}\left(a(t)\right) - c(t)^2 g^{ad}\left(a(t)\right) g^{bc}\left(a(t)\right) - c(t)^3 \sqrt{-\mathrm{det} g\left(a(t)\right)} \epsilon^{abcd}, \quad (5.4)$$

with an additional scale factor $c(t)$ as extra degree of freedom for the spacetime dynamics. The time evolution of the two scale factors $a(t)$ and $c(t)$ is determined by three refined Friedmann equations which can be derived in the framework of the constructive gravity program, as done by [Due20]. The first refined Friedmann equation as given in detail in [Due20], but not stated explicitly here, is basically a constraint equation defining a refined Hubble function $H(a, c)$. The second Friedmann equation is an evolution equation for the scale factor $a(t)$,and, in contrast to general relativistic cosmology, also a third Friedmann equation emerges as evolution equation for the second scale factor $c(t)$ [Due20]; [Fis17]. These Friedmann equations are sourced by an ideal fluid which can be related to the generalized Gotay-Mardsen source tensor (for details refer to [GM01]) in area-metric geometry. Interestingly, this source tensor contains - besides pressure $p(t)$ and density $\rho(t)$ - another fluid degree of freedom $q(t)$ for which no physical interpretation has been found yet [Fis17]; [Due20] other than contributing as gravitational source.

Assuming that to zeroth order the cosmologcial model under consideration is indeed given by ΛCDM cosmology, the second scale factor can be set close to $c(t) = 1$. Then, the area-metric in (5.4) is simply induced by the usual FLRW metric, which is only determined by the the scale factor $a(t)$. Also all time derivatives need to be close to zero $\mathrm{d}^N c(t)/\mathrm{d}t = 0$, such that the scale factor $c(t)$ stays close to one during time evolution. Consequently, the refined Friedmann equations can be expressed perturbatively [Due20]: The first two of them can - with appropriate choice of constants - be expressed in their usual version (see [Bar19a] for instance) in terms of $\rho(t)$ and $p(t)$ only as

$$\left(\frac{\dot{a}}{a}\right)^2 = \frac{8\pi G}{3}\rho + \frac{\Lambda}{3}, \quad (5.5)$$

$$\frac{\ddot{a}}{a} = -\frac{4\pi G}{3}\left(\rho + 3p\right) + \frac{\Lambda}{3}. \quad (5.6)$$

In this case the third Friedmann equation as stated in [Due20], which describes the evolution of the unknown degree of freedom $q(t)$, still remains as

$$0 = q + 3\rho + C_1 + C_2\frac{\dot{a}}{a} + \left(\frac{\dot{a}}{a}\right)^2 C_3 + \frac{\ddot{a}}{a}C_4,$$

with unknown constants C_1 to C_4. Though this gives a relation between the density $\rho(t)$ and pressure $p(t)$ and the unknown degree of freedom $q(t)$, it does not affect the first two Friedmann equations. Thus, the equations (5.5) will be used to effectively describe cosmology as in general relativity. Also, the extra degree of freedom $q(t)$ appears in principle also in the covariant conservation equation of the energy-momentum tensor density and the generalized Gotay-Marsden source tensor density (for details refer to [GM01]; [Due20]):

$$0 = \dot{\rho} + 3\frac{\dot{a}}{a}(\rho + q) + 3\frac{\dot{c}}{c}q.$$

But for $\dot{c} = 0$, which is assumed here, the last term drops out of the conservation equation. It is hence demanded, that the background cosmology evolves according to ΛCDM[2].

To determine the effective metric $P^{\#}_{ab}$ on a cosmological background as described above, a standard assumption from lensing (see for instance [SEF92]; [BS01]; [Bar10]) is adjusted here to include clump contributions. This ansatz is usually done in the context of weak gravitational lensing in general relativity, where the metric is perturbed by local Newtonian potential contributions. Here, local refers to scales which are small compared to the Hubble length. Since the FLRW metric is conformally flat this breaks down to a Minkowski metric being peturbed by a Newtonian potential as discussed in section 4.1. A further requirement to make this ansatz is that the clump contributions sourcing the Newtonian potentials have to move slowly with respect to the Hubble flow.

Now, this idea will be generalized to the case of weakly birefringent spacetime: The prinicpal polynomial and its dual are also conformally[3] flat for a cosmological spacetime with Fresnel tensor

$$P^{\#}_{abcd} = a^2(\eta_c)\,\eta_{(ab}\eta_{cd)},$$

and conformal time η_c with $\mathrm{d}\eta_c = c\mathrm{d}t/a(t)$. Thus, an appropriate ansatz for the effective line-element in weakly birefringent spacetime on a cosmological background can be given by

$$\mathrm{d}s^2 = P^{\#}_{ab}\mathrm{d}x^a\mathrm{d}x^b = a^2(\eta_c)\left((1+2A)\,\mathrm{d}\eta_c^2 - \gamma_{\alpha\beta}\left(1+\frac{1}{2}(V-3U)\right)\mathrm{d}x^\alpha\mathrm{d}x_\alpha\right). \tag{5.7}$$

[2]Even though this assumption can be challenged, one will now continue to explicitly only focus on phenomenology caused by the Yukawa corrections in the weak field limit.

[3]In this context conformality still applies to the Fresnel tensors and hence the principal polynomials as stated in [PWS09].

This may also be derived in a calculation similar to [Lic17] by inserting the following area-metric

$$G^{abcd} = g^{ac}\left(a\left(\eta_c\right)\right) g^{bd}\left(a\left(\eta_c\right)\right) - g^{ad}\left(a\left(\eta_c\right)\right) g^{bc}\left(a\left(\eta_c\right)\right) - \sqrt{-\det g\left(a\left(\eta_c\right)\right)}\epsilon^{abcd} + a^{-4}\left(\eta_c\right) H^{abcd},$$

with the inverse FLRW metric for conformal time $g^{ab}\left(a(\eta_c)\right) = a^{-2}\left(\eta_c\right)\eta^{ab}$, into the definition of the principal polynomial for general linear electrodynamics (see 1.5).
Now, the effective convergence as introduced in the conventional weak lensing formalism by [BS01] is adjusted in the following. This is possible here, since the light propagation is effectively metric [SW17], even though the spacetime under consideration is weakly area-metric. Hence, with the line element as stated in equation (5.7) one can now derive the effective gravitational lensing effect with standard methods [BS01]; [Bar10]; [BM17]. For photons propagating on null geodesics defined by this effective metric the following result for speed of light c' holds to first order:

$$\begin{aligned}
\mathrm{d}s^2 = 0 \quad &\Rightarrow (1+2A)\,\mathrm{d}\eta_c^2 = \left(1 + \frac{1}{2}\left(V - 3U\right)\right)\mathrm{d}x^\alpha \mathrm{d}x_\alpha, \\
&\Rightarrow c' = \left|\frac{\mathrm{d}\vec{x}}{\mathrm{d}t}\right| = \frac{\sqrt{1+2A}}{\sqrt{1+\frac{1}{2}\left(V-3U\right)}} \approx 1 + A - \frac{1}{4}\left(V - 3U\right) \\
&\qquad = 1 - \frac{2M\kappa}{4\pi r} - \frac{M\kappa}{4\pi r}\exp\left(-\eta r\right)\delta\left(\frac{3}{4} - \frac{1}{4}\frac{\tau}{\delta} - \sigma\right) \\
&\qquad = 1 - 2\frac{G}{c^2}\frac{M}{r} - \tilde{\delta}\frac{G}{c^2}\frac{M}{r}\exp\left(-\eta r\right).
\end{aligned}$$

Here, $G/c^2 \equiv \kappa/4\pi$ is the gravitational constant, and the undetermined area-metric constants are summarized as $\tilde{\delta} \equiv \delta\left(3/4 - \tau/(4\delta) - \sigma\right)$. In this form the single constants δ, τ and σ are degenerate and cannot be measured separately via lensing, but only the combined factor $\tilde{\delta}$.
The total deflection potential for a deflecting point mass is thus given by

$$\Phi_{\mathrm{Def}}\left(\vec{r}\right) = -\frac{GM}{c^2\left|\boldsymbol{r} - \boldsymbol{r}_M\right|}\left(1 + \frac{\tilde{\delta}}{2}\exp\left(-\eta\left|\boldsymbol{r} - \boldsymbol{r}_M\right|\right)\right),$$

which is the ordinary Newtonian law $\Phi_N\left(\boldsymbol{r}\right)$ with a Yukawa potential $\Phi_Y\left(\boldsymbol{r}\right)$ refinement. For an extended mass distribution this potential can be expressed in a continuum limit as [Rie20]

$$\frac{\Phi_{\mathrm{Def}}\left(\vec{r}\right)}{c^2} = -\frac{G}{c^2}\int \mathrm{d}^3 r' \, \frac{\rho\left(\boldsymbol{r}'\right)}{\left|\boldsymbol{r} - \boldsymbol{r}'\right|} - \frac{G}{c^2}\frac{\tilde{\delta}}{2}\int \mathrm{d}^3 r' \, \frac{\rho\left(\boldsymbol{r}'\right)}{\left|\boldsymbol{r} - \boldsymbol{r}'\right|}\exp\left(-\eta\left|\boldsymbol{r} - \boldsymbol{r}'\right|\right). \tag{5.8}$$

The corresponding coupled Poisson equation can be given - in a similar way as in [Rie20] - by

$$\begin{aligned}\Delta\Phi_{\mathrm{Def}}(\boldsymbol{r}) - \eta^2\left(\Phi_{\mathrm{Def}}(\boldsymbol{r}) - \Phi_N(\boldsymbol{r})\right) &= 4\pi G(1+\tilde{\delta}/2)\rho(\boldsymbol{r}),\\ \Delta\Phi_N(\boldsymbol{r}) &= 4\pi G\rho(\boldsymbol{r}).\end{aligned} \tag{5.9}$$

Thus, in the continuum limit with (5.8) the expression for c', and thus the refractive index n can be written as

$$\begin{aligned}c' &= 1 + 2\frac{\Phi_N(\boldsymbol{r})}{c^2} + \tilde{\delta}\frac{\Phi_{\mathrm{Y}}(\boldsymbol{r},\eta)}{c^2} = 1 + 2\frac{\Phi_{\mathrm{Def}}(\boldsymbol{r})}{c^2},\\ \Rightarrow n &= \frac{c}{c'} \approx 1 - 2\frac{\Phi_{\mathrm{Def}}(\boldsymbol{r})}{c^2},\end{aligned}$$

where the deflecting potential Φ_{Def} is simply the Newtonian potential Φ_N for vanishing $\tilde{\delta} = 0$. Thus, in this limit standard gravitational lensing can be recovered consistently.
Extremizing the light path from the source S to the observer along the line of sight according to Fermat's priniciple and taking Born's approximation into account, as discussed in more detail in [BM17] and also briefly mentioned in Section 4.1, leads to the following deflection angle $\boldsymbol{\alpha}$, and thus lensing potential Ψ

$$\begin{aligned}\Psi(\boldsymbol{\theta},\chi_S) &= 2\int_0^{\chi_S} \mathrm{d}\chi\, \frac{\chi_S - \chi}{\chi_S\chi}\frac{\Phi_{\mathrm{Def}}(\chi\boldsymbol{\theta},\chi)}{c^2},\\ \boldsymbol{\alpha} &= \boldsymbol{\nabla}_\theta\Psi(\boldsymbol{\theta},\chi_S).\end{aligned}$$

Here, χ is the comoving distance along which the integration is performed, χ_S is the comoving distance between the observer and the source, and $\boldsymbol{\theta}$ is the angular separation in the image plane. Notably, the effective convergence κ_{eff} is still defined as the gradient of the effective deflection angle

$$\kappa_{\mathrm{eff}}(\boldsymbol{\theta},\chi) = \frac{1}{2}\boldsymbol{\nabla}_\theta\cdot\boldsymbol{\alpha}(\boldsymbol{\theta},\chi) = \frac{1}{2}\Delta_\theta\Psi(\boldsymbol{\theta},\chi), \tag{5.10}$$

as in [BS01] for instance.
In comoving coordinates the system of coupled Poisson equations (5.9) becomes

$$\begin{aligned}\Delta_\chi a^{-2}\frac{\Phi_{\mathrm{Def}}(\chi\boldsymbol{\theta},\chi)}{c^2} - \eta^2\left(\frac{\Phi_{\mathrm{Def}}(\chi\boldsymbol{\theta},\chi)}{c^2} - \frac{\Phi_{\mathrm{N}}(\chi\boldsymbol{\theta},\chi)}{c^2}\right) &= \left(1+\frac{\tilde{\delta}}{2}\right)\frac{3\Omega_{m_0}}{2\chi_H^2}\delta_c(\chi\boldsymbol{\theta},\chi)\,a^{-3},\\ \Delta_\chi a^{-2}\frac{\Phi_{\mathrm{N}}(\chi\boldsymbol{\theta},\chi)}{c^2} &= \frac{3\Omega_{m_0}}{2\chi_H^2}\delta_c(\chi\boldsymbol{\theta},\chi)\,a^{-3}.\end{aligned} \tag{5.11}$$

Combining these, the Fourier space representation of the deflection potential $\tilde{\Phi}_{\mathrm{Def}}(k,\chi)$ with $k = \ell/\chi$ and $\Delta_\chi \to -k^2$ becomes

$$\frac{\tilde{\Phi}_{\mathrm{Def}}}{c^2}(k,\chi) = -\left(k^2+\eta^2 a^2\right)^{-1}\left(1+\frac{\tilde{\delta}}{2}+a^2\eta^2k^{-2}\right)\frac{3\Omega_{m_0}}{2\chi_H^2}\tilde{\delta}_c(k,\chi)\,a^{-1}. \tag{5.12}$$

Clearly, in the limit $\eta \to 0$ and $\tilde{\delta} \to 0$ the comoving Newtonian Poisson equation in Fourier space reemerges. Also, one can read off from the comoving Poisson equations (5.11), that the Yukawa refinement likely starts to become of interest for late time universe physics: For early times the scale factor goes to zero, such that the term $\eta^2 a^2$ is suppressed. Thus, for early times it is expected that the Poisson equation is approximately Newtonian, such that structure formation and as a result the density power spectrum can be assumed to be $P_{\delta_c\delta_c}$(k) [Schb].

Now, in a tomographic analysis (for details refer to [MCK14] for instance) an average is performed over the source redshift distribution for a flux limited survey which is - like in section 4.4.4 - given as

$$p(z) = \frac{\beta}{z_0\Gamma\left((\alpha+1)/\beta\right)}\left(\frac{z}{z_0}\right)^\alpha e^{-(z/z_0)^\beta} \propto (z/z_0)^\alpha\, e^{-\left(\frac{z}{z_0}\right)^\beta}, \tag{5.13}$$

with $\alpha = 2, \beta = 1.5$, $z_0 = 0.64$ [Lau+11]; [LHG07]. Then the lensing potential Ψ_B within a tomographic redshift bin B is given as

$$\Psi_B(\boldsymbol{\theta}) = \int_0^{\chi_H} \mathrm{d}\chi\, a W_{\Psi,B}(\chi)\,\frac{\Phi_{\mathrm{Def}}}{c^2},$$
$$\text{with } W_{\Psi,B}(\chi) = \frac{2}{\chi}\frac{D_+(a)}{a}\int_{\max(\chi,\chi_B)}^{\chi_{B+1}} \mathrm{d}\chi'\, p(\chi')\,\frac{\mathrm{d}z}{\mathrm{d}\chi'}\left(1-\frac{\chi}{\chi'}\right),$$

with Hubble-function $-\mathrm{d}\chi' H(\chi') = c\mathrm{d}z$, linear growth factor $D_+(a)$ and Hubble length χ_H. Thus, one can define the following spectrum for the lensing potential taking Limber's approximation [Lim54] into account

$$\begin{aligned} C^{\Psi_A\Psi_B}(\ell) &= \int_0^{\chi_H}\mathrm{d}\chi\, a W_{\Psi,A}(\chi)\int_0^{\chi_H}\mathrm{d}\chi'\, a W_{\Psi,B}(\chi')\left\langle\frac{\Phi_{\mathrm{Def}}}{c^2}(k=\ell/\chi,\chi)\;\frac{\Phi_{\mathrm{Def}}}{c^2}(k'=\ell'/\chi',\chi')\right\rangle \\ &= \int_0^{\chi_H}\mathrm{d}\chi\,\frac{a^2}{\chi^2c^4}W_{\Psi,A}(\chi)W_{\Psi,B}(\chi)P_{\Phi_{\mathrm{Def}}\Phi_{\mathrm{Def}}}(k=\ell/\chi,\chi), \end{aligned}$$

with the potential power spectrum $P_{\Phi_{\mathrm{Def}}\Phi_{\mathrm{Def}}}$. This can be further expressed in terms of the overdensity fluctuation spectrum $P_{\delta_c\delta_c}(k) \propto k^{n_S}T(k)^2$ by insertion of (5.12). Consequently, with the definition (5.10) of the effective convergence the respective spectrum in Fourier space

becomes

$$
\begin{aligned}
C_{AB}^{\kappa_{\rm eff}\,\kappa_{\rm eff}} =& \frac{l^4}{4}\int_0^{\chi_H}\frac{\mathrm{d}\chi}{\chi^2}\,W_{\Psi,A}(\chi)W_{\Psi,B}(\chi)\left(k^2+\eta^2a^2\right)^{-2}\left(1+\frac{\tilde{\delta}}{2}+a^2\eta^2k^{-2}\right)^2\frac{9\Omega_{m_0}^2}{4\chi_H^4}P_{\delta_c\,\delta_c}(k)\\
=& \frac{l^4}{4}\int_0^{\chi_H}\frac{\mathrm{d}\chi}{\chi^2}\,W_{\Psi,A}(\chi)W_{\Psi,B}(\chi)k^{-4}\left(1+\frac{\tilde{\delta}/2\,k^2}{k^2+\eta^2a^2}\right)^2\frac{9\Omega_{m_0}^2}{4\chi_H^4}P_{\delta_c\,\delta_c}(k),
\end{aligned}
\tag{5.14}
$$

where $\Delta_\theta \to -\ell^2$ is used. The effective lensing magnification spectrum is given by

$$
C_{AB}^{\delta\mu_{\rm eff}\,\delta\mu_{\rm eff}}(\ell) = 4C_{AB}^{\kappa_{\rm eff}\,\kappa_{\rm eff}}(\ell).
$$

However, as will be discussed later, the magnification is not only altered by a different kind of deflection potential compared to standard lensing, but also a modification of the Etherington distance dualtiy as discussed in Section 5.3.2.

5.3 Surface brightness fluctuation spectra

The observed surface brightness I and the observed logarithmic surface brightness S of galaxies [FHH20] are defined as

$$
S = \log_{10}\left(\frac{F}{A}\right) = \log_{10}(I)\,, \tag{5.15}
$$

where F is the measured flux, and A is the observed galaxy image area in squared arc seconds. In conventional gravitational lensing within general relativity the observed surface brightness $I(\theta(\beta))$ at image position $\boldsymbol{\theta}$ equals - up to redshift correction factors - the intrinsic surface brightness $I_0(\beta)$ of a source at $\boldsymbol{\beta}$ since it is not changed under light deflection, i.e. $I_0(\beta) = I(\theta(\beta))$ [BS01]; [SEF92].

Now, the influence of local tidal fields $\Delta\Phi$ due to intrinsic alignment changes the intrinsic size and thus also the intrinsic cross-sectional area measure A of the galaxies. The surface brightness scales with inverse area or size of the galaxy, measured in terms of the second moments of the surface brightness distribution, as discussed in the previous Chapter 4. Consequently, it will be directly affected by intrinsic alignment, as will be presented in the following Section 5.3.1. In general relativity, these variations in the intrinisc surface brightness will directly translate to variations in the observed surface brightness.

However, in the framework of weakly birefringent spacetimes, the prediction of the violation of the Etherington distance duality relation, would result in deviations of the surface brightness conservation law in lensing. This will lead to a variation of the observed surface brightness compared to the intrinsic one. This effect looks similar to intrinsic surface bright-

ness variations due to intrinsic alignment in classical astrophysics: For instance, it affects the respective quadrupole moment of the surface brightness distribution. Consequently, this leads to an imprint in the apparent size of observed galaxies, similar to intrinsic effects, however with different parameterization.
Thus, it is important to parameterize both effects separately, as well as to quantify their strength in their respective regimes to decide which of them would actually be dominant in an observation. This will be done in the following three sections. Intrinsic surface brightness fluctuations in classical astrophysics are caused by interaction with local tidal fields. Contrary, the surface brightness fluctuation in the non-metric theory considered here are a lensing effect along the entire line of sight. Hence, the two effects do not influence each other, however in an actual measurement of the surface brightness fluctuation only the sum of both effects can be measured.
In the next section, the surface brightness effect for classical intrinsic alignment is derived. Then, the surface brightness variations in Etherington distance duality violating weak lensing are parameterized. Finally, both effects will be evaluated quantitatively for different parameter values by considering the shape and amplitude of their respective spectra.

5.3.1 Intrinsic surface brightness variations

At first, details on how intrinsic alignment affects the intrinsic surface brightness of galaxies will be discussed. A central assumption is hereby, that the influence of local tidal fiels $\Delta\Phi$ can lead to an effective change in the source area A, while the total number of stars N_{stars} within the galaxies does not change. Since the number of stars determines the light production of a galaxy and thus the measured flux density F the simple proportionality $N_{\text{stars}} \propto F$ is taken to first oder. However, as an aside, tidal fields could possibly enhance star formation (see also [Ren10]) due to increased density of molecular gas making the collapse of these gas clouds more likely. This effect is neglected here for simplicity. Additionally, standard Newtonian gravity is considered to derive the surface brightness fluctuations caused by intrinsic alignment. It shall thus be directly contrasted, how intrinsic surface brightness can vary in a standard description in general relativity, with possible flucutations in lensing due to exotic gravitational physics. Still, it is reasonable to ask whether or not to include the Yukawa corrections also for the intrinsic alignment model. But because the alignment paramer D_{IA} is only determined up to a factor 10, the additional effects would not resolvable. This holds true especially given that the parameterization is chosen here such, that effects due to the areametric modifications only become significant on cosmological scales. As will be discussed later in Section 5.4 this means that the values η and δ will be set to multiples of several inverse Hubble lengthts, what is very small compared to one. Consequently, the additional effects

due to area-metric refinements may be absorbed within the alignment parameter D_{IA}. Yet, it would also be interesting to study, how precisely the linear alignment model itself is modified by including area-metric corrections, too.
Now, the linear alignment model for intrinsic ellipticities first discussed by [GDS21], and extended to intrinsic flexions in Chapter 4, is employed. As stated previoulsy, it is based on the Jeans-equation [Pir+17]

$$\sigma^2 \partial_r \ln\left(\rho(r)\right) = -\partial_r \Phi,$$

where stellar density $\rho(r)$, that is considered to be proportional to the surface brightness distribution $I(r)$, is given by

$$\rho(r) = \bar{\rho}_1 \exp\left(-\frac{\Phi(r)}{\sigma^2}\right) = \frac{N_{\mathrm{stars}}}{A_1} \exp\left(-\frac{\Phi(r)}{\sigma^2}\right). \tag{5.16}$$

Here, $\bar{\rho}_1 = N_{\mathrm{stars}}/A_1 \propto \bar{I}_1 = F/A_1$ is the normalization for $\rho(r)$ with units of stellar area density. The area is measured in square arcsec when going from radial separation r to angular separation with $r = \theta\chi$ and χ as comoving distance. Furthermore, $\bar{I}_1$ is the normalization constant for the surface brightness distribution $I(r)$. Thus, the integration over the galaxy area gives the number of stars, which is proportional to the flux, as

$$\begin{aligned} N_{\mathrm{stars}} &= \int \mathrm{d}^2 r\, \bar{\rho}_1 \exp\left(-\frac{\Phi(r)}{\sigma^2}\right) = \int \mathrm{d}^2 r \frac{N_{\mathrm{stars}}}{A_1} \exp\left(-\frac{\Phi(r)}{\sigma^2}\right) \\ \Rightarrow \quad A_1 &= \int \mathrm{d}^2 r\, \exp\left(-\frac{\Phi(r)}{\sigma^2}\right). \end{aligned}$$

Under the influence of tidal fields the potential becomes, to second order,

$$\Phi(r) \;\rightarrow\; \Phi(r) + \frac{1}{2}\partial_a \partial_b\, \Phi|_{r=0}\, r^a r^b\,, \tag{5.17}$$

which leads to a change in the stellar area density according to

$$\begin{aligned} \rho'(r) &= \bar{\rho}_2 \exp\left(-\frac{\Phi(r)}{\sigma^2}\right)\left(1 - \frac{1}{2\sigma^2}\Phi_{ab} r^a r^b\right) \\ &= \frac{N_{\mathrm{stars}}}{A_2} \exp\left(-\frac{\Phi(r)}{\sigma^2}\right)\left(1 - \frac{1}{2\sigma^2}\Phi_{ab} r^a r^b\right), \end{aligned} \tag{5.18}$$

with $\partial_a \partial_b \Phi \equiv \Phi_{ab}$.

It thus follows for the normalization of the number of stars N_{stars} that

$$\begin{aligned} N_{\text{stars}} &= \int \mathrm{d}^2 r\, \bar{\rho}_2 \exp\left(-\frac{\Phi(r)}{\sigma^2}\right)\left(1 - \frac{1}{2\sigma^2}\Phi_{ab} r^a r^b\right) \\ &= \int \mathrm{d}^2 r\, \frac{N_{\text{stars}}}{A_2} \exp\left(-\frac{\Phi(r)}{\sigma^2}\right)\left(1 - \frac{1}{2\sigma^2}\Phi_{ab} r^a r^b\right), \\ \Rightarrow \quad A_2 &= \int \mathrm{d}^2 r\, \exp\left(-\frac{\Phi(r)}{\sigma^2}\right)\left(1 - \frac{1}{2\sigma^2}\Phi_{ab} r^a r^b\right). \end{aligned}$$

Here, $\bar{\rho}_2 \propto \bar{I}_2$ is again the normalization factor in units of stellar area density such that integration over the density $\rho'(r)$ gives the same number of stars N_{stars} as in the unperturbed case. However, $\bar{\rho}_2$ differs from $\bar{\rho}_1$ due to the different definition of A_2, compared to A_1. Since A_1 and A_2 are both measures of area it can thus be concluded that the intrinsic area of the galaxies changes. To get an analytical expression for this change the Sérsic model is used for the density

$$\rho(r) \propto \exp\left(-\frac{\Phi(r)}{\sigma^2}\right) \hat{=} \exp\left(-b(n)\left[\left(\frac{r}{r_{\text{scale}}}\right)^{n^{-1}} - 1\right]\right), \tag{5.19}$$

with $b(n) \approx 2n - \frac{1}{3}$ and n denoting the Sérsic index. Consequently, by using the two substitutions $x = b\left[(r/r_{\text{scale}})^{n^{-1}} - 1\right]$ and $y = x + b$, one receives the following result for A_1 expressed in terms of the Gamma function $\Gamma(n)$:

$$\begin{aligned} A_1 &= \int \mathrm{d}^2 r\, \exp\left(-b(n)\left[\left(\frac{r}{r_{\text{scale}}}\right)^{n^{-1}} - 1\right]\right) \\ &= \int_0^{2\pi} \mathrm{d}\phi \int_0^{\infty} \mathrm{d}r r\, \exp\left(-b(n)\left[\left(\frac{r}{r_{\text{scale}}}\right)^{n^{-1}} - 1\right]\right) \\ &= 2\pi \int_{-b}^{\infty} \mathrm{d}x\, \exp(-x)\, \frac{n}{b} r_{\text{scale}^2} \left(\frac{x}{b} + 1\right)^{2n-1} \\ &= \frac{2\pi n}{b} r_{\text{scale}}^2 \int_0^{\infty} \mathrm{d}y\, \exp(-(y-b)) \left(\frac{y-b}{b} + 1\right)^{2n-1} \\ &= \frac{2\pi n}{b^{2n}} \exp(b) r_{\text{scale}}^2 \int_0^{\infty} \mathrm{d}y\, \exp(-y)\, y^{2n-1} = \frac{2\pi n}{b^{2n}} \exp(b) r_{\text{scale}}^2 \Gamma(2n). \end{aligned}$$

Similarly the area measure A_2 can be expressed as

$$\begin{aligned}
A_2 &= \int \mathrm{d}^2 r\, \exp\left(-b(n)\left[\left(\frac{r}{r_{\mathrm{scale}}}\right)^{n^{-1}} - 1\right]\right)\left(1 - \frac{1}{2\sigma^2}\Phi_{ab} r^a r^b\right) \\
&= \frac{2\pi n}{b^{2n}} \exp(b) r_{\mathrm{scale}}^2 \Gamma(2n) - \int_0^{2\pi} \mathrm{d}\phi \int_0^{\infty} \mathrm{d}r r\, \exp\left(-b(n)\left[\left(\frac{r}{r_{\mathrm{scale}}}\right)^{n^{-1}} - 1\right]\right) \frac{1}{2\sigma^2}\Phi_{ab} r^a r^b \\
&= A_1 - \int_0^{\infty} \mathrm{d}r\, \exp\left(-b(n)\left[\left(\frac{r}{r_{\mathrm{scale}}}\right)^{n^{-1}} - 1\right]\right) r^3 \\
&\qquad \times \int_0^{2\pi} \frac{\mathrm{d}\phi}{2\sigma^2} \left(\Phi_{00}\cos^2(\phi) + 2\Phi_{01}\cos(\phi)\sin(\phi) + \Phi_{11}\sin^2(\phi)\right) \\
&= A_1 - \frac{\pi\Delta\Phi}{2\sigma^2} \int_{-b}^{\infty} \mathrm{d}x\, \exp(-x)\left(\frac{x}{b} + 1\right)^{4n-1} \frac{r_{\mathrm{scale}}^4}{b} \\
&= A_1 - \frac{\pi\Delta\Phi}{2\sigma^2} \int_0^{\infty} \mathrm{d}y \exp(-y)\, y^{4n-1} \frac{r_{\mathrm{scale}}^4}{b^{4n}} n \exp(b) \\
&= A_1 \left(1 - \frac{r_{\mathrm{scale}}^2}{4b^{2n}\sigma^2} \frac{\Gamma(4n)}{\Gamma(2n)} \Delta\Phi\right) := A_1 \left(1 - F(n)\Delta\Phi\right),
\end{aligned}$$

where the polar coordinates $r_0 = r\cos\phi$ and $r_1 = r\sin\phi$ are inserted and $F(n)$ is defined by

$$F(n) := \frac{r_{\mathrm{scale}}^2}{4b^{2n}\sigma^2} \frac{\Gamma(4n)}{\Gamma(2n)}.$$

To conclude, the relative variation in the density distribution normalization factors, and thus the relative surface brightness, is given by

$$\begin{aligned}
\frac{\bar{\rho}_2 - \bar{\rho}_1}{\bar{\rho}_1} &= \frac{N_{\mathrm{star}}/A_2 - N_{\mathrm{star}}/A_1}{N_{\mathrm{star}}/A_1} = \frac{A_1 - A_2}{A_2} = \frac{F/A_2 - F/A_1}{F/A_1} = \frac{\bar{I}_2 - \bar{I}_1}{\bar{I}_1}, \\
\Rightarrow \frac{\delta\bar{\rho}}{\bar{\rho}_1} &= \frac{\delta\bar{I}}{\bar{I}_1} = \frac{-\delta A}{A_2} = \frac{F(n)\Delta\Phi}{1 - F(n)\Delta\Phi} \approx F(n)\Delta\Phi = -\frac{\delta A}{A_1}.
\end{aligned} \tag{5.20}$$

In the last step all terms of quadratic or higher order in $\Delta\Phi$ are neglected due to the weakness of the tidal fields. For an overdensity it holds that $\Delta\Phi > 0$ due to Poisson's equation. This leads to an increase in the relative density variation $\delta\bar{\rho}/\bar{\rho}_1 > 0$, and hence surface brightness variation $\delta\bar{I}/\bar{I}_1 > 0$. Consequently, the area decreases with $\delta A \equiv A_2 - A_1 < 0$. Insertion of the Sérsic model into expression (5.20) leads to the explicit result

$$\frac{\delta\bar{I}}{\bar{I}} = \frac{1}{4} r_{\mathrm{scale}}^2 b^{-2n} \frac{c^2}{\sigma^2} \frac{\Gamma(4n)}{\Gamma(2n)} \frac{\Delta\Phi}{c^2} = c^2 F(n) \frac{\Delta\Phi}{c^2} \propto \Delta\Phi \propto \frac{\delta s}{s_0} \equiv \Delta s.$$

So, $\Delta\Phi$ causes a change in intrinsic size, and hence also a variation in the surface brightness distribution. Now, the prefactor $c^2F(n)$ can be expressed in terms of the alignment parameter for the intrinsic ellipticites D_{IA}, since both scale with r^2_{scale}. For intrinsic ellipticities the alignment parameter scales like

$$D_{IA} \propto \frac{1}{2}\frac{c^2}{\sigma^2}\frac{\int \mathrm{d}^2 r\, \rho(r) r^4}{\int \mathrm{d}^2 r\, \rho(r) r^2}.$$

By rewritting the integral $\int \mathrm{d}^2 r$ via polar coordinates and performing the angular integrals, keeping in mind that changes in the intrinsic ellipticities scale with $\pi/4$ [GDS21], the parameter D_{IA} can be expressed in terms of the Sérsic model as

$$D_{IA} \propto \frac{1}{2}\frac{c^2}{\sigma^2}\frac{\pi/4}{2\pi}\frac{\int \mathrm{d}r\, \rho(r) r^5}{\int \mathrm{d}r\, \rho(r) r^3} = \frac{1}{2}\frac{c^2}{\sigma^2}\frac{1}{8} r^2_{\text{scale}} b^{-2n}\frac{\Gamma(6n)}{\Gamma(4n)}.$$

Thus, the surface brightness variation can be compactly expressed as

$$\frac{\delta\bar{I}}{\bar{I}} = 4\frac{\Gamma(4n)\Gamma(4n)}{\Gamma(2n)\Gamma(6n)} D_{IA}\frac{\Delta\Phi}{c^2}.$$

To conclude, the following relation between the relative surface brightness fluctuation and the relative size change from [GDS21] in the linear alignment model is obtained as

$$\frac{\delta\bar{I}}{\bar{I}} \propto \frac{1}{2} D_{\text{IA}}\frac{\Delta\Phi}{c^2} = |\Delta s| \quad \Rightarrow \frac{\delta\bar{I}}{\bar{I}} = 2 S_{\text{Sérsic}}(n)\,|\Delta s|\,.$$

Since the galaxy is compressed because of intrinsic alignment its surface brightness is enhanced and vice versa. Here, the proportionality factor

$$S_{\text{Sérsic}}(n) \coloneqq 4\frac{\Gamma(4n)^2}{\Gamma(2n)\Gamma(6n)}$$

is introduced as a scaling relation which takes the internal galactic dynamics into account via the Sérsic index. The II spectrum of self-correlations of the intrinsic surface brightness fluctuations $C_{AB}^{\delta I/I\,\delta I/I}$ is proportional to the intrinsic size spectrum $C_{AB}^{s\,s}$ by [GDS21] because

$$II: \quad C_{AB}^{\delta I/I\,\delta I/I}(\ell) = 4 S_{\text{Sérsic}}(n)^2 C_{AB}^{s\,s}(\ell), \tag{5.21}$$

with

$$C_{AB}^{s\,s}(l) = \ell^4 \int \frac{\mathrm{d}\chi}{\chi^2}\frac{D_{IA}^2}{c^4} W_{\varphi,A} W_{\varphi,B}\frac{9}{4}\frac{\Omega_{m_0}^2}{\chi_H^4} k^{-4} P_{\delta_c\delta_c},$$

and weighting function

$$W_{\varphi,A}(\chi) = \frac{1}{\chi^2} p(z(\chi)) \Theta(\chi - \chi_A) \Theta(\chi_{A+1} - \chi) \frac{H(\chi)}{c} \frac{D_+(a)}{a},$$

as discussed in section 4.4.4 in the context of intrinsic flexions. Here A and B denote the different redshift bins in a tomographic analysis.

As a side remark, the result (5.21) is analogous to the relation between the magnification fluctuation spectrum and the conventional weak lensing convergence spectrum in the linear approximation, namely [BS01]:

$$GG \text{ for GR} : C_{AB}^{\delta\mu\delta\mu}(\ell) \approx 4C_{AB}^{\kappa\kappa}(\ell).$$

However, while for the intrinsic alignment case the equality is exact since it is based on a linear model in the first place, the relation between the convergence and magnification fluctuation spectrum is only valid to first order. This is true because the magnification μ in gravitational lensing is defined non-linearly as the determinant of the inverse Jacobian of the lens map, and only in the weak lensing case an approximate linear relationship between magnification and convergence can be established.
After having discussed how surface brightness fluctuations may arise at the level of general relativity due to intrinsic alignment of galaxies, the next section will show how a similar effect appears if lensing occurs in an area-metric spacetime.

5.3.2 Surface brightness fluctuation in weakly birefringent lensing

In [SEF92] it is thoroughly shown how one can derive a relativistic version of the surface brightness conservation in lensing from the Etherington distance duality relation.
Deviations thereof - like for instance predicted for perturbative area-metric gravity [Sch+17]; [SW17]; [Mor+16]; [Ale20b] or even exotic photon decays [BK04] - would actually lead to violations of surface brightness conservation in gravitational lensing. In the scope of this thesis the first option will be analyzed in more detail.

The following discussion of the Etherington distance duality will - for self-consistency - shortly recapitualte the most important steps in the derivation of the Etherington distance dualilty for metric spacetimes based on [SEF92], and its area-metric modifications as discussed in [SW17]; [Fis17] in more detail.

The Etherington distance duality establishes a relation between the angular diameter distance

$$D_A \equiv \left(\frac{\mathrm{d}A_S}{\mathrm{d}\Omega_O}\right)^{1/2}, \tag{5.22}$$

and the redshift corrected luminosity distance

$$D_{L;\mathrm{cor}} \equiv \left(\frac{\mathrm{d}A_O}{\mathrm{d}\Omega_S}\right)^{1/2}, \tag{5.23}$$

which is given by the following reprocity relation [SEF92]

$$D_{L;\mathrm{cor}} = (1+z)\, D_A, \tag{5.24}$$

on a metric background. The angular diameter D_A distance quantifies how the physical cross-section area of a source $\mathrm{d}A_S$ is mapped to the solid angle $\mathrm{d}\Omega_O$ under which the source appears to the observer. The redshift corrected luminosity distance $D_{L;\mathrm{cor}}$, i.e. the purely geometrically defined luminosity distance, tells how the cross-section surface $\mathrm{d}A_O$ for the photon flux at the observer's position scales with the solid angle $\mathrm{d}\Omega_S$ into which the source radiates[4]. The redshift uncorrected luminosity distance D_L wich will be discussed later contains another factor $(1+z)$, such that

$$D_L \propto (1+z) D_{L;\mathrm{cor}} \propto (1+z)^2 D_A.$$

As discussed previously in Section 5.2 a weakly birefringent background geometry leads to an effectively metric light propagation, so the reciprocity relation (5.24) still holds. For this effective metric $P^{\#}_{ab}$ it is possible to define an effective covariant derivative ∇_a , as stated by [SW17]; [Fis17]. However, as elaborated by [SW17]; [Fis17] and summarized in Section 5.1 in more detail, the local photon flux conservation is now defined differently in terms of an area-metric background geometry as

$$\partial_b \left(\omega_{G^{-1}} N^b\right) = 0.$$

Thus, in the effectively metric description of light propagation the corresponding covariant derivative of the photon flux N^a is not zero $\nabla_a N^a \neq 0$. This results in a change of the observed photon flux at the observer's position due to the geometric structure of spacetime. This would hold true even after having corrected for standard physical processes like photon absorption due to dust [SW17].

[4] In principle, due to aberration, the angular diameter distance also depends on the 4-velocity U^o_O of the observer evaluated at the source position, and the redshift corrected luminosity distance depends on the 4-velocity of the source evaluated at the observer's position [SEF92].

In the standard treatment [SEF92] the number of photons emitted during proper time $\mathrm{d}\tau_S$ into the solid angle $\mathrm{d}\Omega_S$ within the energy interval $\hbar\mathrm{d}\omega_S$ by the source is given by

$$N_{\gamma,\mathrm{emit}} = \mathrm{d}\tau_S\,\mathrm{d}\Omega_S\,\mathrm{d}\omega_S\,\frac{L_{\omega_S}}{4\pi\hbar\omega_S}. \tag{5.25}$$

where the specific luminosity L_{ω_S} has units of $[L_{\omega_S}] = \mathrm{J\,ster^{-2}\,s^{-1}\,Hz^{-1}}$.
For the number of observed photons within a proper time interval $\mathrm{d}\tau_O$, and within the cross-section area $\mathrm{d}A_O$ and energy $\hbar\mathrm{d}\omega_O$ one gets

$$N_{\gamma,\mathrm{obs}} = \mathrm{d}\tau_O\mathrm{d}A_O\mathrm{d}\omega_O\frac{F_{\omega_O}}{\hbar\omega_O}. \tag{5.26}$$

with the specific flux F_{ω_O} with units $[F_{\omega_O}] = \mathrm{J\,m^{-2}\,s^{-1}\,Hz^{-1}}$.
Now, due to the modfication in observed photon flux compared to general relativity it holds according to [SW17]; [Fis17] that

$$N_{\gamma,\mathrm{obs}} = (1+\mu_{\mathrm{vio}})\,N_{\gamma,\mathrm{emit}}. \tag{5.27}$$

Here, the parameter μ_{vio} measures the deviation of $\nabla_a N^a$ from zero, and hence the violation of the Etherington distance duality relation. Its specific functional form will be discussed later in more detail. Consequently, by insertion of the photon number counts $N_{\gamma,\mathrm{emit}}$ (5.25) and $N_{\gamma,\mathrm{obs}}$ (5.26), the definition of the corrected luminosity distance $D_{L;\mathrm{cor}}$ (5.23), as well as the standard redshift law

$$\omega_S = (1+z)\omega_O = (1+z)\omega$$

into relation (5.27), the following specific flux density is obtained [SW17]; [Fis17]

$$F_\omega = \frac{L_{\omega(1+z)}}{4\pi(1+z)D^2_{L;\mathrm{cor}}}(1+\mu_{\mathrm{vio}}). \tag{5.28}$$

Integration over the frequencies then leads to the flux density [SW17]; [Fis17]

$$F = \frac{L}{4\pi(1+z)^2D^2_{L;\mathrm{cor}}}(1+\mu_{\mathrm{vio}}) \overset{!}{=} \frac{L}{4\pi D_L^2}.$$

where $D_L = D_{L;\mathrm{cor}}(1+z)/\sqrt{1+\mu_{\mathrm{vio}}}$ denotes the uncorrected luminosity distance defined via its relation to the bolometric luminosity L [SEF92]. Finally, by insertion of $D_{L;\mathrm{cor}}$ as given in

relation (5.24) into D_L the modified Etherington distance duality follows [SW17]; [Fis17]

$$\frac{D_L}{D_A\,(1+z)^2} = \sqrt{1+\mu_{\text{vio}}}\,. \tag{5.29}$$

Next, the surface brightness violation is derived by following the steps laid out in [SEF92], but now for the modified Etherington distance duality relation (5.29): The specific surface brightness I_ω is given in units of $[I_\omega] = \text{Jm}^{-2}\text{s}^{-1}\text{ster}^{-2}\text{Hz}^{-1}$. According to these units the observed specific surface brightness $I_{\omega;O}$ can be defined as the ratio between the (differential) flux density $\mathrm{d}F_\omega$ at the observer's position[5] and the solid angle $\mathrm{d}\Omega_O$ under which this source appears [SEF92]:

$$I_{\omega;O} = \frac{\mathrm{d}F_\omega}{\mathrm{d}\Omega_O}.$$

Thus, similar to [SEF92], insertion of the specific flux density

$$\mathrm{d}F_\omega = \frac{\mathrm{d}L_{\omega(1+z)}}{4\pi(1+z)D^2_{L;\text{cor}}}(1+\mu_{\text{vio}}) = \frac{\mathrm{d}L_{\omega(1+z)}\mathrm{d}\Omega_S}{4\pi(1+z)\mathrm{d}A_O}(1+\mu_{\text{vio}}),$$

leads to

$$\begin{aligned} I_{\omega;O} &= \frac{\mathrm{d}L_{(1+z)\omega}}{4\pi(1+z)\mathrm{d}A_S}\frac{\mathrm{d}\Omega_S}{\mathrm{d}A_O}\frac{\mathrm{d}A_S}{\mathrm{d}\Omega_O}(1+\mu_{\text{vio}}) \\ &= \frac{\mathrm{d}L_{(1+z)\omega}}{4\pi(1+z)\mathrm{d}A_S}\frac{D_A^2}{D^2_{L;\text{cor}}}(1+\mu_{\text{vio}}) \\ &= \frac{\mathrm{d}L_{(1+z)\omega}}{4\pi\mathrm{d}A_S}\frac{1}{(1+z)^3}(1+\mu_{\text{vio}}) \\ &= I_{(1+z)\omega;S}\frac{1}{(1+z)^3}(1+\mu_{\text{vio}}), \end{aligned} \tag{5.30}$$

where the specific surface brightness of the source is given by the ratio between the source luminosity $\mathrm{d}L_{(1+z)\omega}$ and its respective surface area element $4\pi\mathrm{d}A_S$ as

$$I_{(1+z)\omega;S} = \frac{\mathrm{d}L_{(1+z)\omega}}{4\pi\mathrm{d}A_S}.$$

Integration over all frequencies then leads to the relativistic conversion between the surface brightness distribution for the observer and the source surface brightness distribution:

$$I_O = I_S\,(1+z)^{-4}\,(1+\mu_{\text{vio}}) = I_{O;\text{classic}} + I_{O;\text{classic}}\,\mu_{\text{vio}}.$$

[5] Here, the differential flux density is used to specify that this relation must hold for an extended source rather than a point source (confirm [SEF92] for details).

Here, the classically expected surface brightness conservation law is given by [SEF92]

$$I_{O;\text{classic}} = I_S\,(1+z)^{-4}\,,$$

for $\mu_{\text{vio}} = 0$ and relativistic redshift corrections. Hence, the relative surface brightness variation in weakly birefringent lensing is in general described by

$$\frac{\delta I}{I} = \frac{I_O - I_{O;\text{classic}}}{I_{O;\text{classic}}} = \mu_{\text{vio}}. \tag{5.31}$$

The authors [SW17] have shown that for a weakly birefringent spacetime with gravity sourced by a point mass the Etherington distance duality relation is modified according to

$$D_L = (1+z)^2 D_A \left(1 + \frac{3\delta GM}{2c^2}\left(\frac{e^{-\eta r_{ML}}}{r_{ML}} - \frac{e^{-\eta r_{MO}}}{r_{MO}}\right)\right), \tag{5.32}$$

such that the violating factor μ_{vio} is given in terms of Yukawa refinements. Here, it specifically holds that $\nabla_a N^a = \partial_a\left(-3MG/(2r)\,\delta\exp(-\eta r)\right) N^a$ to first order approximation, so integration of the photon current from source to observer leads to an effective photon excess [SW17]. The inverse length scale of the Yukawa interaction is parameterised by η, while δ, which can be intepreted as a coupling to the Newtonian interaction, is unitless. Here, $\boldsymbol{r}_{\text{ML}} = |\boldsymbol{r}_L - \boldsymbol{r}'|$ is the euclidean distance between the deflector M at position $\boldsymbol{r}'$ and the light source at $\boldsymbol{r}_L$, and $\boldsymbol{r}_{\text{MO}} = |\boldsymbol{r}' - \boldsymbol{r}_O|$ is the distance between observer and deflector. This expression (5.32) can be rewritten in the following way for a continuous mass distribution via the density $\rho(\boldsymbol{r}')$ along the line of sight, due to the lineartiy of the approximate solution [Rie20]

$$\mu_{\text{vio}}\,(\boldsymbol{r}_L, \boldsymbol{r}_O) = \frac{3\delta}{2}\frac{G}{c^2}\int \mathrm{d}^3\, r'\rho(\boldsymbol{r}')\left(\frac{\exp(-\eta|\boldsymbol{r}_{\text{L}} - \boldsymbol{r}'|)}{|\boldsymbol{r}_{\text{L}} - r'|} - \frac{\exp(-\eta|\boldsymbol{r}' - \boldsymbol{r}_O|)}{|\boldsymbol{r}' - \boldsymbol{r}_O|}\right).$$

Then the formula for the Etherington distance duality violation is given by

$$\begin{aligned} D_L =&(1+z)^2 D_A\left(1 + \frac{3\delta}{2}\frac{G}{c^2}\int \mathrm{d}^3 r'\,\rho(\boldsymbol{r}')\left(\frac{1}{|\boldsymbol{r}_{\text{L}} - \boldsymbol{r}'|}\exp(-\eta|\boldsymbol{r}_{\text{L}} - \boldsymbol{r}'|) - \frac{1}{|\boldsymbol{r}'|}\exp(-\eta|\boldsymbol{r}'|)\right)\right) \\ =&(1+z)^2 D_A\left(1 - \frac{3}{2}\frac{G}{c^2}\delta\int \mathrm{d}^3 r'\,\rho(\boldsymbol{r}')K\,(\boldsymbol{r}_{\text{L}} - \boldsymbol{r}') + \int \mathrm{d}^3 r'\,\rho(\boldsymbol{r}')K\,(\boldsymbol{r}_{\text{O}} - \boldsymbol{r}')\right) \\ =&(1+z)^2 D_A\left(1 - \frac{3}{2}\,\delta\left(\frac{\Phi_{\text{Y}}(\boldsymbol{r_L})}{c^2} - \frac{\Phi_{\text{Y}}(\boldsymbol{r_O})}{c^2}\right)\right), \end{aligned} \tag{5.33}$$

where the Yukawa potential $\Phi_{\text{Y}}(\boldsymbol{r}_L)$ was defined as a convolution of the density distribution $\rho(\boldsymbol{r}')$ over the kernel function $K(\boldsymbol{r_S} - \boldsymbol{r}') = -G\exp(-\eta|\boldsymbol{r}_{\text{S}} - \boldsymbol{r}'|)/|\boldsymbol{r}_{\text{S}} - \boldsymbol{r}'|$, similar to [New].

Insertion of a point mass with $\rho(\boldsymbol{r}') = M\delta(\boldsymbol{r}_M - \boldsymbol{r}')$ then reproduces (5.32).
From (5.33) it may now be concluded, that the effective photon excess measured by μ_{vio} as predicted in birefringent spacetimes is determined by the Yukawa potential difference between observer and source:

$$\mu_{\text{vio}}(\boldsymbol{r}_S, \boldsymbol{r}_O) = -3\,\delta\left(\frac{\Phi_{\text{Y}}(\boldsymbol{r}_S)}{c^2} - \frac{\Phi_{\text{Y}}(\boldsymbol{r}_O)}{c^2}\right). \tag{5.34}$$

Now, one makes the assumption that the observer does - on average over different sources and directions - not measure the Yukawa potential at their position. This holds because they are approximated as ideal Friedmann-Lemaître-Robertson-Walker observer, who only measure the FLRW geometry locally and are comoving with the Hubble flow [Schb]. Thus, the effective photon excess factor can be simplified as

$$\mu_{\text{vio}}\,(\boldsymbol{r}_S) = -3\delta\frac{\Phi_{\text{Y}}\,(\boldsymbol{r}_S)}{c^2}. \tag{5.35}$$

This is the photon excess, which reaches the observer from a single source at $\boldsymbol{r}_S$. However, an average over many sources is required, and the light rays emitted feel a Yukawa potential for every point mass they pass by on their way from the source to the observer.
Thus, the expression (5.35) is now rewritten in terms of an integral over the comoving distance, similar to shear or convergence formulas in gravitational lensing. The Yukawa potential $\Phi_{\text{Y}}(\boldsymbol{r})$ is hereby projected along the line of sight, weighted by the source distribution of a flux limited survey (for instance (5.13) as proposed by [Lau+11]). This leads to an averaged violation factor $\bar{\mu}_{\text{vio}}$ with

$$\bar{\mu}_{\text{vio}}(\vec{\theta}) = -3\int_0^{\chi_H} \mathrm{d}\chi\; p\,(z(\chi))\,\Theta\,(\chi_A - \chi)\,\frac{H\,(\chi)}{c}D_+(a)\delta\frac{\Phi_{\text{Y}}(\chi\boldsymbol{\theta},\chi)}{c^2}. \tag{5.36}$$

The line of sight integral can be subdivided into various, extended tomographic bins from the observer position to some upper boundary denoted by χ_A. Furthermore, $H(\chi)$ is the Hubble function while $D_+(a)$ is the linear growth factor of standard structure formation - provided one makes the assumption that the description of cosmology does not to change significantly due to the area-metric structure, as remarked in Section 5.2.
In the linear limit, when generalizing to a continuous mass distribution $\rho(\boldsymbol{r})$, the potential is sourced by a Yukawa field equation according to

$$\left(\Delta - \eta^2\right)\Phi_{\text{Y}}(\boldsymbol{r}) = 4\pi G\rho(\boldsymbol{r}).$$

The comoving Poisson equation thus becomes

$$\left(\Delta_\chi a^{-2} - \eta^2\right) \frac{\Phi_\mathrm{Y}(\chi\boldsymbol{\theta},\chi)}{c^2} = \frac{3\Omega_{m_0}}{2\chi_H^2}\delta_c(\chi\boldsymbol{\theta},\chi)a^{-3},$$

with the Laplacian Δ_χ in comoving coordinates and the density contrast $\delta_c(\chi\boldsymbol{\theta},\chi)$, which is related to the density $\rho\,(\chi\boldsymbol{\theta},\chi)$ via

$$\rho(\chi\boldsymbol{\theta},\chi) = \frac{3H_0^2}{8\pi G}\Omega_{m_0}a^{-3}\delta_c(\chi\boldsymbol{\theta},\chi),$$

and the Hubble length $\chi_H = c/H_0$. In Fourier space the Yukawa field equation becomes

$$\begin{aligned} -\left(k^2a^{-2} + \eta^2\right)\frac{\tilde{\Phi}_\mathrm{Y}\,(k,\chi)}{c^2} =& \frac{3\Omega_{m_0}}{2\chi_H^2}\tilde{\delta}_c\,(k,\chi)\,a^{-3}, \\ \Rightarrow \quad \frac{\tilde{\Phi}_\mathrm{Y}\,(k,\chi)}{c^2} =& -\left(k^2 + \eta^2a^2\right)^{-1}\frac{3\Omega_{m_0}}{2\chi_H^2}\tilde{\delta}_c\,(k,\chi)\,a^{-1}, \end{aligned}$$

where the tilde $\tilde{\cdot}$ denotes the Fourier transforms of the repsective quantities and $k = \ell/\chi$ is the wavenumber associated to $\chi\boldsymbol{\theta}$, while ℓ is the wavenumber associated to angular separations $\boldsymbol{\theta}$. Then the line of sight averaged violation factor becomes

$$\tilde{\tilde{\mu}}_\mathrm{vio}(\ell) = 3\int_0^{\chi_H} \mathrm{d}\chi\; p\,(z(\chi))\,\Theta\,(\chi_A - \chi)\,\frac{H\,(\chi)}{c}\,\frac{D_+(a)}{a}\delta\left(k^2 + \eta^2a^2\right)^{-1}\frac{3\Omega_{m_0}}{2\chi_H^2}\tilde{\delta}_c(k,\chi), \qquad (5.37)$$

in Fourier space. A few of these factors are summarized in an appropriate weighting function as

$$W_{\mathrm{Y},A}\,(\chi) = p\,(z(\chi))\,\Theta\,(\chi_A - \chi)\,\frac{H\,(\chi)}{c}\,\frac{D_+(a)}{a}.$$

Application of Limber's approximation [Lim54] results in the following auto-correlation for the surface brightness fluctuations due to the Etherington distance duality violation in lensing as

$$\left\langle \widetilde{\frac{\delta I}{I}}_\mathrm{Y}(\ell)\,\widetilde{\frac{\delta I}{I}}_\mathrm{Y}(\ell') \right\rangle = (2\pi)^2\delta_D\,(\ell - \ell')\,C_{AB}^{\mu_\mathrm{vio}\,\mu_\mathrm{vio}}(\ell),$$

noting that the density fluctuations are distributed according to a homogeneous, isotropic Gaussian random field (see [Dur08] for instance).

The according GG spectrum for the Etherington distance duality violation factor μ_{vio} is given by

$$\begin{aligned} C_{AB}^{\mu_{\text{vio}}\,\mu_{\text{vio}}}(\ell) =& \left\langle \int_0^{\chi_H} \mathrm{d}\chi\; 3W_{\text{Y},A}(\chi)\,\delta \frac{3\Omega_{m_0}}{2\chi_H^2}\left(k^2+\eta^2 a^2\right)^{-1}\tilde{\delta}_c(k,\chi) \right. \\ & \left. \int_0^{\chi_H} \mathrm{d}\chi'\; 3W_{\text{Y},B}(\chi')\,\delta \frac{3\Omega_{m_0}}{2\chi_H^2}\left(k^2+\eta^2 a^2\right)^{-1}\tilde{\delta}_c(k,\chi') \right\rangle \\ =& 9\int_0^{\chi_H} \frac{\mathrm{d}\chi}{\chi^2}\, W_{\text{Y},A}(\chi)\, W_{\text{Y},B}(\chi)\,\delta^2 \frac{9\Omega_{m_0}^2}{4\chi_H^4}\left(k^2+\eta^2 a^2\right)^{-2} P_{\delta_c\delta_c}(k), \end{aligned} \tag{5.38}$$

where $P_{\delta_c\delta_c} \propto k^{n_S} T(k)^2$ is the standard power spectrum for density fluctuations. As already discussed in Section 5.2 employing this power spectrum is actually also an approximation. For a more precise discussion the effect of the Yukawa correction on structure growth, and hence the power spectrum, needs to be taken into account. This is considered in more detail by [Rie20]. However, modifications to the power spectrum due to the Yukawa corrections are of order $O(\delta)$, while the surface brightness fluctuations are also of $O(\delta)$. Consequently, the combined terms are of order $O\left(\delta^2\right)$, what is neglected here.
Since according to (5.31) the relative surface brightness variation is proportional to μ_{vio}, the GG spectrum for $\delta\bar{I}/\bar{I}_Y$ due to the Yukawa correction in the Etherington distance duality relation is given by

$$GG: \; C_{AB}^{\delta\bar{I}/\bar{I}_Y\,\delta\bar{I}/\bar{I}_Y}(\ell) = C_{AB}^{\mu_{\text{vio}}\,\mu_{\text{vio}}}(\ell). \tag{5.39}$$

Also, with (5.21) one can find a cross-correlation $\left\langle \widetilde{\overline{\delta I}}/I_{\text{Y}}(\ell)\, \widetilde{\overline{\delta I}}/I(\ell') \right\rangle$ of intrinsic surface brightness fluctuations $\widetilde{\overline{\delta I}}/I(\ell')$ in approximately Newtonian tidal fields and surface brightness flucutations $\widetilde{\overline{\delta I}}/I_{\text{Y}}(\ell)$ due to the modified Etherington distance duality in area-metric lensing. The according GI-spectrum is then given by

$$\begin{aligned} GI: \; C_{AB}^{\delta\bar{I}/\bar{I}_Y\,\delta\bar{I}/\bar{I}}(\ell) =& -\delta 3\ell^2 \int \frac{\mathrm{d}\chi}{\chi^2}\, D_{IA} S_{\text{Sérsic}}(n) W_{\varphi,A}(\chi) W_{\text{Y,B}}(\chi) \\ & \times \frac{9\Omega_{m_0}^2}{4\chi_H^4} k^{-2}\left(k^2+\eta^2 a^2\right)^{-1} P_{\delta_c\delta_c}(k). \end{aligned} \tag{5.40}$$

If the area-metric refinement parameters are zero, i.e. $\delta = 0$ and $\eta = 0$, the GG and GI spectra of the surface brightness fluctuation vanish, as expected from the surface brightness conservation law in standard gravitational lensing. Thus, deviations from zero would hint at a modification of the Etherington distance duality relation - given that systematic effects like

light absorption along the line of sight have been taken into account.
In the following section the spectra (5.21), (5.39) and (5.40) are investigated numerically and their relative amplitudes are estimated as functions of the parameter values for η and δ.

5.4 Numerical evaluation of the surface brightness fluctuation spectra

In order to estimate the *II*, *GI* and *GG* spectra as derived in the last two Sections 5.3.1 and 5.3.2 the appropriate numerical values for the constants η and δ need to be estimated. One possibility to find values for these parameters is to consider experimental bounds of Yukawa refinements in the gravitational potential, as done by [Hen+21] for the Milky Way for instance. However, a different approach is followed here: First, it is investiagted which numerical values the coupling δ and the inverse range η need to have, such that the spectra (5.39) and (5.40) are bounded from above by the surface brightness fluctuation spectrum (5.21) due to intrinsic alignment. For estimation of possible values for these parameters a dimensional argument [Schb] can be made: The comoving Poisson equation for the Yukawa potential in Fourier space is given by

$$\delta \frac{\tilde{\Phi}_{\mathrm{Y}}(k,\chi)}{c^2} = -\left(k^2+\eta^2 a^2\right)^{-1} \frac{3\Omega_{m_0}}{2} \frac{\delta}{\chi_H^2} \tilde{\delta}_c(k,\chi)\, a^{-1},$$

where the prefactor δ is the area-metric parameter. Now, since k has units of inverse length, the parameter η has units of inverse length, too. A reasonable choice for a length scale where effects of new physics, which have not been observed so far, could start to become important is a multiple m of the Hubble length χ_H. Therefore, a choice for η^{-1} can be $\eta^{-1} = m\chi_H$ with $m = 1$, $m = 10$ or $m = 100$ for instance.
Similarly, the coupling δ of the Yukawa correction $\tilde{\Phi}_{\mathrm{Y}}$ to the Newtonian potential can be chosen accordingly. By writing the comoving Poisson equation as above δ can be interpreted such, that it scales with inverse Hubble length squared χ_H^{-2}. Thus, one can summarize the coupling δ and the inverse Hubble length into the rescaled coupling $\sqrt{\delta}/\chi_H$ with units of inverse Hubble length. Again, it is estimated, that possible violations from the Newtonian form could become important at m multiples of the Hubble length. This means that in case the Yukawa correction becomes important at a scale of $m\chi_H$, the value corresponding to δ would be $1/m^2$ compared to one. So to conclude, the values of the constants δ and η can be understood in terms of multiples of the inverse Hubble length, giving a scale on which effects of an area-metric refinement could become observable. Notably however, these choices for the parameters are still somewhat arbitrary, but sufficient for estimating the amplitudes of the corresponding *GG* and *GI* spectra, compared to the *II* spectrum.

In Figures 5.1 and 5.2 the surface brightness fluctuation spectra are shown for two extreme choices of Sérsic indices, namely $n = 1$ for the exponential and $n = 4$ for the de Vaucouleurs profile. Also different estimations for the parameters η and δ are made corresponding to length scales of $\eta^{-1} = 10\chi_H$ with $\delta = 10^{-2}$, and $\eta^{-1} = 100\chi_H$ with $\delta = 10^{-4}$, respectively. However, spectra with $m = 1$, i.e. $\eta^{-1} = \chi_H$ and $\delta = 1$ are not depicted here, since the parameter of the Yukawa correction is expected to be small compared to one. The thick curves depict spectra for a non-linear power spectrum according to [Smi+03], while for the thin curves the linear power spectrum is used. Also, there is a Gaussian smoothing of the power spectra, as discussed previously in section 4.4.5.

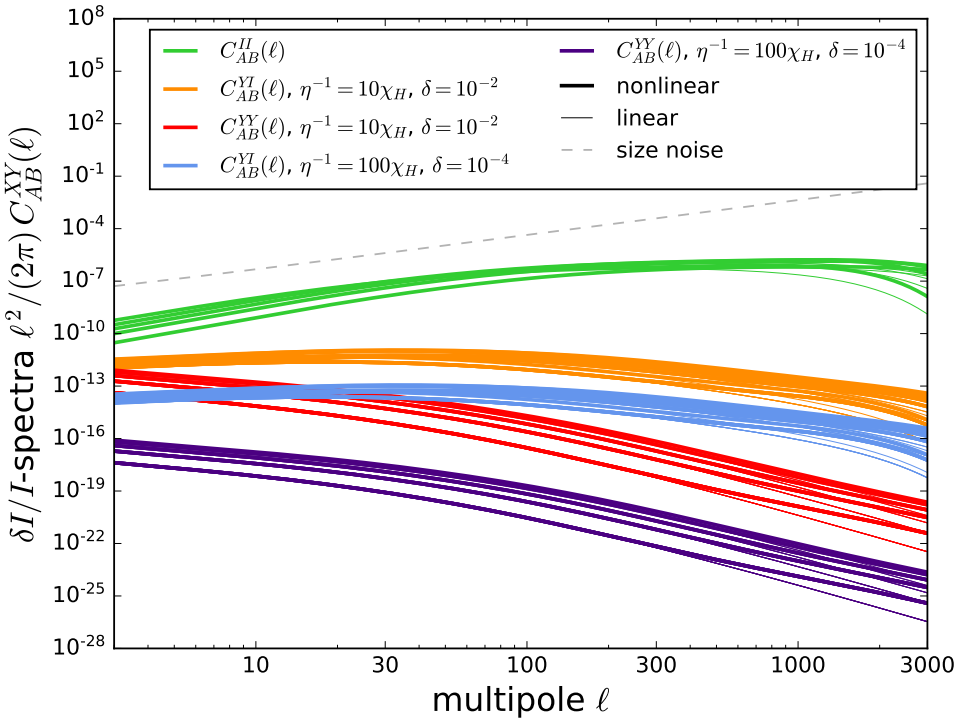

Figure 5.1: **Surface brightness variation spectra for Sérsic index $n = 1$ for a 5-bin tomography:** The amplitudes of the GI and GG spectra are compared to the II spectrum for different choices of area-metric parameters, namely $\eta^{-1} = 10\chi_H$ with $\delta = 10^{-2}$, and $\eta^{-1} = 100\chi_H$ with $\delta = 10^{-4}$.

The II spectrum (denoted as $C^{II}_{AB}(\ell)$) is dominant in both cases, compared to the GG spectrum (denoted as $C^{YI}_{AB}(\ell)$)and the GI spectrum (denoted as $C^{YY}_{AB}(\ell)$). However, for Sérsic index $n = 4$ the amplitudes of the spectra are similar in magnitude for small multipole orders $\ell < 10$, i.e for large length scales. This is because the amplitudes of the alignment self-correlation as well

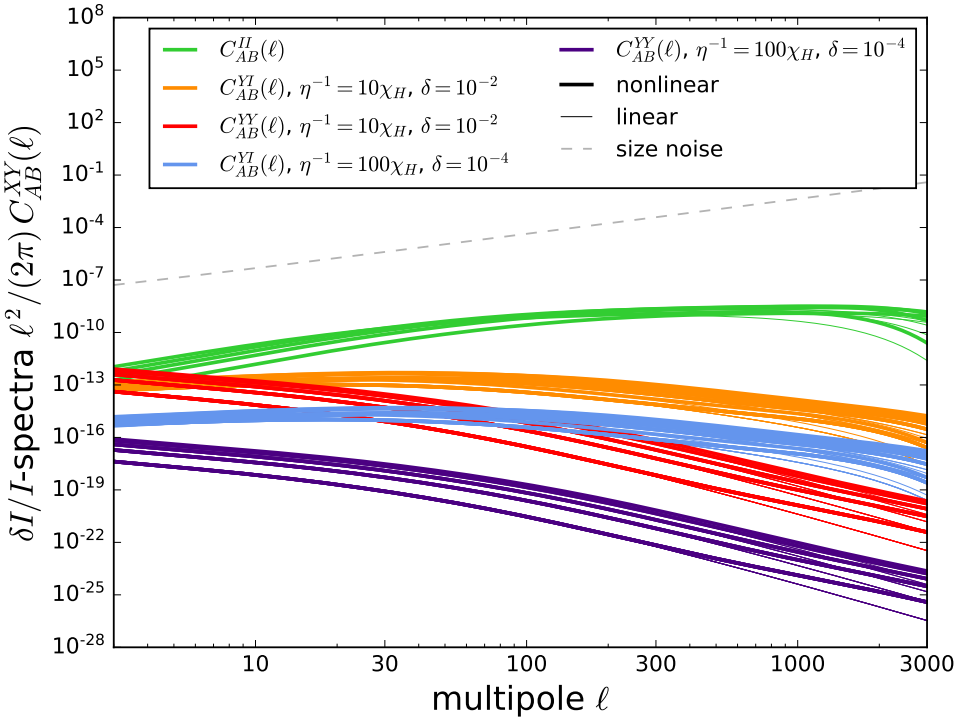

Figure 5.2: **Surface brightness variation spectra for Sérsic index $n = 4$ for a 5-bin tomography:** The amplitudes of the *GI* and *GG* spectra are compared to the *II* spectrum for different choices of area-metric parameters, namely $\eta^{-1} = 10\chi_H$ with $\delta = 10^{-2}$, and $\eta^{-1} = 100\chi_H$ with $\delta = 10^{-4}$.

as the cross-correlation are suppressed by the factor $S_{\text{Sérsic}}(n) = 4\Gamma(4n)^2/\left(\Gamma(2n)\Gamma(6n)\right)$, which decreases with increasing n. For $n = 1$ one has $S_{\text{Sérsic}}(1) = 1.2$, while for $n = 4$ it follows that $S_{\text{Sérsic}}(4) = 0.05$. Also, while the amplitude of the *II* spectrum increases with higher multipole orders and hence smaller structures, it decreases for the *GI* and the *GG* spectra. Thus, the surface brightness variation for Etherington distance duality correction in area-metric lensing is a large scale effect, and suppressed on small scales.

Additionally, the shape for the *GG* spectra and the *GI* spectra does not change significantly for different values of η, and mainly their amplitude is affected by different values of δ, what will be investigated in more detail later. The noise curve is again estimated via the Poissonian error

$$(N_{\text{noise}})_{AB} = \sigma^2_{\text{size}} \frac{n_{\text{tomo}}}{\bar{n}} \delta_{AB}\,,$$

where n_{tomo} is the number of bins, $\sigma_{\text{size}} = 0.8$ the size noise for elliptical galaxies and $\bar{n} = 3.545 \times 10^8 \text{sr}^{-1}$ denotes the number density in the reach of *Euclid* [Lau+11]. The size noise was explicitly used here, since the surface brightness fluctuations $\delta I/I$ are actually pro-

portional to size fluctuations $\delta s/s$. With the same methods as described in Section 4.4.6 for the intrinsic flexion one can also find the cumulated signal-to-noise ratios for the $C_{AB}^{II}(\ell)$, $C_{AB}^{YI}(\ell)$ and $C_{AB}^{YY}(\ell)$ spectra, both for elliptical galaxies and a full galaxy sample for the two choices of Sérsic indices. These are depicted in Figures 5.3 to 5.6.

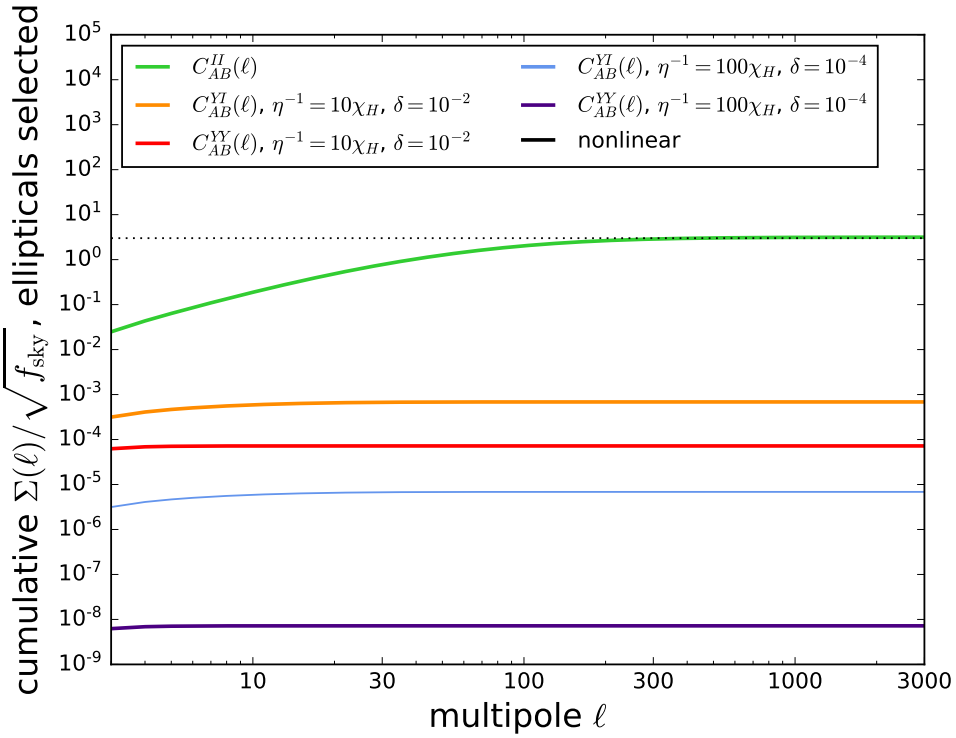

Figure 5.3: **Cumulated signal-to-noise ratio for the surface brightness variation spectra with Sérsic index $n = 1$, a 5-bin tomography, and elliptical galaxy sample:** The cumulated signal-to-noise ratios of the *GI* and *GG* spectra are compared to the one of the *II* spectrum for different choices of area-metric parameters, namely $\eta^{-1} = 10\chi_H$ with $\delta = 10^{-2}$, and $\eta^{-1} = 100\chi_H$ with $\delta = 10^{-4}$.

For a *Euclid*-like survey one can see that in most cases, i.e. for both an exponential galaxy profile or de Vaucouleurs profile, and for ellipticals only, as well as a full galaxy sample, the cumulated signal-to-noise ratios for the $C_{AB}^{YI}(\ell)$ and $C_{AB}^{YY}(\ell)$ signals do - by far - not exceed a signal-to-noise ratio of about $\Sigma(\ell) = 1$. However, observability is possible for $\Sigma(\ell) = 3$, which is only reached by the cumulated signal-to-noise ratio of the $C_{AB}^{II}(\ell)$ spectrum for $n = 1$ and a sample of elliptical galaxies only. For a full galaxy sample the signal-to-noise ratio for $n = 1$ reaches at most $\Sigma(\ell) = 1$, while for $n = 4$ the magnitude of the signal is between 10^{-2} and 10^{-3} for both types of samples.
Furthermore, the cumulated signal-to-noise ratios for the $C_{AB}^{YI}(\ell)$ and $C_{AB}^{YY}(\ell)$ signals generally

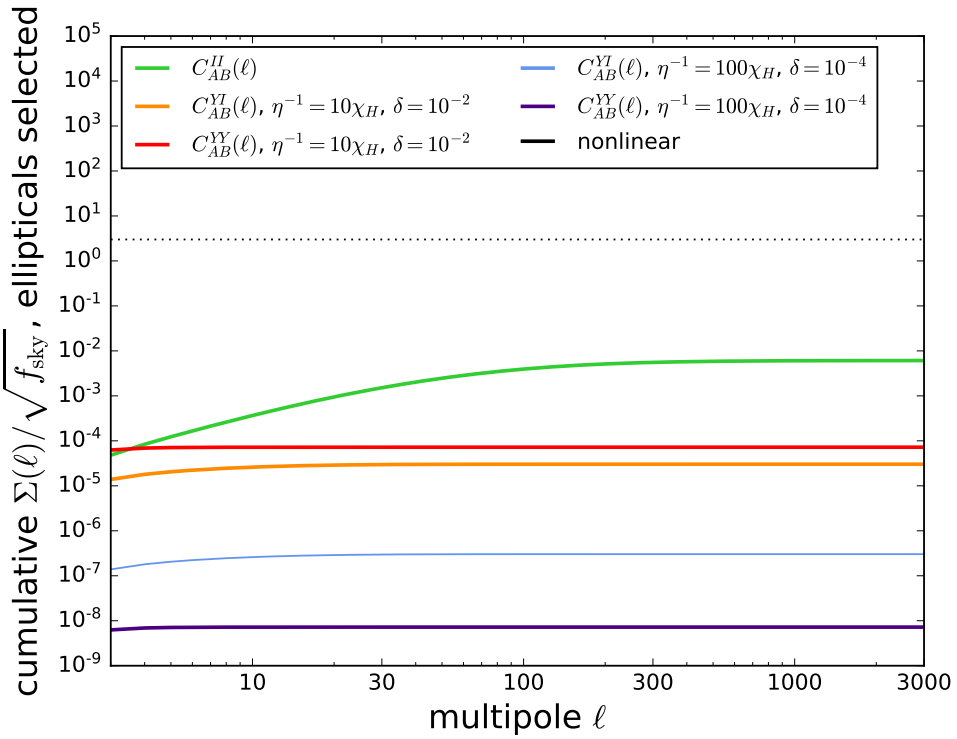

Figure 5.4: **Cumulated signal-to-noise ratio for the surface brightness variation spectra with Sérsic index n = 4, a 5-bin tomography, and elliptical galaxy sample:** The cumulated signal-to-noise ratios of the *GI* and *GG* spectra are compared to the one of the *II* spectrum for different choices of area-metric parameters, namely $\eta^{-1} = 10\chi_H$ with $\delta = 10^{-2}$, and $\eta^{-1} = 100\chi_H$ with $\delta = 10^{-4}$.

remain flat. This is because the spectra themselves decrease for higher multipole order ℓ such that the summed up signal does not increase significantly beyond multipole orders of $\ell > 10$. Thus, it is concluded that surface brightness fluctuations are hard to observe even in the context of general relativity due intrinsic alingment. Additionally, with the surface brightness fluctuation spectra proposed here, it is not possible to measure the area-metric refinements with surveys like *Euclid*, if the corresponding parameters η and δ are to be less than $\eta \leq 1/(10\chi_H)$ and $\delta \leq 0.01$.

Next, it will be investigated in more detail how different choices for the inverse range η would affect the spectra by fixing the coupling δ to a small value. To fix δ to a plausible value one can make the following consideration, similar to [Rie20]: If $\eta \to 0$ the exponential in the Yukawa correction goes to 1. Thus, the gravitational potential would actually be a Newtonian potential

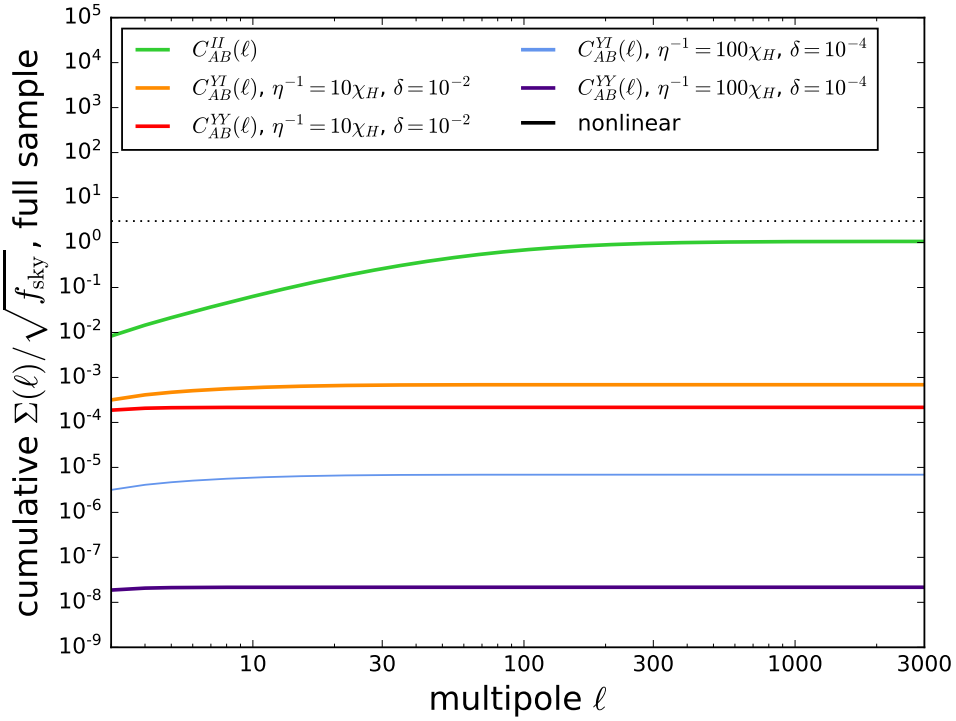

Figure 5.5: **Cumulated signal-to-noise ratio for the surface brightness variation spectra with Sérsic index $n = 1$, a 5-bin tomography, and full galaxy sample:** The cumulated signal-to-noise ratios of the GI and GG spectra are compared to the one of the II spectrum for different choices of area-metric parameters, namely $\eta^{-1} = 10\chi_H$ with $\delta = 10^{-2}$, and $\eta^{-1} = 100\chi_H$ with $\delta = 10^{-4}$.

with gravitational consant $G\,(1+\delta)$:

$$\Phi\left(\boldsymbol{r}-\boldsymbol{r}'\right) = -\frac{GM}{|\boldsymbol{r}-\boldsymbol{r}'|}\,(1+\delta)\,.$$

Consequently, the numerical value of δ should be limited by the relative uncertainty of G, which is stated as 2.2×10^{-5} by *CODATA* [Tie+21]. Thus, for the following considerations the value for the coupling is set to $\delta = 10^{-5}$, while the values for η will be varied to investigate its effect on the shape of the spectra. Also for simplicity, only the curves for non-linear structure formation are plotted. This is depicted in Figure 5.7

The shape of the spectra looks similar to the ones in the previous Figures 5.1 and 5.2, however the amplitdue is suppressed. Accordingly, the cumulated signal-to-noise ratios for elliptical galaxies and a full galaxy sample are given in Figures 5.8 and 5.9.

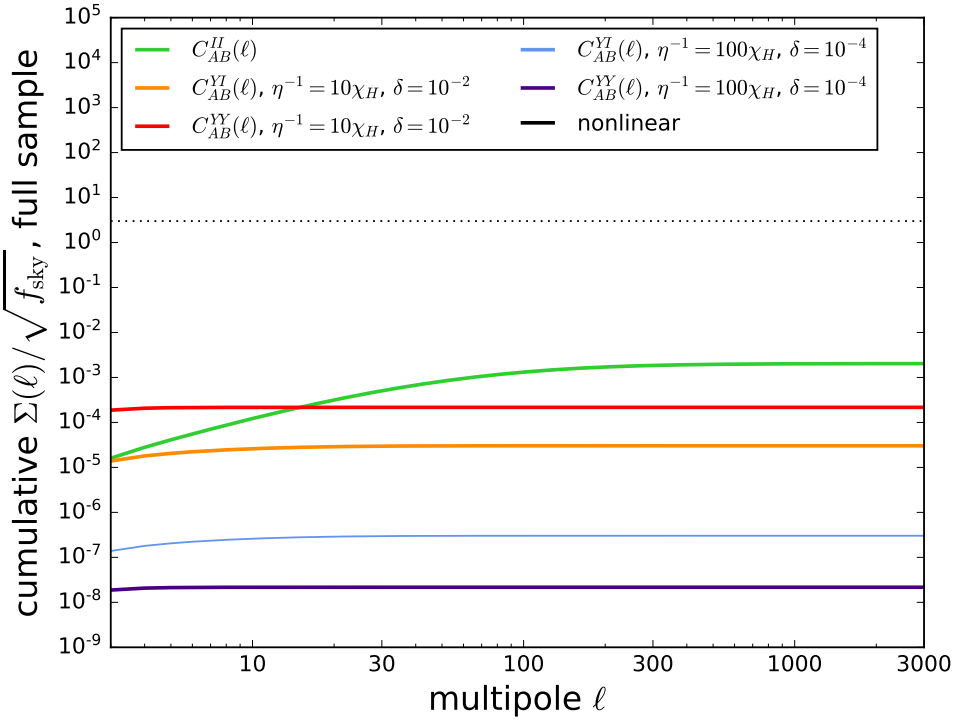

Figure 5.6: **Cumulated signal-to-noise ratio for the surface brightness variation spectra with Sérsic index $n = 4$, a 5-bin tomography, and full galaxy sample:** The cumulated signal-to-noise ratios of the *GI* and *GG* spectra are compared to the one of the *II* spectrum for different choices of area-metric parameters, namely $\eta^{-1} = 10\chi_H$ with $\delta = 10^{-2}$, and $\eta^{-1} = 100\chi_H$ with $\delta = 10^{-4}$.

The *GI* and *GG* spectra, as well as their cumulated signal-to-noise ratios for different values of η, may also be depicted. However, since the shape of the spectra is not strongly affected by this parameter, the curves would overlap and would not be distinguishable. Hence, the curves for different values of η are not plotted here. Yet, it is still possible to compare the ratio of the *GI* spectra and the *GG* spectra for different values of η as shown in Figures 5.10 and 5.11.

The spectra for different η do not vary much in shape and amplitude as long as δ is kept fixed. Thus, the ratio between $C_{AB}^{YI}(\ell)$ spectra, respectively $C_{AB}^{YY}(\ell)$ spectra, is close to one, such that the curves in the Figures 5.10 and 5.11 are close to zero. They even drop exponentially for increasing multipole order ℓ. Therefore, differences in η would - if resolvable - only be noticable for low multipole orders, and hence large scales.

One specifically uses the ratio - instead of the difference - of two spectra to express the difference between them, since they depend on η in a non-linear way.

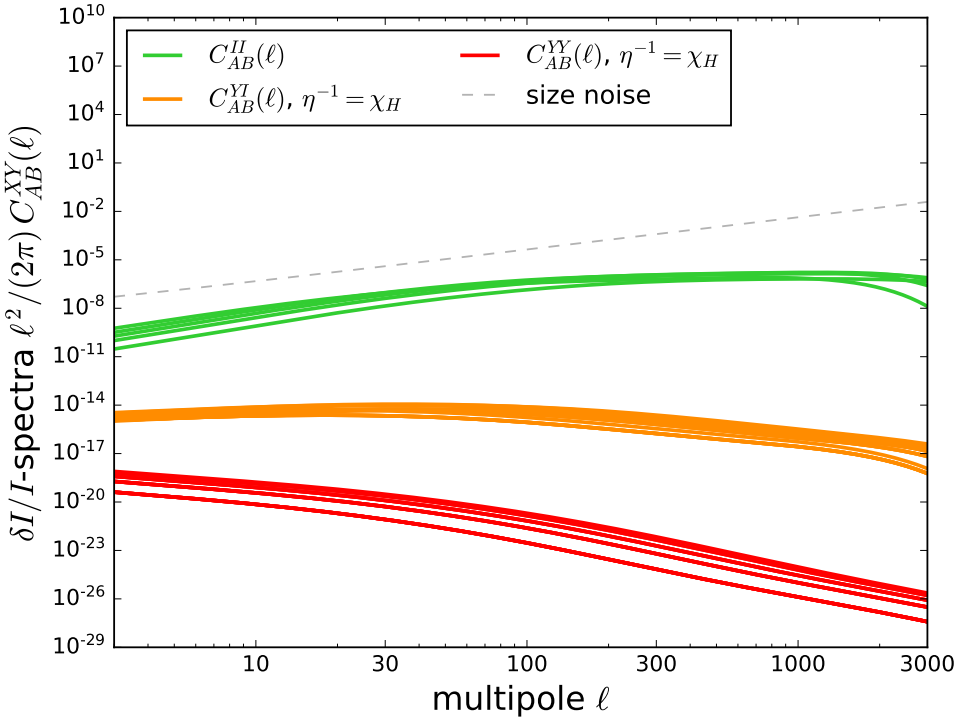

Figure 5.7: **Surface brightness variation spectra for Sérsic index $n = 1$ and a 5-bin tomography:** The amplitudes of the GI and GG spectra are compared to the II spectrum for $\eta^{-1} = \chi_H$, while the value for the coupling is fixed to $\delta = 10^{-5}$.

So, to understand, how the ratio of the different spectra measures a difference in the various η parameters (denoted η_1 and η_2 for instance), the following estimation may be done: The spectra (5.40) and (5.39) depend on η via $C_{AB}^{YI}(\ell) \propto \left(1 + \eta^2 a^2\right)^{-1}$, and $C_{AB}^{YY}(\ell) \propto \left(1 + \eta^2 a^2\right)^{-2}$. Thus, since η is small, this leads to the following approximations:

$$C_{AB}^{YI}(\eta_1) \propto \left(1 + \eta_1^2 a^2\right)^{-1} \approx 1 - \eta_1^2,$$
$$C_{AB}^{YI}(\eta_2) \propto \left(1 + \eta_2^2 a^2\right)^{-1} \approx 1 - \eta_2^2.$$

This leads to

$$\Rightarrow \quad \frac{C_{AB}^{YI}(\eta_1)}{C_{AB}^{YI}(\eta_2)} - 1 \approx \frac{1 - \eta_1^2}{1 - \eta_2^2} - 1 \approx \eta_2^2 - \eta_1^2 = \Delta\eta^2.$$

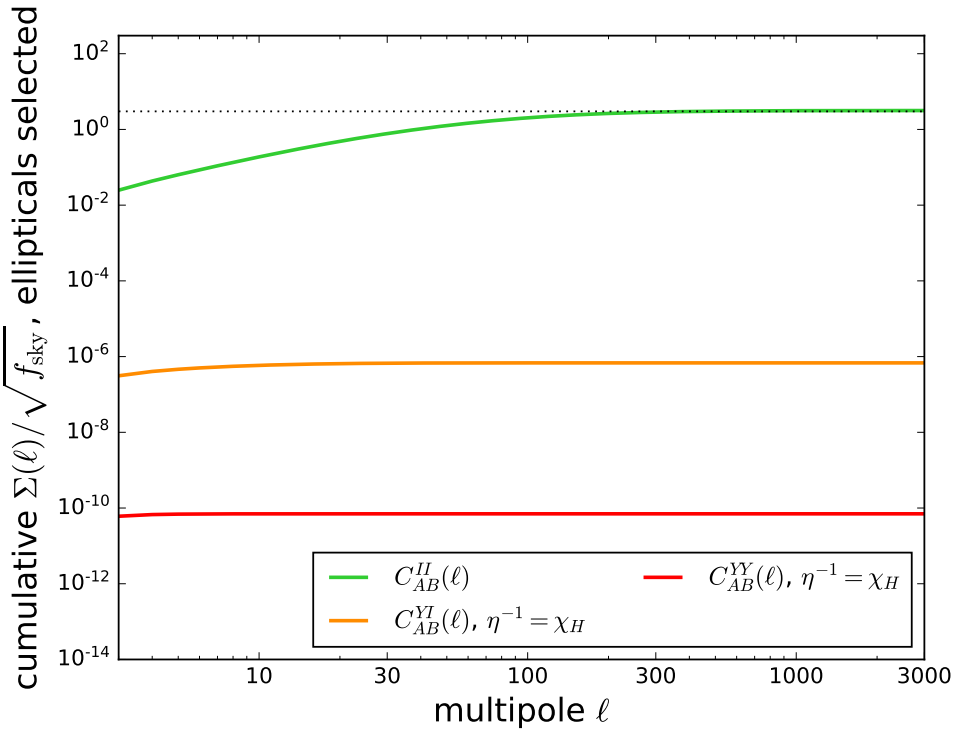

Figure 5.8: **Cumulated signal-to-noise ratio for the surface brightness variation spectra with Sérsic index $n = 1$, a 5-bin tomography, and elliptical galaxy sample:** The cumulated signal-to-noise ratios of the *GI* and *GG* spectra are compared to the cumulated signal-to-noise ratio of the *II* spectrum for $\eta^{-1} = \chi_H$, while the value for the coupling is fixed to $\delta = 10^{-5}$.

Similarly, it holds that

$$\frac{C^{YY}_{AB}(\eta_1)}{C^{YY}_{AB}(\eta_2)} - 1 \approx \frac{1-2\eta_1^2}{1-2\eta_2^2} - 1 \approx 2\eta_2^2 - 2\eta_1^2 = 2\Delta\eta^2.$$

To summarize, two effects of surface brightness variations were compared; once in the context of general relativity and intrinsic alignment, and once for a modified Etherington distance duality in the context of area-metric lensing. Assuming that area-metric corrections are very weak it was demonstrated, that surface brightness variations due to intrinsic alignment are dominating. Especially, with a *Euclid*-like survey only the intrinsic effect may be measured. Larger parameters might be chosen, as for instance discussed in recent studies [Rie20]; [Hen+21], where the data of rotation curves was fitted. However here, cases were discussed, where the modifications to the Etherington distance duality occur on scales of at least a few Hubble lengths.

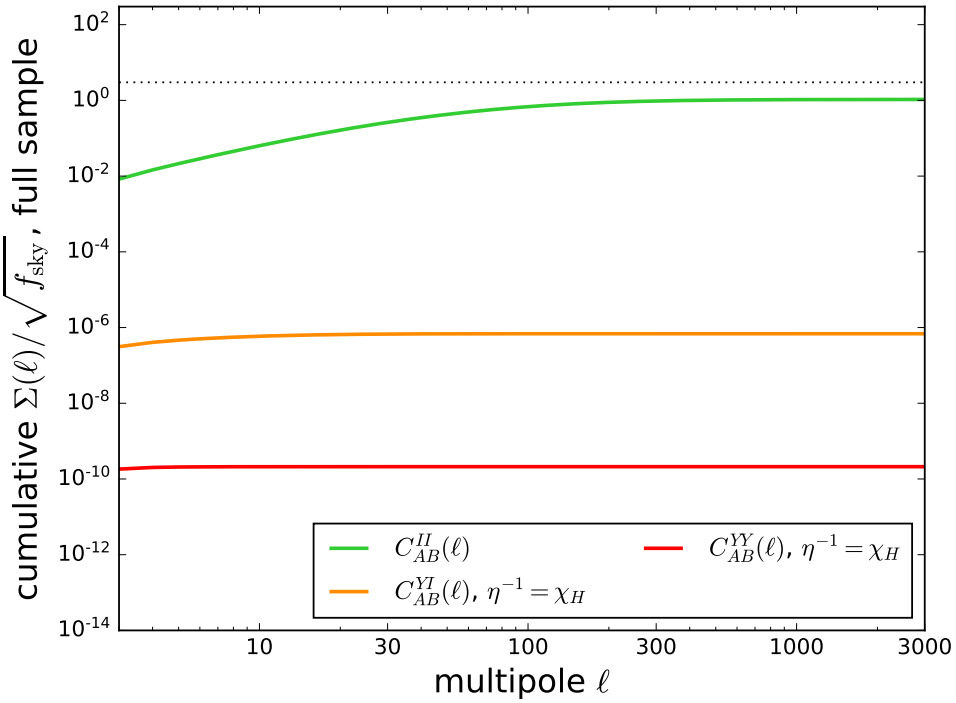

Figure 5.9: **Cumulated signal-to-noise ratio for the surface brightness variation spectra with Sérsic index $n = 1$, a 5-bin tomography, and full galaxy sample:** The cumulated signal-to-noise ratios of the GI and GG spectra are compared to the cumulated signal-to-noise ratio of the II spectrum for $\eta^{-1} = \chi_H$, while the value for the coupling is fixed to $\delta = 10^{-5}$.

Another way to test the modified Etherington distance duality in weak lensing is the magnification bias factor, as will be discussed in the following section.

5.5 Magnification bias in weakly birefringent spacetimes

Before discussing the magnification bias, the derivation of the flux magnification law of weak lensing is summarized, following the discussion by [SEF92]; [BS01]. Then it will demonstrated how this law is altered due to a violation term $\mu_{\rm vio}$ in the Etherington distance duality relation.

The relation between observed specific surface brightness $I_\omega(\beta)$ and observed specific flux density F_ω for an infinitesimal source at angular position $\boldsymbol{\beta}$ is generally given by [BS01]; [SEF92]

$$\mathrm{d}F_{\omega,\mathrm{obs}} = I_\omega(\boldsymbol{\beta})\,\mathrm{d}^2\beta. \tag{5.41}$$

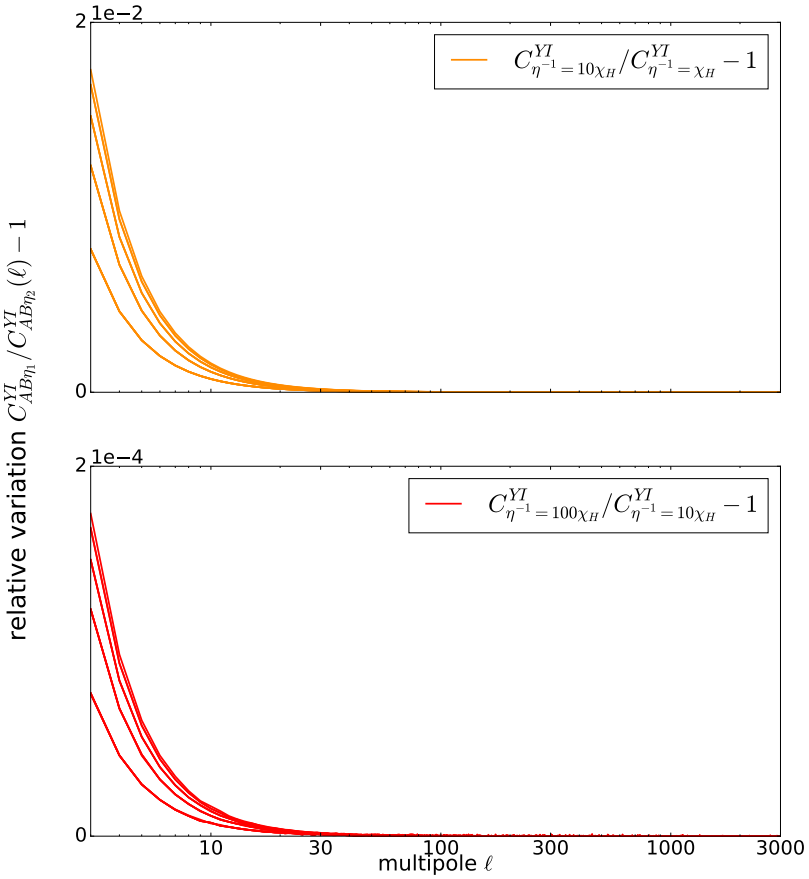

Figure 5.10: **Ratio of the *GI* spectra for different values of η and fixed $\delta = 10^{-5}$:** a) The ratio $C^{YI}_{AB}\left(\ell, \eta^{-1} = 10\chi_H\right)/C^{YI}_{AB}\left(\ell, \eta^{-1} = \chi_H\right) - 1$ is depicted in orange for a 5-bin tomography.
b) The ratio $C^{YI}_{AB}\left(\ell, \eta^{-1} = 100\chi_H\right)/C^{YI}_{AB}\left(\ell, \eta^{-1} = 10\chi_H\right) - 1$ is depicted in red for a 5-bin tomography. In both cases the difference between the spectra is close to zero and exponentially decreasing with increasing multipole order ℓ.

For an extended source integration over the source angular area is required, what leads to

$$F_{\omega;\mathrm{obs}} = \int \mathrm{d}^2\beta \, I_\omega(\boldsymbol{\beta}) \, .$$

The Etherington distance duality shall now be inserted into equation (5.41). Thus, it needs to be expressed via the angular diameter distance D_A in (5.22) and the uncorrected luminosity distance D_L as is discussed in the following paragraph.

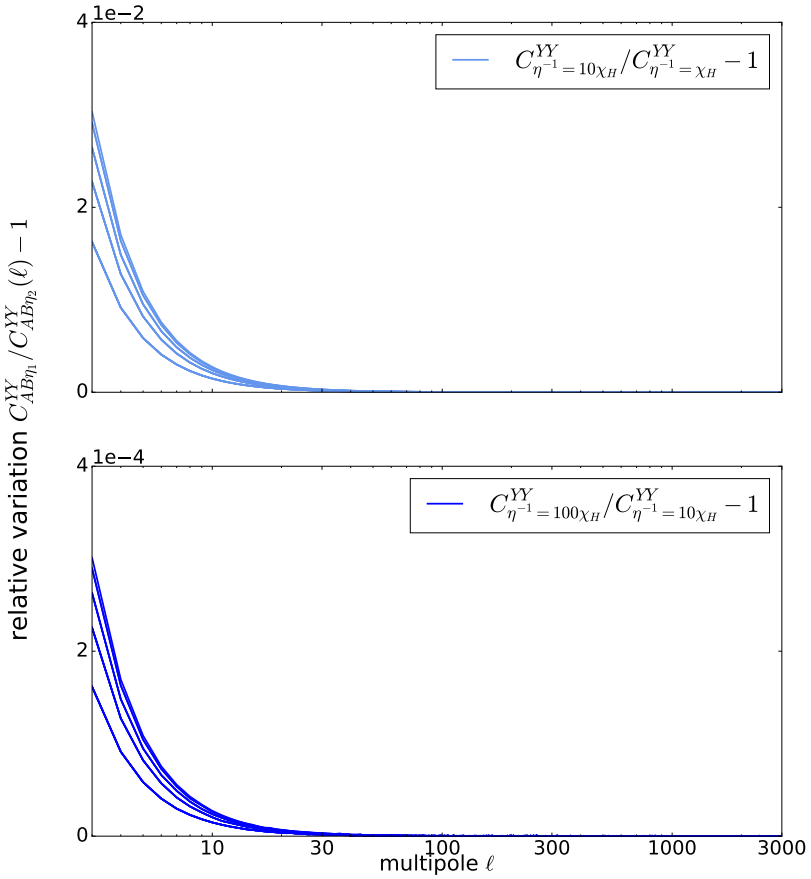

Figure 5.11: **Ratio of the *GG* spectra for different values of η and fixed $\delta = 10^{-5}$:** a) The ratio $C^{YY}_{AB}\left(\ell, \eta^{-1} = 10\chi_H\right)/C^{YY}_{AB}\left(\ell, \eta^{-1} = \chi_H\right) - 1$ is depicted in orange for a 5-bin tomography.
b) The ratio $C^{YY}_{AB}\left(\ell, \eta^{-1} = 100\chi_H\right)/C^{YY}_{AB}\left(\ell, \eta^{-1} = 10\chi_H\right) - 1$ is depicted in red for a 5-bin tomography. In both cases the difference between the spectra is close to zero and exponentially decreasing with increasing multipole order ℓ.

First of all, the definition

$$D_A = \left(\frac{\mathrm{d}A_S}{\mathrm{d}\Omega_O}\right)^{1/2},$$

is inserted into (5.41). Here, the solid angle under which the source appears for the observer is given by $\mathrm{d}\beta^2 = \mathrm{d}\Omega_O$ if no lensing occurs. This leads to

$$\mathrm{d}F_{\omega,\mathrm{obs}} = I_\omega\left(\boldsymbol{\beta}\right)\mathrm{d}A_S\, D_A^{-2}. \tag{5.42}$$

If lensing occurs the solid angle $\mathrm{d}\theta^2$ under which an object appears to the observer in the lense plane at angular position $\boldsymbol{\theta}$ is magnified according to [SEF92]

$$\begin{aligned} \mathrm{d}\theta^2 &= \det\mathcal{A}^{-1}\mathrm{d}\beta^2 = \mu\left(\boldsymbol{\theta}\left(\boldsymbol{\beta}\right)\right)\mathrm{d}\beta^2 = \mu\left(\boldsymbol{\theta}\left(\boldsymbol{\beta}\right)\right)\mathrm{d}A_S\, D_A^{-2} = \mathrm{d}A_S\, {D'}_A^{-2}, \\ \Rightarrow {D'}_A &= \frac{1}{\sqrt{\mu\left(\boldsymbol{\theta}\left(\boldsymbol{\beta}\right)\right)}} D_A. \end{aligned} \tag{5.43}$$

Here, $\mathcal{A}$ is the Jacobian of the lens map and the magnification factor $\mu\left(\boldsymbol{\theta}\left(\boldsymbol{\beta}\right)\right)$ is purely geometrically defined as $\det\mathcal{A}^{-1} \equiv \mu\left(\boldsymbol{\theta}\left(\boldsymbol{\beta}\right)\right)$. The angular diameter distance scales with the inverse of the square root of the magnification factor, and thus effectively becomes smaller if lensing magnification occurs.
Since $D_L \propto D_A$ due to the Etherington reciprocity relation, it follows that magnification affects the luminosity distance as

$$D'_L = \frac{1}{\sqrt{\mu\left(\boldsymbol{\theta}\left(\boldsymbol{\beta}\right)\right)}} D_L.$$

Thus, also the luminosity distance is effectively decreased due to magnification, it may be concluded for the flux that [SEF92]

$$\begin{aligned} F &= \frac{L}{4\pi {D_L}^2}, \\ \Rightarrow F' &\propto \frac{1}{{D'}_L^2} \propto \frac{\mu\left(\boldsymbol{\theta}\left(\boldsymbol{\beta}\right)\right)}{D_L^2} \propto F\mu\left(\boldsymbol{\theta}\left(\boldsymbol{\beta}\right)\right), \end{aligned}$$

where the luminosity L of the source is not changed. All in all, the increase in flux is ultimately caused by the reduction of the angular diameter distance. Further rewriting (5.42) in terms of the luminosity distance measure one can directly read off where modifications of the Etherington distance duality relation will affect the final result for the flux magnification. With the specific surface brightness $I_\omega\left(\boldsymbol{\beta}\right)$ given as

$$I_\omega\left(\boldsymbol{\beta}\right) = \frac{1}{(1+z)^3}\frac{\mathrm{d}L_{(1+z)\omega}}{4\pi\,\mathrm{d}A_S} = \frac{1}{(1+z)^3}\frac{4\pi\,\mathrm{d}F_{(1+z)\omega}\, D_L^2}{4\pi \mathrm{d}A_S} = \frac{1}{(1+z)^4}\frac{\mathrm{d}F_\omega\, D_L^2}{\mathrm{d}A_S},$$

as discussed in (5.30) the flux magnification law can be written as

$$\mathrm{d}F_{\omega,\mathrm{obs}} = \frac{1}{(1+z)^4}\frac{\mathrm{d}F_\omega\, D_L^2}{\mathrm{d}A_S}\mathrm{d}A_S\, {D'}_A^{-2} = \frac{1}{(1+z)^4}\mathrm{d}F_\omega\, D_L^2 {D'}_A^{-2} = \mathrm{d}F_\omega \mu_{\mathrm{eff}}\left(\boldsymbol{\theta}\left(\boldsymbol{\beta}\right)\right)\left(1+\mu_{\mathrm{vio}}\right). \tag{5.44}$$

Here the Etherington distance duality

$$\frac{D_L}{D_A\,(1+z)^2} = \sqrt{1+\mu_{\mathrm{vio}}\left(\boldsymbol{\theta}\left(\boldsymbol{\beta}\right)\right)},$$

and the angular diameter distance

$$D'_A = 1/\sqrt{\mu_{\text{eff}}(\boldsymbol{\theta}(\boldsymbol{\beta}))} D_A$$

for lensing were inserted. The factor μ_{eff} is the effective magnification factor, depending on the explicit lens map. This result can be confirmed for three examples:

- No lensing and $\mu_{\text{vio}} = 0$:

  $$\mathrm{d}F_{\omega,\text{obs}} = \mathrm{d}F_{\omega}.$$

  The observed flux does not change compared to the emitted flux.

- Standard lensing in general relativity and $\mu_{\text{vio}} = 0$:

  $$\mathrm{d}F_{\omega,\text{obs}} = \mathrm{d}F_{\omega}\,\mu(\boldsymbol{\theta}(\boldsymbol{\beta}))\,.$$

  This is the standard flux magnification law in lensing ([SEF92]).

- Area-metric lensing with Yukawa correction term and $\mu_{\text{vio}} \neq 0$:

  $$\mathrm{d}F_{\omega,\text{obs}} = \mathrm{d}F_{\omega}\mu_{\text{eff}}(\boldsymbol{\theta}(\boldsymbol{\beta}))\,(1+\mu_{\text{vio}}(\boldsymbol{\theta}(\boldsymbol{\beta}))\,.$$

  There is an effective magnification factor $\mu_{\text{eff}}(\boldsymbol{\theta}(\boldsymbol{\beta}))$. It looks different compared to the factor for standard lensing in general relativity, due to a different kind of effective metric given in [SW17]. Beyond that there is an additional factor $(1+\mu_{\text{vio}})$, which arises because of the Etherington distance duality modification predicted by [SW17]. Thus, the total flux magnification μ_{tot} is then given by

  $$\mu_{\text{tot}} = \mu_{\text{eff}}(1+\mu_{\text{vio}}) \approx 1 + \delta\mu_{\text{eff}} + \mu_{\text{vio}} + \delta\mu_{\text{eff}}\mu_{\text{vio}} \approx 1 + 2\kappa_{\text{eff}} + \mu_{\text{vio}},$$

  where the magnification μ_{eff} is supposed to be close to one $\mu_{\text{eff}} = 1 + \delta\mu_{\text{eff}}$ in weak lensing [BS01].

Finally, the total magnification spectrum is altered compared to [BS01] and given by

$$C_{AB}^{\delta\mu_{\text{tot}}\delta\mu_{\text{tot}}}(\ell) = 4C_{AB}^{\kappa_{\text{eff}}\kappa_{\text{eff}}}(\ell) + 4C_{AB}^{\kappa_{\text{eff}}\mu_{\text{vio}}}(\ell) + C_{AB}^{\mu_{\text{vio}}\mu_{\text{vio}}}(\ell).$$

Here the cross-correlation $C_{AB}^{\kappa_{\rm eff}\mu_{\rm vio}}(\ell)$ is given by

$$C_{AB}^{\kappa_{\rm eff}\mu_{\rm vio}}(\ell) = \frac{3}{4} l^2 \delta \int_0^{\chi_H} \frac{\mathrm{d}\chi}{\chi^2} W_{\Upsilon,A}(\chi) W_{\Psi,B}(\chi) \left(1 + \frac{\tilde{\delta}}{2} + a^2\eta^2 k^{-2}\right) \times \left(k^2 + \eta^2 a^2\right)^{-2} P_{\delta_c\delta_c}(k),$$

while the auto-correlations $C_{AB}^{\kappa_{\rm eff}\kappa_{\rm eff}}(\ell)$ is given in equation (5.14), and finally $C_{AB}^{\mu_{\rm vio}\mu_{\rm vio}}(\ell)$ is given in equation (5.38).

Generally, the magnification bias describes how the number count of sources can be increased or decreased due to gravitational lensing for a flux limited survey [BS01]; [SEF92].
In the standard treatment (for instance discussed in [BS01]) the number density distribution for observed sources above a certain flux threshold $F_{\rm min}$ of a specific survey within a redshift interval $\mathrm{d}z$ is given by

$$n_0\,(> F_{\rm min}, z)\,\mathrm{d}z.$$

Without lensing the number density of observed sources would be the number of sources $\mathrm{d}N$ counted within a specific solid angle $\mathrm{d}\Omega_O = \mathrm{d}^2\beta$ of the observed sky patch. Hence, the number density scales with the angular diameter distance as

$$n_0\,(> F_{\rm min}, z) = \frac{\mathrm{d}N\,(> F_{\rm min}, z)}{\mathrm{d}\Omega_O} = \frac{\mathrm{d}N\,(> F_{\rm min}, z)}{\mathrm{d}A} D_A^2.$$

Here, $\mathrm{d}A$ denotes the actual area of the observed sky patch in the source plane. Also $F_{\rm min}$ marks the actual flux threshold below which observation of sources is not possible in a flux limited survey. If no lensing occurs this is equal to the minimally observable flux $F = F_{\rm min}$.
If magnification occurs the sources appear brighter, so the actually observable flux threshold $F_{\rm min}$ is effectively lowered to observe fainter sources. However, also the solid angle of observation is stretched, such that the effective density of the sources is lowered. These effects are competing and it depends on the detailed flux law to determine which effect is dominant.

As discussed previously the corresponding flux scales can be expressed via the Etherington distance duality relation as

$$F_{\rm min} = F(1+z)^4 D_L^{-2} D'^2_A.$$

Consequently, if lensing occurs, the number density of the observed galaxies is generally given by

$$\begin{aligned} n\left(>F_{\min},z\right) =& \frac{\mathrm{d}N\left(>F_{\min},z\right)}{\mathrm{d}\Omega_O} = \frac{\mathrm{d}N\left(>F_{\min},z\right)}{\mathrm{d}\theta^2} = \frac{\mathrm{d}N\left(>F(1+z)^4 D_L^{-2} D_A'^2,z\right)}{\mathrm{d}A} D_A'^2 \\ =& \frac{1}{\mu_{\mathrm{eff}}\left(\boldsymbol{\theta}\left(\boldsymbol{\beta}\right)\right)} \frac{\mathrm{d}N\left(>F/\mu_{\mathrm{eff}}\left(\boldsymbol{\theta}\left(\boldsymbol{\beta}\right)\right)(1+z)^4 D_L^{-2} D_A^2,z\right)}{\mathrm{d}A} D_A^2 \\ =& \frac{1}{\mu_{\mathrm{eff}}\left(\boldsymbol{\theta}\left(\boldsymbol{\beta}\right)\right)} n_0\left(>\frac{F}{\mu_{\mathrm{eff}}\left(\boldsymbol{\theta}\left(\boldsymbol{\beta}\right)\right)}(1+z)^4 D_L^{-2} D_A^2,z\right), \end{aligned} \tag{5.45}$$

with

$$\mathrm{d}\Omega_O = \mathrm{d}\theta^2 = \mu_{\mathrm{eff}}\left(\boldsymbol{\theta}\left(\boldsymbol{\beta}\right)\right) \mathrm{d}A D_A^{-2} \mu_{\mathrm{eff}}\left(\boldsymbol{\theta}\left(\boldsymbol{\beta}\right)\right) = \mathrm{d}A D_A'^{-2}.$$

If the Etherington distance duality is not modified, i.e. for general relativity, the result (5.45) reproduces the number density derived in [BS01] for instance.
From observation it is known [BS01]; [SEF92] that the number density distribution scales with a flux power law as

$$n_0\left(>F,z\right) \propto F^{-\alpha} p_0(z;>F), \tag{5.46}$$

with $p_0(z;>F)$ as redshift probability distribution of sources with flux larger than some threshold F. For typical galaxies this distribution is usually given by (5.13).
However, for quasars as sources a different kind of redshift distribution has to be provided, especially since the maximum abundance of quasars appears at redshifts around $z \approx 2.-3.$ [Pei95], while for galaxies it is between $z \approx 0.9-1.5$ [Lau+11]. There are various expressions for the quasar distance distribution in [Pei95], but for simplicity the distribution (5.13) is chosen as functional form for the quasar source distribution $p_0(z)$. Yet, one sets $z_0 = 1.98$ - instead of $z_0 = 0.64$ as for typical galaxies - to ensure that the median of the quasar distance distribution is around $z = 2.8$ with redshift value according to [Pei95].
Consequently, due to the flux power law (5.46), the relation (5.45) can be simplfied to

$$\begin{aligned} n\left(>F_{\min},z\right) =& \frac{1}{\mu_{\mathrm{eff}}\left(\boldsymbol{\theta}\left(\boldsymbol{\beta}\right)\right)} n_0\left(>\frac{F}{\mu_{\mathrm{eff}}\left(\boldsymbol{\theta}\left(\boldsymbol{\beta}\right)\right)}(1+z)^4 D_L^{-2} D_A^2,z\right) \\ \propto& F^{-\alpha} \mu_{\mathrm{eff}}\left(\boldsymbol{\theta}\left(\boldsymbol{\beta}\right)\right)^{\alpha-1} (1+z)^{-4\alpha} D_L^{2\alpha} D_A^{-2\alpha} p_0\left(z;>\frac{F}{\mu_{\mathrm{eff}}\left(\boldsymbol{\theta}\left(\boldsymbol{\beta}\right)\right)}(1+z)^4 D_L^{-2} D_A^2\right). \end{aligned}$$

The bias factor can then be obtained by integration over the number density distribution with respect to the redshift as

$$\begin{aligned} q(\boldsymbol{\theta}) &= \frac{n(>F)}{n_0(>F)} \\ &= \frac{\int \mathrm{d}z\, F^{-\alpha} \mu_{\mathrm{eff}}(\boldsymbol{\theta}(\boldsymbol{\beta}), z)^{\alpha-1} (1+z)^{-4\alpha} D_L^{2\alpha} D_A^{-2\alpha} p_0\left(z; > F/\mu_{\mathrm{eff}}(\boldsymbol{\theta}(\boldsymbol{\beta}), z)\ (1+z)^4 D_L^{-2} D_A^2\right)}{\int \mathrm{d}z\, F^{-\alpha} p_0(>F, z)} \\ &= \int \mathrm{d}z\, \mu_{\mathrm{eff}}(\boldsymbol{\theta}(\boldsymbol{\beta}), z)^{\alpha-1} (1+z)^{-4\alpha} D_L^{2\alpha} D_A^{-2\alpha} p_0\left(z; > \frac{F}{\mu_{\mathrm{eff}}(\boldsymbol{\theta}(\boldsymbol{\beta}), z)}(1+z)^4 D_L^{-2} D_A^2\right), \end{aligned} \tag{5.47}$$

where the magnification $\mu_{\mathrm{eff}}(\boldsymbol{\theta}(\boldsymbol{\beta}), z)$ is also a function of redshift.
If there is no violation of the Etherington distance duality relation, the expression (5.47) will simply yield the standard result for the magnification bias factor [BS01]; [SEF92] given as

$$\begin{aligned} q(\boldsymbol{\theta}) &= \int \mathrm{d}z\, \mu(\boldsymbol{\theta}(\boldsymbol{\beta}), z)^{\alpha-1} (1+z)^{-4\alpha} D_L^{2\alpha} D_A^{-2\alpha} p_0\left(z; > \frac{F}{\mu(\boldsymbol{\theta}(\boldsymbol{\beta}), z)}(1+z)^4 D_L^{-2} D_A^2\right) \\ &= \int \mathrm{d}z\, \mu(\boldsymbol{\theta}(\boldsymbol{\beta}), z)^{\alpha-1} p_0\left(z; > \frac{F}{\mu(\boldsymbol{\theta}(\boldsymbol{\beta}), z)}\right). \end{aligned}$$

If a violation of the Etherington distance duality occurs the magnification bias factor becomes

$$\begin{aligned} q(\boldsymbol{\theta}) &= \int \mathrm{d}z\, \mu_{\mathrm{eff}}(\boldsymbol{\theta}(\boldsymbol{\beta}), z)^{\alpha-1} (1+z)^{-4\alpha} D_L^{2\alpha} D_A^{-2\alpha} p_0\left(z; > \frac{F}{\mu_{\mathrm{eff}}(\boldsymbol{\theta}(\boldsymbol{\beta}), z)}(1+z)^4 D_L^{-2} D_A^2\right) \\ &= \int \mathrm{d}z\, \mu_{\mathrm{eff}}(\boldsymbol{\theta}(\boldsymbol{\beta}), z)^{\alpha-1} (1+\mu_{\mathrm{vio}}(z))^{\alpha} p_0\left(z; > \frac{F}{\mu_{\mathrm{eff}}(\boldsymbol{\theta}(\boldsymbol{\beta}), z)\,(1+\mu_{\mathrm{vio}}(\boldsymbol{\theta}(\boldsymbol{\beta}), z))}\right). \end{aligned}$$

With the magnification factor μ_{eff} close to one and thus

$$\mu_{\mathrm{eff}}^{\alpha-1} = (1+\delta\mu_{\mathrm{eff}})^{\alpha-1} \approx 1 + (\alpha-1)\,\delta\mu_{\mathrm{eff}},$$

and the violating factor μ_{vio} close to zero such that

$$(1+\mu_{\mathrm{vio}})^{\alpha} \approx 1 + \alpha\mu_{\mathrm{vio}},$$

the bias factor is approximately given by

$$\begin{aligned} q(\boldsymbol{\theta}) \approx 1 &+ \int \mathrm{d}z\, (\alpha-1)\delta\mu_{\mathrm{eff}}(\boldsymbol{\theta}(\boldsymbol{\beta}), z)\ p_0(z) + \int \mathrm{d}z\, \alpha\mu_{\mathrm{vio}}(\boldsymbol{\theta}(\boldsymbol{\beta}), z)\ p_0(z) \\ &+ O\left(\delta\mu_{\mathrm{eff}}(\boldsymbol{\theta}(\boldsymbol{\beta}), z)\,\mu_{\mathrm{vio}}(\boldsymbol{\theta}(\boldsymbol{\beta}), z)\right), \end{aligned}$$

with short notation

$$p_0(z) = p_0\left(z; > \frac{F}{\mu_{\rm eff}(\boldsymbol{\theta}, z)\,(1 + \mu_{\rm vio}(\boldsymbol{\theta}(\boldsymbol{\beta}), z))}\right).$$

Here, the term proportional to $\delta\mu_{\rm eff}\mu_{\rm vio}$ is neglected to first order approximation, and it was used that $\int \mathrm{d}z\; p_0(z) = 1$. In this case, the magnification bias factor gets an extra bias term from the Etherington distance duality violation. Additionally, the effective convergence will be different compared to conventional gravitational lensing.
Averaging over the source distribution with

$$\int \mathrm{d}z\,(\alpha - 1)\delta\mu_{\rm eff}(\boldsymbol{\theta}, z)\; p_0(z) \equiv (\alpha - 1)\delta\bar{\mu}_{\rm eff}(\boldsymbol{\theta}),$$

and

$$\int \mathrm{d}z\,\alpha\mu_{\rm vio}(\boldsymbol{\theta}, z)\; p_0(z) \equiv \alpha\bar{\mu}_{\rm vio}(\boldsymbol{\theta}),$$

the bias factor is given by

$$q(\boldsymbol{\theta}) \approx 1 + (\alpha - 1)\delta\bar{\mu}_{\rm eff}(\boldsymbol{\theta}) + \alpha\bar{\mu}_{\rm vio}(\boldsymbol{\theta}). \tag{5.48}$$

Using that in weak lensing the magnification and convergence are related via

$$\delta\mu_{\rm eff}(\boldsymbol{\theta}, \chi(z)) \approx 2\kappa_{\rm eff}(\boldsymbol{\theta}, \chi(z)) = \Delta_\theta\Psi(\boldsymbol{\theta}, \chi(z)) = 2\Delta_\theta \int_0^\chi \mathrm{d}\chi'\,\frac{\chi - \chi'}{\chi\chi'}\Phi_{\rm Def}(\chi'\boldsymbol{\theta}, \chi'),$$

the average over different sources along the line of sight of the effective magnification fluctuation $\delta\bar{\mu}_{\rm eff}\left(\vec{\theta}\right)$ in equation (5.48) becomes

$$\delta\bar{\mu}_{\rm eff}(\boldsymbol{\theta}) = 2\Delta_\theta \int_0^{\chi_H} \mathrm{d}\chi \frac{\mathrm{d}z}{\mathrm{d}\chi}\,(\alpha - 1) \int_0^\chi \mathrm{d}\chi'\,\frac{\chi - \chi'}{\chi\chi'}\Phi_{\rm Def}(\chi'\boldsymbol{\theta}, \chi')\, p_0(z(\chi)).$$

Standard re-arrangement (see for instance also [BS01]) of the integrals according to Fubini's law [AW] and taking the growth factor $D_+(a)$ for the density - and hence potential fluctuations - into account with $-\mathrm{d}\chi H(\chi) = c\mathrm{d}z$, leads to

$$\delta\bar{\mu}_{\rm eff}(\boldsymbol{\theta}) = \Delta_\theta \int_0^{\chi_H} \mathrm{d}\chi\;\frac{\Phi_{\rm Def}}{c^2}(\chi\boldsymbol{\theta}, \chi)\, a W_{\Psi,B}(\chi),$$

with weighting function

$$W_{\Psi,B}(\chi) = \frac{2}{\chi}\frac{D_+(a)}{a}\int_{\max(\chi_B,\chi)}^{\chi_{B+1}} \mathrm{d}\chi'\; p_0(z(\chi'))\,\frac{H(\chi')}{c}\left(1 - \frac{\chi}{\chi'}\right),$$

for a tomographic analysis with red-shift bin B. This is similar to standard results, as for instance discussed by [LHG07], but with a Yukawa refinement of the deflection potential. For the term $\bar{\mu}_{\text{vio}}(\boldsymbol{\theta})$ measuring the averaged photon excess in area-metric spacetime the relation (5.36) holds as discussed previoulsy. With this result an explicit expression for the modified magnification bias factor can be obtained.

Now, the magnification bias factor affects the number count and thus the cross-correlation between observed sources - which could be quasars - and galaxies, tracing the LSS responsible for lensing. In this case the cross-correlation of the relative number counts is generally given by [BS01]

$$\zeta_{QG}(\boldsymbol{\phi}) = \frac{\langle [n_Q(\boldsymbol{\theta}) - \langle n_Q \rangle]\,[n_G(\boldsymbol{\theta}+\boldsymbol{\phi}) - \langle n_G \rangle]\rangle}{\langle n_Q \rangle \langle n_G \rangle}.$$

The number count $n_Q(\boldsymbol{\theta})$ for sources - for instance quasars - within a certain angle is then generally given in terms of the mean number count $\langle n_Q \rangle$ and the magnification bias q as [BS01]

$$n_Q(\boldsymbol{\theta}) = q(\boldsymbol{\theta}) \langle n_Q \rangle .$$

Similarly, the relative number count fluctuation of foreground galaxies ans structures acting as lenses is given in terms of the line of sight integrated mean density contrast

$$\bar{\delta}_c(\boldsymbol{\theta}) = \int_0^{\chi_H} \mathrm{d}\chi\, \frac{H(\chi)}{c} p(z(\chi))\Theta(\chi_B - \chi) D_+(a)\delta_c(\boldsymbol{\theta}\chi, \chi) \equiv \int_0^{\chi_H} \mathrm{d}\chi a W_{\delta_c,B}(\chi)\delta_c(\boldsymbol{\theta}\chi,\chi),$$
$$\text{with weigthing function:} \quad W_{\delta_c,B}(\chi) \equiv \frac{H(\chi)}{c} p(z(\chi))\Theta(\chi_B - \chi)\frac{D_+(a)}{a},$$

via a linear relation [BS01]

$$\frac{\langle [n_G(\boldsymbol{\theta}) - \langle n_G \rangle]\rangle}{\langle n_G \rangle} = b\bar{\delta}_c(\boldsymbol{\theta}),$$

with a possibly scale-dependent galaxy bias factor $b(k)$. This galaxy bias factor measures how the number density of galaxies scales with the mean density contrast. For most applications one can in fact use a constant bias factor with $b \approx 1$ [Dio+13] with a very weak scale dependence only. However, the scale behaviour of the bias factor, especially due to relativistic corrections on horizon scales is involved in its own right. Details can be found in [Tan+18]; [Dio+13]; [Bal+11] for instance.

The galaxy-quasar cross-correlation is then given by

$$\begin{aligned}\zeta_{QG}(\boldsymbol{\phi}) &= \frac{\langle [n_Q(\boldsymbol{\theta}) - \langle n_Q \rangle]\,[n_G(\boldsymbol{\theta}+\boldsymbol{\phi}) - \langle n_G \rangle]\rangle}{\langle n_Q \rangle \langle n_G \rangle} \\ &= b(\alpha - 1)\left\langle \delta\bar{\mu}_{\text{eff}}(\boldsymbol{\theta})\,\bar{\delta}_c(\boldsymbol{\theta}+\boldsymbol{\phi})\right\rangle + b\alpha\left\langle \bar{\mu}_{\text{vio}}(\boldsymbol{\theta})\,\bar{\delta}_c(\boldsymbol{\theta}+\boldsymbol{\phi})\right\rangle,\end{aligned}$$

with the according spectrum in Fourier space

$$C_{AB}^{QG}(\ell) = b(\alpha - 1)C_{AB}^{\delta\bar{\mu}_{\text{eff}}\,\bar{\delta}_c}(\ell) + b\alpha C_{AB}^{\bar{\mu}_{\text{vio}}\,\bar{\delta}_c}(\ell). \tag{5.49}$$

The effective magnification-density spectrum $C_{AB}^{\delta\bar{\mu}_{\text{eff}}\,\bar{\delta}_c}(\ell)$ is then - using Limber's approximation - given by

$$\begin{aligned} C_{AB}^{\delta\bar{\mu}_{\text{eff}}\,\bar{\delta}_c}(\ell) = l^2 \int_0^{\chi_H} \mathrm{d}\chi\, a \frac{W_{\Psi,A}(\chi) W_{\delta_c,B}(\chi)}{\chi^2} \left(k^2 + \eta^2 a^2\right)^{-1} \\ \times \left(1 + \frac{\tilde{\delta}}{2} + a^2\eta^2 k^{-2}\right) \frac{3\Omega_{m_0}}{2\chi_H^2} P_{\delta_c\delta_c}(k), \end{aligned} \tag{5.50}$$

which becomes equivalent to the standard result in [BS01], when setting the constants $\tilde{\delta}$ and η of the area-metric theory to zero. The spectrum measuring the correlation between the averaged photon excess and the foreground lenses $C_{AB}^{\bar{\mu}_{\text{vio}}\,\bar{\delta}_c}(\ell)$ is given by

$$C_{AB}^{\bar{\mu}_{\text{vio}}\,\bar{\delta}_c}(\ell) = \frac{3}{2} \int_0^{\chi_H} \mathrm{d}\chi a \frac{W_{\mathrm{Y},A}(\chi)\, W_{\delta_c,B}(\chi)}{\chi^2} \delta \left(k^2 + \eta^2 a^2\right)^{-1} \frac{3\Omega_{m_0}}{2\chi_H^2} P_{\delta_c\delta_c}(k), \tag{5.51}$$

with weighting function adjusted to account for the quasar distance distribution $p_0(z)$ as

$$W_{\mathrm{Y},A}(\chi) = p_0\left(z(\chi)\right) \Theta\left(\chi_A - \chi\right) \frac{H(\chi)}{c} \frac{D_+(a)}{a}.$$

5.6 Numerical evaluation of the galaxy-quasar cross-correlation spectra

Lastly, the galaxy-quasar cross-correlation spectrum as discussed in Section 5.5 will be depicted graphically and compared to the spectrum expected for general relativity. By the same arguments as in Section 5.4 the coupling parameter δ and the refined parameter $\tilde{\delta}$ are set to $\delta = \tilde{\delta} = 10^{-5}$. In general, these two parameters could differ, but for simplicity they are set equal since, for they should be of similar magnitude. For the range η^{-1} of the Yukawa interaction one Hubble length $\eta^{-1} = \chi_H$ is chosen, noting that different choices for η would not alter the shape of the spectra a lot, as also discussed in Section 5.4. For the exponent of the flux power law of the sources $\alpha = 2.5$ is chosen, what corresponds to an observation in the optical range [BS01]. The galaxy bias is set to $b = 1.5$ and is hence in the admissible range between $b = 1 - 2$ as discussed in [BS01]. Furthermore,no separation into tomographic bins is performed to depict the cross-correlation. The corresponding power spectra for $C^{QG}(\ell) = b(\alpha-1)C_{AB}^{\delta\bar{\mu}_{\text{eff}}\,\bar{\delta}_c}(\ell) + b\alpha C_{AB}^{\bar{\mu}_{\text{vio}}\,\bar{\delta}_c}(\ell)$ in (5.49), as well as its single constituents $C^{\delta\bar{\mu}_{\text{eff}}\,\bar{\delta}_c}(\ell)$ in (5.50) and $C^{\bar{\mu}_{\text{vio}}\,\bar{\delta}_c}(\ell)$ in (5.51) are illustrated in Figure 5.12. The plots show that the shape of the spectrum is mainly dominated by the cross-correlation between the density fluctua-

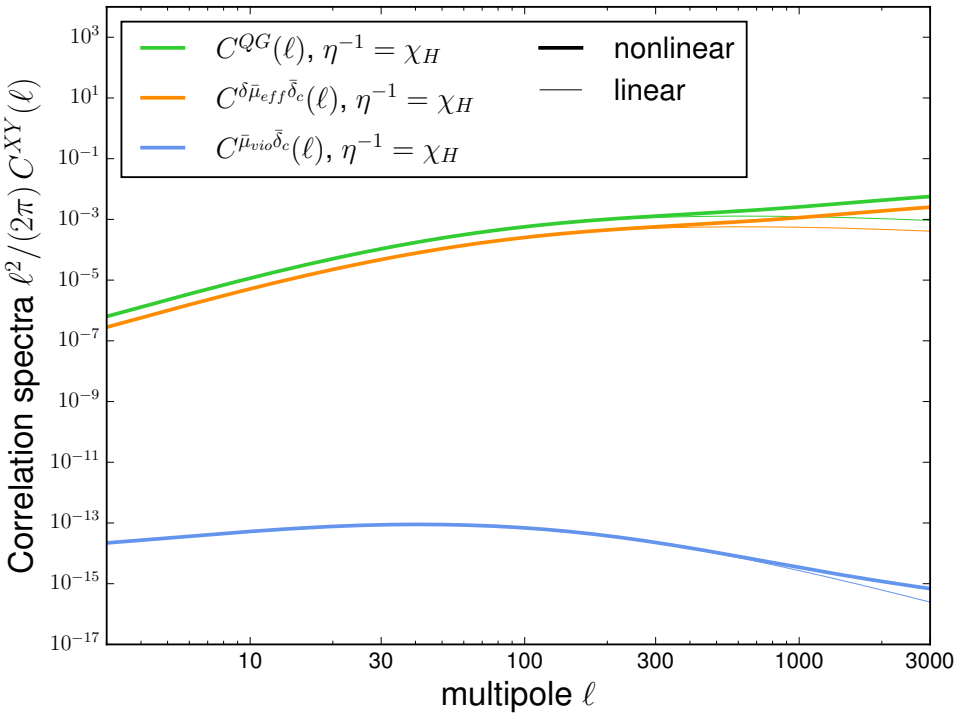

Figure 5.12: **Galaxy-quasar cross-correlation spectrum with area-metric refinements:** The plot shows the power spectrum for the galaxy-quasar cross-correlation $C^{QG}(\ell)$ depicted in green, as well as its single constituents $C^{\delta\bar{\mu}_{\text{eff}}\,\bar{\delta}_c}(\ell)$ in orange and $C^{\bar{\mu}_{\text{vio}}\,\bar{\delta}_c}(\ell)$ in blue for $\delta = \tilde{\delta} = 10^{-5}$ and $\eta = 1/\chi_H$. The thin lines correspond to a spectrum based on linear structure formation, while the thick lines include non-linear refinements in the power spectrum according to [Smi+03].

tions and the effective lensing magnification in the area-metric setting. The magnitude of the spectrum $C^{\bar{\mu}_{\text{vio}}\,\bar{\delta}_c}(\ell)$ containing the Etherington distance duality violating term is strongly suppressed and starts at 10^{-14} for small multipole orders. It then decreases for smaller structures, while the $C^{\delta\bar{\mu}_{\text{eff}}\,\bar{\delta}_c}(\ell)$ spectrum starts at magnitudes between 10^{-7} and 10^{-6}, and increases for larger multipole order. Thus, one may conclude that even for an Etherington distance duality violating term the quasar magnification bias is mainly dominated by the effective lensing convergence for the parameters chosen. The flux enhancement due to an effective photon excess only leads to a subdominant effect.

Furthermore, the galaxy-quasar cross-correlation spectrum with area-metric refinements is compared to the spectrum expected for general relativity. Therefore, setting the area-metric parameters to zero recovers the standard $C^{QG}(\ell)$ spectrum. This is illustrated in Figure 5.13. The $C^{QG}(\ell)_{GR}$ spectrum as expectted in general relativity is subtracted from the spectrum

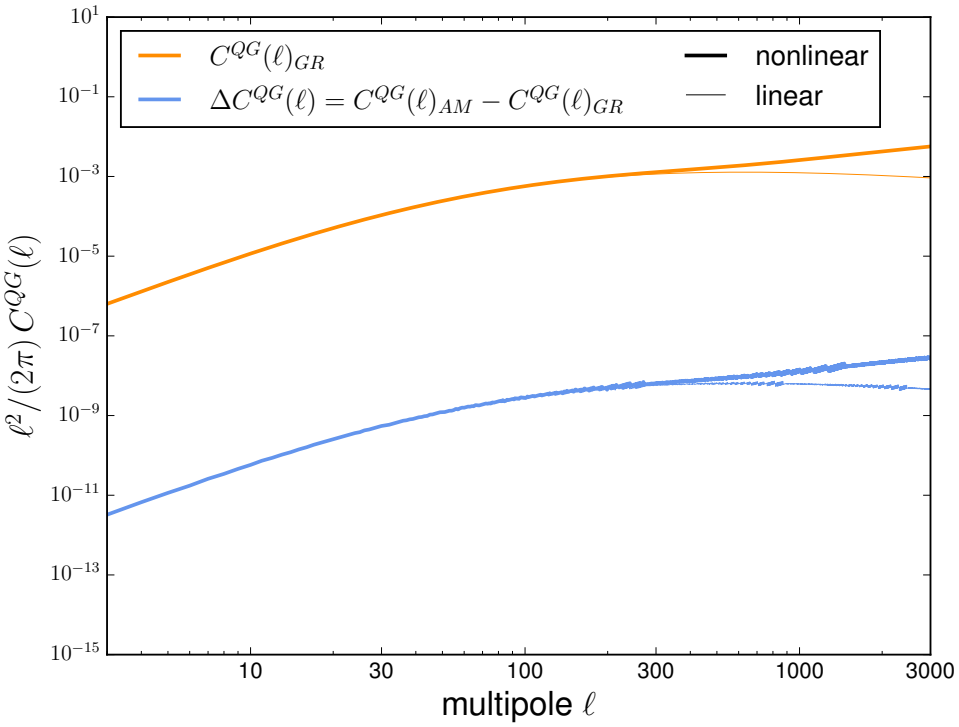

Figure 5.13: **Galaxy-quasar cross-correlation spectrum for general relativity and comparison to spectrum with area-metric refinements:** The plot shows the power spectrum for the galaxy-quasar cross-correlation $C^{QG}(\ell)_{GR}$ as expected for general relativity (orange curve), as well as its difference $\Delta C^{QG}(\ell)$ to the spectrum $C^{QG}(\ell)_{AM}$ containing area-metric refinements (blue curve). Thin lines indicate a linear power spectrum, while the thick lines are spectra based on non-linear structure formation.

$C^{QG}(\ell)_{AM}$ with area-metric refinements. One sees, that in total the area-metric corrections have no substantial effect on the amplitude of the galaxy-quasar cross-correlation spectrum for the chosen parameters δ and η: The magnitude of $\Delta C^{QG}(\ell)$ starts around 10^{-11} for large scales and increases to 10^{-9} for small scales, while the amplitude of the power spectrum $C^{QG}(\ell)_{GR}$ starts at 10^{-7} to 10^{-6} and increases up to 10^{-3} for multipole orders $l \geq 3000$, similar to the total spectrum in Figure 5.12.

5.7 Summary and outlook

To summarize, it was investigated how area-metric refinements in a weakly birefringent spacetime, which lead to a modification in the Etherington distance duality relation, could have an effect on observables in lensing like surface brightness, or the magnification bias. On the

one hand it was demonstrated how surface brightness fluctuations are caused by a modified Etherington distance duality in area-metric lensing. On the other hand a similar effect is also already observable in galaxies at the level of classical astrophysics due to intrinsic alignment. A comparison of both effects shows that the intrinsic alignment effect is dominant and could even by observed with surveys like *Euclid*. Contrary, the effects of area-metric gravity would hardly be observable if the unknown parameters δ and η were as chosen in this work. While η has only very little effect on the amplitudes of the corresponding spectra, they can be increased by tuning δ accordingly. Choosing $\delta \propto 1$ the signal strength would even be of similar magnitude as the signal caused by surface brightness variation due to intrinsic alignment. Yet, such a value is probably unrealistic for δ, as it would imply that the Yukawa refinement and Newtonian potential were of similar magnitude. However, even if effects of weak birefringence in lensing are subdominant, one can still use the spectra as derived in this thesis as a parameterization for Bayesian inference for instance.

As a further remark, the area-metric theory does not constrain these parameters a priori. Thus, they were assumed to scale with the Hubble length on cosmological scales. However, Yukawa corrections can also be investigated locally as done for instance by [Rie20]; [Hen+21] for galaxy rotation curves. A further remark in this context is, that Yukawa corrections of the potential may generally occur in various $f(R)$-gravity classes (see for instance [AT10]; [Cli+12]; [Rie20]), but the violation of the Etherington distance duality is a specific property of the area-metric theory. Furthermore, similar violations may also appear in different contexts, like exotic photon-axion mixing [BK04] for instance.

As a further remark, the results derived here are first order approximations, and various assumptions were made, like assuming a ΛCDM model on an FLRW metric induced cosmologcial background. Also, for a fully consistent study, Yukawa corrections would need to be included on galaxy scales and in structure formation models as discussed in [Rie20]. But then, the questions arises whether these further refinements would actually be resolvabe given that the magnitude of area-metric refinements in lensing in this first order approximation are very low. Beyond that, one could loosen the assumption that a simple ΛCDM model is considered and instead also include higher order corrections of the refined Friedmann equations in area-metric theory as discussed by [Fis17]; [Due20].

6 Summary and outlook

This thesis discussed three different main topics, which are summarized in this final chapter. It will also be discussed which issues and open questions came up within the projects, and how they could be addressed in future work:

Constructive Gravity and solutions for spherically symmetric spacetimes

Firstly, in Chapter 1, basic ideas about of the constructive gravity program (see for instance [Dü+18]; [Due20]; [Wol22]) have been summarized. Furthermore, a massive dispersion relation was postulated in the new observer definition, which is based on [Wie18]; [Wol22]; [Sch20], guided by the steps laid out in [RRS11]. Then, the constructive gravity program was systematically applied to spherically symmetric, metric spacetimes in Chapter 2. The goal was to construct the metric Schwarzschild solution, and similar types of solutions like the Painlevé-Gullstrand solution as proof of principle, without employing the gravitational field equations of general relativity in the process. This calculation also served to demonstrate how the according steps could possibly be adapted to find similar solutions for more general spacetime structures. The calculations were performed in the new observer definition by [Wie18]; [Sch20]; [Wol22], closely guided by steps taken in previous work by [Due20]; [Dü+20]; [Fis17], who used the observer definition by [RRS11] to study FLRW solutions. As expected, the closure equations produced the standard results known from general relativity.
Next, in Chapter 3, a spherically symmetric, stationary area-metric spacetime was considered. An according ansatz for this kind of spacetime was worked out to derive the symmetry reduced input coefficients for the closure equations. Additionally, it was addressed how the notion of staticity as discrete time-reflection symmetry cannot be generalized to an area-metric. But it still survives for the principal polynomial and its dual, and thus the massless and massive particle action. The Schwarzschild spacetime can thus be characterized such, that there is always a frame where Frobenius integrability condition, and thus hypersurface orthogonality, holds for the timelike Killing vector field.
It was subsequently discussed, that the collapse problem within the closure equations is most obstructive for finding a general solution to these even for this symmetry reduced case. This is also problematic, since, according to [Wol22], the principal polynomial for the matter and the geometry do not coincide, what they, however, must for a consistent co-evolution. This

issue could be addressed by explicitly demanding them to be equal. That may lead to more conditions on the output coefficients, and possibly also solve the collapse problem [Wol22] However, it is actually desirable that this condition arises in the constructive gravity program already with sufficient input, and does not have to be enforced in the end to make things consistent.

The difficulty in this case is also, that there is generally a non-vanishing boundary term, which might depend on $\partial^n\varphi$ to arbitrary order n. It does not see the dynamical evolution but still appears in the action. While in the metric case this boundary term $C_A[\varphi] = \delta\Lambda[\varphi]/\delta\varphi^A$ is decoupled from all the other output coefficients [Wol22], this is does not hold for a more general case. Instead, all output coefficients get mixed up in the closure equations due to the non-vanishing $M^{A\gamma}$-coefficient [Wol22]; [Wie]. It is not clear how one could separate them accordingly.

Another issue is whether all information that is contained in the closure equations is actually made explicit, i.e. whether the system of partial differential equations contains hidden integrability conditions, which could somehow simplify the general solution or contain further insights. This problem of involutivity, which was omitted in this thesis, but is still a very important concept for the constructive gravity program in general, was addressed in [Wie18]; [Wol22] for instance. Especially in [Wol22] it was shown that only the covariance part of the closure equations, which comes from the second algebra relation (1.19), is in involutive form. A natural next step would be to show, whether or not this also holds for the system of countably many partial differential equations coming from the first algebra relation (1.18), and what can be learned from that.

So all in all, it is likely, that further conditions need to be specified in the constructive gravity program itself, before further solutions may be found. Another line of thought could be to study if there is possible further information contained in higher order hypersurface deformation brackets. For instance, efforts were made to study the outcome of tertiary brackets like

$$\begin{aligned}[\mathcal{H}(N_1),\mathcal{H}(N_2),\mathcal{H}(N_3)] = {}& \mathcal{H}(N_1)[\mathcal{H}(N_2),\mathcal{H}(N_3)] + \mathcal{H}(N_2)[\mathcal{H}(N_3),\mathcal{H}(N_1)] \\ & + \mathcal{H}(N_3)[\mathcal{H}(N_1),\mathcal{H}(N_2)].\end{aligned}$$

Additionally, also quaternary brackets like

$$\begin{aligned}[\mathcal{H}(N_1),\mathcal{H}(N_2),\mathcal{H}(N_3),\mathcal{H}(N_4)] = {} & \mathcal{H}(N_1)[\mathcal{H}(N_2),\mathcal{H}(N_3),\mathcal{H}(N_4)] \\ & + \mathcal{H}(N_2)[\mathcal{H}(N_3),\mathcal{H}(N_4),\mathcal{H}(N_1)] \\ & + \mathcal{H}(N_3)[\mathcal{H}(N_4),\mathcal{H}(N_1),\mathcal{H}(N_2)] \\ & + \mathcal{H}(N_4)[\mathcal{H}(N_1),\mathcal{H}(N_2),\mathcal{H}(N_3)],\end{aligned}$$

were studied. The goal was to see if the system of closure equations can be enlarged with further equations directly containing higher order components of the principal tensor $p^{\alpha\beta\gamma}$ or $p^{\alpha\beta\gamma\delta}$ for example. This idea was inspired by the so called Nambu-brackets in classical mechanics [Nam73], which can be considered as generalized Poisson brackets. They were thought of as potential candidates to mimic the higher order commutator brackets stated above in the canonical description. Unfortunately, the output of the tertiary and quaternary brackets as given above did not yield functional differential operators on the embedding space X_t. Instead, the results also contained terms proportional to $\delta^2/\delta X_t^2$ and thus these brackets do not close. However, as discussed with [Scha], these outputs could possibly be used as vector fields on the tangent space of the embedding space, to construct a suitable algebra in a second order tangent bundle over X_t, what can be done in future research.
A further interesting idea would be to try to implement the sign conditions which arise when demanding bihyperbolicity for the principal polynomial and the corresponding dual polynomial [Scha] in the canonical description. The sign conditions are discussed in detail in [RRS11] for a general principal polynomial. They were also discussed for a spherically symmetric, stationary area-metric spacetime in Chapter 2 as explicit example.
At last, and as was already mentioned in the introductory Chapter 0, it would also be an interesting case study to apply the constructive gravity program to a matter action describing a spinor with coupling to torsion to see which kind of gravity action would arise from this. One might expect to find a theory similar to ECSK, but of course, this can only be verified by explicit calculation.

Intrinsic and extrinsic gravitational flexions

In Chapter 4 it was first summarized how flexions arise and can be measured in the context of weak gravitational lensing, based on works by [Bac+06]; [GB05]; [OUF07]. Flexions are image distortions caused by variations in the tidal field of the lens via third derivatives $\partial_a\partial_b\partial_c\Phi$ in the gravitational potential Φ of the LSS (large-scale structure). They introduce a centroid shift, as well as a three-fold symmetry in lensed images of sources. Then, a linear intrin-

sic alignment model of elliptical galaxies [GDS21], i.e. an alignment of the galaxies within the local tidal fields, was briefly discussed. In general, it is important to be able to quantify the intrinsic alignment effect precisely, for it is an important systematic error on weak lensing. With the linear alignment model for elliptical galaxies intrinsic gravitational flexions were derived accordingly, using the HOLICs formalism introduced by [OUF07]. The intrinsic flexions introduce an intrinsic shape distortion for elliptical galaxies, similarly to the weak lensing flexion. The goal was to study, whether these intrinsic effects can be measured with *Euclid*-like surveys, and the magnitude of the intrinsic and extrinsic flexion auto- and cross-correlations were compared for a tomographic analysis. It turned out, that even for optimistic choices of flexion noise, as stated by [OUF07], the intrinsic effect was not measurable, but only the lensing flexion auto-correlation spectra. For more realistic choices of flexion dispersions, as discussed in [Row+13], the intrinsic flexion auto-correlation and cross-correlation with lensing flexions is not measurable. Furthermore, this work specified the scaling behavior and analytical form of the alignment parameter D_{IA} in more detail. This parameter is a proportionality constant measuring the strength of the alignment effect. It was specifically analyzed how this parameter changes with Sérsic index n, and how it scales for a galaxy in a virialized model compared to the Sérsic model. This work lead to the publication **Intrinsic and extrinsic gravitational flexions** which appeared in the *Monthly Notices of the Royal Astronomical* Society (December 2021), 510, 2773–2789.

To enhance measurability of the intrinsic flexion effect one could investigate the cross-correlation with intrinsic size and ellipticities, or weak lensing convergence and shear in future work. The cumulated signal-to-noise ratio is expected to be larger, since ellipticities and size can be measured with smaller relative uncertainty. But of course a thorough numerical evaluation would need to be performed to state this more precisely.
A further interesting idea for the linear alignment model in general is to study whether there may also be a time-dependence in the alignment parameter. This loosens the assumption, made by [GDS21] of instantaneous backreaction of the galaxy to tidal forces. As discussed by [SAB21] gravitational potentials of halos can locally be described within a boosted reference frame. This so-called boosted potential can then - according to [SAB21] - be approximated by a self-potential of the system and a time-dependent tidal field. The evolution and alignment of the halos could then be given by this time-dependent tidal field, and thus also the according galaxy alignment. Finally, this be useful for understanding the time dependence of the tidal field of the LSS [SAB21]. It would thus be interesting to study in future work, how this time-dependence might influence the linear alignment model, or whether the alignment parameter itself could become time-dependent, containing the evolution history of the LSS.

Phenomenological tests for weakly birefringent spacetimes in weak lensing

Chapter 5 of this thesis thematized the phenomenology of weakly birefringent spacetimes, which imply a violation of the Etherington distance duality relation. A specific solution in this context is a weakly area-metric spacetime as predicted in a weak field limit of the constructive gravity program, with a point mass as source of the gravitational field [Sch+17]; [Ale20b]. The solution gives rise to additional Yukawa interactions in the gravitational potential, characterized by a coupling parameter δ to the Newtonian interaction, and an inverse interaction range η. As a remark, the numerical values for these parameters are not specified by the constructive gravity program. Here, this solution was considered for a continuous mass distribution, and it was studied how standard quantities in weak gravitational lensing like image convergence are modified by this extra Yukawa potential term.

Another important property of the solution for a weakly birefringent spacetime considered by [Sch+17]; [Ale20b] is that it violates the Etherington distance duality. This relation specifies in what way the angular diameter distance, which measures how apparent object sizes scale compared to their physical size, and the luminosity distance, which is a scaling measure for brightness and fluxes, are related. Now, for metric spacetimes this duality relation between these two distance measures is a fundamental. It is violated for weakly birefingent spacetimes though, as shown by [SW17], and the violation is proportional to a Yukawa potential. The modification of the Etherington distance duality also translates into a violation of the surface brightness conservation law in weak lensing. This leads to relative surface brightness fluctuations $\delta I/I_Y$ which depend on the Yukawa correction. In this thesis the $C_{AB}^{\delta\bar{I}/\bar{I}_Y\,\delta\bar{I}/\bar{I}_Y}(\ell)$ spectra for these surface brightness fluctuations were derived and numerically evaluated. Furthermore, their cumulated signal-to-noise ratio was derived, to estimate their measurability. Here, the parameter values for δ and η were chosen such, that these violations occur on scales corresponding to multiple Hubble lengths. Additionally, the value for δ was chosen to be in the magnitude of the uncertainty of the gravitational constant G.

It was also shown that there is a similar effect of surface brightness fluctuation arising in the context of classical linear intrinsic alignment with Newtonian gravity, as was discussed in Chapter 4. While tidal fields were assumed not to enhance star formation in galaxies to first order, the flux of these galaxies was not affected. However, they caused changes in intrinsic size, what leads to an intrinsic surface brightness fluctuation effect with $\delta I/I$. The according spectra $C_{AB}^{\delta\bar{I}/\bar{I}\,\delta\bar{I}/\bar{I}}(\ell)$ for this effect, as well as the cross-correlation $C_{AB}^{\delta\bar{I}/\bar{I}_Y\,\delta\bar{I}/\bar{I}}(\ell)$ with the Etherington distance duality violating lensing effect were derived. Their shape, amplitude and the corresponding cumulated signal-to-noise ratio were evaluated. It turned out, that only the intrinsic effect can be measured with a *Euclid*-like survey. The magnitude of the surface brightness fluctuation in a weakly area-metric geometry becomes comparable to the intrinsic

effect for $\delta \propto 1$. Thus, with the parameters δ and η chosen in this work it turns out, that the intrinsic effect is always dominant compared to the effect coming from a weakly birefringent spacetime. These findings can also be found in the article **Etherington duality breaking: gravitational lensing in non-metric spacetimes versus intrinsic alignments** *(August 2022)*, arXiv:2208.07197, which was submitted to the *Monthly Notices of the Royal Astronomical Society*.
It was furthermore discussed how a weakly birefringent area-metric spacetime structure, which violates the Etherington distance duality relation, affects other observable lensing quantities like the quasar magnification bias. This bias factor measures how the number count of distant quasars is affected due to weak lensing for a flux limited survey. There are two competing effects: On the one hand there is flux magnification, such that sources appear brighter and are thus more likely to be detected. On the other hand, magnification also leads to an apparent stretching of the observed sky patch, such that the number density of sources is geometrically decreased. It was shown that an area-metric refinement to the lensing potential due to the additional Yukawa potential leads to a change in effective magnification and additional flux magnification due to the Etherington distance duality violation. However, with the numerical values chosen here the modification of the galaxy-quasar cross-correlation spectrum compared to the general relativity case is of magnitude 10^{-11} to 10^{-7}.

In this thesis some assumptions were made, which could be loosened for a more thorough investigation in future work: First of all, it was assumed throughout the calculations that the cosmological model was given by ΛCDM, thereby setting the additional scale factor c, which arises in the flat area-metric cosmology as additional degree of freedom [Due20]; [Fis17], to 1. It would be interesting to study, what happens if one were to use the more general model, though. However, this would still require a better understanding of the flat cosmological solution in general, especially the additional source degree of freedom besides density and pressure found by [Due20]; [Fis17].
Also, it would be interesting to study how the additional Yukawa interaction as predicted in the weakly birefringent set-up affects the intrinsic alignment model. In the current work it was assumed, that the corrections would be small on local scales. Thus, they would not be resolvable within the uncertainty of the alignment parameter D_{IA}, whose numerical value is only determined up to a factor of 10. The parameters η and δ were chosen such, that they only become relevant on cosmological scales, with the classical intrinsic alignment effect setting an upper boundary to the strength of the surface brightness fluctuation. Furthermore, it would be interesting to study whether an according Yukawa modification of the power spectrum (see also [Rie20]) might influence the whole results.

Beyond these additions, it is also important to note, that the observed surface brightness fluctuations are in general also affected by the orientation of the sources with respect to the line of sight. While observing a galaxy face on, the brightness is of course larger, than observing it edge on. Crucially, intrinsic alignment in the tidal fields of the LSS not only affect the shape and size of galaxies. But they also affect, how they get oriented with respect to the field and the observer, as studied for instance by [KH10].
In a flux limited survey this will also lead to a selection bias, which depends on the intrinsic alignment strength: Galaxies which are observed face on get selected preferably, what also affects the galaxy bias b as shown by [KH10]. This in turn can also affect the quasar magnification bias in general, since the galaxy bias also enters in the calculation. It would be interesting to study how this orientation effect might alter the findings in this thesis, which is up to further research.
Another important factor when it comes to measuring the surface brightness of sources is the so-called Malmquist bias [Mal25]: The higher the redshift range observed, i.e. the larger the distance to the observer, in a flux limited survey, the higher the intrinsic brightness of galaxies, which pass the selection process. While galaxies in an overdense region have an increased surface brightness due to intrinsic alignment, galaxies in an underdense region will be fainter, and thus they will be selected less likely with increasing redshift. How this bias might affect the observation of surface brightness fluctuations due to the Etherington distance duality relation is not yet clear, since the sign of δ is not known. If the violating factor μ_{vio} is larger than 0, the sources could appear brighter, therefore being selected with higher probability. On the other hand if $\mu_{\text{vio}} < 0$, sources appear fainter, and would be selected less likely for higher redshifts. How this bias might affect the overall results concerning the spectra and the cumulated signal-to-noise ratio, especially as functions of wavenumber k, is indeed interesting, especially in regards to actual observations, and up to future research.

To summarize, in the weak field limit it is possible to study the effect of area-metric geometries on weak lensing observables, like surface brightness variations or the quasar magnification bias. This comes with a caveat, since the corresponding signatures of this exotic geometry structure are very weak. Especially, when considering surface brightness fluctuations for instance, effects from classical astrophysics like intrinsic alignment have to be taken into account as well. These were shown to dominate any signatures coming from a non-metric geometry, such that different ways to test for area-metric spacetimes need to be proposed as well. Thus, besides analyzing weak lensing observables there is also the perspective to learn more about the strong gravity regime with modern experiments like LIGO or EHT. How-

ever, explicit application of the constructive gravity program for deriving solutions in the strong gravity regime, like the Schwarzschild solution, for area-metric geometries is still out of reach. Thus, a better understanding of the program itself forms the basis to find different types of astrophysical solutions on an area-metric spacetime in the future.

Part I

Appendix

A Gravitational closure equations

This is the complete set of gravitational closure equations worked out by [Dü+18]; [Due20]; [Wol22]. Here, the *LaTex* template of [Due20] was adapted to display them within the new, alternative observer definition based on [Wie18]; [Sch20]; [Wol22], similar to [Wie18]. The equations split up in the seven individual equations ($C1$)-($C7$), and the sequence equations ($C8_{N\geq 2}$)-($C21_{\text{odd } N\geq 3}$).

Seven individual equations

$$\begin{aligned}
\textbf{(C1)}\quad 0 &= -C\,\delta^{\gamma}_{\mu} + \sum_{K=0}^{\infty}(K+1)\,\Big[C_{:A}{}^{\alpha_1\ldots\alpha_K\gamma}\,\left(\varphi^{A}{}_{,\mu\alpha_1\ldots\alpha_K} + F^{A}{}_{\mu}{}^{\alpha_{K+1}}{}_{,\alpha_1\ldots\alpha_{K+1}}\right) \\
&\qquad - C_{:A}{}^{(\alpha_1\ldots\alpha_K|}\,F^{A}{}_{\mu}{}^{|\gamma)}{}_{,\alpha_1\ldots\alpha_K}\Big] \\
\textbf{(C2)}\quad 0 &= -C_B\,\delta^{\gamma}_{\mu} - C_A\,F^{A}{}_{\mu}{}^{\gamma}{}_{:B} + \sum_{K=0}^{\infty}(K+1)\Big[C_{B:A}{}^{\gamma\alpha_1\ldots\alpha_K}\,\left(\varphi^{A}{}_{,\mu\alpha_1\ldots\alpha_K} + F^{A}{}_{\mu}{}^{\alpha_{K+1}}{}_{,\alpha_1\ldots\alpha_{K+1}}\right)\Big] \\
&\quad - \sum_{K=0}^{\infty}(K+1)\,C_{B:A}{}^{(\alpha_1\ldots\alpha_K|}\,F^{A}{}_{\mu}{}^{|\gamma)}{}_{,\alpha_1\ldots\alpha_K} \\
\textbf{(C3)}\quad 0 &= 2\,(\deg P^{\#}-1)^{-1}\,C_{AB}\,p^{\#\rho(\mu|}\,F^{A}{}_{\rho}{}^{|\nu)} + \sum_{K=0}^{\infty}(K+1)\,C_{B:A}{}^{\alpha_1\ldots\alpha_K(\mu|}\,M^{A|\nu)}{}_{,\alpha_1\ldots\alpha_K} \\
&\quad - \sum_{K=0}^{\infty}(-1)^K\begin{pmatrix}K+2\\K\end{pmatrix}\left(\partial^{K}_{\alpha_1\ldots\alpha_K}\,C_{:B}{}^{\alpha_1\ldots\alpha_K\mu\nu}\right) \\
\textbf{(C4)}\quad 0 &= 2\,(\deg P^{\#}-1)^{-1}\,C_{AB}\left(p^{\#\mu\nu}\,\varphi^{A}{}_{,\nu} - p^{\#\mu\nu}{}_{,\gamma}\,F^{A}{}_{\nu}{}^{\gamma}\right) - C_A\,M^{A\mu}{}_{:B} \\
&\quad - \sum_{K=0}^{\infty}C_{B:A}{}^{\alpha_1\ldots\alpha_K}\,M^{A\mu}{}_{,\alpha_1\ldots\alpha_K} - \sum_{K=0}^{\infty}(-1)^K\,(K+1)\left(\partial^{K}_{\alpha_1\ldots\alpha_K}C_{:A}{}^{\alpha_1\ldots\alpha_K\mu}\right) \\
\textbf{(C5)}\quad 0 &= 2\,\partial_{\mu}\left(C_A\,M^{A[\mu|}{}_{:B}\,M^{B|\gamma]}\right) - 2\,(\deg P^{\#}-1)^{-1}\,p^{\#\rho\gamma}[C_A\,\varphi^{A}{}_{,\rho} + \partial_{\mu}(C_A\,F^{A}{}_{\rho}{}^{\mu})] \\
&\quad + \sum_{K=0}^{\infty}C_{:A}{}^{\alpha_1\ldots\alpha_K}\,M^{A\gamma}{}_{,\alpha_1\ldots\alpha_K} \\
&\quad + \sum_{K=0}^{\infty}\sum_{J=0}^{K}(-1)^J\begin{pmatrix}K\\J\end{pmatrix}(J+1)\,\partial^{J}_{\alpha_1\ldots\alpha_J}\left(C_{:A}{}^{\beta_1\ldots\beta_{K-J}(\alpha_1\ldots\alpha_J|}\,M^{A|\gamma)}{}_{,\beta_1\ldots\beta_{K-J}}\right)
\end{aligned}$$

$$(\boldsymbol{C6}) \quad 0 = 6\,(\deg P^{\#}-1)^{-1}\,C_{AB_1B_2}\left(p^{\#\mu\nu}\,\varphi^{A}{}_{,\nu} - p^{\#\mu\nu}{}_{,\gamma}\,F^{A}{}_{\nu}{}^{\gamma}\right) - 4\,C_{A(B_1|}\,M^{A\mu}{}_{:|B_2)}$$
$$- 2\,C_{B_1B_2:A}\;M^{A\mu} - 2\,C_{B_1B_2:A}{}^{\alpha}\;M^{A\mu}{}_{,\alpha} - 2\,C_{B_1B_2:A}{}^{\alpha\beta}\;M^{A\mu}{}_{,\alpha\beta} - C_{B_2:B_1}{}^{\mu}$$
$$- \sum_{K=0}^{\infty}(-1)^K\,(K+1)\left(\partial^{K}_{\alpha_1\ldots\alpha_K}C_{B_1:B_2}{}^{\mu\alpha_1\ldots\alpha_K}\right)$$

$$(\boldsymbol{C7}) \quad 0 = \sum_{K=0}^{\infty}\sum_{J=2}^{K+1}(-1)^J\binom{K}{J-1}\binom{J}{N}\,(J-1)\,\partial^{J+1}_{\gamma\alpha_1\ldots\alpha_J}\left(C_{:A}{}^{\beta_1\ldots\beta_{K-J}(\alpha_1\ldots\alpha_J|}\;M^{A|\gamma)}{}_{,\beta_1\ldots\beta_{K-J}}\right)$$

Fourteen sequence equations

$$(\boldsymbol{C8}_{N\geq 2}) \quad 0 = \sum_{K=0}^{\infty}\binom{K+N}{N}\Big[C_{:A}{}^{\beta_1\ldots\beta_N\alpha_1\ldots\alpha_K}\left(\varphi^{A}{}_{,\mu\alpha_1\ldots\alpha_K} + F^{A}{}_{\mu}{}^{\alpha_{K+1}}{}_{,\alpha_1\ldots\alpha_{K+1}}\right)$$
$$- C_{:A}{}^{(\beta_1\ldots\beta_N\alpha_1\ldots\alpha_{K-1}|}\;F^{A}{}_{\mu}{}^{|\alpha_K)}{}_{,\alpha_1\ldots\alpha_K}\Big]$$

$$(\boldsymbol{C9}_{N\geq 2}) \quad 0 = \sum_{K=0}^{\infty}\binom{K+N}{N}\Big[C_{B:A}{}^{\beta_1\ldots\beta_N\alpha_1\ldots\alpha_K}\left(\varphi^{A}{}_{,\mu\alpha_1\ldots\alpha_K} + F^{A}{}_{\mu}{}^{\alpha_{K+1}}{}_{,\alpha_1\ldots\alpha_{K+1}}\right)$$
$$- C_{B:A}{}^{(\beta_1\ldots\beta_N\alpha_1\ldots\alpha_{K-1}|}\;F^{A}{}_{\mu}{}^{|\alpha_K)}{}_{,\alpha_1\ldots\alpha_K}\Big]$$

$$(\boldsymbol{C10}_{N\geq 2}) \quad 0 = -C_{B_1\ldots B_N}\,\delta^{\gamma}_{\mu} - N\,C_{A(B_1\ldots B_{N-1}|}\,F^{A}{}_{\mu}{}^{\gamma}{}_{:|B_N)} - C_{B_1\ldots B_N:A}\;F^{A}{}_{\mu}{}^{\gamma} + C_{B_1\ldots B_N:A}{}^{\gamma}\;\varphi^{A}{}_{,\mu}$$
$$- C_{B_1\ldots B_N:A}{}^{\alpha}\;F^{A}{}_{\mu}{}^{\gamma}{}_{,\alpha} - C_{B_1\ldots B_N:A}{}^{\alpha_1\alpha_2}\;F^{A}{}_{\mu}{}^{\gamma}{}_{,\alpha_1\alpha_2} + 2\,C_{B_1\ldots B_N:A}{}^{\alpha\gamma}\;\varphi^{A}{}_{,\alpha\mu}$$

$$(\boldsymbol{C11}_{N\geq 2}) \quad 0 = C_{B_1\ldots B_N:A}{}^{\beta_1\beta_2}\;\varphi^{A}{}_{,\mu} - 2\,C_{B_1\ldots B_N:A}{}^{\alpha(\beta_1|}\;F^{A}{}_{\mu}{}^{|\beta_2)}{}_{,\alpha} - C_{B_1\ldots B_N:A}{}^{(\beta_1|}\;F^{A}{}_{\mu}{}^{|\beta_2)}$$

$$(\boldsymbol{C12}_{N\geq 2}) \quad 0 = C_{B_1\ldots B_N:A}{}^{(\beta_1\beta_2|}\;F^{A}{}_{\mu}{}^{|\beta_3)}$$

$$(\boldsymbol{C13}_{N\geq 2}) \quad 0 = C_{B_1\ldots B_N:A}{}^{(\beta_1\beta_2|}\;M^{A|\beta_3)}$$

$$(\boldsymbol{C14}_{N\geq 2}) \quad 0 = C_{AB_1\ldots B_{N-1}}\left[(\deg P^{\#}-1)^{-1}\,p^{\#\rho\mu}F^{A}{}_{\rho}{}^{\nu} - M^{B[\mu|}\,M^{A|\nu]}{}_{:B}\right]$$

$$(\boldsymbol{C15}_{N\geq 2}) \quad 0 = C_{B_1\ldots\widetilde{B_J}\ldots B_{N+1}:B_J}{}^{\mu\nu} - C_{B_1\ldots B_N:B_{N+1}}{}^{\mu\nu} \qquad \text{for } J = 1\ldots N+1$$

$$(\boldsymbol{C16}_{N\geq 2}) \quad 0 = N\,(N+1)\,(\deg P^{\#}-1)^{-1}\,C_{AB_1\ldots B_N}\,p^{\#\rho(\mu|}\,F^{A}{}_{\rho}{}^{|\nu)} + N\,C_{B_1\ldots B_N:A}{}^{(\mu|}\;M^{A|\nu)}$$
$$+ 2\,N\,C_{B_1\ldots B_N:A}{}^{\alpha(\mu|}\;M^{A|\nu)}{}_{,\alpha} + (N-2)\,C_{B_1\ldots B_{N-1}:B_N}{}^{\mu\nu}$$

$$(\boldsymbol{C17}_{N\geq 2}) \quad 0 = (N+2)\,(N+1)\,(\deg P^{\#}-1)^{-1}\,C_{AB_1\ldots B_{N+1}}\left(p^{\#\mu\gamma}\varphi^{A}{}_{,\gamma} - p^{\#\mu\nu}{}_{,\gamma}\,F^{A}{}_{\nu}{}^{\gamma}\right)$$
$$- (N+1)^2\,C_{A(B_1\ldots B_N|}\,M^{A\mu}{}_{:|B_{N+1})} - (N+1)\,C_{B_1\ldots B_N:A}\;M^{A\mu}$$
$$- (N+1)\,C_{B_1\ldots B_N:A}{}^{\alpha}\;M^{A\mu}{}_{,\alpha} - (N+1)\,C_{B_1\ldots B_N:A}{}^{\alpha\beta}\;M^{A\mu}{}_{,\alpha\beta}$$
$$- \sum_{K=0}^{N+1}C_{B_1\ldots\widetilde{B_K}\ldots B_{N+1}:B_K}{}^{\mu} + 2\left(\partial_{\gamma}C_{B_1\ldots B_N:B_{N+1}}{}^{\mu\gamma}\right)$$

$$(\boldsymbol{C18_{N\geq 2}}) \quad 0 = C_{B_2:B_1}{}^{\mu_1\ldots\mu_N} - \sum_{K=0}^{\infty}(-1)^{K+N}\binom{K+N}{N}\left(\partial^K_{\alpha_1\ldots\alpha_K} C_{B_1:B_2}{}^{\alpha_1\ldots\alpha_K\mu_1\ldots\mu_N}\right)$$

$$(\boldsymbol{C19_{N\geq 2}}) \quad 0 = \sum_{K=0}^{\infty}\left[\binom{K+N}{N} C_{B:A}{}^{\alpha_1\ldots\alpha_K(\mu_1\ldots\mu_N|}\ M^{A|\mu_{N+1})}{}_{,\alpha_1\ldots\alpha_K} + (-1)^{K+N}\binom{K+N+1}{N+1}\left(\partial^K_{\alpha_1\ldots\alpha_K} C_{:B}{}^{\alpha_1\ldots\alpha_K\mu_1\ldots\mu_{N+1}}\right)\right]$$

$$(\boldsymbol{C20_{\text{even } N\geq 2}}) \quad 0 = \sum_{K=N}^{\infty}\sum_{J=N+1}^{K+1}(-1)^J\binom{K}{J-1}\binom{J}{N} \times \partial^{J-N}_{\alpha_1\ldots\alpha_{J-N}}\left(C_{:A}{}^{\beta_J\ldots\beta_K(\alpha_1\ldots\alpha_{J-N}\mu_1\ldots\mu_{N-1}|}\ M^{A|\mu_N)}{}_{,\beta_J\ldots\beta_K}\right)$$

$$(\boldsymbol{C21_{\text{odd } N\geq 3}}) \quad 0 = 2\sum_{K=N-1}^{\infty}\binom{K}{N-1} C_{:A}{}^{\beta_N\ldots\beta_K(\mu_1\ldots\mu_{N-1}|}\ M^{A|\mu_N)}{}_{,\beta_N\ldots\beta_K} - \sum_{K=N}^{\infty}\sum_{J=N+1}^{K+1}\binom{K}{J-1}\binom{J}{N} \times \partial^{J-N}_{\alpha_1\ldots\alpha_{J-N}}\left(C_{:A}{}^{\beta_J\ldots\beta_K(\alpha_1\ldots\alpha_{J-N}\mu_1\ldots\mu_{N-1}|}\ M^{A|\mu_N)}{}_{,\beta_J\ldots\beta_K}\right)$$

B Frobenius's integrability theorem

As described in detail in the literature (for instance [Str13];[Wal84];[Sei10]) and briefly summarized here the Frobenius integrability theorem arises in the context of integrability of manifolds [Wal84]: For a n-dimensional manifold a k-dimensional subspace S_p of the tangent space $S_p \subset T_pM$ at every point $p \in M$ is considered. Now, the question is, whether there exists a k-dimensional submanifold N such that its tangent space T_pN at every point $p \in N$ corresponds to S_p. According to the definition in [Str13], S is a k-dimensional distribution on M, i.e. a smooth map[1] $p \to S_p$ from the point p to the tangent subspace S_p, and N is an integrable manifold of S if for each point p it holds that [Str13]

$$T_p\iota \cdot T_pN = S_p.$$

Here, ι denotes the inclusion map of the submanifold N into M as $\iota : N \hookrightarrow M$. The distribution S is then called integrable if one can find an integral submanifold through each point $p \in N$ [Str13]. In one dimension, finding this integral submanifold specializes to finding the integral curve of a vector field through every point p. Another version of the Frobenius integrability theorem states that, if integral submanifolds for S can be found, it is involute [Wal84]. This means that, if two vector fields $X, Y \in S$ then the commutator $[X, Y] \in S$, too.
As demonstrated in [Str13]; [Wal84], the theorem can also be rephrased in terms of differential one-forms $\omega \in \Omega^1(M)$ (for more details on differential forms see [Nak03] for instance). First, these one-forms ω are required to annihilate the vector fields $X \in S$, i.e.

$$\omega(X) = 0.$$

According to [Wal84] they thus form a $(n-k)$-dimensional co-space $W_p^* \subset T_p^*(M)$. Now, $W^* \subset \Omega(M)$ shall be associated to the distribution S [Str13] as according co-distribution. With $\omega \in W^*$, $\mu^\alpha \in W^*$ and $\nu^\alpha \in \Omega^1(M)$ one can finally show that the Frobenius integrability theorem can also be formulated such, that

$$\mathrm{d}\omega = \sum_{\alpha=1}^{n-k} \mu^\alpha \wedge \nu^\alpha, \tag{B.1}$$

[1] To phrase it differently the distribution S can be considered as a subspace of the tangent bundle TM, i.e. $S \subseteq TM$ [Sei10]

needs to hold to ensure integrability of S [Wal84]. Here, $\mathrm{d}\omega$ denotes the exterior derivative of the one-form and $\wedge$ the exterior product.
As an explicit example a one-dimensional co-space can be considered, where ω is the one-form associated with a vector field V such that $\omega = V^\flat$. Complementary, there is an associated distribution S as collection of tangent spaces T_pN at each point p with N as $(n-1)$-dimensional hypersurface of M, and $\omega(X) = 0$ with $X \in S$. The integrability condition (B.1) for S then simplifies to [Str13]

$$\omega \wedge \mathrm{d}\omega = 0.$$

This is necessary and sufficient for

$$\omega = g\mathrm{d}f$$

with integrating factor g and $\mathrm{d}f$ as a kind of gradient on the hypersurfaces of $f = \text{const}$ [Str13]. Thus, the integral submanifold of the distribution S under consideration can locally be described by a constant function $f(\boldsymbol{y})$ with coordinates $\boldsymbol{y}$, as also discussed more generally in [Sei10].

Consequently, for the case of a Lorentzian manifold (M, g) it may be shown, that the vector field X must be orthogonal to the induced spatial hypersufaces, what corresponds to staticity of the spacetime (see for instance section 2.2.1).
In case of a manifold with an area-metric as underlying geometric structure equipped with a Legendre map defined by the (dual) principal polynomial one can still establish a notion of hypersurface orthogonality for a specific choice of foliation. However, the association to staticity in its original sense as time-reflection symmetry $t \to -t$ is generally different, as discussed in Section 3.3.

C Killing condition for the dual principal polynomial

According to [PWS09] the area-metric isomorphism, generated by Killing vector fields K is, similar to the metric case, given by

$$G_{f(p)}\left(f_* u, f_* w, f_* g, f_* h\right) = G_p\left(u, w, g, h\right). \tag{C.1}$$

Here, $f : M \to M$ is a diffeomorphism mapping a point $p \in M$ to $f(p) \in M$ with coordinate charts $\phi(p) = x^a$ and $\phi(f(p)) = y^{a'}$. A push-forward map f_* is applied to the vector fields u, w, g and h.
If f corresponds to a small displacement such that $\phi(f(p)) = y^{a'} = x^{a'} + \epsilon K^{a'}$, with $\epsilon > 0$ being infinitesimally small, standard methods as for instance discussed in [Nak03] show that the isometry condition (C.1) leads to the Killing condition

$$\mathcal{L}_K G = 0.$$

Now, it can be shown that the isometry condition in G also leads to an isometry for $P^{\#}$, such that the Killing condition also applies to $P^{\#}$: First, one takes the pull-back f^* of $P^{\#}_{f(p)}$ and explicitly evaluates the expression in the coordinate map as

$$f^* P^{\#}_{f(p)}(u, w, g, h) = P^{\#}_{f(p)}\left(f_* u, f_* w, f_* g, f_* h\right),$$
$$\Rightarrow \quad P^{\#}_{a'b'c'd'}(y)\frac{\partial y^{a'}}{\partial x^a}\frac{\partial y^{b'}}{\partial x^b}\frac{\partial y^{c'}}{\partial x^c}\frac{\partial y^{d'}}{\partial x^d} = -\tfrac{1}{24}\omega_G^2(y)\epsilon^{m'n'p'q'}\epsilon^{r's't'u'}G_{m'n'r'(a'}(y)G_{b'|p's'|c'}(y)G_{d')q't'u'}(y).$$

Explicit insertion of the isometry condition for the area-metric

$$G_{a'b'c'd'}(y)\frac{\partial y^{a'}}{\partial x^a}\frac{\partial y^{b'}}{\partial x^b}\frac{\partial y^{c'}}{\partial x^c}\frac{\partial y^{d'}}{\partial x^d} = G_{abcd}(x),$$

as well as the according transformation behavior of ϵ^{abcd} under diffeomorphisms [Car14]

$$\epsilon^{a'b'c'd'} = \det\left|\frac{\partial y}{\partial x}\right|^{-1}\epsilon^{abcd}\frac{\partial y^{a'}}{\partial x^a}\frac{\partial y^{b'}}{\partial x^b}\frac{\partial y^{c'}}{\partial x^c}\frac{\partial y^{d'}}{\partial x^d},$$

and thus consequently

$$\omega_G(y)^2 = \omega_G(x)^2 \det\left|\frac{\partial y}{\partial x}\right|^2,$$

leads to

$$P^{\#}_{a'b'c'd'}(y)\frac{\partial y^{a'}}{\partial x^{a}}\frac{\partial y^{b'}}{\partial x^{b}}\frac{\partial y^{c'}}{\partial x^{c}}\frac{\partial y^{d'}}{\partial x^{d}} = P^{\#}_{abcds}(x).$$

Thus, the isometry condition for $P^{\#}$ is obtained as

$$f^{*}P^{\#}_{f(p)}(u,w,g,h) = P^{\#}_{f(p)}\left(f_{*}u, f_{*}w, f_{*}g, f_{*}h\right) = P^{\#}_{p}\left(u,w,g,h\right),$$

for which the Killing equation

$$\mathcal{L}_{K}P^{\#} = 0,$$

follows from infinitesimal shifts sourced by the Killing vector field K.

D Bibliography

[ADW08] R. Arnowitt, S. Deser, and M. C. W. “Republication of: The dynamics of general relativity”. In: *General Relativity and Gravitation* (2008).

[Ale20a] N. Alex. “Gravitational radiation from birefringent matter dynamics”. In: *Physical Review D* 102.10 (2020). DOI: 10.1103/physrevd.102.104017. URL: https://doi.org/10.1103%2Fphysrevd.102.104017.

[Ale20b] N. Alex. *Solutions of gravitational field equations for weakly birefringent spacetimes*. 2020. DOI: 10.48550/ARXIV.2009.07540. URL: https://arxiv.org/abs/2009.07540.

[Ale22] N. Alex. PhD thesis, Friedrich-Alexander-Universität Erlangen-Nürnberg. in preparation. 2022.

[AR07] A. Amara and A. Refregier. “Optimal Surveys for Weak Lensing Tomography”. In: *Monthly Notices of the Royal Astronomical Society* 381.3 (Oct. 10, 2007), pp. 1018–1026. ISSN: 00358711, 13652966. DOI: 10.1111/j.1365-2966.2007.12271.x. arXiv: astro-ph/0610127. URL: http://arxiv.org/abs/astro-ph/0610127.

[AT10] L. Amendola and S. Tsujikawa. *Dark Energy: Theory and Observations*. Cambridge University Press, 2010. DOI: 10.1017/CBO9780511750823.

[AW] R. M. Aarts and E. W. Weisstein. - visited 10.01.2022. URL: https://mathworld.wolfram.com/FubiniTheorem.html.

[AW05] G. Arfken and H. J. Weber. *Mathematical methods for Physicists*. Elsevier Academic Press, 2005.

[Bac+06] D. J. Bacon et al. “Weak gravitational flexion”. In: *Monthly Notices of the Royal Astronomical Society* 365.2 (Jan. 2006), pp. 414–428. ISSN: 0035-8711. DOI: 10.1111/j.1365-2966.2005.09624.x. eprint: https://academic.oup.com/mnras/article-pdf/365/2/414/2978831/365-2-414.pdf. URL: https://doi.org/10.1111/j.1365-2966.2005.09624.x.

[Bal+11] T. Baldauf et al. “Galaxy bias and non-linear structure formation in general relativity”. In: *Journal of Cosmology and Astroparticle Physics* 2011.10 (2011), 031–031. ISSN: 1475-7516. DOI: 10.1088/1475-7516/2011/10/031. URL: http://dx.doi.org/10.1088/1475-7516/2011/10/031.

[Bar10] M. Bartelmann. “Gravitational lensing”. In: *Classical and Quantum Gravity* 27.23 (2010), p. 233001. DOI: 10.1088/0264-9381/27/23/233001. URL: https://doi.org/10.1088%2F0264-9381%2F27%2F23%2F233001.

[Bar19a] M. Bartelmann. *Das kosmologische Standardmodell*. Heidelberg: Springer-Verlag, 2019.

[Bar19b] M. Bartelmann. *General Relativity*. Heidelberg: Heidelberg University Publishing, 2019.

[Bar+86] J. M. Bardeen et al. “The Statistics of Peaks of Gaussian Random Fields”. In: *Astrophysical Journal* 304 (May 1986), p. 15. DOI: 10.1086/164143.

[BK04] B. A. Bassett and M. Kunz. “Cosmic distance-duality as a probe of exotic physics and acceleration”. In: *Physical Review D* 69.10 (2004). ISSN: 1550-2368. DOI: 10.1103/physrevd.69.101305. URL: http://dx.doi.org/10.1103/PhysRevD.69.101305.

[Bla20] M. Blau. *Lecture Notes on General Relativity*. Albert Einstein Center for Fundamental Physics, Institut für Theoretische Physik Universit at Bern CH-3012 Bern, Switzerland, Lecture notes - visited at 15.08.2022. 2020. URL: http://www.blau.itp.unibe.ch/GRLecturenotes.html.

[BM17] M. Bartelmann and M. Maturi. “Weak gravitational lensing”. In: *Scholarpedia* 12 (2017), p. 32440.

[Boo21] J. Boos. *Effects of Non-locality in Gravity and Quantum Theory*. Springer Cham, 2021. DOI: https://doi.org/10.1007/978-3-030-82910-0.

[BS01] M. Bartelmann and P. Schneider. “Weak gravitational lensing”. In: *Physics Reports* 340.4-5 (2001), 291–472. ISSN: 0370-1573. DOI: 10.1016/s0370-1573(00)00082-x. URL: http://dx.doi.org/10.1016/S0370-1573(00)00082-X.

[BS03] A. Bernal and M. Sánchez. “On Smooth Cauchy Hypersurfaces and Geroch’s Splitting Theorem”. In: *Communications in Mathematical Physics* 243 (Dec. 2003), pp. 461–470. DOI: 10.1007/s00220-003-0982-6.

[Car14] S. Carroll. *Spacetime and Geometry, An Introduction to General Relativity*. Essex: Pearson New International Edition, 2014. ISBN: 10: 1-292-02663-4.

[CH01] A. Cooray and W. Hu. “Power Spectrum Covariance of Weak Gravitational Lensing”. In: *The Astrophysical Journal* 554.1 (2001), pp. 56–66. DOI: 10.1086/321376. URL: https://doi.org/10.1086/321376.

[Cli+12] T. Clifton et al. “Modified gravity and cosmology”. In: *Physics Reports* 513.1 (2012). Modified Gravity and Cosmology, pp. 1–189. ISSN: 0370-1573. DOI: https://doi.org/10.1016/j.physrep.2012.01.001. URL: https://www.sciencedirect.com/science/article/pii/S0370157312000105.

[Daa+22] J. Daas et al. *Probing Quadratic Gravity with the Event Horizon Telescope*. 2022. DOI: 10.48550/ARXIV.2204.08480. URL: https://arxiv.org/abs/2204.08480.

[Dio+13] E. D. Dio et al. “The CLASSgal code for relativistic cosmological large scale structure”. In: *Journal of Cosmology and Astroparticle Physics* 2013.11 (2013), 044–044. ISSN: 1475-7516. DOI: 10.1088/1475-7516/2013/11/044. URL: http://dx.doi.org/10.1088/1475-7516/2013/11/044.

[DL03] C. Doran and A. Lasenby. *Geometric Algebra for Physicists*. Cambridge: Cambridge University Press, 2003.

[Due20] M. Duell. *Gravitational closure of matter field equations - General Theory & Symmetrization*. PhD Thesis under supervision of Bjoern M. Schaefer and Frederic P. Schuller at the University of Heidelberg. 2020.

[Dur08] R. Durrer. *The Cosmic Microwave Background*. Cambridge: Cambridge University Press, 2008.

[Dü+18] M. Düll et al. “Gravitational closure of matter field equations”. In: *Phys. Rev. D* 97 (8 2018), p. 084036. DOI: 10.1103/PhysRevD.97.084036. URL: https://link.aps.org/doi/10.1103/PhysRevD.97.084036.

[Dü+20] M. Düll et al. *Symmetric gravitational closure*. 2020. arXiv: 2003.07109 [gr-qc].

[FHH20] J. K. C. Freudenburg, E. M. Huff, and C. M. Hirata. “A Framework for Measuring Weak-Lensing Magnification Using the Fundamental Plane”. In: *Mon. Not. Roy. Astron. Soc.* 496.3 (2020), pp. 2998–3014. DOI: 10.1093/mnras/staa1505. arXiv: 1910.02906 [astro-ph.CO].

[Fis17] N. L. Fischer. *Cosmological closure of metric and area-metric ideal fluids*. Master Thesis under supervision of Bjoern M. Schaefer and Frederic P. Schuller at the University of Heidelberg. 2017.

[FT02] M. E. Fels and C. G. Torre. “The principle of symmetric criticality in general relativity”. In: *Classical and Quantum Gravity* 19.4 (2002), pp. 641–675. DOI: 10.1088/0264-9381/19/4/303. URL: https://doi.org/10.1088%2F0264-9381%2F19%2F4%2F303.

[Fuj+21] T. Fujita et al. “Detection of isotropic cosmic birefringence and its implications for axionlike particles including dark energy”. In: *Physical Review D* 103.4 (2021). DOI: 10.1103/physrevd.103.043509. URL: https://doi.org/10.1103%2Fphysrevd.103.043509.

[GB05] D. Goldberg and D. Bacon. “Galaxy-Galaxy Flexion: Weak Lensing to Second Order”. In: *The Astrophysical Journal* 619 (Feb. 2005). DOI: 10.1086/426782.

[GD05] A. W. Graham and S. P. Driver. “A Concise Reference to (Projected) Sérsic R 1/n Quantities, Including Concentration, Profile Slopes, Petrosian Indices, and Kron Magnitudes”. In: *Publications of the Astronomical Society of Australia* 22.2 (2005), 118–127. DOI: 10.1071/AS05001.

[GDS21] B. Ghosh, R. Durrer, and B. M. Schäfer. “Intrinsic and extrinsic correlations of galaxy shapes and sizes in weak lensing data”. In: *Monthly Notices of the Royal Astronomical Society* 505.2 (2021), pp. 2594–2609. DOI: 10.1093/mnras/stab1435. URL: https://doi.org/10.1093%2Fmnras%2Fstab1435.

[Gie+12] K. Giesel et al. “Gravitational dynamics for all tensorial spacetimes carrying predictive, interpretable, and quantizable matter”. In: *Physical Review D* 85.10 (2012). ISSN: 1550-2368. DOI: 10.1103/physrevd.85.104042. URL: http://dx.doi.org/10.1103/PhysRevD.85.104042.

[GL07] D. M. Goldberg and A. Leonard. “Measuring Flexion”. In: *The Astrophysical Journal* 660.2 (May 10, 2007), pp. 1003–1015. ISSN: 0004-637X, 1538-4357. DOI: 10.1086/513137. arXiv: astro-ph/0607602. URL: http://arxiv.org/abs/astro-ph/0607602 (visited on 03/11/2020).

[GM01] M. Gotay and J. Marsden. “Stress-Energy-Momentum Tensors and the Belinfante-Rosenfeld Formula”. In: *Contemp. Math.* 132 (May 2001). DOI: 10.1090/conm/132/1188448.

[Gou07] E. Gourgoulhon. *3+1 Formalism and Bases of Numerical Relativity*. 2007. DOI: 10.48550/ARXIV.GR-QC/0703035. URL: https://arxiv.org/abs/gr-qc/0703035.

[Hen+21] J. Henrichs et al. “Testing gravity with the Milky Way: Yukawa potential”. In: *Phys. Rev. D* 104 (4 2021), p. 043009. DOI: 10.1103/PhysRevD.104.043009.

[Hil+17] S. Hilbert et al. “Intrinsic alignments of galaxies in the Illustris simulation”. In: *Monthly Notices of the Royal Astronomical Society* 468.1 (2017), 790–823. ISSN: 1365-2966. DOI: 10.1093/mnras/stx482. URL: http://dx.doi.org/10.1093/mnras/stx482.

[Hir+04] C. M. Hirata et al. “Galaxy-galaxy weak lensing in the Sloan Digital Sky Survey: intrinsic alignments and shear calibration errors”. In: *Monthly Notices of the Royal Astronomical Society* 353.2 (Sept. 2004), pp. 529–549. ISSN: 00358711, 13652966. DOI: 10.1111/j.1365-2966.2004.08090.x. URL: http://mnras.oxfordjournals.org/cgi/doi/10.1111/j.1365-2966.2004.08090.x (visited on 09/26/2015).

[Hir+07] C. M. Hirata et al. “Intrinsic galaxy alignments from the 2SLAQ and SDSS surveys: luminosity and redshift scalings and implications for weak lensing surveys: Intrinsic alignments”. In: *Monthly Notices of the Royal Astronomical Society* 381.3 (Sept. 26, 2007), pp. 1197–1218. ISSN: 00358711, 13652966. DOI: 10.1111/j.1365-2966.2007.12312.x. URL: http://mnras.oxfordjournals.org/cgi/doi/10.1111/j.1365-2966.2007.12312.x (visited on 09/26/2015).

[HKT76] S. A. Hojman, K Kuchar, and C Teitelboim. “Geometrodynamics regained”. In: *Ann. Phys. (N.Y.); (United States)* (1976). DOI: 10.1016/0003-4916(76)90112-3. URL: https://www.osti.gov/biblio/7194714.

[HO03] F. W. Hehl and Y. N. Obukhov. *Foundations of Classical Electrodynamics*. Birkhäuser Boston, MA, 2003. DOI: https://doi.org/10.1007/978-1-4612-0051-2.

[HO06] F. Hehl and Y. Obukhov. “Spacetime Metric from Local and Linear Electrodynamics: A New Axiomatic Scheme”. In: *Special Relativity*. Springer Berlin Heidelberg, 2006, pp. 163–187. DOI: 10.1007/3-540-34523-x_7. URL: https://doi.org/10.1007%2F3-540-34523-x_7.

[Hol+17] R. Holanda et al. “Probing the distance-duality relation with high-z-data”. In: *Journal of Cosmology and Astroparticle Physics* 2017.09 (2017), pp. 039–039. DOI: 10.1088/1475-7516/2017/09/039. URL: https://doi.org/10.1088%2F1475-7516%2F2017%2F09%2F039.

[Hor74] G. W. Horndeski. “Second-order scalar-tensor field equations in a four-dimensional space”. In: *International Journal of Theoretical Physics* 10 (1974), 363–384. DOI: https://doi.org/10.1007/BF01807638.

[HS10] C. M. Hirata and U. Seljak. “Intrinsic alignment-lensing interference as a contaminant of cosmic shear”. In: *Physical Review D* 82.4 (Aug. 24, 2010), p. 049901. ISSN: 1550-7998, 1550-2368. DOI: 10.1103/PhysRevD.82.049901. arXiv: astro-ph/0406275. URL: http://arxiv.org/abs/astro-ph/0406275 (visited on 05/09/2017).

[HT05] D. Huterer and M. Takada. “Calibrating the nonlinear matter power spectrum: Requirements for future weak lensing surveys”. In: *Astroparticle Physics* 23.4 (2005), pp. 369–376. ISSN: 0927-6505. DOI: https://doi.org/10.1016/j.astropartphys.2005.02.006. URL: https://www.sciencedirect.com/science/article/pii/S092765050500023X.

[HT99] W. Hu and M. Tegmark. “Weak Lensing: Prospects for Measuring Cosmological Parameters”. In: *The Astrophysical Journal Letters* 514 (Apr. 1999), pp. L65–L68. DOI: 10.1086/311947.

[Hu02] W. Hu. “Dark energy and matter evolution from lensing tomography”. In: *Phys.Rev.* 66.08 (2002), p. 083515. DOI: 10.1103/PhysRevD.66.083515.

[HW05] D. Huterer and M. White. “Nulling tomography with weak gravitational lensing”. In: *Phys. Rev. D* (Aug. 2005). DOI: 10.1103/PhysRevD.72.043002.

[IK85a] C. Isham and K. Kuchar. “Representations of spacetime diffeomorphisms. I. Canonical parametrized field theories”. In: *Annals of Physics* 164.2 (1985), pp. 288–315. ISSN: 0003-4916. DOI: https://doi.org/10.1016/0003-4916(85)90018-1. URL: https://www.sciencedirect.com/science/article/pii/0003491685900181.

[IK85b] C. Isham and K. Kuchar. “Representations of spacetime diffeomorphisms. II. Canonical geometrodynamics”. In: *Annals of Physics* 164.2 (1985), pp. 316–333. ISSN: 0003-4916. DOI: https://doi.org/10.1016/0003-4916(85)90019-3. URL: https://www.sciencedirect.com/science/article/pii/0003491685900193.

[Iti09] Y. Itin. “On light propagation in premetric electrodynamics: the covariant dispersion relation”. In: *Journal of Physics A: Mathematical and Theoretical* 42.47 (2009), p. 475402. DOI: 10.1088/1751-8113/42/47/475402. URL: https://doi.org/10.1088/1751-8113/42/47/475402.

[JT03] B. Jain and A. Taylor. “Cross-Correlation Tomography: Measuring Dark Energy Evolution with Weak Lensing”. In: *Phys. Rev. Lett.* 91.14 (Oct. 2003), p. 141302. DOI: 10.1103/PhysRevLett.91.141302.

[KH10] E. Krause and C. M. Hirata. “Tidal alignments as a contaminant of the galaxy bispectrum”. In: *Monthly Notices of the Royal Astronomical Society* 410.4 (2010), pp. 2730–2740. DOI: 10.1111/j.1365-2966.2010.17638.x. URL: https://doi.org/10.1111%2Fj.1365-2966.2010.17638.x.

[Kuc74] K. Kuchar. “Geometrodynamics regained: A Lagrangian approach”. In: *Journal of Mathematical Physics* 15.6 (1974), pp. 708–715. DOI: 10.1063/1.1666715. eprint: https://doi.org/10.1063/1.1666715. URL: https://doi.org/10.1063/1.1666715.

[Lau+11] R. Laureijs et al. *Euclid Definition Study Report*. 2011. arXiv: 1110.3193 [astro-ph.CO].

[LH04] C. Lämmerzahl and F. W. Hehl. “Riemannian light cone from vanishing birefringence in premetric vacuum electrodynamics”. In: *Phys. Rev. D* 70 (10 2004), p. 105022. DOI: 10.1103/PhysRevD.70.105022. URL: https://link.aps.org/doi/10.1103/PhysRevD.70.105022.

[LHG07] M. LoVerde, L. Hui, and E. Gaztañaga. “Magnification-temperature correlation: The dark side of integrated Sachs-Wolfe measurements”. In: *Physical Review D* 75.4 (2007). ISSN: 1550-2368. DOI: 10.1103/physrevd.75.043519. URL: http://dx.doi.org/10.1103/PhysRevD.75.043519.

[Lic17] S. Licklederer. *Planetary motion in weakly birefringent spacetime*. Bacherlor’s Thesis at the Friedrich Alexander University of Erlangen-Nürnberg under supervision of Frederic P. Schuller. 2017.

[Lim54] D. N. Limber. “The Analysis of Counts of the Extragalactic Nebulae in Terms of a Fluctuating Density Field. II.” In: *Astrophysical Journal* 119 (May 1954), p. 655. DOI: 10.1086/145870.

[Mal25] K. G. Malmquist. “A contribution to the problem of determining the distribution in space of the stars”. In: *Meddelanden fran Lunds Astronomiska Observatorium Serie I* 106 (Feb. 1925), pp. 1–12.

[MC18] C. Ma and P.-S. Corasaniti. “Statistical Test of Distance–Duality Relation with Type Ia Supernovae and Baryon Acoustic Oscillations”. In: *The Astrophysical Journal* 861.2 (2018), p. 124. DOI: 10.3847/1538-4357/aac88f. URL: https://doi.org/10.3847%2F1538-4357%2Faac88f.

[MCK14] D. Munshi, P. Coles, and M. Kilbinger. “Tomography and weak lensing statistics”. In: *Journal of Cosmology and Astroparticle Physics* 2014.04 (2014), 004–004. ISSN: 1475-7516. DOI: 10.1088/1475-7516/2014/04/004. URL: http://dx.doi.org/10.1088/1475-7516/2014/04/004.

[MK20] Y. Minami and E. Komatsu. “New Extraction of the Cosmic Birefringence from the Planck 2018 Polarization Data”. In: *Physical Review Letters* 125.22 (2020). DOI: 10.1103/physrevlett.125.221301. URL: https://doi.org/10.1103%2Fphysrevlett.125.221301.

[Mor+16] S. More et al. *Modifications to the Etherington Distance Duality Relation and Observational Limits*. 2016. arXiv: 1612.08784 [astro-ph.CO].

[MSW73] C. W. Misner, T. K. S., and J. A. Wheeler. *Gravitation*. W. H. Freeman and Company, 1973. ISBN: 0-7167-0344-0.

[Nak03] M. Nakahara. *Geometry, Topology and Physics*. Boca Raton, Florida: Taylor & Francis Group, 2003. ISBN: 0-7503-0606-8.

[Nam73] Y. Nambu. “Generalized Hamiltonian Dynamics”. In: *Phys. Rev. D* 7 (8 1973), pp. 2405–2412. DOI: 10.1103/PhysRevD.7.2405. URL: https://link.aps.org/doi/10.1103/PhysRevD.7.2405.

[New] *Newton potential. Encyclopedia of Mathematics.* - visited 24.11.2021. URL: http://encyclopediaofmath.org/index.php?title=Newton_potential&oldid=11686.

[NO12] M. Nedeljkov and M. Oberguggenberger. “Ordinary differential equations with delta function terms”. In: *Publications de l’Institut Mathematique* 91 (Jan. 2012). DOI: 10.2298/PIM1205125N.

[OR02] Y. N. Obukhov and G. F. Rubilar. “Fresnel analysis of wave propagation in nonlinear electrodynamics”. In: *Phys. Rev. D* 66 (2 2002), p. 024042. DOI: 10.1103/PhysRevD.66.024042. URL: https://link.aps.org/doi/10.1103/PhysRevD.66.024042.

[OUF07] Y. Okura, K. Umetsu, and T. Futamase. “A New Measure for Weak-Lensing Flexion”. In: *The Astrophysical Journal* 660.2 (2007), pp. 995–1002. DOI: 10.1086/513135. URL: https://doi.org/10.1086/513135.

[OUF08] Y. Okura, K. Umetsu, and T. Futamase. “A Method for Weak Lensing Flexion Analysis by the HOLICs Moment Approach”. In: *The Astrophysical Journal* 680.1 (June 10, 2008), pp. 1–16. ISSN: 0004-637X, 1538-4357. DOI: 10.1086/587676. arXiv: 0710.2262. URL: http://arxiv.org/abs/0710.2262 (visited on 03/11/2020).

[Pei95] Y. C. Pei. “The Luminosity Function of Quasars”. In: *The Astrophysical Journal* 438 (Jan. 1995), p. 623. DOI: 10.1086/175105.

[Pir+17] D. Piras et al. “The mass dependence of dark matter halo alignments with large-scale structure”. In: *Monthly Notices of the Royal Astronomical Society* 474.1 (2017), 1165–1175. ISSN: 1365-2966. DOI: 10.1093/mnras/stx2846. URL: http://dx.doi.org/10.1093/mnras/stx2846.

[PWS09] R. Punzi, M. N. R. Wohlfarth, and F. P. Schuller. “Propagation of light in area metric backgrounds”. In: *Class. Quant. Grav.* 26 (2009), p. 035024. DOI: 10.1088/0264-9381/26/3/035024. arXiv: 0711.3771 [hep-th].

[QMZ21] J. Qin, F. Melia, and T.-J. Zhang. “Test of the cosmic distance duality relation for arbitrary spatial curvature”. In: *Monthly Notices of the Royal Astronomical Society* 502.3 (2021), pp. 3500–3509. DOI: 10.1093/mnras/stab124. URL: https://doi.org/10.1093%2Fmnras%2Fstab124.

[Rei+22] R. Reischke et al. “Testing modified (Horndeski) gravity by combining intrinsic galaxy alignments with cosmic shear”. In: *Monthly Notices of the Royal Astronomical Society* 510.3 (2022), pp. 4456–4462. DOI: 10.1093/mnras/stab3219. URL: https://doi.org/10.1093%2Fmnras%2Fstab3219.

[Ren10] F. Renaud. *Dynamics of the Tidal Fields and Formation of Star Clusters in Galaxy Mergers*. 2010. arXiv: 1008.0331 [astro-ph.CO].

[Rie20] H.-M. G. Rieser. *Cosmological and Astrophysical Tests of Constructive Gravity*. PhD Thesis under supervision of Bjoern M. Schaefer and Frederic P. Schuller at the University of Heidelberg. 2020.

[Rie+98] A. G. Riess et al. “Observational Evidence from Supernovae for an Accelerating Universe and a Cosmological Constant”. In: *The Astronomical Journal* 116.3 (1998), pp. 1009–1038. DOI: 10.1086/300499. URL: https://doi.org/10.1086%2F300499.

[Row+13] B. Rowe et al. “Flexion measurement in simulations of Hubble Space Telescope data”. In: *Monthly Notices of the Royal Astronomical Society* 435.1 (2013), pp. 822–844. ISSN: 0035-8711. DOI: 10.1093/mnras/stt1353. URL: http://dx.doi.org/10.1093/mnras/stt1353.

[RRS11] D. Raetzel, S. Rivera, and F. P. Schuller. “Geometry of physical dispersion relations”. In: *Physical Review D* 83.4 (2011). ISSN: 1550-2368. DOI: 10.1103/physrevd.83.044047. URL: http://dx.doi.org/10.1103/PhysRevD.83.044047.

[RS11] S. Rivera and F. P. Schuller. "Quantization of general linear electrodynamics". In: *Physical Review D* 83.6 (2011). DOI: 10.1103/physrevd.83.064036. URL: https://doi.org/10.1103%2Fphysrevd.83.064036.

[Rub02] G. Rubilar. "Linear pre-metric electrodynamics and deduction of the light cone". In: *Annalen der Physik* 11.10-11 (2002), pp. 717–782. DOI: 10.1002/1521-3889(200211)11:10/11<717::aid-andp717>3.0.co;2-6. URL: https://doi.org/10.1002%2F1521-3889%28200211%2911%3A10%2F11%3C717%3A%3Aaid-andp717%3E3.0.co%3B2-6.

[Ryd09] L. Ryder. *Introduction to General Relativity*. Cambridge: Cambridge University Press, 2009. ISBN: 978-0-521-84563-2.

[SAB21] J. Stücker, R. E. Angulo, and P. Busch. "The boosted potential". In: *Monthly Notices of the Royal Astronomical Society* 508.4 (2021), pp. 5196–5216. DOI: 10.1093/mnras/stab2913. URL: https://doi.org/10.1093%2Fmnras%2Fstab2913.

[SBD17] J. G. de Swart, G. Bertone, and J. van Dongen. "How dark matter came to matter". In: *Nature Astronomy* 1.3 (2017). DOI: 10.1038/s41550-017-0059. URL: https://doi.org/10.1038%2Fs41550-017-0059.

[Scha] F. P. Schuller. private communication.

[Schb] B. M. Schäfer. private communication.

[SCH09] B. M. SCHÄFER. "Galactic angular momenta and angular momentum correlations in the cosmological large-scale structure". In: *International Journal of Modern Physics D* 18.02 (2009), 173–222. ISSN: 1793-6594. DOI: 10.1142/s0218271809014388. URL: http://dx.doi.org/10.1142/S0218271809014388.

[Sch11] B. M. Schäfer. *Dark energy and evolution of the cosmic large-scale structure - Habilitation dissertation; Ruprecht-Karls Universtiy of Heidelberg*. 2011.

[Sch+12] B. M. Schäfer et al. "On the validity of the Born approximation for weak cosmic flexions". In: *Monthly Notices of the Royal Astronomical Society* 420.1 (Feb. 2012), pp. 455–467. DOI: 10.1111/j.1365-2966.2011.20051.x. arXiv: 1101.4769 [astro-ph.CO].

[Sch+17] J. Schneider et al. *Gravitational closure of weakly birefringent electrodynamics*. 2017. arXiv: 1708.03870 [hep-th].

[Sch20] F. P. Schuller. *Constructive Gravity: Foundations and Applications*. 2020. DOI: 10.48550/ARXIV.2003.09726. URL: https://arxiv.org/abs/2003.09726.

[SEF92] P. Schneider, J. Ehlers, and E. E. Falco. *Gravitational Lenses*. Springer-Verlag, 1992.

[Sei10] W. M. Seiler. *Involution - The Formal Theory of Differential Equations and its Applications in Computer Algebra*. Springer-Verlag Berlin Heidelberg, 2010. DOI: 10.1007/978-3-642-01287-7.

[Sér63] J. L. Sérsic. "Influence of the atmospheric and instrumental dispersion on the brightness distribution in a galaxy". In: *Boletin de la Asociacion Argentina de Astronomia La Plata Argentina* 6 (Feb. 1, 1963), pp. 41–43. ISSN: 0571-3285. URL: http://adsabs.harvard.edu/abs/1963BAAA....6...41S (visited on 03/04/2020).

[SH11] B. M. Schaefer and L. Heisenberg. "Weak lensing tomography with orthogonal polynomials". In: *Monthly Notices of the Royal Astronomical Society* 423 (July 2011). DOI: 10.1111/j.1365-2966.2012.21137.x.

[She01] Z. Shen. *Lectures on Finsler Geometry*. 2001. DOI: 10.1142/9789812811622.

[SKW06] P. Schneider, C. Kochanek, and J. Wambsganss. *Gravitational Lensing: Strong, Weak and Micro*. Berlin Heidelberg: Springer-Verlag, 2006.

[Smi+03] R. E. Smith et al. "Stable clustering, the halo model and non-linear cosmological power spectra". In: *Monthly Notices of the Royal Astronomical Society* 341.4 (June 2003), pp. 1311–1332. ISSN: 0035-8711. DOI: 10.1046/j.1365-8711.2003.06503.x. eprint: https://academic.oup.com/mnras/article-pdf/341/4/1311/3500043/341-4-1311.pdf. URL: https://doi.org/10.1046/j.1365-8711.2003.06503.x.

[SR16] B. Schäfer and R. Reischke. "Describing variations of the Fisher-matrix across parameter space". In: *Monthly Notices of the Royal Astronomical Society* 460 (Mar. 2016). DOI: 10.1093/mnras/stw1221.

[SSR20] M. Sipp, B. Schäfer, and R. Reischke. "Optimising tomography for weak gravitational lensing surveys". In: *Monthly Notices of the Royal Astronomical Society* 501 (Nov. 2020). DOI: 10.1093/mnras/staa3710.

[Str13] N. Straumann. *General Relativity*. Dordrecht: Springer, 2013. DOI: 10.1007/978-94-007-5410-2.

[SW14] F. P. Schuller and C. Witte. "How quantizable matter gravitates: A practitioner's guide". In: *Phys. Rev. D* 89 (10 2014), p. 104061. DOI: 10.1103/PhysRevD.89.104061. URL: https://link.aps.org/doi/10.1103/PhysRevD.89.104061.

[SW17] F. P. Schuller and M. C. Werner. “Etherington’s Distance Duality with Birefringence”. In: *Universe* 3.3 (2017). ISSN: 2218-1997. DOI: 10.3390/universe3030052. URL: https://www.mdpi.com/2218-1997/3/3/52.

[SWW10] F. P. Schuller, C. Witte, and M. N. Wohlfarth. “Causal structure and algebraic classification of non-dissipative linear optical media”. In: *Annals of Physics* 325.9 (2010), 1853–1883. ISSN: 0003-4916. DOI: 10.1016/j.aop.2010.04.008. URL: http://dx.doi.org/10.1016/j.aop.2010.04.008.

[Tan+18] V. Tansella et al. “The full-sky relativistic correlation function and power spectrum of galaxy number counts. Part I: theoretical aspects”. In: *Journal of Cosmology and Astroparticle Physics* 2018.03 (2018), 019–019. ISSN: 1475-7516. DOI: 10.1088/1475-7516/2018/03/019. URL: http://dx.doi.org/10.1088/1475-7516/2018/03/019.

[Tie+21] E. Tiesinga et al. “CODATA Recommended Values of the Fundamental Physical Constants: 2018”. In: *Journal of Physical and Chemical Reference Data* 50.3 (2021), p. 033105. DOI: 10.1063/5.0064853. eprint: https://doi.org/10.1063/5.0064853. URL: https://doi.org/10.1063/5.0064853.

[Tra06] A. Trautman. *Einstein-Cartan Theory*. 2006. DOI: 10.48550/ARXIV.GR-QC/0606062. URL: https://arxiv.org/abs/gr-qc/0606062.

[TS18] T. M. Tugendhat and B. M. Schäfer. “Angular ellipticity correlations in a composite alignment model for elliptical and spiral galaxies and inference from weak lensing”. In: *Monthly Notices of the Royal Astronomical Society* 476.3 (Feb. 2018), pp. 3460–3477. ISSN: 0035-8711. DOI: 10.1093/mnras/sty323. eprint: https://academic.oup.com/mnras/article-pdf/476/3/3460/24502734/sty323.pdf. URL: https://doi.org/10.1093/mnras/sty323.

[TTH97] M. Tegmark, A. N. Taylor, and A. F. Heavens. “Karhunen-Loève Eigenvalue Problems in Cosmology: How should we tackle large data sets?” In: *The Astrophysical Journal* 480.1 (1997), pp. 22–35.

[TW04] M. Takada and M. White. “Tomography of Lensing Cross-Power Spectra”. In: *The Astrophysical Journal* 601 (Jan. 2004), pp. L1–L4. DOI: 10.1086/381870.

[Vau48] G. de Vaucouleurs. “Recherches sur les Nebuleuses Extragalactiques”. In: *Annales d’Astrophysique* 11 (Jan. 1, 1948), p. 247. ISSN: 0365-0499. URL: http://adsabs.harvard.edu/abs/1948AnAp...11..247D (visited on 03/04/2020).

[Wal84] R. M. Wald. *General Relativity*. Chicago: The Universty of Chicago Press, 1984. ISBN: 0-226-87033-2.

[Wie] A. A. Wierzba. private communication.

[Wie18] A. A. Wierzba. *Parametrodynamics*. Master Thesis under supervision of Frederic P. Schuller and Ivo Sachs at the Ludwig-Maximillian University, Munich. 2018.

[Wit14] C. Witte. *Gravity actions from matter actions*. PhD Thesis under supervision of Frederic P. Schuller, Thomas Thiemann and Matthias Staudacher at the Humboldt-University, Berlin. 2014.

[Wol22] F. Wolz. *Gravitational Closure of Matter field equations*. PhD Thesis under supervision of Frederic P. Schuller and Domenico Guillini at the Leibniz-University, Hannover. 2022.

[ZSH22] J. Zjupa, B. M. Schäfer, and O. Hahn. "Intrinsic alignments in IllustrisTNG and their implications for weak lensing: Tidal shearing and tidal torquing mechanisms put to the test". In: *Monthly Notices of the Royal Astronomical Society* 514.2 (Aug. 2022), pp. 2049–2072. DOI: 10.1093/mnras/stac042.

[Zwi33] F. Zwicky. "Die Rotverschiebung von extragalaktischen Nebeln". In: *Helvetica Physica Acta* 6 (Jan. 1933), pp. 110–127.

Own Publications

The results on intrinsic flexions presented in section 4.4.1 and partly 4.2 of this thesis have been published in

E. S. Giesel, B. Ghosh and B. M. Schäfer,

Monthly Notices of the Royal Astronomical Society (December 2021), 510, 2773–2789,

Intrinsic and extrinsic gravitational flexions.

Further discussion concerning details on the numerical value of the alignment parameter and updated plots have been updated on *ArXiv* arXiv:2107.09000v3.

The results discussed in sections 5.3 and 5.4 are also published as

E. S. Giesel, B. Ghosh and B. M. Schäfer,

ArXiv: arXiv:2208.07197, *(August 2022)*

Etherington duality breaking: gravitational lensing in non-metric spacetimes versus intrinsic alignments.

and submitted to the *Monthly Notices of the Royal Astronomical Society*.

Acknowledgements

First and foremost I would like to thank my thesis supervisor Professor Dr. Björn Malte Schäfer for several years of very successful cooperation, with many highly interesting and fascinating scientific discussion, invaluable advice, be it scientific or professional, and active support throughout the years. I am very thankful for the respectful interaction at eye level and his reliance on my abilities to be head tutor for his lecture on general relativity, as well as entrusting me with the supervision of students during the summer academy of Studienstiftung des deutschen Volkes. I highly appreciate that he promoted me to autonomously drive my scientific projects, at all times showing a high level of confidence in my work.

I would like to thank Professor Dr. Jan Pawlowski for being the second referee of this thesis, as well as being part of my Ph.D. committee. In this context, I would also like to thank Professor Dr. Andre Butz as well as Privatdozent Dr. Maarten DeKieviet to complete my committee as examiners.

Many thanks also to Professor Dr. Frederic Paul Schuller for his co-supervision. I greatly appreciate the inspiring and fascinating joint discussions, and I am very thankful for his invitation to the University of Twente, a visit from which I benefited a lot. I am also very grateful for his time to follow my invitation to the Heidelberg Graduate Days in winter semester 2022 to give a lecture on constructive gravity.

Concerning the funding I would like to express my gratitude to the Studienstiftung des Deutschen Volkes for providing me with a scholarship to pursue my doctoral studies from 01.11.2019 until the 31.10.2022, funding a major part of this work.
Furthermore, I would like to thank the ARI (Astronomisches Rechen-Institut) at ZAH (Center for Astronomy of the University of Heidelberg) for providing me with a workplace, as well as a scholarship from the 01.11.2022 until the 31.12.2022 to finish my doctoral studies.
I am also thankful for being accepted as a member of the Young Researchers Convent (YRC) STRUCTURES Heidelberg, and for receiving the YRC Travel Grant to visit my co-supervisor Frederic P. Schuller at the University of Twente, Netherlands.

I would further like to thank Professor Dr. Marcus Werner for valuable common discussions,

especially on his joint work with Frederic P. Schuller, and scientific exchange.

A special thank you also again goes out to Maarten DeKieviet for introducing me to the very interesting field of geometric algebra, as well as sharing his ideas and excitement on this topic with me. I am also very grateful that I was invited to contribute to his seminar on geometric algebra, being invited to his group seminar and the DAI talk on cosmology by George Ellis.

I am also greatly indebted to my former colleague Maximilian Düll, as well as Florian Wolz for taking their time to share with me their very deep insights and technical expertise concerning the constructive gravity program and solution strategies. I really valued the common discussions with them both, which were of enormous support for me. I am also very thankful for Max's very helpful comments to improve this thesis, and Florian's thorough proofreading of larger parts of the thesis with valuable suggestions for improvements.

I would also like to thank Basundhara Ghosh for our joint work during the last few years and our valuable discussions leading to the two publications cited in this thesis.

Many thanks also to my colleague Robert Reischke for our successful cooperation on the publication *Information geometry in cosmological inference problems*, as well as our joint working-group management during the summer academy of Studienstiftung des deutschen Volkes. I also appreciated his personal and scientific advice and support, and I am very grateful for his proofreading of parts of my thesis.

Many thanks also to Alexander Wierzba with whom I hand many interesting conversations during my visit in Twente, and I would also like to thank him for his contributions to the Heidelberg Graduate Days lecture course held by Frederic Schuller.

A special thank you also goes out to my former colleague Hans-Martin Rieser who invited me to the Quantum Computing seminar at the DLR (German Aerospace Center) at Ulm, which he had organized associated with Stiftung der deutschen Wirtschaft, as well as introducing me to his colleagues, and providing me with a highly interesting insight into his workplace and his work as such.

I am also thankful for my current and former colleagues at ZAH and STRUCTURES, namley Lennert Röver, Pedro Riba, Rafael Arutjunjan, Mascha Teich, Marvin Sipp, Sebastian Stapelberg, Alexander Kunkel, Veronika Öhl, Christian Sorgenfrei, Johannes Schwinn, Iris

Feldt, Tristan Daus, Carsten Littek, Sara Konrad, Alexander Oestreicher, Ricardo Waibel, Felix Kuhn, Christophe Pixius and Elena Kozlikin. I really enjoyed our valuable discussions, as well as the supportive environment, and highly interesting exchange on modern topics in cosmology during our seminars.

I highly appreciate the successful cooperation with Hannes Keppler, Jonah Cedric Strauß, Rafael Arutjunjan, Saswato Sen, Philipp Saake, Jeff Kuntz, Parham Radpay, Jonas Rezacek and Benedikt Jung as tutors for the general relativity lecture and their strong commitment and creative ideas concerning the exercises and exercise groups, especially in challenging times during the pandemic. In this context I would also like to thank my former colleagues Christian Angrick, again Robert Reischke, Nils Leif Vu and again Maximilian Düll for sharing material and exercise suggestions for the exercise sheets, as well as sharing general advice concerning my function as head tutor.

Many thanks to Tobias Haas, Christian Schmidt and Jiahan Shi for the great teamwork during the STRUCTURES Schöntal workshop on entanglement, leading to the contribution on the black hole information paradox.

I am also indebted to Ralf Rath, who has accompanied me as my mentor for the last few years with invaluable counsel concerning career options and decisions, as well as professional and personal development.
I am also grateful to Claudia Götzigner for her mindful advice concerning my professional and personal development throughout the last few years.
Finally, I would like to thank my family for their unfailing support.